Copper-Catalyzed Stereoselective Silylfunctionalization of Internal Alkynes with Silylboronates

Hirokazu Moniwa

March 2025

Copper-Catalyzed Stereoselective Silylfunctionalization of Internal Alkynes with Silylboronates

A dissertation submitted to
THE GRADUATE SCHOOL OF ENGINEERING SCIENCE
OSAKA UNIVERSITY
in partial fulfillment of the requirements for the degree of
DOCTOR OF PHILOSOPHY IN SCIENCE

by

Hirokazu Moniwa

March 2025

Abstract

Silylalkenes are known as useful synthetic intermediates of various functional molecules, such as pharmaceuticals and optical organic materials. For the synthesis of silylalkenes, transition-metal-catalyzed 1,2-hydrosiylation and 1,2-silylfunctionalization of alkynes are known as straightforward and efficient methods. Although such reactions have been extensively developed, most of them are *syn*-selective addition to introduce substituents to the same side of alkynes, and *anti*-selective addition is limited so far. In particular, there are very few reactions of unsymmetric internal alkynes with high regio- and *anti*-selectivity.

Silylborane compounds having a silicon–boron bond are useful silylating reagents due to their unique reactivity. Silylcopper nucleophiles, which can be generated by the reaction of a copper salt and a silylboronate, have been utilized in the synthesis of various silylalkene compounds from alkynes, but most of the reported reactions proceed *syn*-selectively.

In this context, the author developed novel copper-catalyzed *anti*-selective 1,2-silylfunctionalization reactions of internal alkynes with silylboronates for the synthesis of multi-substituted silylalkenes. These reactions allowed to access various alkene-containing compounds by using the resulting silylalkenes as synthetic intermediates.

Chapter 1 provides an overview of the pioneering works and the recent development on transition-metal-catalyzed *anti*-selective 1,2-hydrosilylation and 1,2-silylfunctionalization of alkynes and the reactivity of silylboronates with copper catalysts.

Chapter 2 describes the development of copper-catalyzed regio- and *anti*-selective silylboration of internal alkynes to synthesize silylborated alkenes. This reaction proceeds with very high regio- and *anti*-selectivity and can afford synthetically useful silicon- and boron-substituted alkenes as these moieties can be transformed into various other

functional groups. In addition, the detailed reaction mechanism of the silylboration was elucidated based on the experimental and theoretical studies. The author found that the *syn*-*anti* isomerization of alkenyl metals proceeds through an allenyl anion transition state and the *anti*-selectivity is likely controlled by the steric hindrance of the silicon substituent.

Chapter 3 describes *anti*-selective cyclative silylarylation of benzylalkynes to give silylindenes by using a similar reaction system with a copper catalyst and silylboronates. It is an unusual process in that the aromatic C–H bond is activated via an elimination of the hydrogen atom as a hydride.

Finally, Chapter 4 describes the development of copper-catalyzed regio- and *syn*-selective formal hydro(borylmethylsilyl)ation reaction of internal alkynes with silylboronates. Although this reaction does not proceed *anti*-selectively, it shows a novel reactivity of the reaction system using a copper catalyst and silylboronates. This reaction proceeds via alkenyl-to-alkyl 1,4-copper migration, which has not been previously reported.

Contents

Chapter 1

General Introduction

This dissertation describes novel copper-catalyzed *anti*-silylboration, *anti*-silylarylation, and *syn*-hydro(borylmethylsilyl)ation of internal alkynes with silylboronates, which the author developed. Before describing these reactions, Chapter 1 introduces previously studied transition-metal-catalyzed *anti*-selective silylfunctionalization of alkynes and copper-catalyzed reactions using silylboronates.

1.1 Transition-metal-catalyzed *anti*-selective 1,2-hydrosilylation and 1,2-silylfunctionalization of alkynes

Alkenes having silicon substituents (= silylalkenes) are used as synthetic intermediates for various useful alkene-containing compounds because of their unique and diverse reactivity of the silicon moiety.[1] For the synthesis of silylalkenes, 1,2-hydrosilylation and 1,2-silylfunctionalization of alkynes are most straightforward and efficient methods.[2] However, high regio- and stereoselectivity is required for synthetically useful reactions because up to four isomers can be generated depending on the position and configuration of the introduced substituents (Scheme 1). Since the pioneering hydrosilylation reactions of alkynes were developed in 1950s and 1960s,[3] various hydrosilylation and silylfunctionalization reactions of alkynes using transition-metal catalysts have been studied. To date, catalytic reactions using Mn,[4] Fe,[5] Ni,[6] Cu,[7] Rh,[8] Pd,[9] Ir,[10] Pt,[11] Au,[12], La[13] etc. have been reported, but most of them are *syn*-selective additions. On the other hand, transition-metal-catalyzed *anti*-selective reactions, which are complementary to *syn*-addition reactions, are limited compared to *syn*-selective

reactions. As a pioneering work of *anti*-selective silylation of alkynes, Ojima *et al*. developed *anti*-selective hydrosilylation of terminal alkynes.[14a] Since then, particularly in the last decade, many *anti*-selective hydrosilylation and silylfunctionalization reactions have been intensively investigated. In this section, selected pioneering works and recent developments on *anti*-selective hydrosilylation and silylfunctionalization of alkynes are described.

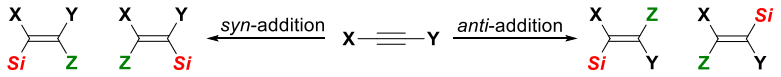

Scheme 1. Hydrosilylation (**Z** = H) and silylfunctionalization (**Z** = B, C, Si etc.) of alkynes (left: *syn*-addition, right: *anti*-addition).

1.1.1 Transition-metal-catalyzed *anti*-selective 1,2-hydrosilylation of alkynes

Catalytic *anti*-hydrosilylation and silylfunctionalization reactions of terminal alkynes using radical, Lewis acid, or transition-metal have been well-studied for a long time.[3,15,16] For the transition-metal-catalyzed *anti*-selective reactions, rhodium-catalyzed hydrosilylation of terminal alkynes was developed as a pioneering work by Ojima *et al*. in 1974.[14a] In the reaction using 1-hexyne and dimethylethylsilane, silylalkene **1** was obtained in a high yield with 81% *anti*-selectivity. They proposed the reaction mechanism involving the insertion of 1-hexyne to silylrhodium **2** followed by *syn*-*anti* isomerization between silylalkenylrhodium **3** and **5** via zwitterionic carbene structure **4**. The *anti*-selectivity was controlled by the steric difference of silylalkenylrhodium intermediates (Scheme 2).[14d]

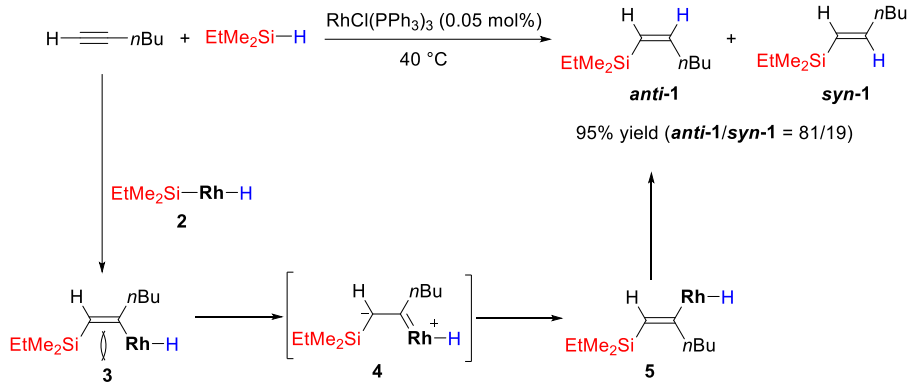

Scheme 2. Rhodium-catalyzed *anti*-selective hydrosilylation of terminal alkynes and the proposed mechanism by Ojima *et al*.

In 1990, Crabtree *et al*. reported an iridium-catalyzed *anti*-selective hydrosilylation of terminal alkynes. When using phenylacetylene as a substrate, the *anti*-selectivity was extremely high, and the regioisomer was not observed at all (Scheme 3).[14e] They proposed *syn-anti* isomerization through η^2-vinyliridium (iridacyclopropene) **8** instead of a zwitterionic carbene. Based on this pioneering report, mechanisms of various other transition-metal-catalyzed reactions involving *syn-anti* isomerization of alkenylmetals were elucidated.[17]

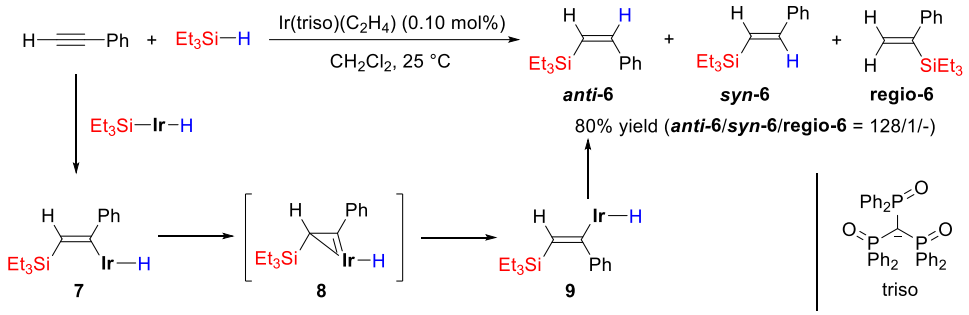

Scheme 3. Iridium-catalyzed *anti*-selective hydrosilylation of terminal alkynes and the proposed mechanism by Crabtree *et al*.

Since these Ojima's and Crabtree's reports, *anti*-hydrosilylation reactions of

alkynes have been widely studied, but most of them are not applicable to internal alkynes.[14,18]

Trost *et al*. achieved an *α*-selective hydrosilylation of alkynes to synthesize branch-type silylalkenes by using a cationic ruthenium catalyst (Scheme 4a).[19] A deuterium labeling experiment with triethylsilane-*d* provided a completely deuterated α-silylalkene at the *anti*-position of the silyl group, confirming that this hydrosilylation proceeded *anti*-selectively. This reaction is a rare example that is applicable not only to terminal alkynes but also to internal alkynes. As shown in Scheme 4b, reactions using dialkylalkynes or propargyl alcohols proceeded in high yields with high *anti*-selectivity to give the corresponding silylalkenes.

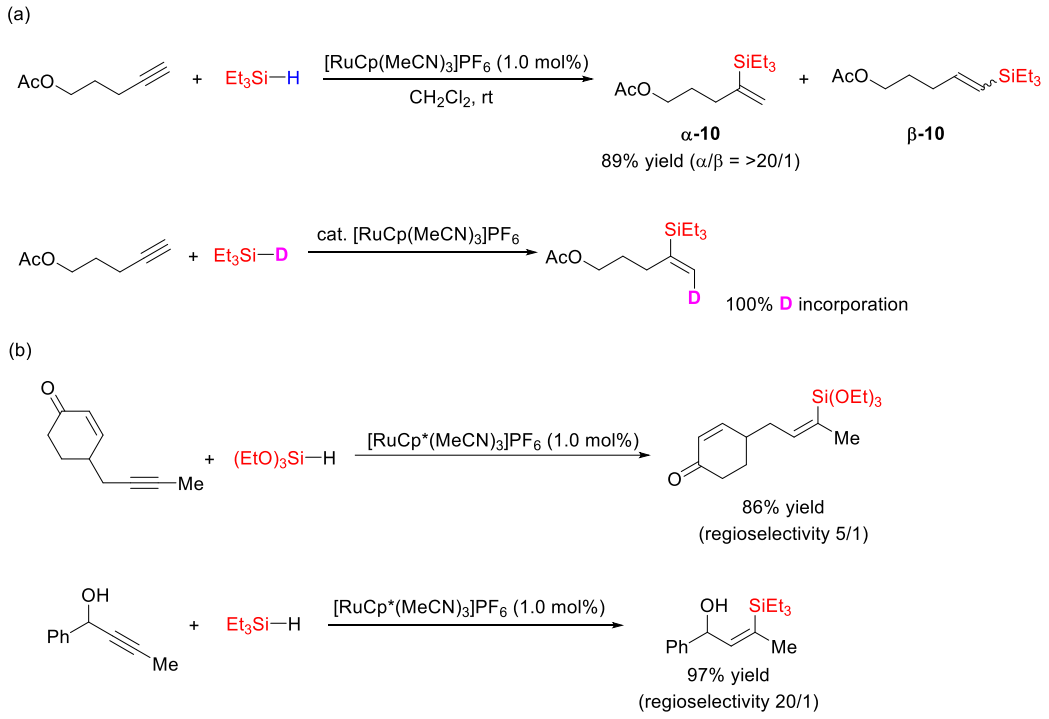

Scheme 4. Ruthenium-catalyzed *anti*- and regio-selective hydrosilylation of (a) terminal and (b) internal alkynes.

In 2002, Matsuda *et al*. reported silylative cyclization of 1,6-heptadiynes by using a rhodium catalyst (Scheme 5).[20] In the presence of $Rh(H)(SiMe_2Ph)(Cl)(PPh_3)_2$ as a catalyst, silylative cyclization proceeded to afford (*E*)-dialkylidenecyclopentane **11** predominantly. On the other hand, the use of $RhCl(PPh_3)_3$ as a catalyst resulted in the formation of indanes **13** and **14** instead of **11** via cyclotrimerization of alkynes.

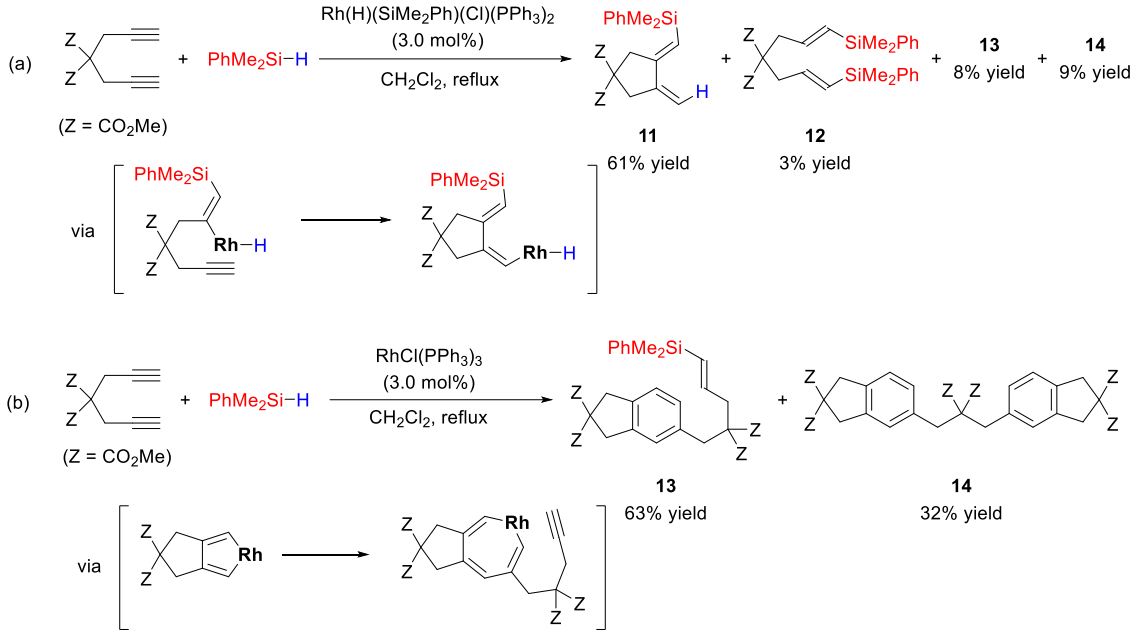

Scheme 5. (a) Silylative cyclization of 1,6-heptadiynes by $Rh(H)(SiMe_2Ph)(Cl)(PPh_3)_2$. (b) Dimerization and trimerization of 1,6-heptadiynes by $RhCl(PPh_3)_3$.

In 2010, Ferreira *et al*. achieved a platinum-catalyzed synthesis of silylenone **(*Z*)-16a** via intramolecular *anti*-selective hydrosilylation (silylprotonation) of silylpropargyl alcohol **15a** (Scheme 6a).[21] A π-acidic platinum plays a key role in this reaction, and *anti*-selective silyl migration proceeds from the platinum-coordinated intermediate to give vinylplatinum species **17**. Subsequent protodemetalation leads to silylenone product **(*Z*)-16a** with high stereoselectivity. In addition, they also reported that **(*E*)-16b** was obtained with high *syn*- and regioselectivity under the same platinum catalyst system by changing

the starting materials to an alkynone and a hydrosilane (Scheme 6b).

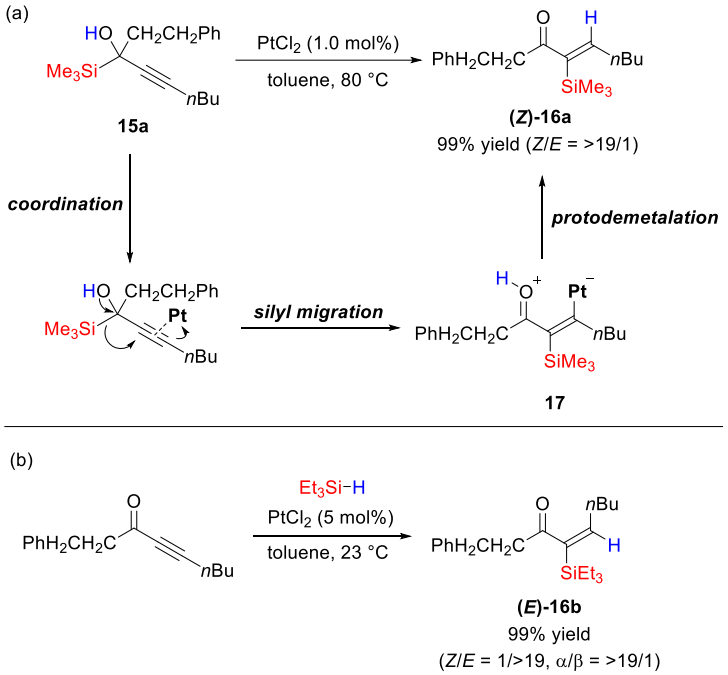

Scheme 6. Platinum-catalyzed reaction: (a) *anti*-selective hydrosilylation of propargyl alcohols and (b) *syn*-selective hydrosilylation of alkynones.

1.1.2 Transition-metal-catalyzed *anti*-selective carbosilylation of alkynes

In contrast to the progress of *anti*-hydrosilylation, the development of *anti*-selective carbosilylation reactions, which simultaneously introduce silicon and carbon substituents into alkynes, had been delayed for a long time. However, in 2010s, the development of *anti*-carbosilylation reactions by transition-metal catalysts was rapidly achieved.

In 2011, Fukumoto and Chatani *et al*. found rhodium-catalyzed silylimination of alkynes and the stereochemistry was controlled by changing the substituents of isocyanides (Scheme 7).[22] The reaction of phenylacetylene and dimethylphenylsilane with xylyl isocyanide gave imine **18a** with 98% (*E*)-selectivity, whereas the use of *tert*-

octyl isocyanide afforded imine **18b** with 93% (*Z*)-selectivity. For the reaction mechanism, they proposed the following pathway. Initially, *syn*-addition of Rh–Si bond to an alkyne occurs, which is followed by insertion of an isocyanide to form iminorhodium intermediate ***syn*-19**. If the substituent on isocyanide is a *tert*-alkyl group, (*Z*)-product is obtained by the subsequent reaction with a hydrosilane. On the other hand, in the case of the reaction with an aryl isocyanide, zwitterionic intermediate **20** is formed due to the stabilization of an anion on the nitrogen by the electron-withdrawing aryl group, and it isomerizes to intermediate ***anti*-21**. However, they were unable to obtain experimental evidence to support their hypothesis.

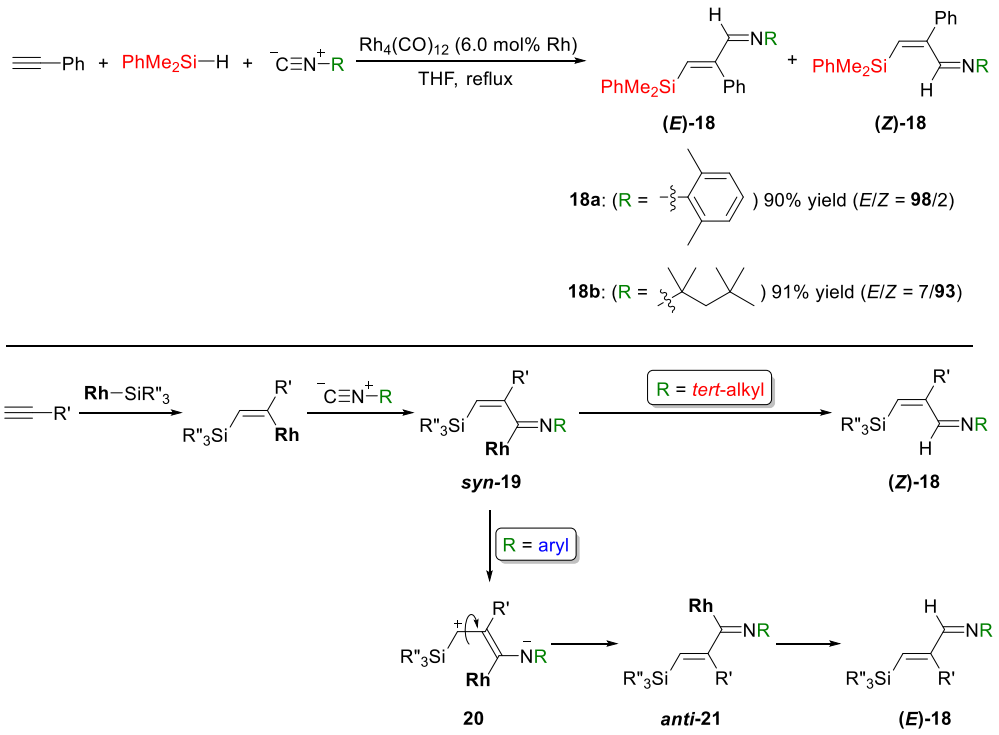

Scheme 7. Rhodium-catalyzed stereo-controlled silylimination of alkynes.

Wu *et al*. achieved a rhodium-catalyzed synthesis of silylindenones by the reaction of internal alkynes with hydrosilanes and carbon monoxide (Scheme 8).[23] The proposed

reaction mechanism is shown as follows. The reaction begins with oxidative addition of a silane to a rhodium, then the resulting silylrhodium undergoes 1,2-addition to an alkyne. Subsequently, C–H bond activation proceeds with the assistance of TEMPO, followed by insertion of carbon monoxide into the Rh–C bond. Finally, Compound **22** is afforded by reductive elimination.

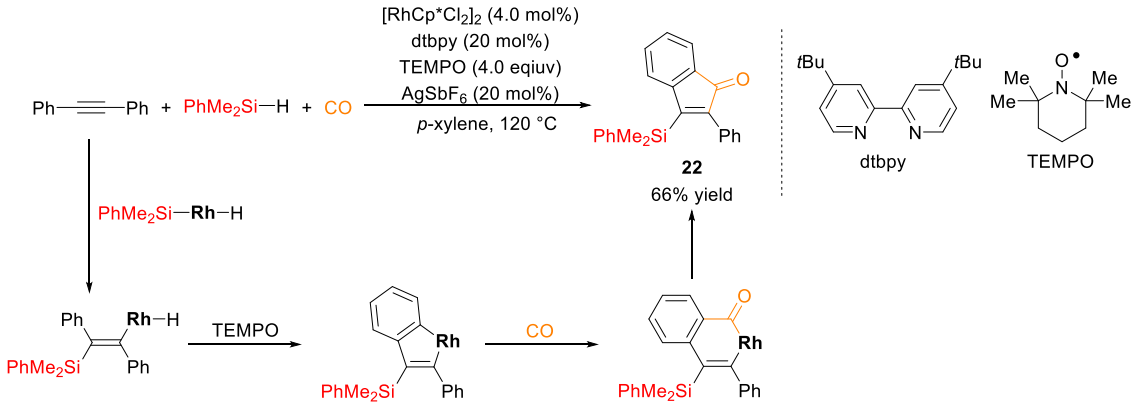

Scheme 8. Rhodium-catalyzed synthesis of silylindenones by *anti*-carbosilylation of internal alkynes.

Most of the reactions mentioned above used hydrosilanes as silicon sources, but reactions using other silicon sources have also been developed. For example, Riant *et al*. developed a stereo-tunable silylallylation of alkynoates using a silylboronic ester under a copper/palladium dual catalytic system (Scheme 9a).[24] The reaction of an alkynoate with a silylboronate and an allyl carbonate in the presence of copper(I) salt, $Pd(OAc)_2$, and PPh_3 yielded silylalkene **(*Z*)-23** with 91% *anti*-selectivity. On the other hand, the reaction without PPh_3 gave **(*E*)-23** with 96% *syn*-selectivity. They proposed that the difference of stereoselectivity was attributable to the difference in reactivity of π-allylpalladium intermediates. In the absence of PPh_3, less electrophilic dimeric π-allylpalladium **27** is generated, and this undergoes direct transmetalation with *syn*-silylalkenylcopper **24** to

give **(*E*)-23**. In contrast, the reaction with PPh_3 gives monomeric cationic π-allylpalladium **28**, which inhibits transmetalation by the phosphine ligand, and intermediate ***syn*-24** isomerizes to ***anti*-26** via allenolate **25**. Cationic palladium enhances electrophilicity of the allyl moiety, and forms **(*Z*)-23** by subsequent nucleophilic attack from **25** to **28** from the less hindered side. Recently, by using a similar catalytic system consisting of copper and palladium, Li *et al*. developed *anti*-selective allenylsilylation of a terminal alkyne with a silylboronic ester to give allenylalkene **29** (Scheme 9b).[25]

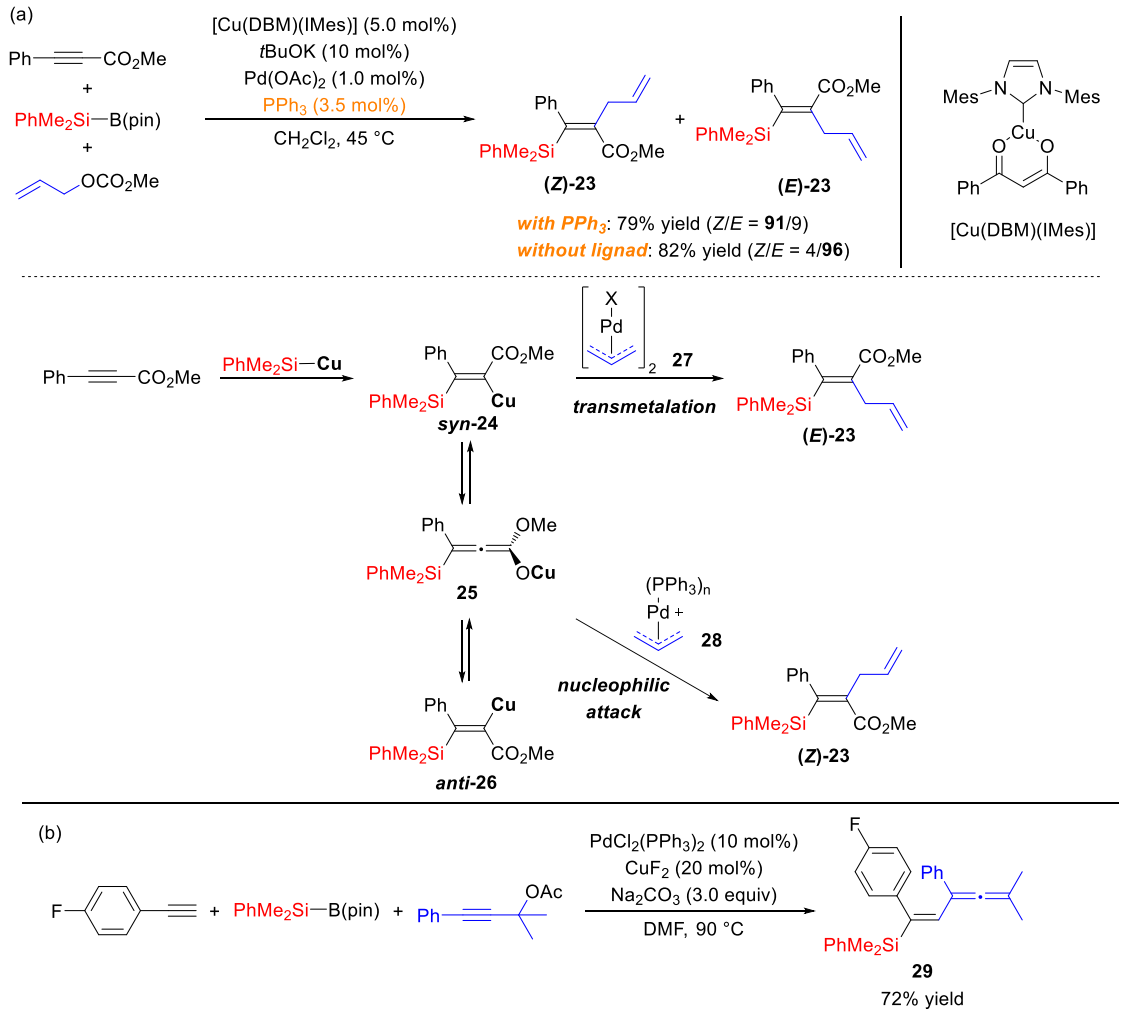

Scheme 9. (a) Copper/palladium-catalyzed stereo-tunable silylallylation of internal alkynes. (b) Copper/palladium-catalyzed *anti*-selective allenylsilylation of terminal alkynes.

In 2017, Nakamura *et al*. reported an iron-catalyzed *anti*-selective carbosilylation of internal alkynes with alkyl halides and silylboronates (Scheme 10).[26] The stereoselectivity of this reaction can be switched depending on the substituents on the silylboronic ester. Whereas the carbosilylation proceeded with high *anti*-selectivity to afford silylalkene **30a** by using (dimethylphenyl)silylboronic ester, the use of (dimethoxyphenyl)silylboronic ester led to the formation of **30b** with high *syn*-selectivity. This reaction was applicable to various alkyl halides and unactivated alkynes such as diphenylacetylene, and in the case of the reaction using alkyl(aryl)alkynes, the corresponding silylalkenes were obtained with high regio- and stereoselectivity. This is a rare example that achieved high regio- and *anti*-selectivity in silylfunctionalization of unactivated unsymmetric internal alkynes.

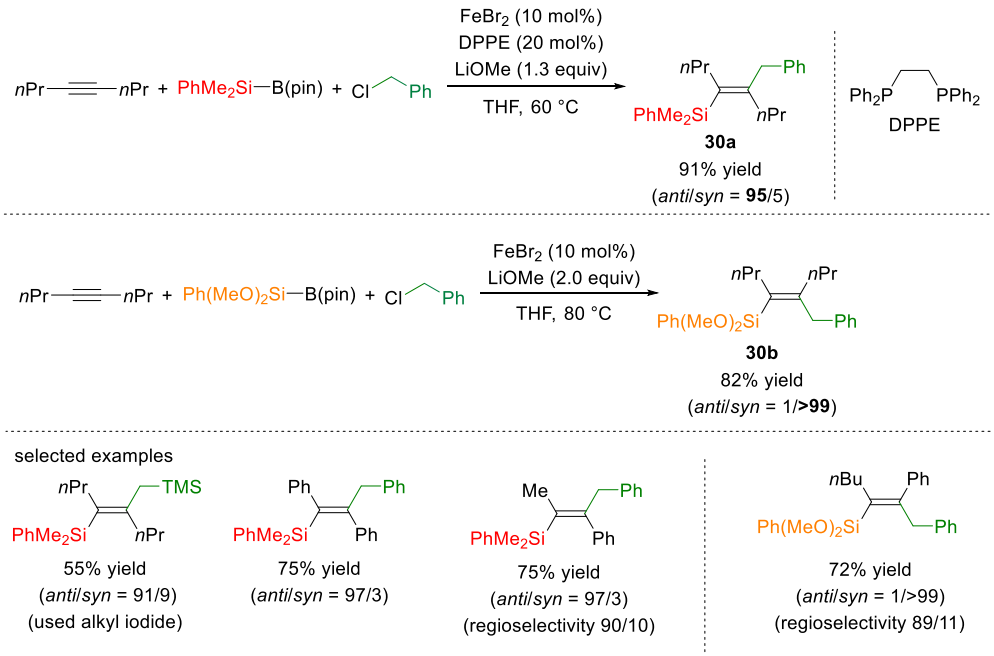

Scheme 10. Iron-catalyzed carbosilylation of internal alkynes.

Watson *et al*. achieved a palladium-catalyzed carbosilylation of symmetric internal alkynes with alkylzincs and silyl iodides (Scheme 11).[27] In this reaction, the

stereochemical outcome could be controlled by the ligands. When JessePhos was used, an *anti*-adduct was obtained, and when PPh_3 or DrewPhos was used, a *syn*-adduct was given.

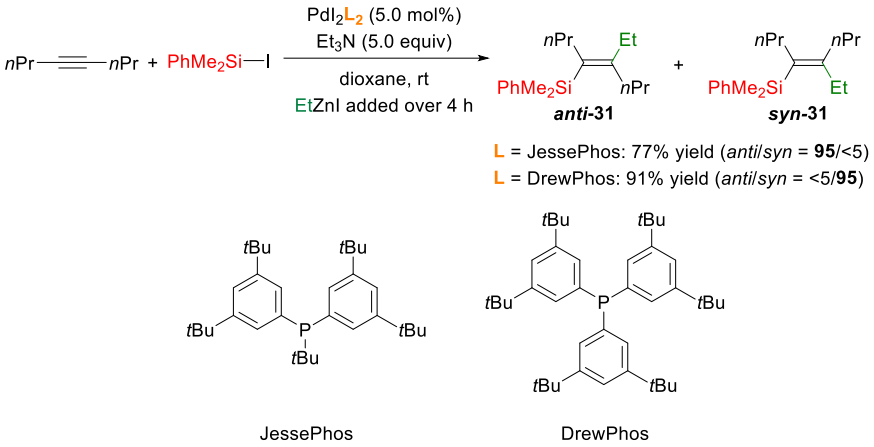

Scheme 11. Palladium-catalyzed carbosilylation of internal alkynes with silyl iodides and alkylzinc reagents.

Silylzinc reagents have been known as efficient silylating agents for alkynes.[7c,15a,b] Recently, Rasappan *et al*. developed stable silylzinc reagent **32** and achieved a nickel-catalyzed *anti*-selective carbosilylation of terminal alkynes with it (Scheme 12).[28] They investigated the reaction mechanism by DFT calculation and suggested that the *syn*-*anti* isomerization between alkenylnickel species **34** and **36** proceeded via nickelacyclopropene-type transition state **35** similar to the one proposed by Crabtree *et al*.[14e]

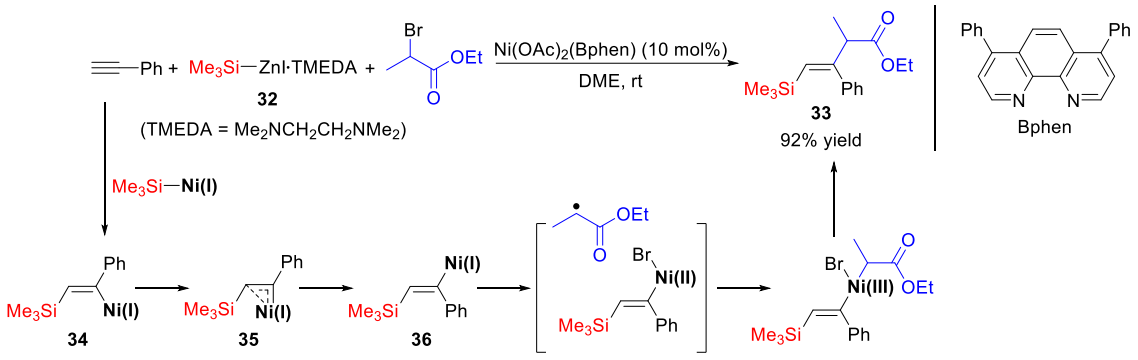

Scheme 12. Nickel-catalyzed *anti*-selective carbosilylation of terminal alkynes with silylzinc reagents.

Zhang *et al*. reported the use of disilanes as silylating reagents for the synthesis of isoquinolinones having a silicon substituent by *anti*-carbosilylation of alkynes (Scheme 13).[29]

Scheme 13. Palladium-catalyzed *anti*-carbosilylation using disilanes.

Clark *et al*. achieved the synthesis of silyldienes by a ruthenium-catalyzed *anti*-selective silylvinylation of internal alkynes through activation of intramolecular silicon substituents.[30] The reaction of alkyne **38** having a vinylsilyl ether with an acrylate was conducted in the presence of $RuHCl(CO)(PCy_3)_2$, giving compound **39** (Scheme 14). As an initial step of this proposed reaction mechanism, a ruthenium hydride adds to the vinyl group of compound **38** followed by β-silicon elimination to give silylruthenium **40**. Subsequently, compound **39** is generated from intermediate **40** by insertion of an alkyne into the Si–Ru bond, *syn*-*anti* isomerization, and the Heck-type addition to an acrylate.

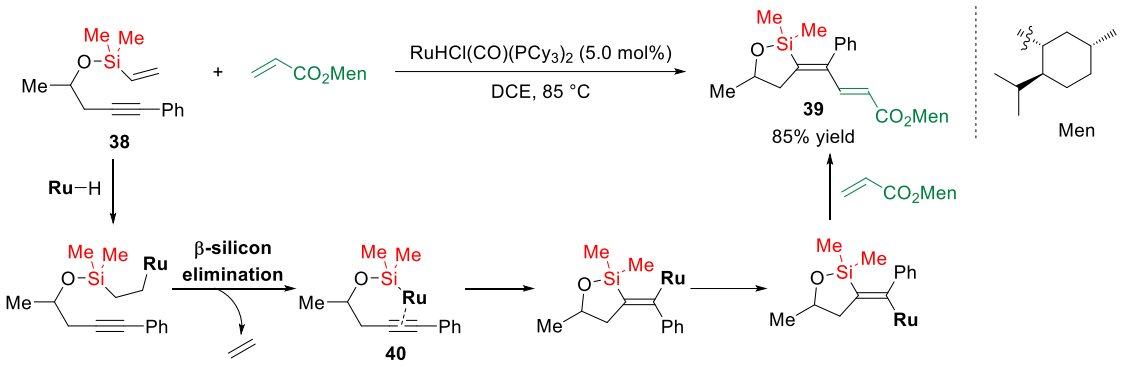

Scheme 14. Ruthenium-catalyzed *anti*-selective silylvinylation of internal alkynes.

1.1.3 Transition-metal-catalyzed *anti*-selective silylboration of alkynes

Silylboration of alkynes is a powerful method for the synthesis of useful synthetic intermediates because it allows the introduction of boron substituents that can be converted to a variety of other functional groups. Various *syn*-selective silylboration reactions of alkynes have been developed mainly by using palladium catalysts,[9a–c] whereas *anti*-selective reactions are very limited.[31] In 2008, as the first example of *anti*-selective silylboration of alkynes, Suginome *et al*. reported that the stereoselectivity could be switched from *syn* to *anti* by using an excess amount of silylboronic ester **42** over alkyne **41** in the palladium-catalyzed reaction between them (Scheme 15).[32]

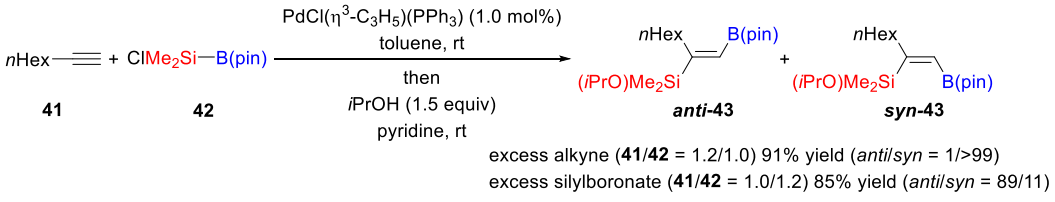

Scheme 15. Palladium-catalyzed *syn*- and *anti*-silylboration of terminal alkynes.

1.1.4 Transition-metal-catalyzed *anti*-selective disilylation of alkynes

Disilanes have been used as a powerful silicon donor for the silylation of

alkynes.[2d,e] The first report of *anti*-disilylation of alkynes was by Matsuda *et al*. on the rhodium-catalyzed reaction of alkynes **44** bearing a pendant disilane moiety (Scheme 16).[33a] They proposed the mechanism as follows. Initially, the Si–Si bond of compound **44** undergoes oxidative addition to a rhodium(I) complex to give intermediate **46**, and then intramolecular insertion of the alkyne to the Rh–Si bond takes place *syn*-selectively. Subsequently, η^2-vinylrhodium (1-rhodacyclopropene) species **48** is formed from alkenylrhodium **47**, and (dimethyl)silylene migrates to the electrophilic carbene carbon to afford **50** through **49**. Finally, carbon–silicon bond-forming reductive elimination of **50** gives silylbenzosilole **45**. In 2022, Kobayashi and Naka *et al*. developed a similar *anti*-disilylation of alkynes following the Sonogashira coupling under palladium catalysis.[33b]

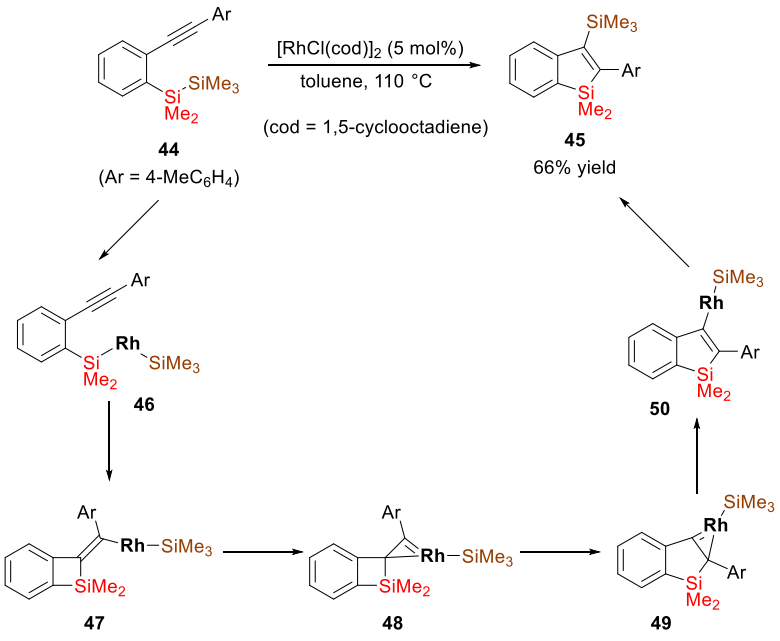

Scheme 16. Rhodium-catalyzed synthesis of silylbenzosiloles via *anti*-disilylation of alkynes.

Intermolecular *anti*-disilylation of alkynes was first achieved by He and Zhang *et al*. (Scheme 17).[34] This rhodium-catalyzed reaction was applicable to alkynones and

alkynoates, whereas the use of diphenylacetylene as a starting material gave *syn*-disilylated alkene **55**. For the reaction mechanism, they proposed that *syn-anti* isomerization between alkenylrhodium **52** and **54** proceeded via allenic intermediate **53**.

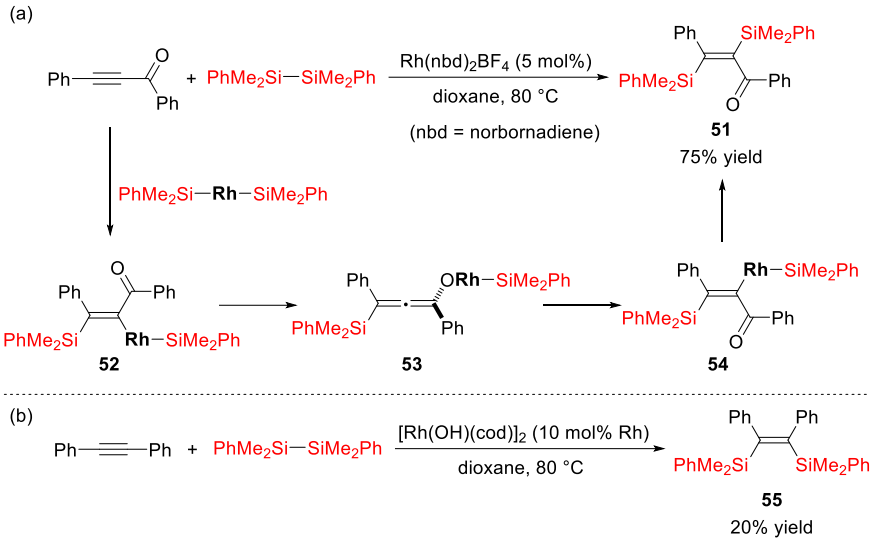

Scheme 17. Rhodium-catalyzed intermolecular (a) *anti*-disilylation of alkynones and (b) *syn*-disilylation of diphenylacetylene.

1.2 Reactions of silylboronates with copper catalysts

The first silylborane compound having a Si–B bond was reported around 1960,[35] and after the pioneering research by Nöth *et al*.,[36a,b] synthetically useful silylboranes were developed by Y. Ito, Suginome *et al*., Hartwig *et al*., and H. Ito *et al*.[36] Among silylborane compounds, several silylboronates (silylboronic esters) are now commercially available and are used in many reactions. In contrast to classical silicon sources such as chlorosilanes and hydrosilanes whose silicon acts as an electrophile, a silicon of silylboranes acts as a nucleophile. Due to their unique reactivities, many reactions have been developed so far by using silylboranes, as partially described in the previous section (1.1).[37]

Various methods have been established to activate silylboranes (silylboronates) as shown in Scheme 18. For example, Ito *et al.* and Tanaka *et al*. reported that silylboranes were activated by oxidative addition of the Si–B bond to low-valent transition metals (Scheme 18a).[38] Suginome *et al*. discovered that silylenes could be generated from silylboranes bearing amino group on the silicon atom by heating or the reaction with a transition metal (Scheme 18b).[39] It is known that transmetalation with transition metals or alkaline (earth) metals or reactions with nucleophiles generate silicon nucleophiles from silylboronates (Scheme 18c).[40] In addition, several reports recently described that the Si–B bond was cleaved by light irradiation in the presence of a photocatalyst or addition of a nucleophile to generate a silyl radical (Scheme 18d).[41]

A reaction of silylboronates with copper salts proceeded through a path as shown in Scheme 18c (i) to give a nucleophilic silylcopper, which is known to react with unsaturated compounds such as carbonyl compounds and alkynes. In this section, representative copper-catalyzed reactions using silylboronates are summarized, and in particular the reactions of alkynes with silylcopper species are described.

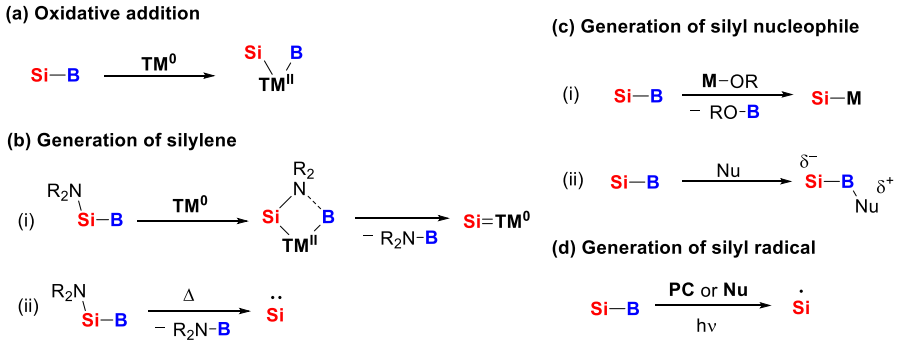

Scheme 18. Reactivity of silylboranes: (a) oxidative addition to transition metals, (b) generation of silylenes, (c) generation of silyl nucleophiles, and (d) generation of silyl radicals.

1.2.1 Copper-catalyzed reactions of alkynes with silylboronates

For the copper-catalyzed addition of silylboronates to alkynes, *syn*-selective reactions have been studied more than *anti*-selective reactions as described in Section 1.1.[24,25] As a pioneering study on copper-catalyzed reactions of alkynes with silylboronates, in 1986, Oshima *et al*. reported a silylprotonation (hydrosilylation) reaction using $PhMe_2Si–BEt_3Li$ and a catalytic amount of CuCN (Scheme 19a).[42a] Although this rection proceeded in a highly *syn*-selective manner, the regioselectivity was greatly influenced by the substituents of the alkyne substrates. On the other hand, Loh *et al*. developed a reaction that can control the regioselectivity of silylprotonation by modifying the Oshima's catalytic system (Scheme 19b).[42b] When CuCl, NaO*t*Bu, and JohnPhos, an electron-rich and bulky monophosphine ligand, were used, the reaction of a terminal alkylalkyne with a silylboronate gave branched silylalkene compound **57** with high selectivity. Since this report, several copper-catalyzed silylprotonation reactions of alkynes have been developed.[42]

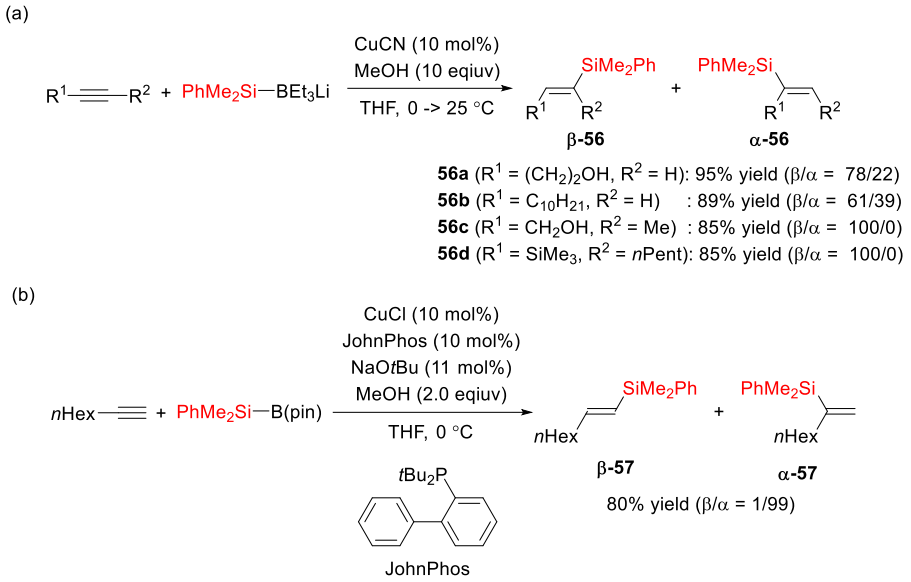

Scheme 19. (a) A pioneering work of copper-catalyzed silylprotonation of alkynes. (b) Branch-selective silylprotonation of alkynes by CuCl/JohnPhos catalyst.

Although the silylprotonation reaction described in Scheme 19 required the addition of MeOH as a proton donor, it is also known that silylboronates can function as both nucleophiles and electrophiles, leading to silylboration reactions. Fu and Xu *et al*. reported that *syn*-selective silylboration of alkynes proceeded in the simple reaction system using a copper catalyst, an alkyne and a silylboronate, and its regioselectivity could be controlled by changing the ligand on copper (Scheme 20).[43] When CuTc and PCy_3 were used as a copper precursor and a ligand, silylborated alkene **58** having silicon at the terminal position was obtained, while the reaction using $PPh(tBu)_2$ as the ligand selectively gave compound **59** having a boron moiety at the terminal position.

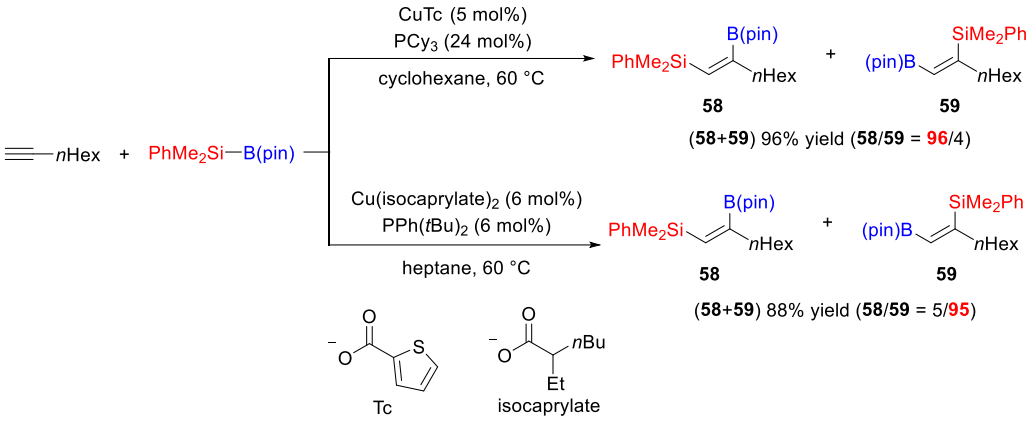

Scheme 20. Regio-controllable copper-catalyzed silylboration of alkynes.

Copper-catalyzed reactions using other electrophiles in addition to silylboronates and alkynes have also been developed to synthesize tri- or tetrasubstituted silylalkenes. Tsuji *et al*. found that cyclative silylcarboxylation proceeded when silylboronates were reacted with alkynes under CO_2 atmosphere (Scheme 21).[44] The reaction mechanism of this process was explained as follows. Initially, the *in-situ* generated silylcopper nucleophile adds to an alkyne, and then resulting alkenylcopper **61** attacks carbon dioxide to give copper carboxylate **62**. Subsequently, this undergoes cyclization via cleavage of the Si–Ph bond to afford phenylcopper **63** and silalactone **60**. Transmetalation of phenylcopper **63** with a silylboronate regenerates the silylcopper. In this reaction, the presence of a phenyl group on the silylboronate was essential, and, in the case of the reaction using a trialkylsilylboronate, *syn*-silylcarboxylated alkene **64** was obtained without cyclization.

Yoshida *et al.* achieved a copper-catalyzed silylstannylation of alkynes through a three-component reaction using tin alkoxides as the electrophile (Scheme 22).[45]

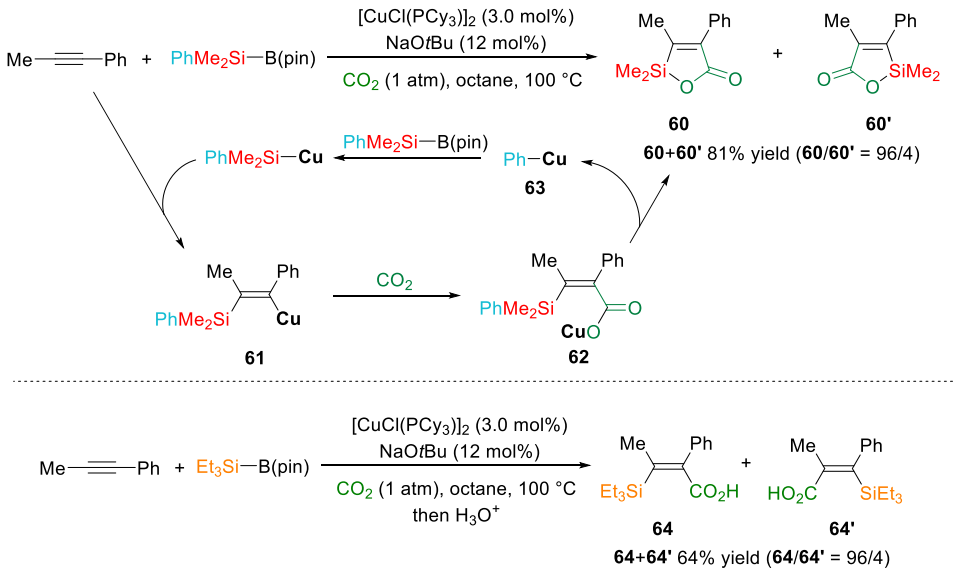

Scheme 21. Copper-catalyzed silylcarboxylation of alkynes with CO_2 as an electrophile.

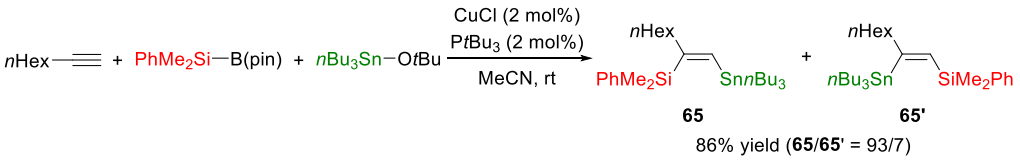

Scheme 22. Copper-catalyzed silylstannylation of terminal alkynes with tin alkoxides.

By combining a palladium catalyst and a silylcopper nucleophile, it is possible to incorporate other electrophiles as well.[24,25,46] For example, Shintani and Nozaki *et al*. achieved silylarylation of internal alkynes using a palladium catalyst and aryl halides in addition to a copper catalyst and silylboronates (Scheme 23a).[46a] In addition, Nishihara *et al*. recently reported silylarylation of alkynes via decarbonylation using acyl fluorides as an electrophile (Scheme 23b).[46b]

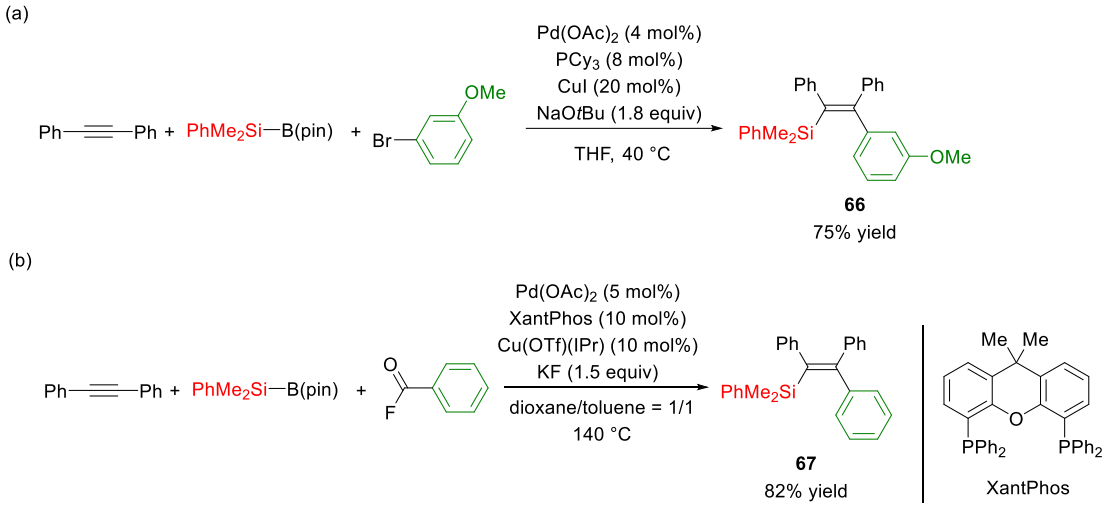

Scheme 23. Palladium- and copper-catalyzed silylarylation of internal alkynes with silylboronates.

Moreover, by changing the substituents on alkynes, it is possible to carry out other silylation reactions of alkynes in addition to simple 1,2-addition. In 2015, Loh *et al.* achieved a synthesis of silylallenes by the enantioselective silylation of enynoates (Scheme 24a).[47a] In this reaction, the alkene geometry of the substrate was important. While the use of (*Z*)-enynoates gave high yields with high enantioselectivity, the use of (*E*)-enynoates led to significantly reduced yields and enantioselectivity.

They also developed a similar reaction using a copper catalyst and a silylboronate for enantioselective disilylation of enynoate **70** (Scheme 24b).[47b] In the first step of this reaction, the copper works as a catalyst for the silylprotonation of the alkyne, and then further silylcupration of the resulting diene **72** takes place in a 1,6-fashion to give β,γ-unsaturated carbonyl compound **71**.

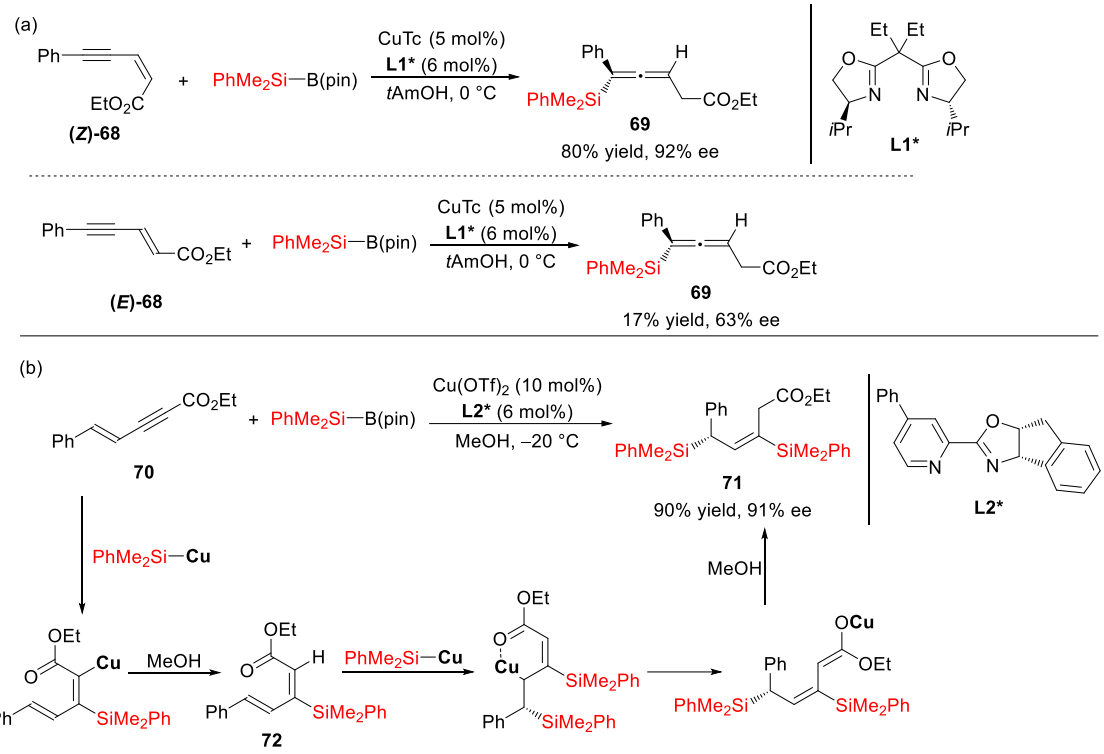

Scheme 24. (a) Copper-catalyzed synthesis of silylallenes from enynoates. (b) Copper-catalyzed disilylation of enynes.

Xu *et al*. reported that several different types of silylated compounds can be synthesized for the copper-catalyzed reaction of alkynes having an epoxide with silylboronates depending on the conditions (Scheme 25).[48] When the reaction was conducted in the presence of diisopropylethylamine (DIPEA) in MeOH, silylallene **73** was obtained in a high yield. On the other hand, the use of K_2CO_3 as a base and DMF as a solvent gave silyldiene **74**, and in the case of using 1-pentanol as a solvent at 60 °C, allyl alcohol **75** was given.

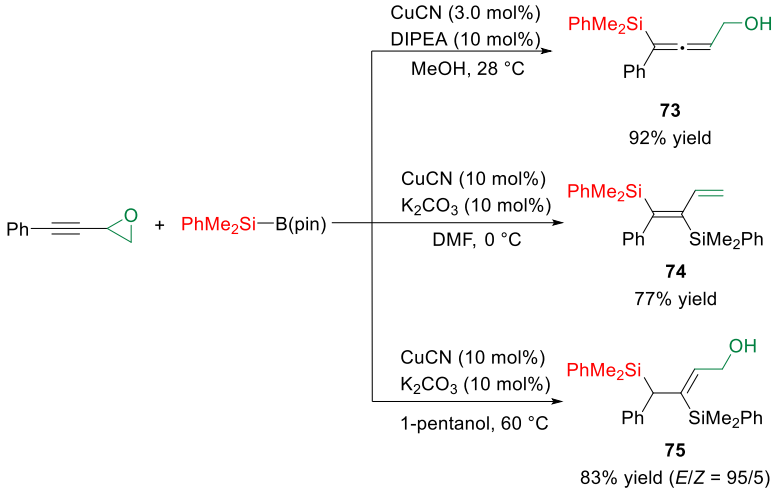

Scheme 25. Copper-catalyzed silylation of propargyl epoxides.

1.2.2 Copper-catalyzed reactions of C–C double bonds with silylboronates

Silylcopper nucleophiles are known to add not only to alkynes but also to other unsaturated C–C bonds. For example, Fujihara *et al*. found that β,γ-unsaturated carbonyl compound **76** could be synthesized by reacting a 1,3-diene with silylcopper in the presence of benzonitrile as an electrophile (Scheme 26).[49] In addition, the reaction of silylcopper with allenes has also been well studied.[45,50] Tsuji *et al*. and Procter *et al*. independently achieved carbosilylation of allenes using carbonyl compounds and silylboronates in the presence of a copper catalyst (Scheme 27). Under Tsuji's conditions using a phosphine ligand, homoallylic alcohol **77** was obtained from an alkylallene through the selective addition to the terminal double bond,[50a] whereas in the case of Procter's reaction using an NHC ligand, compound **78** was given via selective reaction at the internal double bond of an arylallene.[50b]

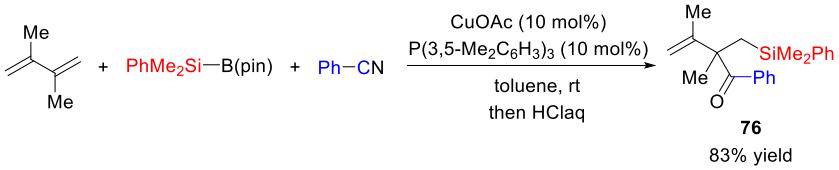

Scheme 26. Copper-catalyzed carbosilylation of 1,3-dienes with silylboronates and benzonitriles.

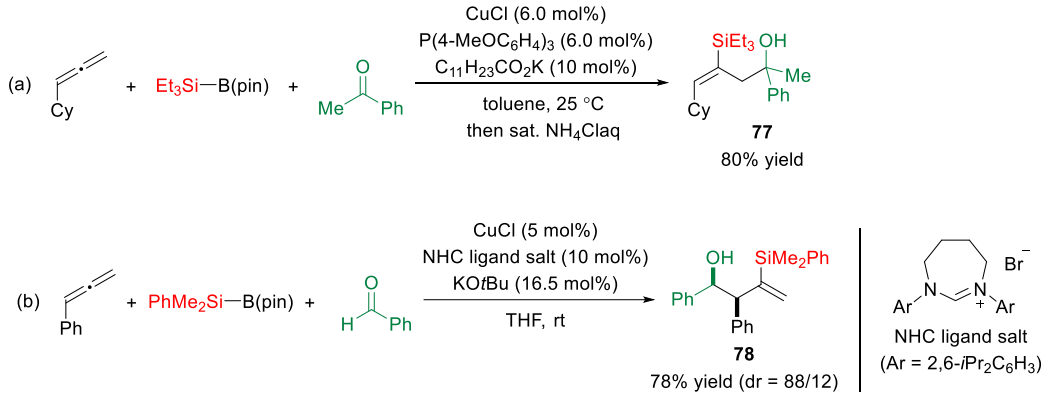

Scheme 27. Copper-catalyzed carbosilylation of allenes (a) reported by Tsuji *et al*. and (b) reported by Procter *et al*.

The most well-studied reaction of silylcopper nucleophiles with carbon–carbon double bonds is 1,4-addition to α,β-unsaturated carbonyls. Hoveyda *et al*. reported that when a chiral NHC was used as a ligand for copper, enantioselective 1,4-addition proceeded to give β-silyl ketone **79**. (Scheme 28)[51a] Since then, many catalytic 1,4-addition reactions to α,β-unsaturated carbonyl compounds using silylcopper nucleophiles have been developed.[51] In addition, Jia *et al*. reported that when a silylboronate was reacted with an α,β-unsaturated amide having an iodophenyl group in the presence of a copper catalyst, cyclative silylarylation proceeded to afford oxindole **80** (Scheme 29).[52]

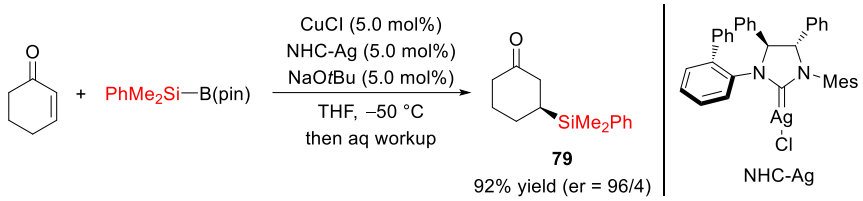

Scheme 28. Copper-catalyzed enantioselective 1,4-conjugate addition to α,β-unsaturated ketones with silylboronates.

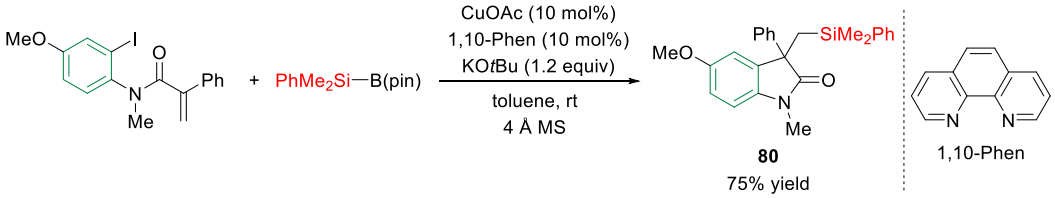

Scheme 29. Copper-catalyzed cyclative silylarylation of acrylamides.

Silylcopper has also been used for alkene substitution and allylic substitution reactions.[53,54] For example, Mankad *et al*. developed a dehydrosilylation of styrene with silylboronates by adding a ketone as an oxidant (Scheme 30).[53a] This reaction proceeds through addition of silylcopper to an alkene followed by β-hydrogen elimination, giving silylalkene **81** and copper hydride. The resulting copper hydride adds to a ketone, and subsequent transmetalation with a silylboronate regenerates the silylcopper.

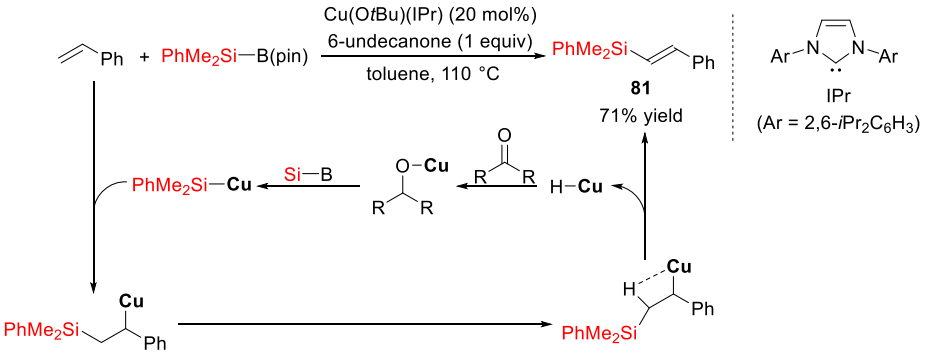

Scheme 30. Copper-catalyzed dehydrosilylation of alkenes.

In 2010, Oestreich *et al*. developed an allylic substitution reaction of compounds **82** having a leaving group at the allylic position with silylboronates (Scheme 31a).[54a] The selectivity of S_N2' and S_N2 (nucleophilic attack to γ-position or α-position) depended on the leaving group. In the case with chloride or phosphate, allylsilane **γ-83** was selectively yielded, and the reaction using allyl acetate afforded **α-83**. In addition, in 2013, they and Hayashi *et al*. achieved the asymmetric reaction by using chiral NHCs as the ligand (Scheme 31b,c).[54b,c]

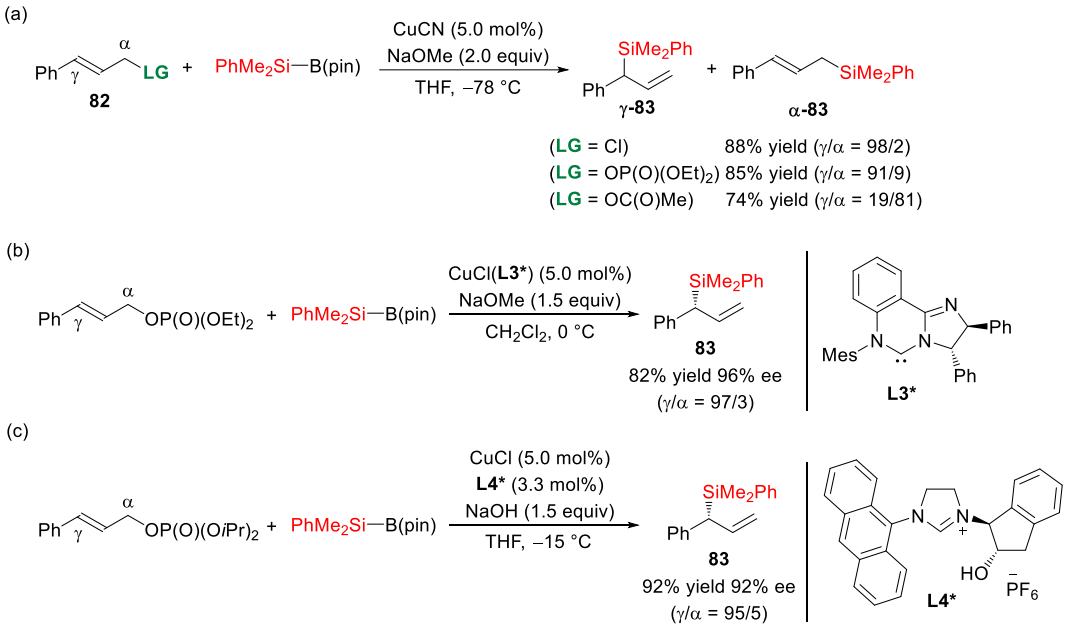

Scheme 31. (a) Copper-catalyzed γ-selective allylic substitution with silylboronates. (b) and (c) Copper-catalyzed enantioselective silylation via allylic substitution.

1.2.3 Copper-catalyzed 1,2-addition to carbon–heteroatom double bonds with silylboronates

The reaction system combining a copper catalyst and silylboronates is useful for the silylation of carbonyl and imine compounds. For example, in 2011, Kleeberg *et al*. reported silylation of aldehydes, and the rate-determining step was found to be the

addition of a silylcopper to an aldehyde by stoichiometric reactions and NMR analysis (Scheme 32).[55] In the same year, Oestreich *et al*. discovered that the copper-catalyzed reaction system with siylboronates could also be used in the reactions of imines as electrophiles.[56]

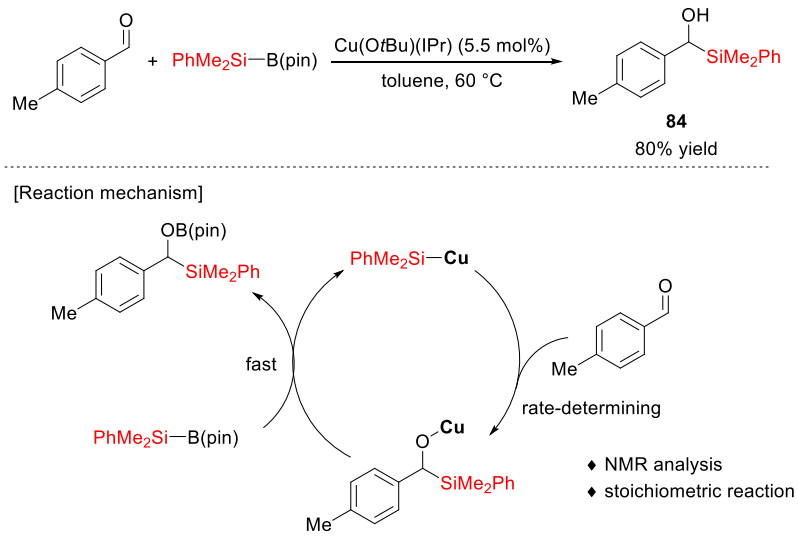

Scheme 32. Copper-catalyzed nucleophilic addition of silylboronates to aldehydes.

Kleeberg *et al*. investigated reduction of carbon dioxide with a copper catalyst and silylboronates and unveiled the mechanism by *in-situ* ^{13}C NMR spectroscopy, single crystal X-ray diffraction studies, and IR spectroscopy.[57] The proposed reaction mechanism is shown in Scheme 33. Initially, silylcopper **85**, which is generated from a copper alkoxide and a silylboronate, adds to carbon dioxide to give copper complex **86**. Some of this intermediate **86** is transformed to silylcopper **85** and compound **87** via transmetalation with a silylboronate. **86** can also be decomposed to copper complex **88** with the elimination of carbon monoxide. While compound **87** turns into compounds **89**, **90**, and **91** with the extrusion of carbon monoxide at ambient temperature, intermediate **88** gives compound **89** by transmetalation with a silylboronate to regenerate silylcopper

85. They confirmed the structures of complexes **85**, **86**, **88** and compound **87** by single-crystal X-ray diffraction analysis, and conducted the stoichiometric reactions to observe the decomposition pathways of complex **86** and compound **87** by ^{13}C NMR.

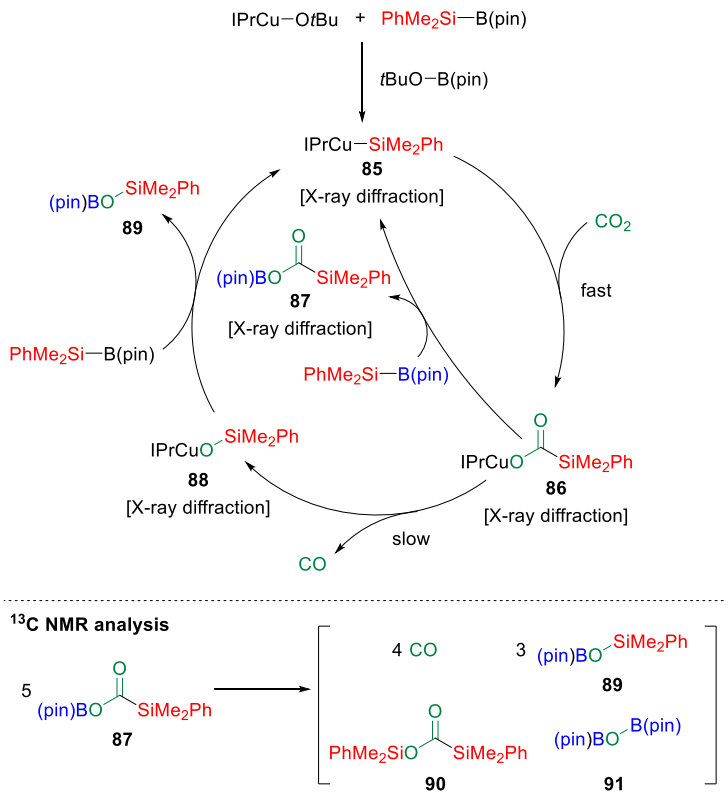

Scheme 33. The proposed mechanism on the reduction of carbon dioxide by a copper catalyst and silylboronates.

1.2.4 Copper-catalyzed coupling reactions to form a C–Si bond with silylboronates

Several studies have shown that the cross-coupling reactions of silylcopper with alkyl and aryl electrophiles can proceed to form C–Si bonds efficiently. In 2013, Shintani and Hayashi *et al*. found that the silylation of benzyl phosphate could be achieved in a moderate yield in the presence of a copper catalyst.[54c]

In 2014, Martin *et al*. developed a silylation reaction of aryl pivalates and alkyl pivalates through the C–O bond cleavage using a nickel/copper-cocatalyst system

(Scheme 34).[58] In this reaction, the silylcopper nucleophile was proposed to undergo transmetalation with nickel complex **93**, which is generated by oxidative addition of the C–O bond of an aryl pivalate to nickel.

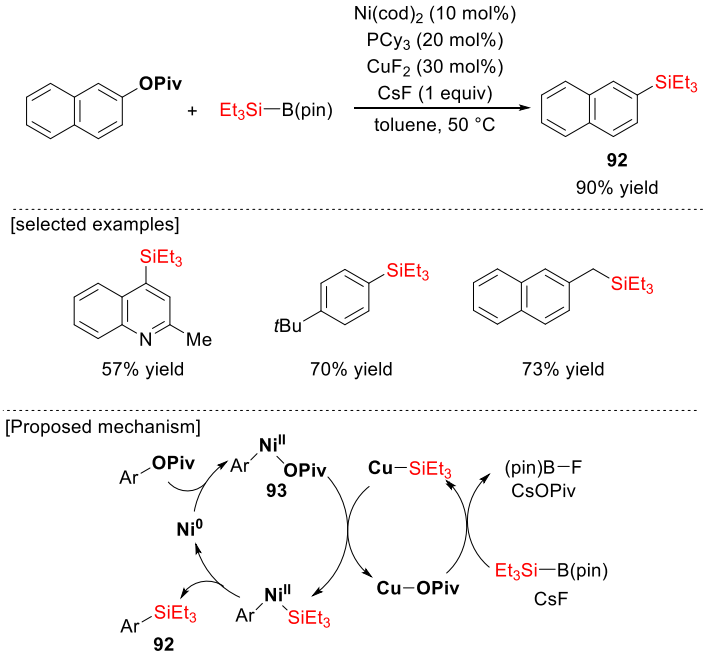

Scheme 34. Nickel/copper-catalyzed silylation of aryl pivalates via C–O cleavage.

In 2020, Oestereich *et al*. achieved deaminative C(sp^3)–Si cross-coupling with silylbonates by using benzylic ammonium triflates as electrophiles (Scheme 35).[59] This reaction was confirmed to proceed stereospecifically by using a highly enantioenriched benzylammonium salt. Thus, the reaction of **(*R*)-94** with a silylboronate in the presence of CuBr and NaO*t*Bu gave benzylsilane **(*S*)-95** with inversion of configuration, indicating that the reaction proceeds via an S_N2-type mechanism.

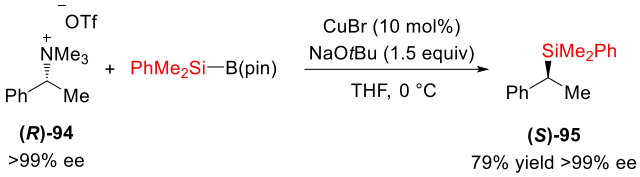

Scheme 35. Copper-catalyzed stereospecific substitution of benzylammonium triflates.

In addition, Oestereich *et al*. developed coupling reactions to form a C–Si bond via radical mechanism through a silylcopper intermediate.[60] For example, aliphatic esters derived from *N*-hydroxyphthalimide can be transformed into silylalkanes by the reaction with silylboronates in the presence of a copper catalyst via decarboxylative silylation (Scheme 36).[60a] To understand the reaction mechanism, the reaction of aliphatic ester **96b** having a cyclopropane was conducted, which resulted in the formation of ring-opened compound **98b** instead of directly silylated compound **97b**. In addition, the reaction of **96a** in the presence of TEMPO gave TEMPO-adduct **99a** along with the generation of **97a**. From these results, the following radical mechanism was proposed. As the first step, Si–Cu$^{\bullet+}$ and **96a**$^{\bullet-}$ are generated by single-electron transfer (SET) from a silylcopper to **96a**. Subsequently, alkyl radical is generated through the elimination of carbon dioxide, and then a C–Si bond is formed.

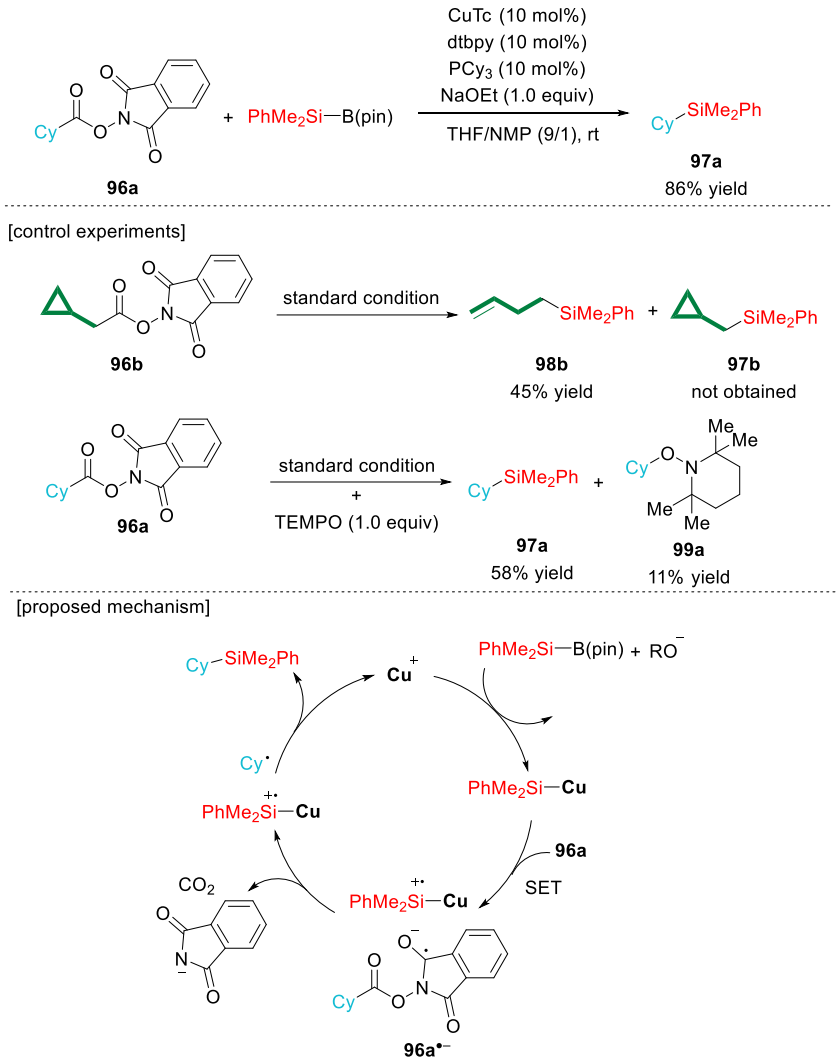

Scheme 36. Copper-catalyzed decarboxylative radical silylation of aliphatic carboxylic acid derivatives.

1.3 Overview of this dissertation

Silylalkenes are known as useful synthetic intermediates of various organic compounds. As described in Section 1.1, transition-metal-catalyzed 1,2-silylfunctionalization of alkynes is one of the most powerful methods to synthesize silylalkenes, but *anti*-selective additions are limited compared to *syn*-selective reactions. In particular, there are very few reactions of unsymmetric internal alkynes with high regio- and *anti*-selectivity, leading to compounds that require multiple synthesis steps by conventional methods. To solve this problem, the author focused on the use of a copper catalyst in combination with silylboronates. As described in Section 1.2, silylcopper nucleophiles can provide various silylalkene compounds from alkynes by the addition of suitable electrophiles or changing the substituents on the alkynes. In this context, as novel copper-catalyzed reactions with silylboronates, the author found that regio- and *anti*-selective 1,2-silylfunctionalization reactions of internal alkynes can be promoted by using a copper catalyst in the presence of an alkoxide base. The author explored these regio- and *anti*-selective reactions including their reaction mechanisms, to expand the scope of accessible silylalkene compounds.

Chapter 2 describes the development of a copper-catalyzed regio- and *anti*-selective silylboration of internal alkynes to synthesize silylborated alkenes. This reaction proceeds with very high regio- and *anti*-selectivity and can afford synthetically useful silicon- and boron-substituted alkenes as these moieties can be transformed into various other functional groups (Scheme 37a). In addition, the detailed reaction mechanism of the silylboration was elucidated based on the experimental and theoretical studies. The author found that the *syn-anti* isomerization of alkenyl metals does not proceed through a commonly proposed metallacyclopropene (η^2-vinylmetal) structure. Instead, involvement of an allenyl anion transition state was found to be more plausible. Furthermore, the *anti*-

selectivity was likely controlled by the steric hindrance of the silicon substituent (Scheme 37b).

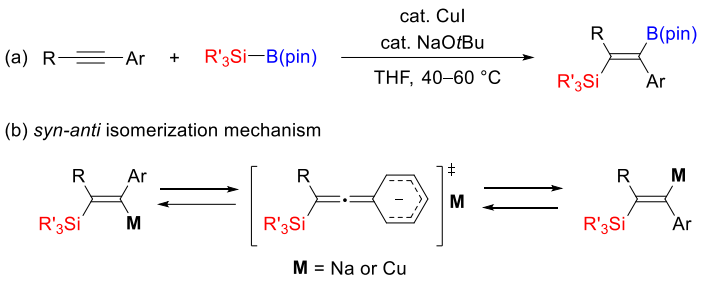

Scheme 37. (a) Copper-catalyzed regio- and *anti*-selective silylboration of internal alkynes. (b) The mechanism on *syn-anti* isomerization.

Chapter 3 describes *anti*-selective cyclative silylarylation of benzylalkynes to synthesize silylindenes by using a similar reaction system with a copper catalyst and silylboronates. It is an unusual process in that the aromatic C–H bond is activated as an electrophile by eliminating the hydrogen atom as a hydride (Scheme 38).

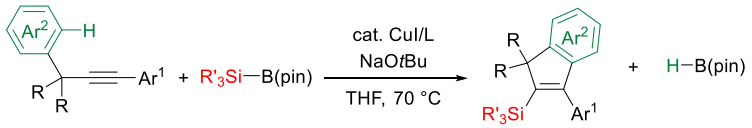

Scheme 38. Copper-catalyzed cyclative silylarylation of benzylalkynes with silylboronates.

Finally, Chapter 4 describes the development of a regio- and *syn*-selective formal hydro(borylmethylsilyl)ation reaction of internal alkynes. Although this reaction does not proceed *anti*-selectivity, it shows a novel reactivity of the reaction system using a copper catalyst and silylboronates. This reaction proceeds via alkenyl-to-alkyl 1,4-copper migration, which has not been previously reported (Scheme 39).

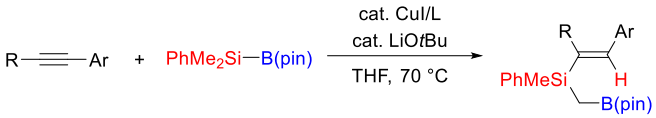

Scheme 39. Copper-catalyzed formal hydro(borylmethylsilyl)ation reaction of internal alkynes via 1,4-copper migration.

Through the development of these reactions, accessible silylalkenes have been significantly expanded, which also enabled the synthesis of various useful organic compounds by using these silylalkenes as synthetic intermediates. In addition, understanding the detailed mechanism of each reaction is beneficial for further development of new reactions using similar strategies. In fact, our group also found a copper-catalyzed synthesis of 3-silyl-1-silacyclopentenes via regio- and *anti*-selective addition of silylboronates to silicon-containing internal alkynes (Scheme 40).[61]

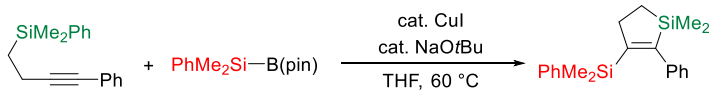

Scheme 40. Copper-catalyzed *anti*-disilylation of internal alkynes having a silyl group with silylboronates.

1.4 References

[1] Reviews on transformation of silylalkenes: (a) Langkopf, E.; Schinzer, D. *Chem. Rev*. **1995**, *95*, 1375–1408. (b) Fleming, I.; Barbero, A.; Walter, D. *Chem. Rev*. **1997**, *97*, 2063–2192. (c) Curtis-Long, M. J.; Aye, Y. *Chem. Eur. J.* **2009**, *15*, 5402–5416. (d) Denmark, S. E.; Liu, J. H.-C. *Angew*. *Chem*., *Int*. *Ed*. **2010**, *49*, 2978–2986. (e) Nakao, Y.; Hiyama, T. *Chem. Soc. Rev.* **2011**, *40*, 4893–4901.

[2] Reviews on the synthesis of silylalkenes: (a) Lim, D. S. W.; Anderson, E. A. *Synthesis* **2012**, *44*, 983–1010. (b) Ansell, M. B.; Navarro, O.; Spencer, J. *Coord. Chem. Rev.* **2017**, *336*, 54–77. (c) Pal, P. P.; Ghosh, S.; Hajra, A. *Org. Biomol. Chem*. **2023**, *21*, 2272–2294. (d) Beletskaya, I.; Moberg, C. *Chem. Rev*. **2006**, *106*, 2320–2354. (e) Suginome, M.; Ito, Y. *Chem. Rev*. **2000**, *100*, 3221–3256.

[3] (a) Benkeser, R. A.; Hickner, R. A. *J. Am. Chem. Soc.* **1958**, *80*, 5298–5300. (b) Benkeser, R. A.; Burrous, M. L.; Nelson, L. E.; Swisher, J. V. *J. Am. Chem. Soc*. **1961**, *83*, 4385–4389.

[4] Selected examples on manganese-catalyzed silylation of alkynes: (a) Hibino, J.; Nakatsukasa, S.; Fugami, K.; Matsubara, S.; Oshima, K.; Nozaki, H. *J. Am. Chem. Soc.* **1985**, *107*, 6416–6417. (b) Tang, J.; Shinokubo, H.; Oshima, K. *Bull. Chem. Soc. Jpn*. **1997**, *70*, 245–251.

[5] Selected examples on iron-catalyzed silylation of alkynes: (a) Belger, C.; Plietker, B. *Chem. Commun.* **2012**, *48*, 5419–5421. (b) Sen, A.; Tewari, T.; Kumar, R.; Vinod, C. P.; Sharma, H.; Vanka, K.; Chikkali, S. H. *Catal. Sci. Technol.* **2024**, *14*, 2752–2760. (c) Simonian, N. G.; Féo, M.; Tanguy, C.; Troufflard, C.; Lefèvre, G. *ACS Catal.* **2024**, *14*, 12163–12172. (d) Hu, M.-Y.; He, P.; Qiao, T.-Z.; Sun, W.; Li, W.-T.; Lian, J.; Li, J.-H.; Zhu, S.-F. *J. Am. Chem. Soc*. **2020**, *142*, 16894–16902.

[6] Selected examples on nickel-catalyzed silylation of alkynes: (a) Tamao, K.; Miyake,

N.; Kiso, Y.; Kumada, M. *J. Am. Chem. Soc.* **1975**, *97*, 5603–5605. (b) Zhang, Y.; Wang, X.-C.; Ju, C.-W.; Zhao, D. *Nat. Commun*. **2021**, *12*, 68. (c) Lee, C.; Jeon, J. H.; Lee, S.; Choe, W.; Kwak, J.; Seo, S.; Hong, S. Y.; Jung, B. *ACS Catal*. **2024**, *14*, 5077–5087. (d) Zhou, Y.-B.; Liu, Z.-K.; Fan, X.-Y.; Li, R.-H.; Zhang, G.-L.; Chen, L.; Pan, Y.-M.; Tang, H.-T.; Zheng, J.-H.; Zhan, Z.-P. *Org. Lett*. **2018**, *20*, 7748–7752.

[7] Selected examples on copper-catalyzed silylation of alkynes: (a) Wakamatsu, K.; Nonaka, T.; Okuda, Y.; Tückmantel, W.; Oshima, K.; Utimoto, K.; Nozaki, H. *Tetrahedron* **1986**, *42*, 4427–4436. (b) Liepins, V.; Karlström, A. S. E.; Bäckvall, J.-E. *J. Org. Chem*. **2002**, *67*, 2136–2143. (c) Auer, G.; Oestreich, M. *Chem. Commun.* **2006**, 311–313. (d) Wang, Z.-L.; Zhang, F.-L.; Xu, J.-L.; Shan, C.-C.; Zhao, M.; Xu, Y.-H. *Org. Lett.* **2020**, *22*, 7735–7742.

[8] Selected examples on rhodium-catalyzed silylation of alkynes: (a) Cornish, A. J.; Läppert, M. F. *J. Organomet. Chem*. **1984**, *271*, 153–168. (b) Matsuda, I.; Ogiso, A.; Sato, S.; Izumi, Y. *J. Am. Chem. Soc*. **1989**, *111*, 2332–2333. (c) Ojima, I.; Vidal, E.; Tzamarioudaki, M.; Matsuda, I. *J. Am. Chem. Soc*. **1995**, *117*, 6797–6798. (d) Biffis, A.; Conte, L.; Tubaro, C.; Basato, M.; Aronica, L. A.; Cuzzola, A.; Caporusso, A. M. *J. Organomet. Chem.* **2010**, *695*, 792–798. (e) Yang, L.; Yi, M.; Wu, X.; Lu, Y.; Zhang, Z. *Chem. Eur. J.* **2024**, *30*, e202402406.

[9] Selected examples on palladium-catalyzed silylation of alkynes: (a) Saito, N.; Saito, K.; Sato, H.; Sato, Y. *Adv. Synth. Catal*. **2013**, *355*, 853–856. (b) Ansell, M. B.; Spencer, J.; Navarro, O. *ACS Catal*. **2016**, *6*, 2192–2196. (c) Ohmura, T.; Oshima, K.; Taniguchi, H.; Suginome, M. *J. Am. Chem. Soc.* **2010**, *132*, 12194–12196. (d) Chatani, N.; Amishiro, N.; Murai, S. *J. Am. Chem. Soc.* **1991**, *113*, 7778–7780. (e) Chatani, N.; Amishiro, N.; Morii, T.; Yamashita, T.; Murai, S. *J. Org. Chem*. **1995**, *60*, 1834–1840. (f) Ito, Y.; Suginome, M.; Murakami, M. *J. Org. Chem*. **1991**, *56*,

1948–1951. (g) Ansell, M. B.; Roberts, D. E.; Cloke, F. G. N.; Navarro, O.; Spencer, J. *Angew. Chem.*, *Int. Ed.* **2015**, *54*, 5578–5582. (h) Casson, S.; Kocienski, P.; Reid, G.; Smith, N.; Street, J. M.; Webster, M. *Synthesis* **1994**, *12*, 1301–1309.

[10] Selected examples on iridium-catalyzed silylation of alkynes (a) Song, L.-J.; Ding, S.; Wang, Y.; Zhang, X.; Wu, Y.-D.; Sun, J. *J. Org. Chem*. **2016**, *81*, 6157–6164. (b) Gao, W.; Ding, H.; Yu, T.; Wang, Z.; Ding, S. *Org. Biomol. Chem.* **2021**, *19*, 6216–6220.

[11] Selected examples on platinum-catalyzed silylation of alkynes: (a) Tanaka, M.; Uchimaru, Y.; Lautenschlage, H.-J. *Organometallics* **1991**, *10*, 16–18. (b) Rooke, D. A.; Ferreira, E. M. *J. Am. Chem. Soc.* **2010**, *132*, 11926–11928. (c) Rooke, D. A.; Ferreira, E. M. *Angew. Chem.*, *Int. Ed.* **2012**, *51*, 3225–3230. (d) Kawasaki, Y.; Ishikawa, Y.; Igawa, K.; Tomooka, K. *J. Am. Chem. Soc.* **2011**, *133*, 20712–20715.

[12] Selected examples on gold-catalyzed silylation of alkynes: (a) Lykakis, I. N.; Psyllaki, A.; Stratakis, M. *J. Am. Chem. Soc.* **2011**, *133*, 10426–10429. (b) Gryparis, C.; Stratakis, M. *Org. Lett*. **2014**, *16*, 1430–1433. (c) Kidonakis, M.; Stratakis, M. *Eur. J. Org. Chem*. **2017**, *29*, 4265–4271.

[13] Lanthanum-catalyzed silylation of alkynes: Xu, X.; Gao, A.; Chen, W.; Xu, X.; Li, J.; Cui, C. *ACS Catal*. **2023**, *13*, 3743–3748.

[14] (a) Ojima, I.; Kumagai, M.; Nagai, Y. *J. Organomet. Chem.* **1974**, *66*, C14–C16. (b) Dickers, H. M.; Haszeldine, R. N.; Mather, A. P.; Parish, R. V. *J. Organomet. Chem.* **1978**, *161*, 91–95. (c) Brady, K. A.; Nile, T. A. *J. Organomet. Chem.* **1981**, *206*, 299–304. (d) Ojima, I.; Clos, N.; Donovan, R. J.; Ingallina, P. *Organometallics* **1990**, *9*, 3127–3133. (e) Tanke, R. S.; Crabtree, R. H. *J. Am. Chem. Soc.* **1990**, *112*, 7984–7989.

[15] Selected examples on *anti*-silylfunctionalization of alkynes by radical systems: (a)

Romain, E.; Fopp, C.; Chemla, F.; Ferreira, F.; Jackowski, O.; Oestreich, M.; Perez-Luna, A. *Angew. Chem.*, *Int. Ed.* **2014**, *53*, 11333–11337. (b) Romain, E.; de la Vega-Hernández, K.; Guégan, F.; Sanz García, J.; Fopp, C.; Chemla, F.; Ferreira, F.; Gerard, H.; Jackowski, O.; Halbert, S.; Oestreich, M.; Perez-Luna, A. *Adv. Synth. Catal*. **2021**, *363*, 2634–2647. See also: (c) Yamaguchi, S.; Xu, C.; Tamao, K. *J. Am. Chem. Soc*. **2003**, *125*, 13662–13663.

[16] Selected examples and a review on Lewis acid-catalyzed *anti*-silylfunctionalization of alkynes: (a) Asao, N.; Yoshikawa, E.; Yamamoto, Y. *J. Org. Chem.* **1996**, *61*, 4874–4875. (b) Asao, N.; Yamamoto, Y. *Bull. Chem. Soc. Jpn*. **2000**, *73*, 1071–1087. (c) Zuo, H.; Irran, E.; Klare, H. F. T.; Oestreich, M. *Angew. Chem.*, *Int. Ed.* **2024**, *63*, e202401599. (d) Zuo, H.; Klare, H. F. T.; Oestreich, M. *J. Org. Chem.* **2023**, *88*, 4024–4027. See also: (e) Kinoshita, H.; Ueda, A.; Fukumoto, H.; Miura, K. *Org. Lett*. **2017**, *19*, 882–885.

[17] Selected examples on transition-metal-catalyzed reactions involving *syn-anti* isomerization of alkenylmetals: (a) Lv, W.; Liu, S.; Chen, Y.; Wen, S.; Lan, Y.; Cheng, G. *ACS Catal.* **2020**, *10*, 10516–10522. (b) Zell, D.; Kingston, C.; Jermaks, J.; Smith, S. R.; Seeger, N.; Wassmer, J.; Sirois, L. E.; Han, C.; Zhang, H.; Sigman, M. S.; Gosselin, F. *J. Am. Chem. Soc.* **2021**, *143*, 19078–19090. (c) Shan, C.; He, M.; Luo, X.; Li, R.; Zhang, T. *Org. Chem. Front.* **2023**, *10*, 4243–4249.

[18] Recently developed *anti*-selective hydrosilylation of alkynes: (a) Behera, R. R.; Saha, R.; Kumar, A. A.; Sethi, S.; Jana, N. C.; Bagh, B. *J. Org. Chem*. **2023**, *88*, 8133–8149. (b) Zheng, N.; Song, W.; Zhang, T.; Li, M.; Zheng, Y.; Chen, L. *J. Org. Chem*. **2018**, *83*, 6210–6216. (c) Zhao, X.; Yang, D.; Zhang, Y.; Wang, B.; Qu, J. *Org. Lett*. **2018**, *20*, 5357–5361. (d) Puerta-Oteo, R.; Munarriz, J.; Polo, V.; Jiménez, M. V.; Pérez-Torrente, J. J. *ACS Catal*. **2020**, *10*, 7367–7380.

[19] Trost, B. M.; Ball, Z. T. *J. Am. Chem. Soc.* **2005**, *127*, 17644–17655.

[20] Muraoka, T.; Matsuda, I.; Itoh, K. *Organometallics* **2002**, *21*, 3650–3660.

[21] Rooke, D. A.; Ferreira, E. M. *J. Am. Chem. Soc.* **2010**, *132*, 11926–11928.

[22] Fukumoto, Y.; Hagihara, M.; Kinashi, F.; Chatani, N. *J. Am. Chem. Soc.* **2011**, *133*, 10014–10017.

[23] Zhu, F.; Spannenberg, A.; Wu, X.-F. *Chem. Commun.* **2017**, *53*, 13149–13152.

[24] Vercruysse, S.; Cornelissen, L.; Nahra, F.; Collard, L.; Riant, O. *Chem. Eur. J*. **2014**, *20*, 1834–1838.

[25] Yang, L.-F.; Wang, Q.-A.; Li, J.-H. *Org. Lett.* **2021**, *23*, 6553–6557.

[26] Iwamoto, T.; Nishikori, T.; Nakagawa, N.; Takaya, H.; Nakamura, M. *Angew. Chem.*, *Int. Ed.* **2017**, *56*, 13298–13301.

[27] Wisthoff, M. F.; Pawley, S. B.; Cinderella, A. P.; Watson, D. A. *J. Am. Chem. Soc*. **2020**, *142*, 12051–12055.

[28] (a) Chandrasekaran, R.; Selvam, K.; Rajeshkumar, T.; Chinnusamy, T.; Maron, L.; Rasappan, R. *Angew. Chem.*, *Int. Ed.* **2024**, *63*, e202318689. See also: (b) Chandrasekaran, R.; Pulikkottil, F. T.; Elama, K. S.; Rasappan, R. *Chem. Sci.* **2021**, *12*, 15719–15726.

[29] Cheng, C.; Zhang, Y. *Org. Lett*. **2021**, *23*, 5772–5776.

[30] (a) Zhao, J.; Liu, S.; Marino, N.; Clark, D. A. *Chem. Sci*. **2013**, *4*, 1547–1551. (b) Liu, S.; Zhao, J.; Kaminsky, L.; Wilson, R. J.; Marino, N.; Clark, D. A. *Org. Lett*. **2014**, *16*, 4456–4459.

[31] Non-transition-metal-catalyzed *anti*-selective silylboration: (a) Nagao, K.; Ohmiya, H.; Sawamura, M. *Org. Lett*. **2015**, *17*, 1304–1307. (b) Fritzemeier, R.; Santos, W. L. *Chem. Eur. J*. **2017**, *23*, 15534–15537.

[32] Ohmura, T.; Oshima, K.; Suginome, M. *Chem. Commun.* **2008**, 1416–1418.

[33] (a) Matsuda, T.; Ichioka, Y. *Org. Biomol. Chem.* **2012**, *10*, 3175–3177. (b) Naka, A.; Shimomura, N.; Kobayashi, H. *ACS Omega* **2022**, *7*, 30369–30375.

[34] He, T.; Liu, L.-C.; Guo, L.; Li, B.; Zhang, Q.-W.; He, W. *Angew. Chem*., *Int. Ed*. **2018**, *57*, 10868–10872.

[35] (a) Cowley, A. H.; Sisler, H. H.; Ryschkewitsch, G. E. *J. Am. Chem. Soc.* **1960**, *82*, 501–502. (b) Seyferth, D.; Kögler, H. P. *J. Inorg. Nucl. Chem.* **1960**, *15*, 99–104.

[36] (a) Nöth, H.; Höllerer, G. *Chem. Ber.* **1966**, *99*, 2197–2205. (b) Habereder, T.; Nöth, H. *Appl. Organomet. Chem*. **2003**, *17*, 525–538. (c) Suginome, M.; Matsuda, T.; Ito, Y. *Organometallics* **2000**, *19*, 4647–4649. (d) Ohmura, T.; Masuda, K.; Furukawa, H.; Suginome, M. *Organometallics* **2007**, *26*, 1291–1294. (e) Boebel, T. A.; Hartwig, J. F. *Organometallics* **2008**, *27*, 6013–6019. (f) Yamamoto, E.; Shishido, R.; Seki, T.; Ito, H. *Organometallics* **2017**, *36*, 3019–3022. (g) Shishido, R.; Uesugi, M.; Takahashi, R.; Mita, T.; Ishiyama, T.; Kubota, K.; Ito, H. *J. Am. Chem. Soc.* **2020**, *142*, 14125–14133. (h) Takeuchi, T.; Shishido, R.; Kubota, K.; Ito, H. *Chem. Sci*. **2021**, *12*, 11799–11804.

[37] Reviews on reactivity of silylborane: (a) Oestreich, M.; Hartmann, E.; Mewald, M. *Chem. Rev.* **2013**, *113*, 402–441. (b) Feng, J.-J.; Mao, W.; Zhang, L.; Oestreich, M. *Chem. Soc. Rev.* **2021**, *50*, 2010–2073. (c) Ohmura, T.; Suginome, M. *Bull. Chem. Soc. Jpn.* **2009**, *82*, 29–49.

[38] (a) Suginome, M.; Nakamura, H.; Ito, Y. *Chem. Commun.* **1996**, 2777–2778. (b) Suginome, M.; Matsuda, T.; Nakamura, H.; Ito, Y. *Tetrahedron* **1999**, 55, 8787–8800. (c) Onozawa, S.-y.; Hatanaka, Y.; Tanaka, M. *Chem. Commun*. **1997**, 1229–1230.

[39] (a) Ohmura, T.; Masuda, K.; Suginome, M. *J. Am. Chem. Soc*. **2008**, *130*, 1526–1527. (b) Sasaki, I.; Maebashi, A.; Li, J.; Ohmura, T.; Suginome, M. *Eur. J. Org. Chem*. **2022**, e202101573.

[40] (a) Kawauchi, A.; Minamimoto, T.; Tamao, K. *Chem. Lett.* **2001**, *30*, 1216–1217. (b) O'Brien, J. M.; Hoveyda, A. H. *J. Am. Chem. Soc.* **2011**, *133*, 7712–7715. (c) Ito, H.; Horita, Y.; Yamamoto, E. *Chem. Commun*. **2012**, *48*, 8006–8008. (d) Morimasa, Y.; Kabasawa, K.; Ohmura, T.; Suginome, M. *Asian J. Org. Chem.* **2019**, *8*, 1092–1096.

[41] (a) Matsumoto, A.; Ito, Y. *J. Org. Chem*. **2000**, *65*, 5707–5711. (b) Zhong, M.; Pannecoucke, X.; Jubault, P.; Poisson, T. *Chem. Eur. J.* **2021**, *27*, 11818–11822. (c) Takemura, N.; Sumida, Y.; Ohmiya, H. *ACS Catal*. **2022**, *12*, 7804–7810. (d) Ishigaki, S.; Nagashima, Y.; Yukimori, D.; Tanaka, J.; Matsumoto, T.; Miyamoto, K.; Uchiyama, M.; Tanaka, K. *Nat. Commun.* **2023**, *14*, 652. (e) Zhou, J.; Zhao, Z.; Mori, S.; Yamamoto, K.; Shibata, N. *Chem. Sci*. **2024**, *15*, 5113–5122. (f) Arai, R.; Nagashima, Y.; Koshikawa, T.; Tanaka, K. *J. Org. Chem*. **2023**, *88*, 10371–10380.

[42] (a) Nozaki, K.; Wakamatsu, K.; Nonaka, T.; Tückmantel, W.; Oshima, K.; Utimoto, K. *Tetrahedron Lett.* **1986**, *27*, 2007–2010. (b) Wang, P.; Yeo, X.-L.; Loh, T.-P. *J. Am. Chem. Soc*. **2011**, *133*, 1254–1256. (c) Zhou, H.; Wang, Y.-B. *ChemCatChem* **2014**, *6*, 2512–2156. (d) Hazra, C. K.; Fopp, C.; Oestreich, M. *Chem. Asian J.* **2014**, *9*, 3005–3010. (e) Garcia-Rubia, A.; Romero-Revilla, J. A.; Mauleon, P.; Arrayás, R. G; Carretero, J. C. *J. Am. Chem. Soc*. **2015**, *137*, 6857–6865.

[43] Zhao, M.; Shan, C.-C.; Wang, Z.-L.; Yang, C.; Fu, Y.; Xu, Y.-H. *Org. Lett.* **2019**, *21*, 6016–6020.

[44] Fujihara, T.; Tani, Y.; Semba, K.; Terao, J.; Tsuji, Y. *Angew*. *Chem*., *Int*. *Ed*. **2012**, *51*, 11487–11490.

[45] Yoshida, H.; Hayashi, Y.; Ito, Y.; Takaki, K. *Chem. Commun.* **2015**, *51*, 9440–9442.

[46] (a) Shintani, R.; Kurata, H.; Nozaki, K. *J. Org. Chem*. **2016**, *81*, 3065–3069. (b) Chen, Q.; Li, Z.; Nishihara, Y. *Org. Lett.* **2022**, *24*, 385–389.

[47] (a) Wang, M.; Liu, Z.-L.; Zhang, X.; Tian, P.-P.; Xu, Y.-H.; Loh, T.-P. *J. Am. Chem.*

Soc. **2015**, *137*, 14830–14833. (b) Meng, F.-F.; Xie, J.-H.; Xu, Y.-H.; Loh, T.-P. *ACS Catal*. **2018**, *8*, 5306–5312.

[48] Chang, X.-H.; Liu, Z.-L.; Luo, Y.-C.; Yang, C.; Liu, X.-W.; Da, B.-C.; Li, J.-J.; Ahmad, T.; Loh, T.-P.; Xu, Y.-H. *Chem. Commun*. **2017**, *53*, 9344–9347.

[49] Matsuda, Y.; Tsuji, Y.; Fujihara, T. *Chem. Commun*. **2020**, *56*, 4648–4651.

[50] (a) Tani, Y.; Yamaguchi, T.; Fujihara, T.; Terao, J.; Tsuji, Y. *Chem. Lett*. **2015**, *44*, 271–273. (b) Rae, J.; Hu, Y. C.; Procter, D. J. *Chem. Eur. J*. **2014**, *20*, 13143–13145. (c) Rae, J.; Yeung, K.; McDouall, J. J. W.; Procter, D. J. *Angew. Chem.*, *Int. Ed.* **2016**, *55*, 1102–1107. (d) Tani, Y.; Fujihara, T.; Terao, J.; Tsuji, Y. *J. Am. Chem. Soc*. **2014**, *136*, 17706–17709.

[51] (a) Lee, K.-S.; Hoveyda, A. H. *J. Am. Chem. Soc.* **2010**, *132*, 2898–2900. (b) Ibrahem, I.; Santoro, S.; Himo, F.; Córdova, A. *Adv. Synth. Catal*. **2011**, *353*, 245–252. (c) Calderone, J. A.; Santos, W. L. *Org. Lett*. **2012**, *14*, 2090–2093. (d) Mao, W.; Oestreich, M. *Org. Lett*. **2020**, *22*, 8096–8100. See also: (e) Lee, K.-S.; Wu, H.; Haeffner, F.; Hoveyda, A. H. *Organometallics* **2012**, *31*, 7823–7826. (f) López, A.; Parra, A.; Jarava-Barrera, C.; Tortosa, M. *Chem. Commun*. **2015**, *51*, 17684–17687.

[52] Liang, R.-X.; Chen, R.-Y.; Zhong, C.; Zhu, J.-W.; Cao, Z.-Y.; Jia, Y.-X. *Org. Lett.* **2020**, *22*, 3215–3218.

[53] (a) Mazzacano, T.; Mankad, N. P. *ACS Catal.* **2017**, *7*, 146–149. (b) Sakaguchi, H.; Ohashi, M.; Ogoshi, S. *Angew. Chem.*, *Int. Ed.* **2018**, *57*, 328–332.

[54] (a) Vyas, D. J.; Oestreich, M. *Angew. Chem.*, *Int. Ed.* **2010**, *49*, 8513–8515. (b) Delvos, L. B.; Vyas, D. J.; Oestreich, M. *Angew. Chem.*, *Int. Ed.* **2013**, *52*, 4650–4653. (c) Takeda, M.; Shintani, R.; Hayashi, T. *J. Org. Chem.* **2013**, *78*, 5007–5017. (d) Delvos, L. B.; Oestreich, M. *Synthesis* **2015**, *47*, 924–933.

[55] Kleeberg, C.; Feldmann, E.; Hartmann, E.; Vyas, D. J.; Oestreich, M. *Chem. Eur. J.*

2011, *17*, 13538–13543.

[56] Vyas, D. J.; Fröhlich, R.; Oestreich, M. *Org. Lett.* **2011**, *13*, 2094−2097.

[57] Kleeberg, C.; Cheung, M. S.; Lin, Z.; Marder, T. B. *J. Am. Chem. Soc*. **2011**, *133*, 19060−19063.

[58] Zarate, C.; Martin, R. *J. Am. Chem. Soc.* **2014**, *136*, 2236–2239.

[59] Scharfbier, J.; Gross, B. M.; Oestreich, M. *Angew. Chem*., *Int. Ed.* **2020**, *59*, 1577–1580.

[60] (a) Xue, W.; Oestreich, M. *Angew. Chem.*, *Int. Ed*. **2017**, *56*, 11649–11652. (b) Xue, W.; Qu, Z.-W.; Grimme, S.; Oestreich, M. *J. Am. Chem. Soc.* **2016**, *138*, 14222–14225. (c) Hazrati, H.; Oestreich, M. *Org. Lett.* **2018**, *20*, 5367–5369. (d) Cheng, L.-J.; Mankad, N. P. *J. Am. Chem. Soc.* **2020**, *142*, 80–84.

[61] Kondo, R.; Moniwa, H.; Shintani, R. *Org. Lett*. **2023**, *25*, 4193–4197.

Chapter 2

Copper-Catalyzed Synthesis of Tetrasubstituted Alkenes via Regio- and *anti*-Selective Addition of Silylboronates to Internal Alkynes

2.1 Introduction

Alkenes constitute a fundamental structural component in various organic molecules and widely appear in biologically active compounds as well as functional organic materials. It is therefore highly important to develop efficient synthetic methods of alkenes with precise control of the regio- and stereochemistry. In particular, synthesis of tetrasubstituted alkenes can be quite challenging because of the steric congestion and the number of isomers that need to be distinguished when the substituents are different with one another.[1] Among the possible synthetic strategies to tetrasubstituted alkenes, 1,2-difunctionalization of internal alkynes is one of the most straightforward approaches, and addition of silylboronates would be highly attractive in view of the synthetic utility of silyl and boryl groups.[2] Indeed, silylboration of alkynes have been extensively investigated since pioneering work by Suginome, Nakamura, and Ito under palladium and platinum catalysis,[3a] and several effective catalyst systems have been developed to date.[3] However, most of the existing methods employ either terminal alkynes or symmetric internal alkynes as substrates, and silicon and boron are introduced *syn*-selectively across the C–C triple bond (Scheme 1a). With regard to the *anti*-selective addition of silylboronates to internal alkynes, only two approaches have been reported to date: a tributylphosphine-catalyzed addition to 3-substituted propiolates[4] and a PhLi/12-crown-4-mediated addition to 3-substituted propiolamides,[5] both of which require carbonyl substituted alkynes as substrates (Scheme 1b).[6] In this context, herein the author describe

a copper-catalyzed regio- and *anti*-selective addition of silylboronates to unactivated unsymmetric internal alkynes to give the corresponding tetrasubstituted alkenes under simple and mild conditions (Scheme 1c).[7]

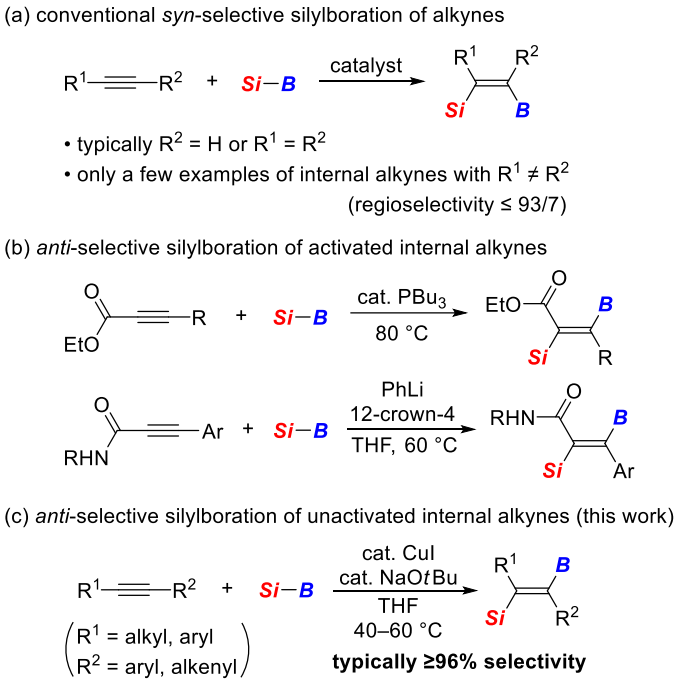

Scheme 1. Silylboration of alkynes for the synthesis of silicon- and boron-substituted alkenes: (a) conventional *syn*-selective silylboration of alkynes, (b) *anti*-selective silylboration of activated internal alkynes, and (c) this work: *anti*-selective silylboration of unactivated internal alkynes.

2.2 Results and discussion

2.2.1 Reaction development and product derivatization

Initially, 1-phenyl-1-propyne (**1a**) was employed as the substrate and a reaction with silylboronate **2a** was conducted in the presence of CuI (10 mol%) and LiO*t*Bu (40 mol%) in THF at 40 °C (Table 1, entry 1). Under these conditions, silylboration product **3aa** was obtained in 81% yield with 96% selectivity via regio- and *anti*-selective addition.[3b,c] it was subsequently found that the use of NaO*t*Bu in place of LiO*t*Bu improved the selectivity to >99% in 79% yield (entry 2), but the use of KO*t*Bu led to a significant decrease of the yield while keeping the high selectivity (29% yield, >99% selectivity; entry 3). On the other hand, no reaction took place by using NaOMe (entry 4), and the reaction using NaO*t*Bu in the absence of CuI gave only 9% yield of the product with much lower selectivity (72% selectivity; entry 5). The present reaction also proceeded with similar efficiency and high regio- and *anti*-stereoselectivity by using several ligands for copper such as PPh_3, PCy_3, XantPhos, and IPr (entries 6–9), but no reaction occurred in the presence of Phen (entry 10).

Table 1. Copper-catalyzed reaction of **1a** with **2a**: effect of base and ligand.

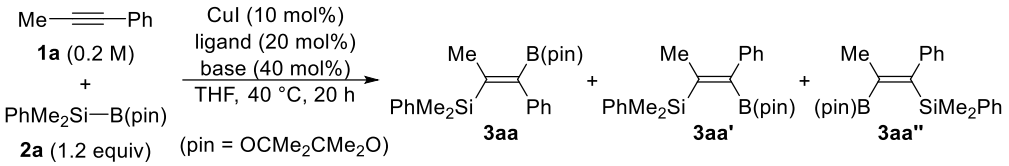

Entry	Ligand	Base	Yield (%) [a]	**3aa**/**3aa'**/**3aa''** [a]
1	None	LiO*t*Bu	81	96/0/4
2	None	NaO*t*Bu	79	>99/<1/<1
3	None	KO*t*Bu	29	>99/<1/0
4	None	NaOMe	0	–
5[b]	None	NaO*t*Bu	9	72/6/22
6	PPh_3	NaO*t*Bu	71	96/1/3
7	PCy_3	NaO*t*Bu	78	99/<1/<1
8	XantPhos [c]	NaO*t*Bu	75	>99/1/0
9	IPr [c,d]	NaO*t*Bu	75	99/1/0
10	Phen [c]	NaO*t*Bu	0	–

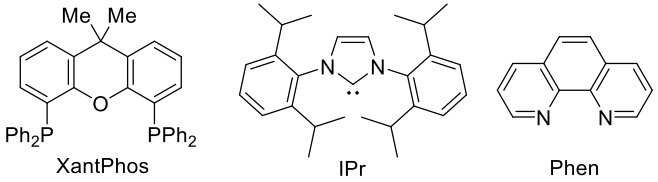

[a] Determined by ^{1}H NMR against internal standard (dimethyl terephthalate). [b] No CuI was used. [c] 10 mol% of ligand was used. [d] (IPr)CuCl was used instead of CuI/ligand.

Under the conditions in Table 1, entry 2, the scope of alkyl(aryl)alkynes **1** was found to be fairly broad in the addition of **2a**, giving products **3** with high regio- and *anti*-selectivity as summarized in Scheme 2 (typically ≥96% selectivity). For example, in addition to compound **3aa** having a methyl group, primary, secondary, and even tertiary alkyl group-substituted compounds **3ba–ea** could be synthesized in 77–86% yield with ≥94% selectivity. Several functional groups such as alkene, ether, silyl ether, and carbazole on the alkyl chain were tolerated as shown for the synthesis of compounds **3fa–ia**. Regarding the substituents on the aromatic rings, various groups including ether (**3ka**, **3qa**, **3sa**), halide (**3ja**,[8] **3ma**, **3na**), ester (**3oa**), and acetal (**3pa**) could be introduced at either *para*-, *meta*-, or *ortho*-position without affecting the regio- and *anti*-stereoselectivity. Heteroaryl groups as well as an alkenyl group could also be used in place of an aryl group to give the corresponding products **3ua–wa**[8] with similarly high selectivity.

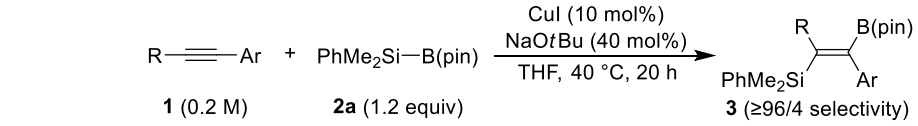

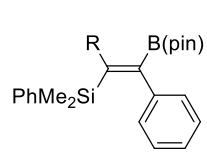

3aa (R = Me): 79% yield
3ba (R = *n*Pr): 80% yield
3ca (R = *i*Bu): 86% yield
3da (R = *i*Pr): 77% yield
3ea (R = *t*Bu): 85% yield[a,b]

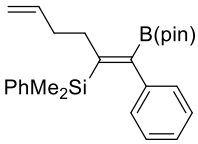

3fa: 74% yield[c]

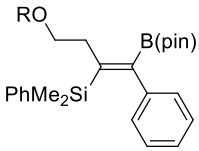

3ga (R = Me): 70% yield[d]
3ha (R = $SiMe_2tBu$): 83% yield[d]

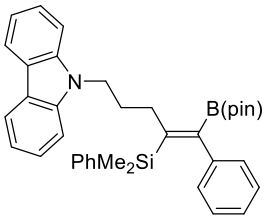

3ia: 84% yield[b,d]

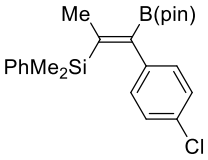

3ja: 72% yield[d]

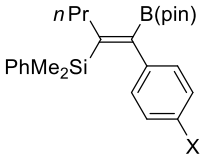

3ka (X = OMe): 82% yield
3la (X = Me): 84% yield
3ma (X = F): 60% yield[d]
3na (X = Cl): 67% yield[d]
3oa (X = CO_2tBu): 53% yield[d,e]

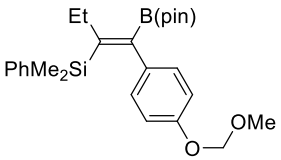

3pa: 84% yield

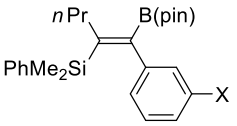

3qa (X = OMe): 83% yield
3ra (X = Me): 84% yield

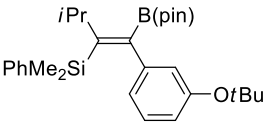

3sa: 85% yield

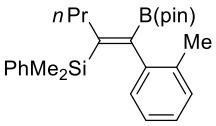

3ta: 76% yield

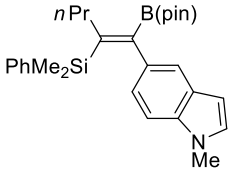

3ua: 83% yield[d]

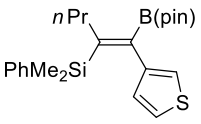

3va: 43% yield

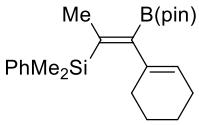

3wa: 85% yield

[a] The reaction was conducted using **2a** (2.0 equiv), CuI (20 mol%), and NaO*t*Bu (80 mol%) at 10 °C for 70 h. [b] Selectivity = 94/6. [c] Selectivity = 93/7. [d] The reaction was conducted at 60 °C. [e] The reaction was conducted using **1o** (1.2 equiv) and **2a** (1.0 equiv).

Scheme 2. Scope of copper-catalyzed silylboration of unsymmetric internal alkynes.

The present *anti*-selective silylboration reaction is also applicable to symmetric diarylalkynes **4** as briefly examined in Scheme 3. The use of excess silylboronate **2a** for the reaction of diarylalkynes resulted in somewhat lower *anti*-selectivity. For example, when the reaction was conducted with diphenylacetylene (**4a**) (1.0 equiv) and **2a** (1.2 equiv), the silylboration product was obtained in 82% yield with *anti*/*syn* = 87/13.[9] On the other hand, the reaction using excess amount of **4a** gave **5aa** with 99/1 *anti*-selectivity. In addition to **2a**, (triethylsilyl)boronate **2b** could be used for the reaction of **4a** to give corresponding product **5ab** with high selectivity. Several substituted diphenylacetylenes including a sterically congested one underwent silylboration with **2a** to give compounds **5ba–ea** as well.

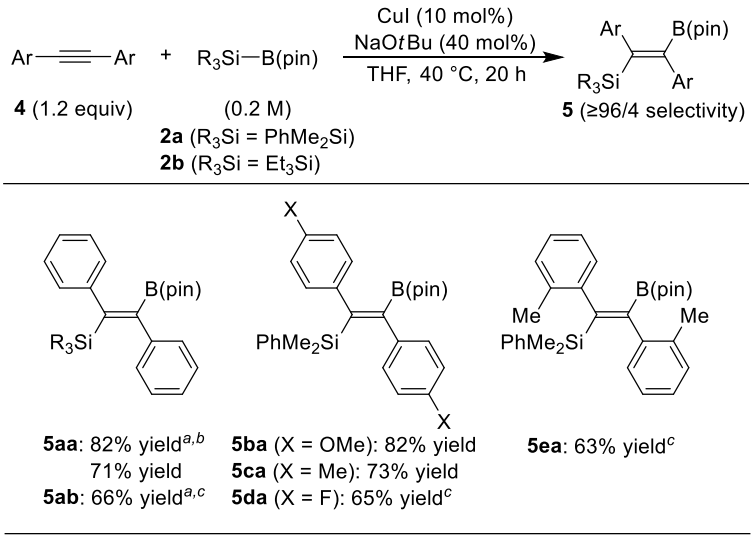

[a] The reaction was conducted using **4** (1.0 equiv) and **2** (1.2 equiv). [b] Selectivity = 87/13. [c] The reaction was conducted at 60 °C.

Scheme 3. Scope of copper-catalyzed silylboration of symmetric diarylalkynes.

In contrast, the use of dialkylalkynes such as 3-hexyne (**4f**) and 5-decyne (**4g**) led to the formation of *syn*-addition products such as **5fa'** and **5ga'** with no formation of the corresponding *anti*-adducts (eq 1).

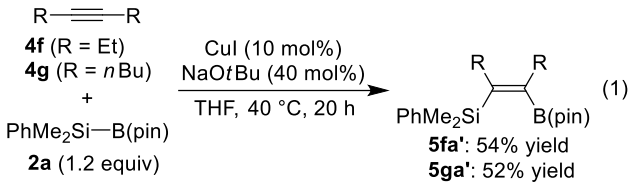

(1)

The tetrasubstituted alkenes obtained in the present catalysis can be further transformed into various other compounds by utilizing the silyl and/or boryl groups installed into the molecules. For example, alkylation of the alkenylboronate of **3ha** could be achieved by a rhodium-catalyzed 1,4-addition to a vinyl ketone to give stereochemically defined γ,δ-unsaturated ketone **6** in 72% yield (Scheme 4a).[10] In addition, Suzuki coupling of **3pa** with iodobenzene efficiently proceeded to give alkenylsilane **7** and this could be readily transformed into the corresponding bromoalkene **8** by reacting it with *N*-bromosuccinimide (NBS) (Scheme 4b). Subsequent deprotection of the MOM group of **8** led to compound **9**, a known precursor for the synthesis of (*Z*)-tamoxifen.[11] On the other hand, similarly cross-coupled compound **10** obtained from **3sa** having a 3-*tert*-butoxyphenyl group preferentially underwent bromination on the aromatic ring, rather than desilylative bromination on the alkene, by the reaction with NBS/NaBr to give compound **11**,[12] and this could be converted to benzosilole **12** by treating it with *t*BuLi (Scheme 4c).

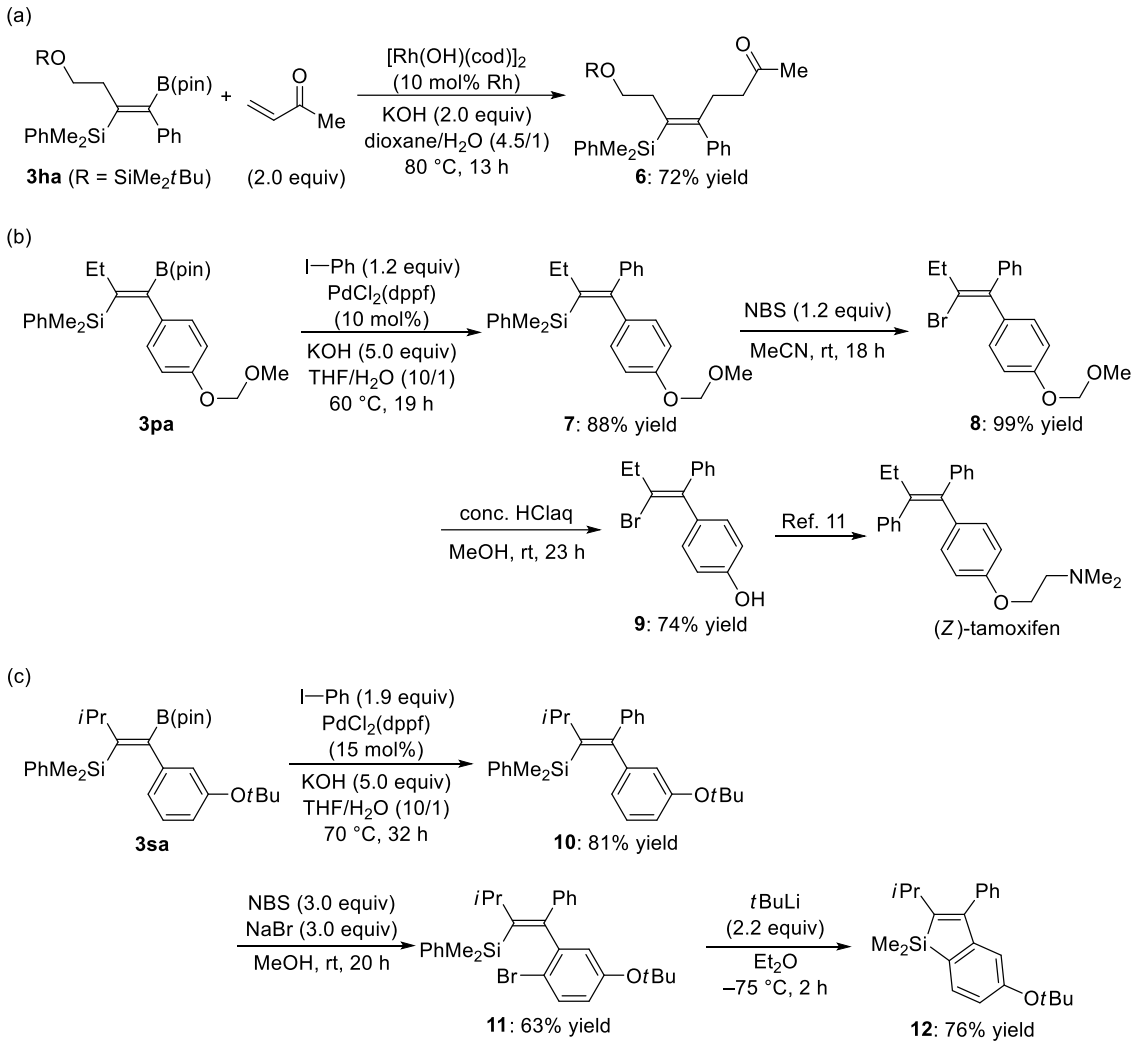

Scheme 4. Functionalization of silylborated tetrasubstituted alkenes **3**: (a) Rhodium-catalyzed 1,4-addition of **3ha**, (b) the synthesis of (*Z*)-tamoxifen from **3pa**, and (c) the synthesis of benzosilole **12** from **3sa**.

2.2.2 Mechanistic Investigation

As an experimental result on this reaction mechanism, it was found that the amount of NaO*t*Bu used in the present catalysis showed a significant impact on the reaction outcome (Table 2). Thus, in the presence of 10 mol % of CuI, no reaction took place when the amount of NaO*t*Bu was 0–30 mol % (entry 1). In contrast, high yields of **3aa** were realized with 40–50 mol % (entries 2 and 3), and the yield became gradually lower by further increasing the amount to 100–200 mol % (entries 4 and 5). Because alkoxides are known to displace halogens on copper(I) and can form cuprate complexes when an excess amount is used with respect to copper,[13] the cuprate species could be the key intermediate, considering that the amount of NaO*t*Bu needs to be sufficiently high (≥40 mol%) to promote the present reaction. In addition, alkoxides are also known to coordinate to the boron of silylboronates[14] and the resulting species become less electrophilic at boron, which could lead to lower efficiency of the borylation process. This is probably why the yields become lower when a stoichiometric amount of NaO*t*Bu is used in the present reaction.

Table 2. Effect of the amount of base in the copper-catalyzed reaction of **1a** with **2a**.

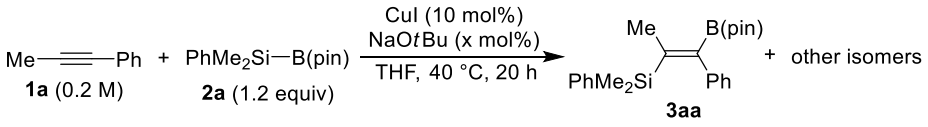

Entry	x (mol%)	Yield (%) [a]	**3aa**/other isomers [a]
1	0–30	0	–
2	40	79	>99/1
3	50	74	99/1
4	100	66	99/1
5	200	50	>99/1

[a] Determined by ^{1}H NMR against internal standard (dimethyl terephthalate).

To gain further insights into the active copper species, stoichiometric reactions were carried out and monitored by ^{1}H NMR. Initially, a stochiometric reaction using NaO*t*Bu was attempted, but ^{1}H NMR signals of the reaction mixture were broadened due to the low solubility. Therefore, LiO*t*Bu was used instead for the NMR experiments. A 1:1 mixture of CuI and silylboronate **2a** in the presence of LiO*t*Bu (4.0 equiv) in THF-d_8 gave a distinct singlet at 0.31 ppm, which can be assigned as methyl protons on the silicon of Cu(SiMe$_2$Ph) (**A^0**) (Figure 1a). When 1-phenyl-1-propyne (**1a**) was added to *in-situ* generated **A^0**, no reaction took place (Figure 1b). On the other hand, a 1:2 mixture of CuI and **2a** with LiO*t*Bu (4.0 equiv) gave a new singlet at 0.02 ppm as the major peak, presumably corresponding to methyl protons of $Li^+Cu^-(SiMe_2Ph)_2$ (**A**) (Figure 1c). When **1a** was added to *in-situ* generated **A**, new signals appeared at room temperature, which can be assigned as silylalkenylcuprates **B** and **B^2** (Figure 1d). Protonolysis of these species led to the formation of silylprotonated alkene **13a** as the major product along with the minor amount of its regioisomer **13a'**.[15] These results suggested that a disilylcuprate, not a neutral silylcopper(I), is the catalytically active species, and the reaction proceeds through *syn*-insertion of an alkyne to the silicon–copper bond.

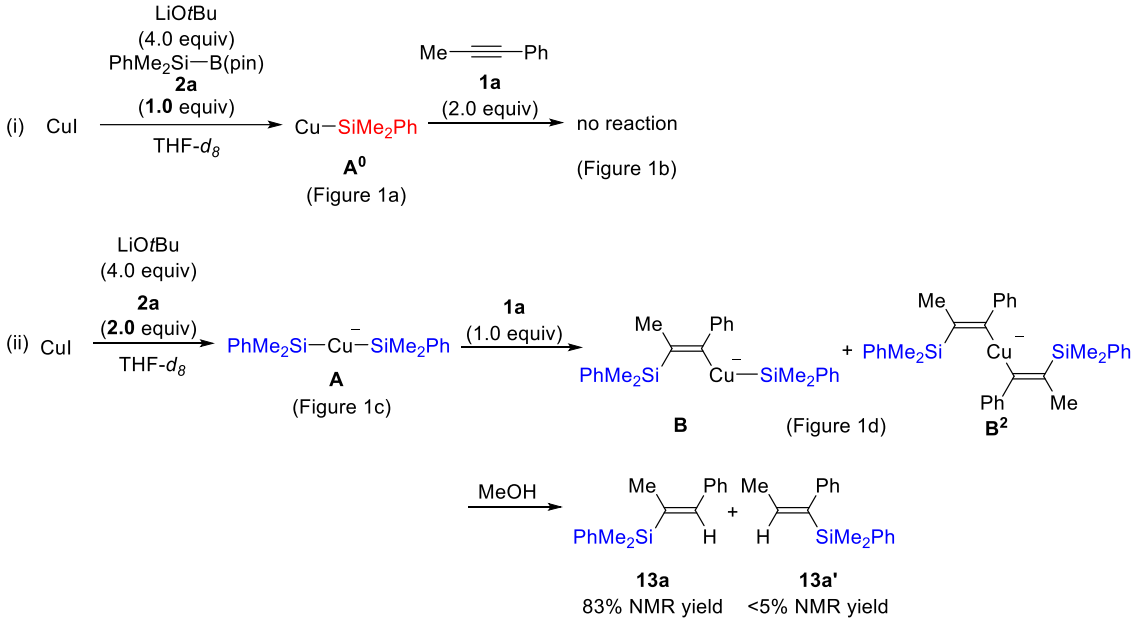

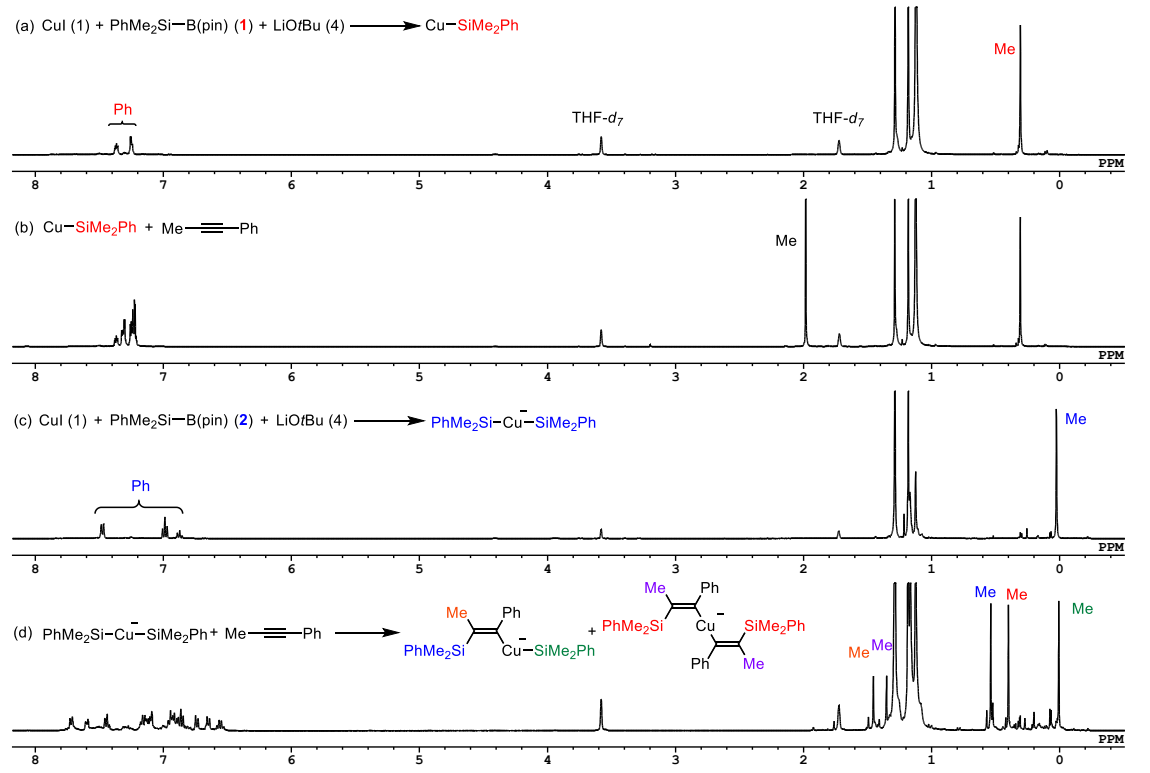

Figure 1. ^{1}H NMR spectra of (a) *in-situ* generated Cu(SiMe$_2$Ph), (b) *in-situ* generated Cu(SiMe$_2$Ph) + alkyne **1a** (2.0 equiv), (c) *in-situ* generated Li$^+$Cu$^-$(SiMe$_2$Ph)$_2$, (d) *in-situ* generated Li$^+$Cu$^-$(SiMe$_2$Ph)$_2$ + alkyne **1a** (1.0 equiv) (400 MHz in THF-*d*$_8$).

Based on these data, a proposed catalytic cycle for the reaction of alkyne **1a** with silylboronate **2a** is shown in Scheme 5. Thus, disilylcuprate **A** undergoes regioselective *syn*-insertion of alkyne **1a** to give *syn*-alkenyl(silyl)cuprate **B**. Instead of direct borylation of **B** giving **3aa'**, *syn*-to-*anti* isomerization of **B** takes place to give *anti*-alkenyl(silyl)cuprate **C**, which then reacts with silylboronate **2a** to give *anti*-silylboration product **3aa** along with regeneration of disilylcuprate **A**.

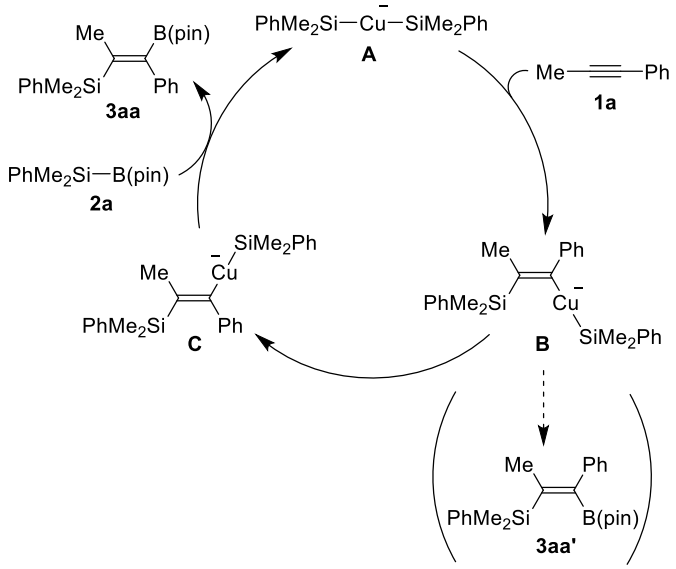

Scheme 5. Proposed catalytic cycle for the copper-catalyzed reaction of alkyne **1a** with silylboronate **2a** to give **3aa**.

To understand the mechanism of the present catalysis more in detail, DFT calculations were conducted. All calculations were performed with the Gaussian 16 package.[16] Geometries were fully optimized by the DFT-B3LYP functional[17] using LANL2DZ for Cu, 6-31G(d) for C, H, B, O, Na atoms, and 6-31+G(d) for Si atom. Frequency analyses were carried out to confirm that each structure was a local minimum (no imaginary frequency) or a transition state (only one imaginary frequency). The energies were estimated by the geometry optimization including the solvation effect with the SCRF-SMD model using THF solvent.[18] The 3D optimized structures were displayed by the CYLview visualization program.[19]

The first step in Scheme 5, the insertion of alkyne **1a** to disilylcuprate **A**, was initially investigated with a focus on the regioselectivity. The reaction of **1a** with **A** toward *syn*-alkenyl(silyl)cuprate **B** is exergonic by 24.9 kcal/mol via **TS A–B** ($\Delta G^{\ddagger}$ = 15.5 kcal/mol) (Scheme 6). The reaction with the opposite regioselectivity needs to go through energetically higher **TS A–B'** ($\Delta G^{\ddagger}$ = 21.1 kcal/mol) to give its regioisomer **B'** (−22.1 kcal/mol). This indicates that the formation of **B** is energetically more favorable than **B'**, which is in good agreement with the experimentally observed regioselectivity. Comparison of the transition-state structures between **TS A–B** and **TS A–B'** showed that **TS A–B** retains a stronger conjugate nature of the alkyne with the phenyl group in **1a** than **TS A–B'** (C1–C3 = 1.45 Å for **TS A–B** vs. C1–C3 = 1.47 Å for **TS A–B'**; Figure 2). In addition, **TS A–B** is sterically more favorable than **TS A–B'** due to the smaller steric repulsion with the incoming dimethylphenylsilyl group (∠C2–C1–Cu–Si = 23.9° for **TS A–B** vs. ∠C1–C2–Cu–Si = 28.3° for **TS A–B'**). Thus, the energy difference between **TS A–B** and **TS A–B'** is caused by both electronic and steric effects, leading to the preferential attack of a silicon nucleophile at the β-position to the phenyl group.

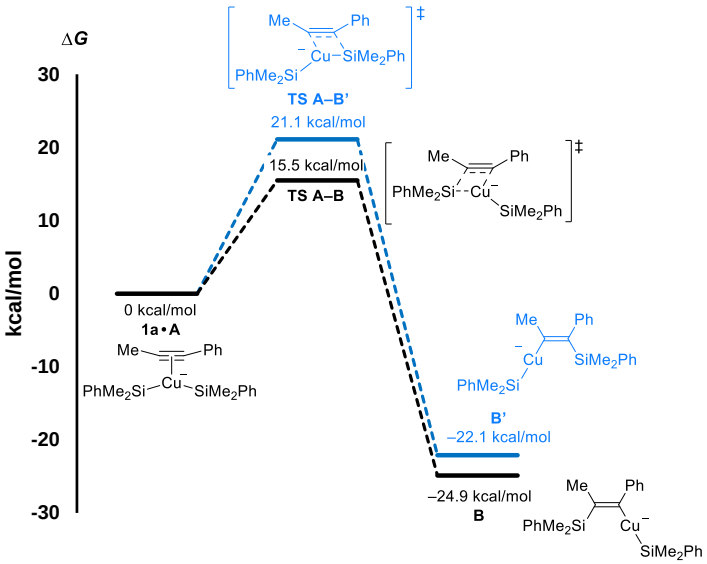

Scheme 6. Calculated reaction pathways for the alkyne insertion to **A**.

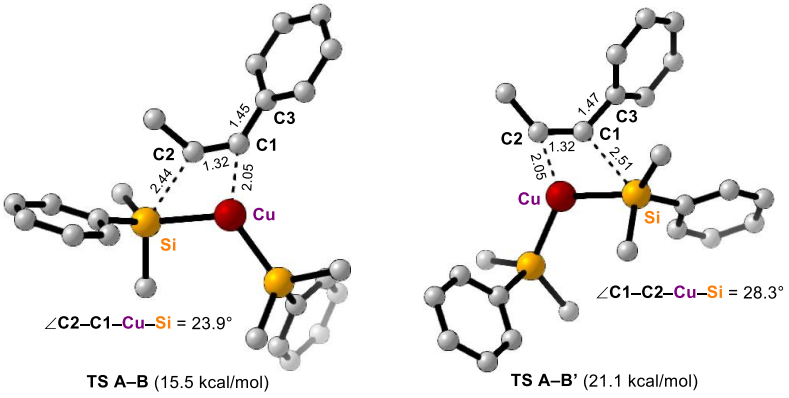

Figure 2. Structures of **TS A–B** and **TS A–B'**. Bond lengths are in Å.

The *syn*-to-*anti* isomerization step from **B** to **C** in Scheme 5 was then explored. Unlike the previously reported processes with other transition metals, the transition states with zwitterionic metal carbene or η^2-vinylmetal structures could not be identified (path 1 in Scheme 7).[20] Although there could be anion stabilization by α-effect of silicon, the zwitterionic carbene may not be so stable without other stabilization effect.[21] In addition, the formation of an η^2-vinylmetal would also be unfavorable presumably due to the lack of an empty d-orbital on copper of the alkenyl(silyl)cuprate species, because the

formation of an η^2-vinylmetal structure requires donation of electrons from an occupied π-orbital of the alkene to an empty d-orbital of the metal center and back donation from an occupied d-orbital of the metal to a π*-orbital of the alkene.[22] As an alternative pathway, an anionic allenic structure stabilized by the benzene ring was found as a possible transition state (path 2 in Scheme 7). However, the energy barrier from **B** to **C** through this pathway was somewhat high ($\Delta G^{\ddagger}$ = 27.4 kcal/mol), and the subsequent borylation of **C** required even higher $\Delta G^{\ddagger}$ of 38.2 kcal/mol, although it is lower by 7.2 kcal/mol than the barrier for direct borylation of **B** to give **3aa'** (Scheme 8).

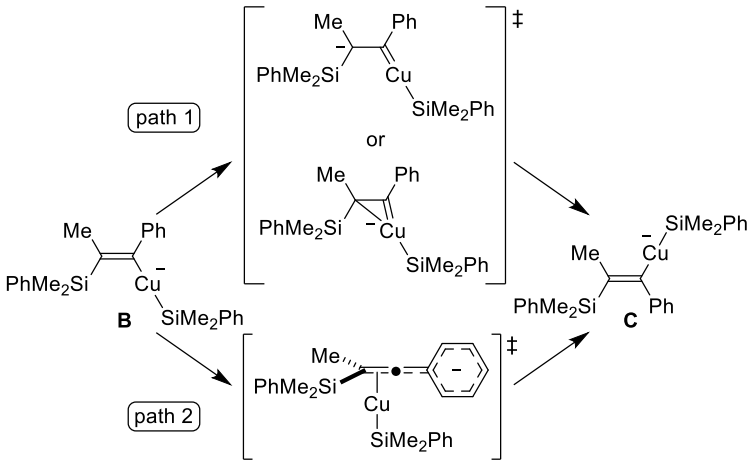

Scheme 7. Possible reaction pathways from **B** to **C**.

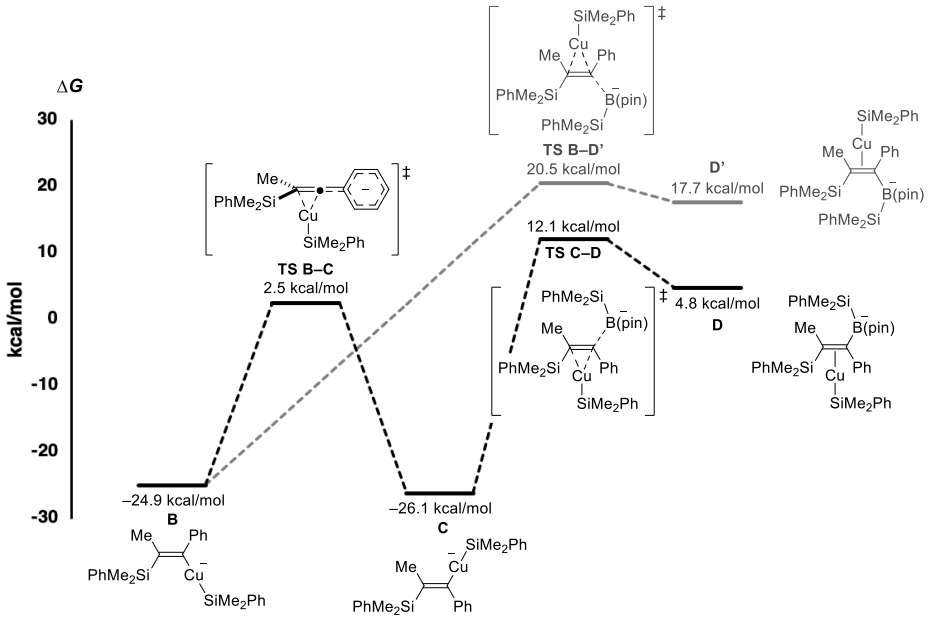

Scheme 8. Calculated reaction pathways for the isomerization of **B** followed by borylation.

Further exploration of more plausible scenarios was carried out based on this promising but not exactly convincing isomerization pathway. As a result, it was found that dissociation of the silylalkenyl moiety from (dimethylphenylsilyl)copper with the assistance of NaO*t*Bu gives more configurationally labile anionic species **E** (−14.3 kcal/mol; Scheme 9). This then undergoes isomerization to **F** (−12.6 kcal/mol) with a much lower barrier of $\Delta G^{\ddagger}$ = 5.9 kcal/mol via **TS E–F** (−8.4 kcal/mol) having a similar anionic allenic structure stabilized by the conjugation with the benzene ring ($\Delta G^{\ddagger}$ = 16.5 kcal/mol from **B**; Figure 3).[23] The strong *trans* influence of the silyl ligand on copper in **B** would facilitate the carbon–copper bond cleavage at its *trans*-position.[24] In the actual experimental system, dissociation of the silylalkenyl moiety from **B** would be assisted by NaO*t*Bu. Therefore, the dissociated alkenyl anion equivalent should be stabilized by a nearby sodium cation, but the calculations in Scheme 9 were performed without explicitly locating the sodium cation to simplify various possible local minima in ion-paired structures. A representative calculated pathway with incorporation of a sodium cation is

shown in Scheme 10. From *syn*-alkenyl(silyl)cuprate **B**, dissociated alkenyl anion equivalent **J** is generated via intermediates **H** and **I**. This then undergoes *syn*-to-*anti* isomerization through **TS J–K** with a sodium-stabilized allenyl anion structure to give isomerized alkenyl anion equivalent **K**, which eventually becomes *anti*-silylalkenylsodium **L**.

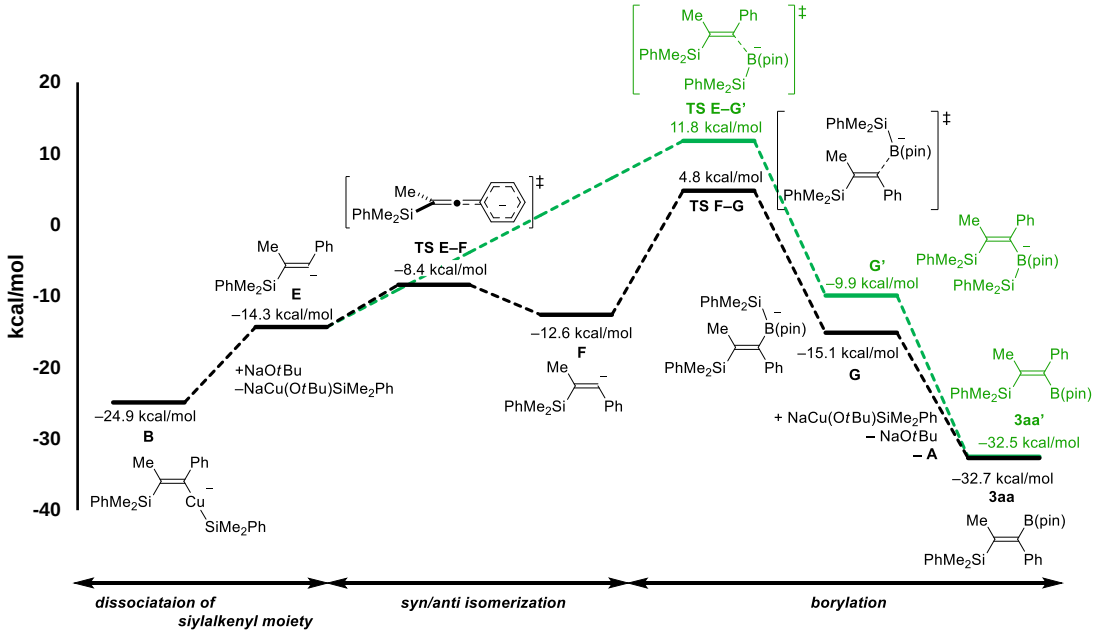

Scheme 9. Calculated reaction pathways for the isomerization of **E** followed by borylation.

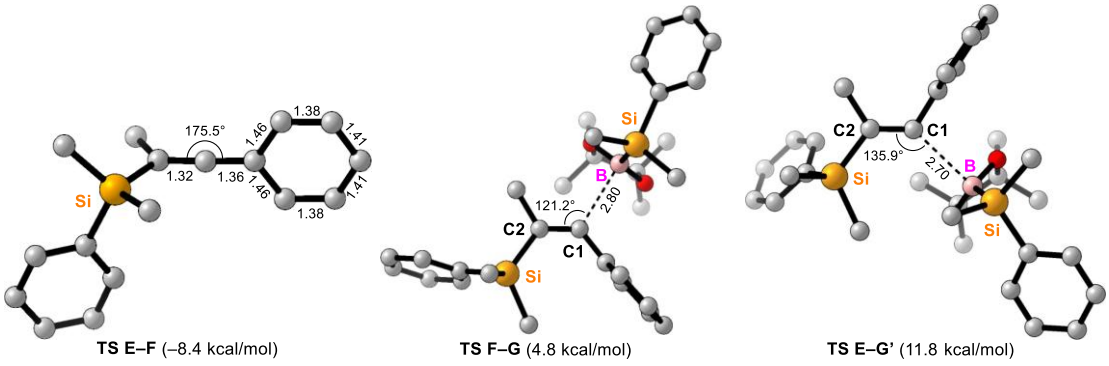

Figure 3. Structures of **TS E–F**, **TS F–G**, and **TS E–G'**. Bond lengths are in Å.

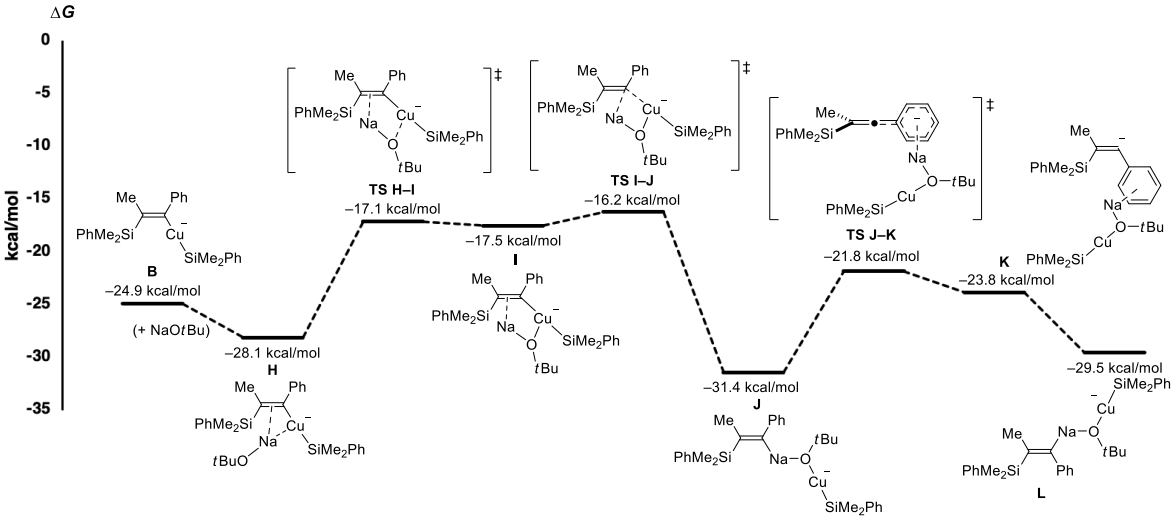

Scheme 10. Calculated reaction pathways for the isomerization of **B** to **L** with assistance of NaO*t*Bu.

For the borylation step in Scheme 9, the isomerized intermediate **F** reacts with silylboronate **2a** to form a carbon–boron bond via **TS F–G** (4.8 kcal/mol, $\Delta G^{\ddagger}$ = 17.4 kcal/mol), giving alkenyl(silyl)borate **G** (−15.1 kcal/mol). Subsequent transfer of the dimethylphenylsilyl group from boron to copper gives product **3aa** with regeneration of disilylcuprate **A** (−32.7 kcal/mol). In comparison, the reaction of **E** with **2a** toward the formation of **3aa'** via intermediate **G'** (−9.9 kcal/mol) required the energy barrier of $\Delta G^{\ddagger}$ = 26.1 kcal/mol at the carbon–boron bond-forming **TS E–G'** (11.8 kcal/mol), which is significantly higher in energy than **TS F–G**. The overall energy profile matches well with the experimental results of selective formation of **3aa**, and the stereoselectivity of the product is determined at the borylation step with reversible *syn*/*anti* isomerization of the alkenyl nucleophile.

The origin of *anti*-selectivity for the reaction of **1a** with **2a** is caused by the steric repulsion between the dimethylphenylsilyl group on the alkene and the incoming boryl group. Indeed, the bond angle of the alkene and the boron (∠C2–C1–B) of **TS F–G** is 121.2°, whereas that of **TS E–G'** is 135.9° and the silylboronate unit is distorted outside

(Figure 3). These computational results indicate that *anti*-borylation **TS F–G** is sterically more favored than *syn*-borylation **TS E–G'**, leading to the selective formation of **3aa**.

To gain further information on the *syn*/*anti*-selectivity at the borylation step for the reaction of **1a**, distortion/interaction analysis of the carbon–boron bond-forming transition states **TS F–G** and **TS E–G'** was conducted (Scheme 11).[25] As a result, distortion energies of **TS F–G** and **TS E–G'** were estimated to be ΔE_{strain} = 5.8 kcal/mol and 11.0 kcal/mol, respectively, and **TS E–G'** has greater strain than **TS F–G**. On the other hand, the stabilization by interaction energy of **TS F–G** (ΔE_{int} = −4.5 kcal/mol) is larger than that of **TS E–G'** (ΔE_{int} = −3.1 kcal/mol).

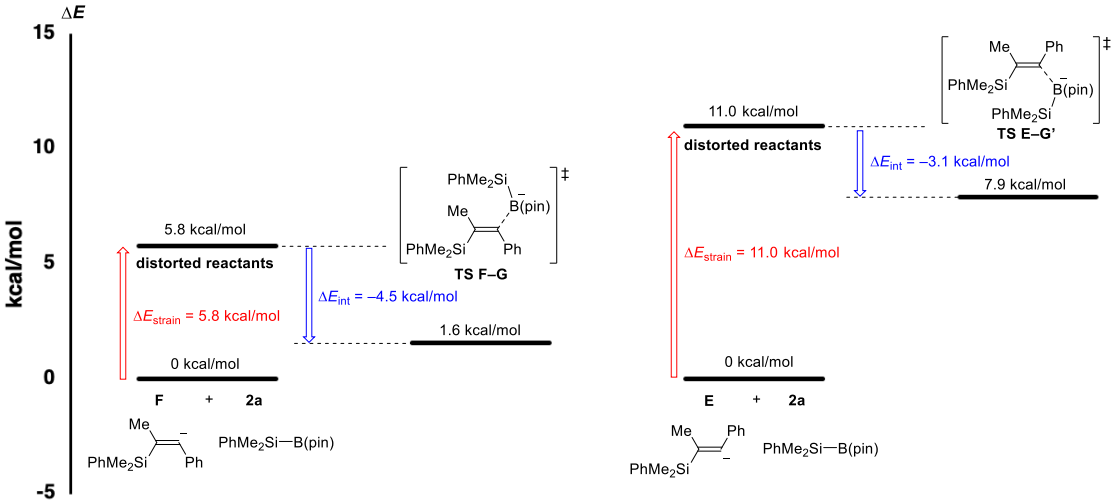

Scheme 11. Plots of distortion, interaction, and activation energies for the transition states **TS F–G** (left) and **TS E–G'** (right).

The overall reaction mechanism proposed by the result of DFT calculations is summarized in Scheme 12. Thus, disilylcuprate **A** undergoes regioselective *syn*-insertion of alkyne **1a**, which is controlled by the electronic and steric effect of an alkyne, to give *syn*-alkenyl(silyl)cuprate **B**. Alkenyl anion equivalent **E** was then generated with the

assistance of NaO*t*Bu, and it isomerizes to *anti*-alkenyl anion **F** via anionic allenic transition state **TS E–F** with the stabilization by conjugation with the benzene ring. Subsequently, **F** reacts with silylboronate **2a** to give silylborated alkene **3aa**. The selectivity between *anti*-borylation from **F** and *syn*-borylation from **E** is controlled by the steric effect.

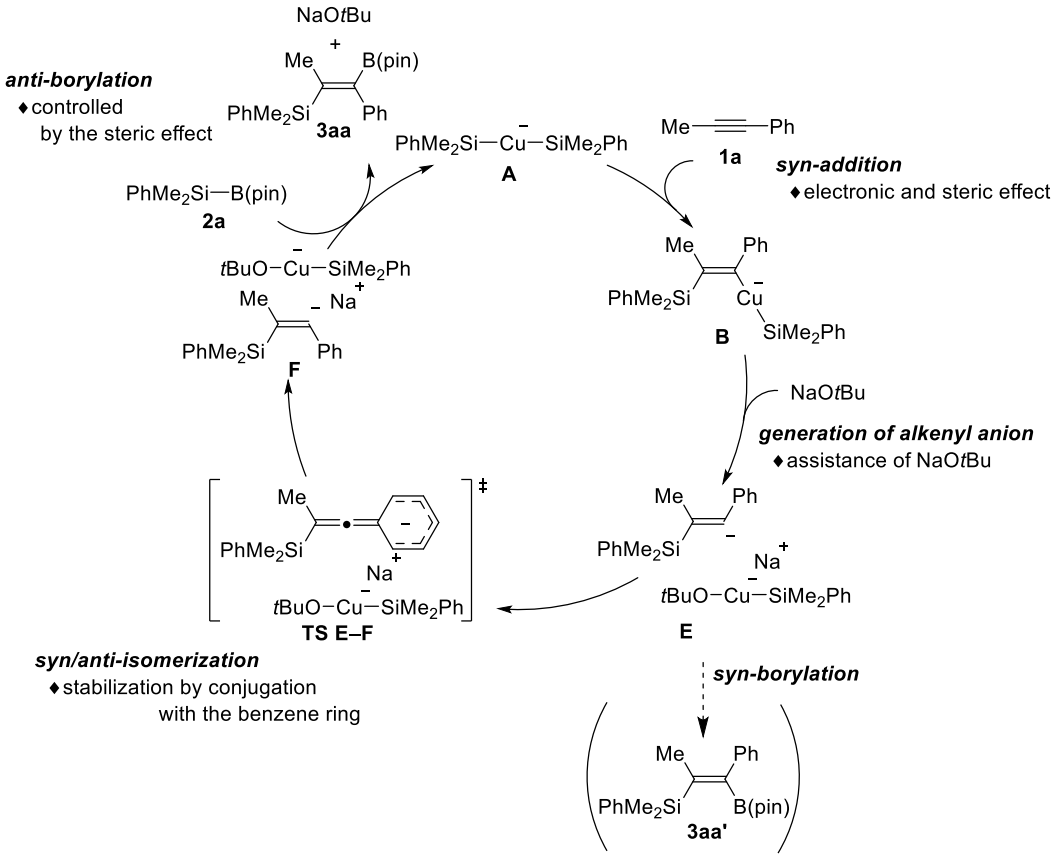

Scheme 12. Catalytic cycle for the copper-catalyzed *anti*-silylboration of alkyne **1a** with **2a** based on DFT calculations.

In this silylboration reaction, alkynes having a bulky alkyl substituent such as 3,3-dimethyl-1-phenyl-1-butyne (**1e**) also gave *anti*-addition product **3ea** selectively as shown in Scheme 2. Even for this bulky substrate, the steric control toward *anti*-addition was found to be operative. Thus, according to the DFT calculations for the reaction of **1e** (Scheme 13), **TS F$_e$–G$_e$** ($\Delta G^{\ddagger}$ = 28.6 kcal/mol) toward *anti*-addition product was found to be energetically more favorable than **TS E$_e$–G'$_e$** ($\Delta G^{\ddagger}$ = 33.6 kcal/mol) toward *syn*-addition product, which is consistent with the experimental result. In addition, the same structural analysis of the borylation transition states was performed and it was suggested that the formation of **3ea** is more favorable than **3ea'** and each bond angle around the alkene is slightly closer to 120° for the transition state toward **3ea** than that toward *syn*-**3ea'** (Table 3).

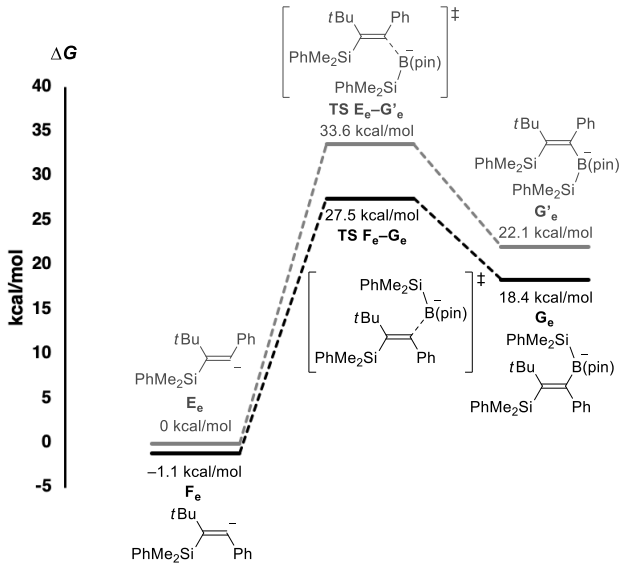

Scheme 13. Calculated borylation pathways for the silylboration of 3,3-dimethyl-1-phenyl-1-butyne (**1e**).

Table 3. Structures of **TS F$_e$–G$_e$** and **TS E$_e$–G'$_e$**.

	TS F$_e$–G$_e$	**TS E$_e$–G'$_e$**
	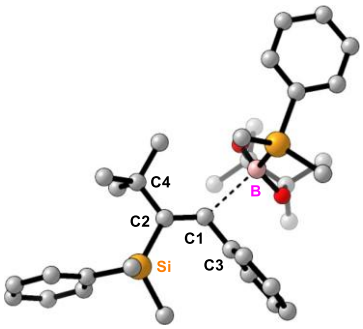	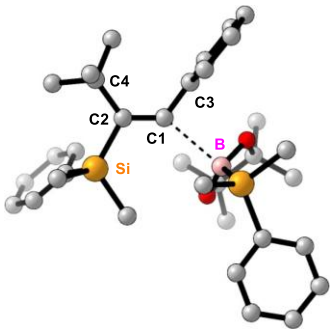
C1–B	2.55 Å	2.57 Å
∠C2–C1–B	138.5°	138.8°
∠C3–C1–B	97.8°	95.9°
∠C2–C1–C3	123.7°	125.3°
∠C4–C2–C1	122.9°	125.3°
∠C4–C2–Si	116.6°	115.6°
∠C1–C2–Si	120.5°	118.9°

With regard to the reaction of dialkylalkynes, the reaction of 2-butyne (dimethylacetylene; **4h**) with silylboronate **2a** was theoretically examined at the *syn*/*anti*-isomerization and borylation steps (Scheme 14). As was the case for 1-phenyl-1-propyne (**1a**), zwitterionic metal carbene or η^2-vinylmetal structures could not be identified as the transition state for the isomerization of *syn*-alkenylcuprate **B$_{4h}$** to *anti*-alkenylcuprate **C$_{4h}$**. Instead, copper-coordinated linear structure **TS B$_{4h}$–C$_{4h}$** was observed with a high activation energy ($\Delta G^{\ddagger}$ = 48.1 kcal/mol). For the path from alkenyl anion **E$_{4h}$**, the isomerization transition state **TS E$_{4h}$–F$_{4h}$** ($\Delta G^{\ddagger}$ = 27.5 kcal/mol) was lower in energy than that of **TS B$_{4h}$–C$_{4h}$**, but *syn*-borylation transition state **TS E$_{4h}$–G'$_{4h}$** from **E$_{4h}$** toward **5ha'** was energetically much lower ($\Delta G^{\ddagger}$ = 20.4 kcal/mol). Thus, in the reaction of dialkylalkynes, *syn*-silylboration proceeds more favorably than *anti*-silylboration. This is consistent with the stereoselectivity switch for the reaction of dialkylacetylenes as shown in eq 1.

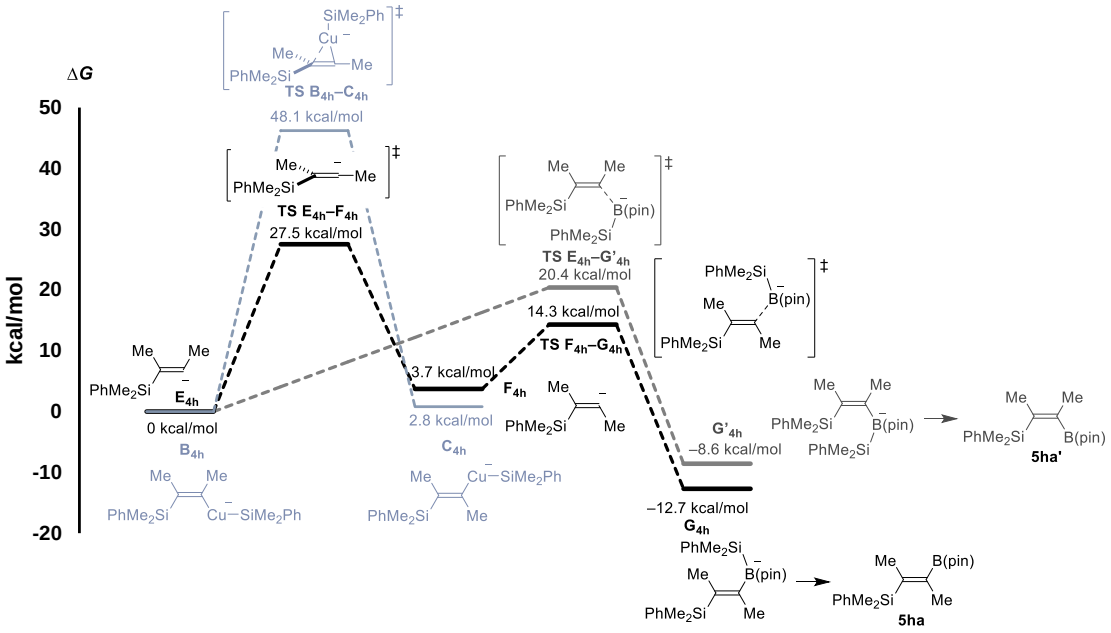

Scheme 14. Calculated borylation pathways for the silylboration of 2-butyne (**4h**).

2.3 Conclusion

The author developed a copper-catalyzed regio- and *anti*-selective addition of silylboronates to unsymmetric internal alkynes to give the corresponding tetrasubstituted alkenes under simple and mild conditions. A variety of alkynes could be employed with high selectivity and the resulting products were further functionalized by utilizing silyl and boryl groups on the alkene, demonstrating the complementary nature of the present catalysis to the existing methods. In addition, the author examined the mechanism of this copper-catalyzed reaction to understand the reaction pathway and the origin of selectivity. As a result, the overall profile of this catalysis for the reaction of 1-phenyl-1-propyne (**1a**) with silylboronate **2a** was elucidated. It was found that the regioselectivity is determined by both electronic and steric effects at the alkyne insertion step, and that the *syn*-to-*anti* isomerization takes place reversibly through an anionic allenic transition state stabilized by the existence of the benzene ring rather than a typical η^2-vinylmetal (metalacyclopropene) species. The *anti*-selectivity was found to be determined at the borylation step with the control by the steric effect of the silyl group introduced on the alkyne carbon. The importance of the aryl group on the alkyne to electronically induce *syn*-to-*anti* isomerization was further confirmed by conducting the reactions with dialkylalkynes for comparison. The results obtained in this study would be highly informative for the development of new catalytic transformations involving *syn*/*anti*-isomerization processes.

2.4 Experimental section

General

All reactions were carried out with standard Schlenk techniques under nitrogen or in a glove box under argon unless otherwise noted. NMR spectra were recorded on JEOL JNM-ECS400 or Agilent Unity-Inova500 spectrometer. High resolution mass spectra were recorded on JEOL JMS700 spectrometer. X-ray crystallographic analysis was performed by RIGAKU XTaLAB P200. Preparative GPC was performed with JAI LaboACE LC-5060 equipped with JAIGEL-2HR columns using $CHCl_3$ as an eluent. Computations were performed using workstation at Rikkyo University, Tokyo, Japan.

Et_3N (FUJIFILM Wako Chemicals) and *i*Pr_2NH (FUJIFILM Wako Chemicals) were distilled over KOH under vacuum. THF (Kanto Chemical; dehydrated), 1,4-dioxane (FUJIFILM Wako Chemicals; dehydrated), Et_2O (FUJIFILM Wako Chemicals: dehydrated), acetonitrile (FUJIFILM Wako Chemicals; dehydrated), methanol (FUJIFILM Wako Chemicals), 1-phenyl-1-propyne (TCI), 1-phenyl-1-pentyne (TCI), diphenylacetylene (TCI), 4-methyl-1-pentyne (TCI), 1-pentyne (TCI), 3-hexyne (TCI), 5-decyne (TCI), iodobenzene (FUJIFILM Wako Chemicals), 1-chloro-4-iodobenzene (TCI), iodoethene (FUJIFILM Wako Chemicals), 3-buten-2-one (TCI), *N*-bromosuccinimide (FUJIFILM Wako Chemicals), hexamethylphosphoric triamide (TCI), (dimethylphenylsilyl)boronic acid pinacol ester (FUJIFILM Wako Chemicals), *n*BuLi (Kanto Chemical; 1.58 M solution in hexane), *t*BuLi (Kanto Chemical; 1.60 M solution in pentane), 1-propynylmagnesium bromide (Aldrich; 0.5 M solution in THF), PPh_3 (FUJIFILM Wako Chemicals), PCy_3 (Aldrich), Xantphos (FUJIFILM Wako Chemicals), 1,10-phenanthroline (Aldrich), P*t*Bu_3•HBF_4 (TCI), LiO*t*Bu (Aldrich), NaO*t*Bu (TCI), KO*t*Bu (Nacalai Tesque), NaOMe (FUJIFILM Wako Chemicals), KOH (FUJIFILM Wako Chemicals), hydrochloric acid (FUJIFILM Wako Chemicals), NaBr (FUJIFILM

Wako Chemicals), CuI (FUJIFILM Wako Chemicals), and $ZnCl_2$ (Kishida Chemical) were used as received.

1d,[26] **1e**,[26] **1g**,[27] **1k**,[28] **1l**,[29] **1m**,[29] **1n**,[29] **1q**,[30] **1t**,[29] **1w**,[31] **4b**,[26] **4c**,[32] **4d**,[32] **4e**,[30] (triethylsilyl)boronic acid pinacol ester,[33] 9-(4-pentyn-1-yl)-9*H*-carbazole,[34] 4-(methoxymethoxy)phenylacetylene,[35] *N*-(4-iodophenyl)-*N*-methylacetamide,[36] 5-boromo-1-methyl-1*H*-indole,[37] (IPr)CuCl,[38] $[Rh(OH)(cod)]_2$,[39] $PdCl_2(MeCN)_2$,[40] $PdCl_2(PPh_3)_2$,[41] $Pd(PPh_3)_4$,[42] and $PdCl_2(dppf)$[43] were synthesized following the literature procedures.

Synthesis of substrates

Representative procedures for substrates:

4-Methyl-1-phenyl-1-pentyne (1c) (CAS 42049-53-6)

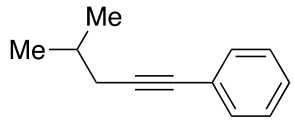

A mixture of 4-methyl-1-pentyne (258 μL, 2.20 mmol), iodobenzene (411 mg, 2.01 mmol), $PdCl_2(PPh_3)_2$ (27.6 mg, 39.3 μmol), CuI (15.2 mg, 79.8 μmol), and Et_3N (836 μL, 6.00 mmol) in THF (4.0 mL) was stirred for 22 h at room temperature. The reaction mixture was directly passed through a pad of silica gel with EtOAc and the solvent was removed under vacuum. The residue was chromatographed on silica gel with hexane and further purified by GPC with $CHCl_3$ to afford compound **1c** as a colorless oil (208 mg, 1.31 mmol; 65% yield).

^{1}H NMR ($CDCl_3$): δ 7.42-7.38 (m, 2H), 7.30-7.24 (m, 3H), 2.30 (d, $^3J_{HH}$ = 6.6 Hz, 2H), 1.91 (sept, $^3J_{HH}$ = 6.6 Hz, 1H), 1.05 (d, $^3J_{HH}$ = 6.6 Hz, 6H). $^{13}C\{^1H\}$ NMR ($CDCl_3$): δ 131.7, 128.3, 127.6, 124.3, 89.5, 81.6, 28.7, 28.4, 22.2.

9-(5-Phenyl-4-pentyn-1-yl)-9*H*-carbazole (1i) (CAS 434935-37-2)

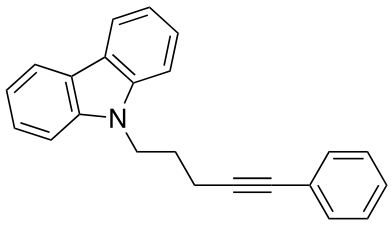

A mixture of 9-(4-pentyn-1-yl)-9*H*-carbazole (524 mg, 2.24 mmol), iodobenzene (457 mg, 2.24 mmol), $Pd(PPh_3)_4$ (86.9 mg, 86.9 μmol), CuI (29.3 mg, 153 μmol), and Et_3N (940 μL, 6.74 mmol) in THF (5.0 mL) was stirred for 19 h at room temperature. The reaction mixture was directly passed through a pad of silica gel with EtOAc and the

solvent was removed under vacuum. The residue was chromatographed on silica gel with CH_2Cl_2/hexane = 1/4 to afford compound **1i** as a white solid (659 mg, 2.13 mmol; 95% yield).

^{1}H NMR ($CDCl_3$): δ 8.11 (d, $^3J_{HH}$ = 7.8 Hz, 2H), 7.52 (d, $^3J_{HH}$ = 8.2 Hz, 2H), 7.49-7.43 (m, 4H), 7.36-7.30 (m, 3H), 7.24 (dd, $^3J_{HH}$ = 7.8 and 6.9 Hz, 2H), 4.53 (t, $^3J_{HH}$ = 6.9 Hz, 2H), 2.46 (t, $^3J_{HH}$ = 6.9 Hz, 2H), 2.20 (quint, $^3J_{HH}$ = 6.8 Hz, 2H). ^{13}C{^{1}H} NMR ($CDCl_3$): δ 140.6, 131.7, 128.5, 128.0, 125.8, 123.8, 123.1, 120.5, 119.1, 108.8, 89.1, 81.9, 41.8, 28.1, 17.3.

1-(4-Chlorophenyl)-1-propyne (1j) (CAS 2809-65-6)

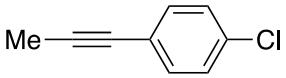

1-Propynylmagnesium bromide (4.40 mL, 2.20 mmol; 0.5 M solution in THF) was added slowly over 6 min with additional THF (5.0 mL) to $ZnCl_2$ (335 mg, 2.46 mmol) at 0 °C, and the mixture was stirred for 30 min at 0 °C. $Pd(PPh_3)_4$ (69.7 mg, 60.3 μmol) and 1-chloro-4-iodobenzene (481 mg, 2.02 mmol) were successively added to it with THF (2.0 mL), and the mixture was stirred for 45 h at 50 °C. The reaction mixture was directly passed through a pad of silica gel with EtOAc and the solvent was removed under vacuum. The residue was chromatographed on silica gel with hexane to afford compound **1j** as a colorless oil (235 mg, 1.57 mmol; 78% yield).

^{1}H NMR ($CDCl_3$): δ 7.31 (d, $^3J_{HH}$ = 8.2 Hz, 2H), 7.25 (d, $^3J_{HH}$ = 8.7 Hz, 2H), 2.04 (s, 3H). ^{13}C{^{1}H} NMR ($CDCl_3$): δ 133.6, 132.9, 128.7, 122.7, 87.1, 78.8, 4.5.

1-(4-(Methoxymethoxy)phenyl)-1-butyne (1p) (CAS 2271220-73-4)

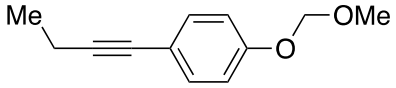

*n*BuLi (1.29 mL, 2.04 mmol; 1.58 M solution in hexane) was added slowly to a solution of *i*Pr$_2$NH (320 μL, 2.20 mmol) in THF (2.0 mL) at −78 °C, and the mixture was stirred for 30 min at −78 °C. The resulting solution was then added slowly over 10 min with additional THF (1.5 mL) to a solution of 4-(methoxymethoxy)phenylacetylene (278 mg, 1.71 mmol) in THF (2.0 mL) at −78 °C, and the mixture was stirred for 1 h at −78 °C. Hexamethylphosphoric triamide (350 μL, 2.04 mmol) and iodoethane (230 μL, 2.78 mmol) were successively added to it, and the mixture was stirred for 30 min at −78 °C and for 12.5 h at room temperature. The reaction was quenched with saturated NH$_4$Claq and this was extracted with Et$_2$O. The organic layer was washed with saturated NaClaq, dried over MgSO$_4$, filtered, and concentrated under vacuum. The residue was chromatographed on silica gel with EtOAc/hexane = 1/20. To remove inseparable remaining 4-(methoxymethoxy)phenylacetylene, this was added to a mixture of *N*-(4-iodophenyl)-*N*-methylacetamide (51.7 mg, 0.188 mmol), Pd(PPh$_3$)$_4$ (11.0 mg, 9.50 μmol), CuI (3.7 mg, 19 μmol) in Et$_3$N (1.0 mL) and THF (1.0 mL), and the resulting mixture was stirred for 44 h at 40 °C. The reaction mixture was directly passed through a pad of silica gel with EtOAc and the solvent was removed under vacuum. The residue was chromatographed on silica gel with EtOAc/hexane = 1/30 to afford compound **1p** as a pale yellow oil (278 mg, 1.46 mmol; 85% yield).

^{1}H NMR (CDCl$_3$): δ 7.32 (d, $^3J_{HH}$ = 9.2 Hz, 2H), 6.94 (d, $^3J_{HH}$ = 8.7 Hz, 2H), 5.16 (s, 2H), 3.47 (s, 3H), 2.40 (q, $^3J_{HH}$ = 7.5 Hz, 2H), 1.22 (t, $^3J_{HH}$ = 7.6 Hz, 3H). ^{13}C{^{1}H} NMR (CDCl$_3$): δ 156.8, 133.0, 117.6, 116.2, 94.5, 90.5, 79.6, 56.2, 14.1, 13.2.

1-Methyl-5-(1-pentynyl)-1*H*-indole (1u) (CAS 2520341-72-2)

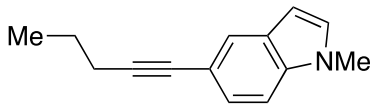

A mixture of 1-pentyne (234 μL, 2.40 mmol), 5-bromo-1-methyl-1*H*-indole (423 mg, 2.01 mmol), $PdCl_2(MeCN)_2$ (15.6 mg, 60.1 μmol), P*t*Bu$_3$•HBF$_4$ (34.8 mg, 0.120 mmol), CuI (7.8 mg, 41 μmol), and *i*Pr$_2$NH (355 μL, 2.53 mmol) in 1,4-dioxane (3.0 mL) was stirred for 2 h at room temperature. The reaction mixture was directly passed through a pad of silica gel with EtOAc and the solvent was removed under vacuum. The residue was chromatographed on silica gel with EtOAc/hexane = 1/20 and further purified by GPC with $CHCl_3$ to afford compound **1u** as an orange oil (261 mg, 1.32 mmol; 66% yield).

^{1}H NMR ($CDCl_3$): δ 7.71 (s, 1H), 7.28 (dd, $^3J_{HH}$ = 8.2 Hz and $^4J_{HH}$ = 1.4 Hz, 1H), 7.22 (d, $^3J_{HH}$ = 8.7 Hz, 1H), 7.04 (d, $^3J_{HH}$ = 3.2 Hz, 1H), 6.44 (d, $^3J_{HH}$ = 3.2 Hz, 1H), 3.77 (s, 3H), 2.42 (t, $^3J_{HH}$ = 7.1 Hz, 2H), 1.66 (sext, $^3J_{HH}$ = 7.2 Hz, 2H), 1.08 (t, $^3J_{HH}$ = 7.3 Hz, 3H). ^{13}C{^{1}H} NMR ($CDCl_3$): δ 136.1, 129.6, 128.4, 125.3, 124.5, 114.8, 109.2, 101.1, 87.4, 82.1, 32.9, 22.6, 21.6, 13.7.

Analytical data for other substrates:

6-Phenyl-1-hexen-5-yne (1f) (CAS 16664-52-1)

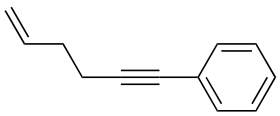

^{1}H NMR ($CDCl_3$): δ 7.43-7.35 (m, 2H), 7.32-7.22 (m, 3H), 5.93 (ddt, $^3J_{HH}$ = 17.0, 10.6, and 6.4 Hz, 1H), 5.13 (dd, $^3J_{HH}$ = 17.1 Hz and $^2J_{HH}$ = 1.4 Hz, 1H), 5.06 (dd, $^3J_{HH}$ = 10.1 Hz and $^2J_{HH}$ = 0.9 Hz, 1H), 2.50 (t, $^3J_{HH}$ = 7.1 Hz, 2H), 2.36 (q, $^3J_{HH}$ = 7.0 Hz, 2H). ^{13}C{^{1}H} NMR ($CDCl_3$): δ 137.1, 131.7, 128.3, 127.7, 124.1, 115.8, 89.7, 81.2, 33.1, 19.4.

4-(*tert*-Butyldimethylsiloxy)-1-phenyl-1-butyne (1h) (CAS 141427-90-9)

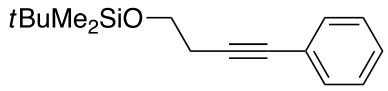

^{1}H NMR ($CDCl_3$): δ 7.41-7.37 (m, 2H), 7.30-7.25 (m, 3H), 3.82 (t, $^{3}J_{HH}$ = 6.9 Hz, 2H), 2.63 (t, $^{3}J_{HH}$ = 7.1 Hz, 2H), 0.92 (s, 9H), 0.10 (s, 6H). ^{13}C{^{1}H} NMR ($CDCl_3$): δ 131.7, 128.3, 127.8, 123.9, 87.3, 81.7, 62.1, 26.1, 24.0, 18.5, −5.1.

***tert*-Butyl 4-(1-pentynyl)benzoate (1o)** (CAS 2474249-77-7)

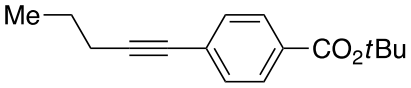

^{1}H NMR ($CDCl_3$): δ 7.89 (d, $^{3}J_{HH}$ = 8.2 Hz, 2H), 7.42 (d, $^{3}J_{HH}$ = 8.2 Hz, 2H), 2.41 (t, $^{3}J_{HH}$ = 7.1 Hz, 2H), 1.64 (sext, $^{3}J_{HH}$ = 7.3 Hz, 2H), 1.59 (s, 9H), 1.06 (t, $^{3}J_{HH}$ = 7.6 Hz, 3H). ^{13}C{^{1}H} NMR ($CDCl_3$): δ 165.5, 131.4, 130.9, 129.4, 128.5, 93.5, 81.3, 80.5, 28.3, 22.2, 21.6, 13.7.

1-(3-Methylphenyl)-1-pentyne (1r) (CAS 1416339-67-7)

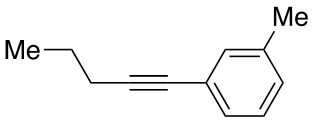

^{1}H NMR ($CDCl_3$): δ 7.23 (s, 1H), 7.20 (d, $^{3}J_{HH}$ = 7.8 Hz, 1H), 7.16 (t, $^{3}J_{HH}$ = 7.3 Hz, 1H), 7.07 (d, $^{3}J_{HH}$ = 7.3 Hz, 1H), 2.38 (t, $^{3}J_{HH}$ = 7.1 Hz, 2H), 2.31 (s, 3H), 1.63 (sext, $^{3}J_{HH}$ = 7.2 Hz, 2H), 1.05 (t, $^{3}J_{HH}$ = 7.3 Hz, 3H). ^{13}C{^{1}H} NMR ($CDCl_3$): δ 137.9, 132.3, 128.7, 128.5, 128.2, 124.0, 90.0, 81.0, 22.4, 21.5, 21.3, 13.7.

3-Methyl-1-(3-*tert*-butoxyphenyl)-1-butyne (1s)

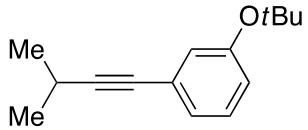

^{1}H NMR ($CDCl_3$): δ 7.16 (t, $^{3}J_{HH}$ = 7.6 Hz, 1H), 7.11 (dt, $^{3}J_{HH}$ = 7.8 Hz and $^{4}J_{HH}$ = 1.4 Hz, 1H), 7.03 (dd, $^{4}J_{HH}$ = 2.3 and 1.8 Hz, 1H), 6.90 (ddd, $^{3}J_{HH}$ = 7.3 Hz and $^{4}J_{HH}$ = 2.3 and 1.4 Hz, 1H), 2.77 (sept, $^{3}J_{HH}$ = 6.9 Hz, 1H), 1.34 (s, 9H), 1.26 (d, $^{3}J_{HH}$ = 6.9 Hz, 6H). $^{13}C\{^{1}H\}$ NMR ($CDCl_3$): δ 155.3, 128.8, 127.3, 126.9, 124.7, 124.0, 95.7, 79.7, 78.8, 29.0, 23.1, 21.2. HRMS (EI) calcd for $C_{15}H_{20}O$ (M^+) 216.1509, found 216.1515.

1-(3-Thienyl)-1-pentyne (1v) (CAS 1221442-00-7)

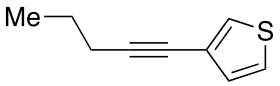

^{1}H NMR ($CDCl_3$): δ 7.34 (dd, $^{4}J_{HH}$ = 3.2 and 0.9 Hz, 1H), 7.22 (dd, $^{3}J_{HH}$ = 5.0 Hz and $^{4}J_{HH}$ = 3.2 Hz, 1H), 7.07 (dd, $^{3}J_{HH}$ = 5.0 Hz and $^{4}J_{HH}$ = 0.9 Hz, 1H), 2.36 (t, $^{3}J_{HH}$ = 6.9 Hz, 2H), 1.62 (sext, $^{3}J_{HH}$ = 7.2 Hz, 2H), 1.04 (t, $^{3}J_{HH}$ = 7.6 Hz, 3H). $^{13}C\{^{1}H\}$ NMR ($CDCl_3$): δ 130.2, 127.6, 125.1, 123.2, 89.9, 75.8, 22.3, 21.5, 13.7.

Catalytic reactions and derivatization

General procedure for Scheme 2.

Compound **1** (0.200 mmol) and (dimethylphenylsilyl)boronic acid pinacol ester (**2a**) (65.4 μL, 0.240 mmol) were added with the aid of THF (0.20 mL) to a mixture of CuI (3.8 mg, 20 μmol) and NaO*t*Bu (7.7 mg, 80 μmol) in THF (0.80 mL), and the resulting mixture was stirred for 20 h at 40 °C. This was passed through a pad of silica gel with EtOAc and the solvent was removed under vacuum. The residue was purified by GPC with $CHCl_3$ to afford compound **3**.

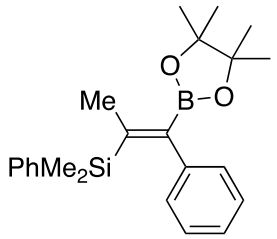

Compound 3aa. Colorless oil. 79% yield (59.5 mg; **3aa**/other isomers > 99/1).

^{1}H NMR ($CDCl_3$): δ 7.46-7.40 (m, 2H), 7.32-7.27 (m, 3H), 7.18-7.12 (m, 3H), 7.07-7.01 (m, 2H), 2.06 (s, 3H), 1.25 (s, 12H), −0.04 (s, 6H). ^{13}C{^{1}H} NMR ($CDCl_3$): δ 149.3, 143.8, 140.1, 133.9, 128.64, 128.62, 127.8, 127.7, 126.3, 83.7, 24.8, 23.9, −1.5. HRMS (FD) calcd for $C_{23}H_{31}BO_2Si$ (M^+) 378.2181, found 378.2200.

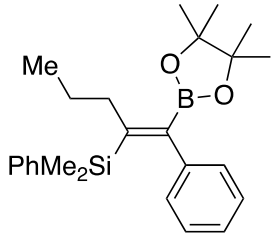

Compound 3ba. Colorless oil. 80% yield (65.3 mg; **3ba**/other isomers = 96/4).

^{1}H NMR ($CDCl_3$): δ 7.42-7.36 (m, 2H), 7.29-7.22 (m, 3H), 7.14-7.09 (m, 3H), 7.04-6.99 (m, 2H), 2.37-2.30 (m, 2H), 1.50-1.39, (m, 2H), 1.23 (s, 12H), 0.86 (t, $^3J_{HH}$ = 7.3 Hz,

3H), 0.00 (s, 6H). $^{13}C\{^{1}H\}$ NMR ($CDCl_3$): δ 153.6, 143.5, 140.5, 134.0, 128.6, 128.5, 127.7, 127.5, 126.2, 83.6, 40.1, 25.1, 24.8, 14.4, −0.6. HRMS (FD) calcd for $C_{25}H_{35}BO_2Si$ (M^+) 406.2494, found 406.2499.

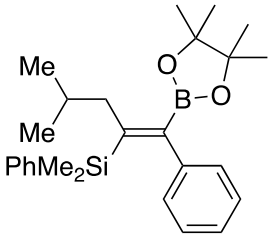

Compound 3ca. Yellow oil. 86% yield (71.4 mg; **3ca**/other isomers = 99/1).

^{1}H NMR ($CDCl_3$): δ 7.36-7.32 (m, 2H), 7.27-7.20 (m, 3H), 7.14-7.09 (m, 3H), 7.04-6.99 (m, 2H), 2.27 (d, $^{3}J_{HH}$ = 7.1 Hz, 2H), 1.73 (sept, $^{3}J_{HH}$ = 6.7 Hz, 1H), 1.22 (s, 12H), 0.87 (d, $^{3}J_{HH}$ = 6.5 Hz, 6H), 0.03 (s, 6H). $^{13}C\{^{1}H\}$ NMR ($CDCl_3$): δ 153.0, 143.8, 140.5, 134.0, 128.7, 128.4, 127.7, 127.4, 126.3, 83.6, 47.5, 28.6, 24.8, 22.6, −0.3. HRMS (FD) calcd for $C_{26}H_{37}BO_2Si$ (M^+) 420.2650, found 420.2669.

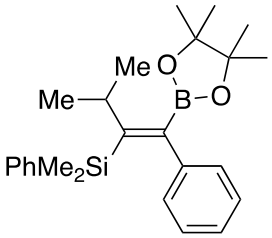

Compound 3da. White solid. 77% yield (61.4 mg; **3da**/other isomers > 99/1).

^{1}H NMR ($CDCl_3$): δ 7.43-7.37 (m, 3H), 7.26-7.20 (m, 3H), 7.14-7.06 (m, 3H), 7.05-6.99 (m, 2H), 2.72 (sept, $^{3}J_{HH}$ = 7.0 Hz, 1H), 1.19 (s, 12H), 1.16 (d, $^{3}J_{HH}$ = 7.4 Hz, 6H), 0.01 (s, 6H). $^{13}C\{^{1}H\}$ NMR ($CDCl_3$): δ 157.0, 143.2, 141.1, 134.0, 128.7, 128.3, 127.7, 127.5, 126.2, 83.7, 37.3, 24.7, 23.4, 0.6. HRMS (FD) calcd for $C_{25}H_{35}BO_2Si$ (M^+) 406.2494, found 406.2492.

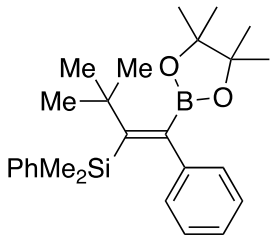

Compound 3ea. The reaction was conducted using **2a** (2.0 equiv), CuI (20 mol%), and NaO*t*Bu (80 mol%) at 10 °C for 70 h. White solid. 85% yield (70.9 mg; **3ea**/other isomers = 94/6).

^{1}H NMR ($CDCl_3$): δ 7.29-7.24 (m, 2H), 7.20-7.12 (m, 3H), 7.02-6.95 (m, 3H), 6.92-6.88 (m, 2H), 1.29 (s, 9H), 1.06 (s, 12H), 0.10 (s, 6H). ^{13}C{^{1}H} NMR ($CDCl_3$): δ 157.8, 142.9, 142.7, 133.6, 129.8, 127.8, 127.34, 127.29, 126.0, 83.6, 39.8, 31.9, 24.4, 3.8. HRMS (FAB) calcd for $C_{26}H_{37}BO_2Si$ (M^+) 420.2650, found 420.2662.

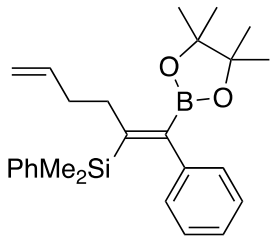

Compound 3fa. Colorless oil. 74% yield (62.3 mg; **3fa**/other isomers = 93/7).

^{1}H NMR ($CDCl_3$): δ 7.41-7.38 (m, 2H), 7.31-7.24 (m, 3H), 7.16-7.12 (m, 3H), 7.04-7.01 (m, 2H), 5.75 (ddt, $^{3}J_{HH}$ = 17.0, 10.2, and 5.0 Hz, 1H), 4.96-4.87 (m, 2H), 2.47-2.40 (m, 2H), 2.18-2.10 (m, 2H), 1.22 (s, 12H), 0.01 (s, 6H). ^{13}C{^{1}H} NMR ($CDCl_3$): 152.9, 143.4, 140.2, 138.7, 134.0, 128.9, 128.6, 127.8, 127.6, 126.3, 114.3, 83.7, 37.1, 36.0, 24.8, −0.7. HRMS (FAB) calcd for $C_{26}H_{36}BO_2Si$ ($M+H^+$) 419.2572, found 419.2590.

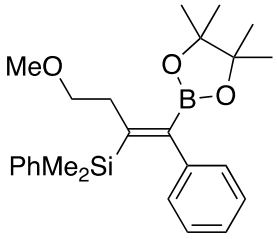

Compound 3ga. The reaction was conducted at 60 °C. Colorless oil. 70% yield (58.9 mg; **3ga**/other isomers = 96/4).

^{1}H NMR ($CDCl_3$): δ 7.41-7.36 (m, 2H), 7.30-7.23 (m, 3H), 7.16-7.11 (m, 3H), 7.04-6.98 (m, 2H), 3.37 (t, $^{3}J_{HH}$ = 7.8 Hz, 2H), 3.25 (s, 3H), 2.69 (dd, $^{3}J_{HH}$ = 8.0 and 7.3 Hz, 2H), 1.23 (s, 12H), 0.01 (s, 6H). ^{13}C{^{1}H} NMR ($CDCl_3$): δ 149.0, 143.4, 140.1, 134.0, 128.6, 128.5, 127.8, 127.6, 126.4, 83.8, 73.5, 58.4, 37.0, 24.8, −0.8. HRMS (FD) calcd for $C_{25}H_{35}BO_3Si$ (M^+) 422.2443, found 422.2461.

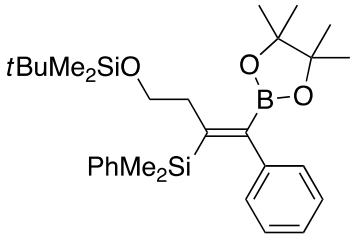

Compound 3ha. The reaction was conducted at 60 °C. Pale yellow solid. 83% yield (86.5 mg; **3ha**/other isomers = 97/3). The reaction using 1.00 g (3.84 mmol) of **1h** gave **3ha** in 79% yield (1.58 g; **3ha**/other isomers = 97/3).

^{1}H NMR ($CDCl_3$): δ 7.42-7.36 (m, 2H), 7.31-7.23 (m, 3H), 7.17-7.11 (m, 3H), 7.05-6.99 (m, 2H), 3.56 (dd, $^{3}J_{HH}$ = 8.7 and 7.3 Hz, 2H), 2.64 (dd, $^{3}J_{HH}$ = 8.3 and 7.8 Hz, 2H), 1.23 (s, 12H), 0.86 (s, 9H), 0.01 (s, 6H), −0.01 (s, 6H). ^{13}C{^{1}H} NMR ($CDCl_3$): δ 149.1, 143.5, 140.2, 134.0, 128.6, 128.5, 127.8, 127.7, 126.4, 83.8, 64.3, 40.7, 26.1, 24.8, 18.4, −0.8, −5.1. HRMS (FD) calcd for $C_{30}H_{47}BO_3Si_2$ (M^+) 522.3151, found 522.3129.

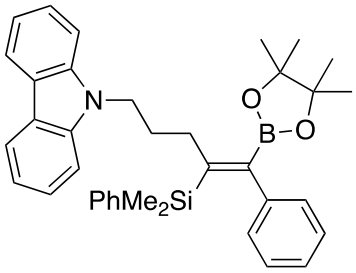

Compound 3ia. The reaction was conducted at 60 °C. White solid. 84% yield (97.1 mg; **3ia**/other isomers = 94/6).

^{1}H NMR ($CDCl_3$): δ 8.08 (d, $^{3}J_{HH}$ = 7.8 Hz, 2H), 7.43 (dd, $^{3}J_{HH}$ = 7.8 and 6.9 Hz, 2H), 7.37 (dd, $^{3}J_{HH}$ = 7.8 and 6.4 Hz, 2H), 7.33-7.23 (m, 5H), 7.21 (dd, $^{3}J_{HH}$ = 7.8 and 7.3 Hz, 2H), 7.18-7.12 (m, 3H), 7.03-6.98 (m, 2H), 4.13 (t, $^{3}J_{HH}$ = 7.3 Hz, 2H), 2.50-2.40 (m, 2H), 1.99-1.89 (m, 2H), 1.07 (s, 12H), −0.03 (s, 6H). ^{13}C{^{1}H} NMR ($CDCl_3$): δ 153.1, 143.4, 140.5, 139.9, 134.0, 128.7, 128.6, 127.8, 127.7, 126.4, 125.6, 123.0, 120.4, 118.8, 108.8, 83.6, 43.3, 35.7, 30.8, 24.6, −0.7. HRMS (FD) calcd for $C_{37}H_{42}BNO_2Si$ (M^+) 571.3072, found 571.3067.

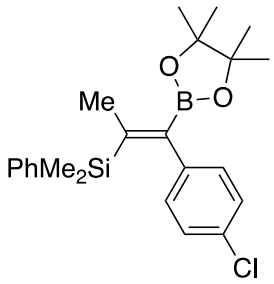

Compound 3ja. The reaction was conducted at 60 °C. White solid. 72% yield (59.8 mg; **3ja**/other isomers > 99/1). The structure was determined by X-ray crystallographic analysis.

^{1}H NMR ($CDCl_3$): δ 7.39-7.35 (m, 2H), 7.32-7.25 (m, 3H), 7.08 (d, $^{3}J_{HH}$ = 8.2 Hz, 2H), 6.92 (d, $^{3}J_{HH}$ = 8.2 Hz, 2H), 2.08 (s, 3H), 1.24 (s, 12H), 0.01 (s, 6H). ^{13}C{^{1}H} NMR ($CDCl_3$): δ 150.9, 142.3, 139.7, 133.8, 132.1, 130.0, 128.7, 127.9, 127.8, 83.8, 24.8, 23.8, −1.4. HRMS (FAB) calcd for $C_{23}H_{30}BClO_2Si$ (M^+) 412.1791, found 412.1802.

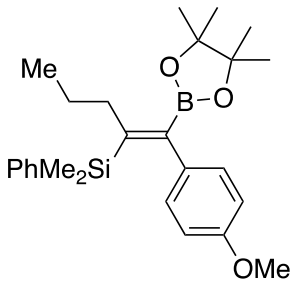

Compound 3ka. Yellow oil. 82% yield (71.5 mg; **3ka**/other isomers = 99/1).

^{1}H NMR ($CDCl_3$): δ 7.41-7.36 (m, 2H), 7.30-7.22 (m, 3H), 6.94-6.89 (m, 2H), 6.67-6.63 (m, 2H), 3.75 (s, 3H), 2.35-2.29 (m, 2H), 1.50-1.37 (m, 2H), 1.23 (s, 12H), 0.86 (t, $^{3}J_{HH}$ = 7.3 Hz, 3H), 0.04 (s, 6H). ^{13}C{^{1}H} NMR ($CDCl_3$): δ 158.3, 153.3, 140.7, 136.0, 134.0, 129.6, 128.4, 127.5, 113.1, 83.6, 55.2, 40.1, 25.1, 24.8, 14.4, −0.5. HRMS (FAB) calcd for $C_{26}H_{37}BO_3Si$ (M^+) 436.2600, found 436.2614.

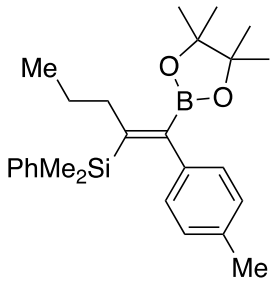

Compound 3la. Colorless oil. 84% yield (70.5 mg; **3la**/other isomers > 99/1).

^{1}H NMR ($CDCl_3$): δ 7.42-7.36 (m, 2H), 7.30-7.21 (m, 3H), 6.96-6.88 (m, 4H), 2.37-2.28 (m, 2H), 2.27 (s, 3H), 1.49-1.38 (m, 2H), 1.23 (s, 12H), 0.85 (t, $^{3}J_{HH}$ = 7.3 Hz, 3H), 0.01 (s, 6H). ^{13}C{^{1}H} NMR ($CDCl_3$): δ 153.3, 140.7, 140.6, 135.6, 134.0, 128.5, 128.40, 128.37, 127.4, 83.6, 40.1, 25.1, 24.8, 21.3, 14.4, −0.5. HRMS (FD) calcd for $C_{26}H_{37}BO_2Si$ (M^+) 420.2650, found 420.2638.

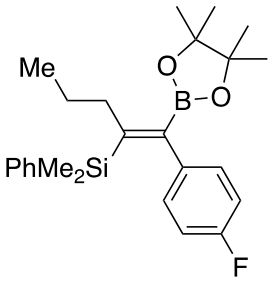

Compound 3ma. The reaction was conducted at 60 °C. Yellow oil. 60% yield (50.7 mg; **3ma**/other isomers = 99/1).

^{1}H NMR ($CDCl_3$): δ 7.36-7.31 (m, 2H), 7.30-7.21 (m, 2H), 6.94-6.89 (m, 2H), 6.80-6.74 (m, 2H), 2.39-2.33 (m, 2H), 1.50-1.40 (m, 2H), 1.22 (s, 12H), 0.88 (t, $^{3}J_{HH}$ = 7.3 Hz, 3H), 0.05 (s, 6H). ^{13}C{^{1}H} NMR ($CDCl_3$): δ 161.8 (d, $^{1}J_{CF}$ = 244 Hz), 154.8, 140.3, 139.4 (d, $^{4}J_{CF}$ = 3.8 Hz), 133.9, 130.1 (d, $^{3}J_{CF}$ = 7.7 Hz), 128.5, 127.6, 114.5 (d, $^{2}J_{CF}$ = 21.1 Hz), 83.7, 40.0, 25.1, 24.8, 14.4, −0.6. HRMS (FD) calcd for $C_{25}H_{34}BFO_2Si$ (M^+) 424.2400, found 424.2410.

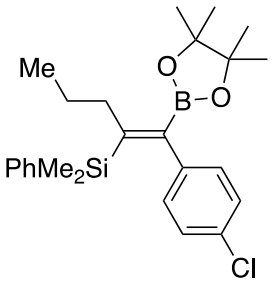

Compound 3na. The reaction was conducted at 60 °C. Yellow oil. 67% yield (58.4 mg; **3na**/other isomers = 99/1).

^{1}H NMR ($CDCl_3$): δ 7.34-7.30 (m, 2H), 7.30-7.20 (m, 2H), 7.04 (d, $^{3}J_{HH}$ = 8.2 Hz, 2H), 6.88 (d, $^{3}J_{HH}$ = 8.2 Hz, 2H), 2.40-2.33 (m, 2H), 1.50-1.39 (m, 2H), 1.22 (s, 12H), 0.88 (t, $^{3}J_{HH}$ = 7.3 Hz, 3H), 0.07 (s, 6H). ^{13}C{^{1}H} NMR ($CDCl_3$): δ 155.2, 142.1, 140.1, 133.8, 132.0, 130.0, 128.5, 127.8, 127.6, 83.7, 40.0, 25.1, 24.8, 14.4, −0.5. HRMS (FD) calcd for $C_{25}H_{34}BClO_2Si$ (M^+) 440.2104, found 440.2123.

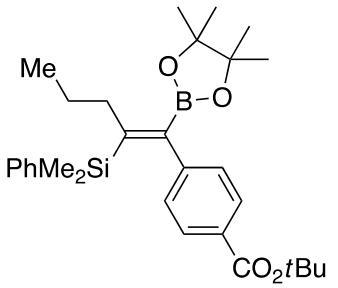

Compound 3oa. The reaction was conducted using **1n** (1.2 equiv) and **2a** (1.0 equiv) at 60 °C. Yellow oil. 53% yield (54.1 mg; **3oa**/other isomers > 99/1).

^{1}H NMR ($CDCl_3$): δ 7.73 (d, $^{3}J_{HH}$ = 7.8 Hz, 2H), 7.37-7.32 (m, 2H). 7.30-7.20 (m, 3H), 7.04 (d, $^{3}J_{HH}$ = 8.2 Hz, 2H), 2.41-2.32 (m, 2H), 1.59 (s, 9H), 1.50-1.38 (m, 2H), 1.21 (s, 12H), 0.87 (t, $^{3}J_{HH}$ = 7.1 Hz, 3H), 0.04 (s, 6H). ^{13}C{^{1}H} NMR ($CDCl_3$): δ 166.1, 155.1, 148.3, 140.0, 133.9, 129.8, 128.9, 128.6, 128.5, 127.6, 83.7, 80.8, 40.1, 28.4, 25.1, 24.8, 14.4, −0.5. HRMS (FD) calcd for $C_{30}H_{43}BO_4Si$ (M^+) 506.3018, found 506.3021.

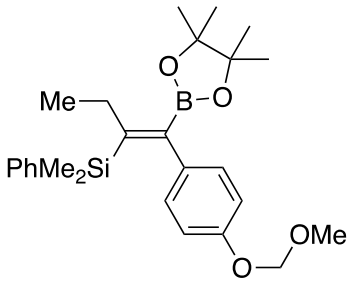

Compound 3pa. Yellow oil. 84% yield (75.5 mg; **3pa**/other isomers > 99/1).

^{1}H NMR ($CDCl_3$): 7.41-7.35 (m, 2H), 7.30-7.21 (m, 3H), 6.91 (d, $^{3}J_{HH}$ = 8.3 Hz, 2H), 6.77 (d, $^{3}J_{HH}$ = 8.2 Hz, 2H), 5.12 (s, 2H), 3.47 (s, 3H), 2.39 (q, $^{3}J_{HH}$ = 7.5 Hz, 2H), 1.23 (s, 12H), 1.03 (t, $^{3}J_{HH}$ = 7.6 Hz, 3H), 0.05 (s, 6H). ^{13}C{^{1}H} NMR ($CDCl_3$): 156.0, 154.8, 140.5, 137.1, 133.9, 129.6, 128.4, 127.5, 115.5, 94.8, 83.6, 56.0, 30.6, 24.7, 16.4, −0.5. HRMS (FD) calcd for $C_{26}H_{37}BO_4Si$ (M^+) 452.2549, found 452.2561.

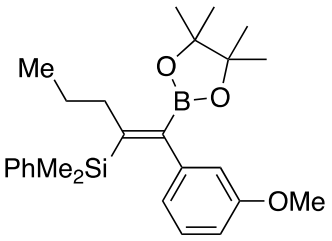

Compound 3qa. Colorless oil. 83% yield (73.1 mg; **3qa**/other isomers = 99/1).

^{1}H NMR ($CDCl_3$): δ 7.43-7.37 (m, 2H), 7.28-7.22 (m, 3H), 7.04 (t, $^{3}J_{HH}$ = 7.8 Hz, 1H), 6.68-6.63 (m, 2H), 6.53 (dd, $^{4}J_{HH}$ = 2.3 and 1.8 Hz, 1H), 3.52 (s, 3H), 2.39-2.31 (m, 2H), 1.51-1.41 (m, 2H), 1.24 (s, 12H), 0.89 (t, $^{3}J_{HH}$ = 7.3 Hz, 3H), 0.04 (s, 6H). ^{13}C{^{1}H} NMR ($CDCl_3$): δ 159.1, 153.2, 144.8, 140.8, 134.0, 128.7, 128.4, 127.6, 121.1, 113.3, 112.9, 83.7, 55.0, 40.3, 25.1, 24.8, 14.4, −0.6. HRMS (FAB) calcd for $C_{26}H_{37}BO_3Si$ (M^+) 436.2600, found 436.2606.

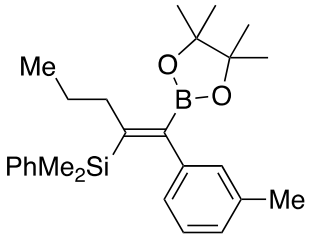

Compound 3ra. Colorless oil. 84% yield (70.2 mg; **3ra**/other isomers = 99/1).

^{1}H NMR ($CDCl_3$): δ 7.39-7.34 (m, 2H), 7.29-7.21 (m, 3H), 7.02 (t, $^{3}J_{HH}$ = 7.6 Hz, 1H), 6.91 (d, $^{3}J_{HH}$ = 7.3 Hz, 1H), 6.83 (d, $^{3}J_{HH}$ = 7.8 Hz, 1H), 6.77 (s, 1H), 2.37-2.30 (m, 2H), 2.14 (s, 3H), 1.52-1.41 (m, 2H), 1.23 (s, 12H), 0.88 (t, $^{3}J_{HH}$ = 7.3 Hz, 3H), 0.01 (s, 6H). ^{13}C{^{1}H} NMR ($CDCl_3$): δ 153.2, 143.3, 140.8, 137.1, 133.9, 129.6, 128.4, 127.51, 127.47, 127.0, 125.5, 83.6, 40.2, 25.1, 24.8, 21.3, 14.4, −0.6. HRMS (FD) calcd for $C_{26}H_{37}BO_2Si$ (M^+) 420.2650, found 420.2655.

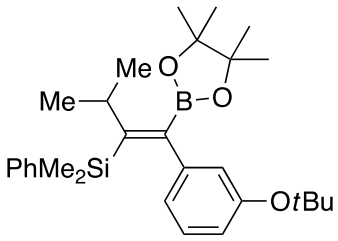

Compound 3sa. White solid. 85% yield (81.6 mg; **3sa**/other isomers > 99/1).

^{1}H NMR ($CDCl_3$): 7.49-7.43 (m, 2H), 7.32-7.23 (m, 3H), 7.06-6.99 (m, 1H), 6.82-6.75 (m, 3H), 2.68 (sept, $^{3}J_{HH}$ = 7.0 Hz, 1H), 1.28 (s, 9H), 1.18 (s, 12H), 1.13 (d, $^{3}J_{HH}$ = 7.3 Hz, 6H), 0.00 (s, 6H). $^{13}C\{^{1}H\}$ NMR ($CDCl_3$): 156.4, 154.9, 144.2, 141.0, 134.2, 128.5, 128.3, 127.5, 124.3, 124.2, 122.4, 83.7, 78.4, 37.1, 29.1, 24.7, 23.4, 0.6. HRMS (FD) calcd for $C_{29}H_{43}BO_3Si$ (M^+) 478.3069, found 478.3064.

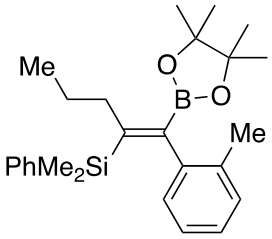

Compound 3ta. Colorless oil. 76% yield (64.0 mg; **3ta**/other isomers = 97/3).

^{1}H NMR ($CDCl_3$): δ 7.33-7.29 (m, 2H), 7.28-7.20 (m, 3H), 7.05 (td, $^{3}J_{HH}$ = 7.3 Hz and $^{4}J_{HH}$ = 1.4 Hz, 1H), 6.99 (t, $^{3}J_{HH}$ = 7.5 Hz, 1H), 6.95 (d, $^{3}J_{HH}$ = 7.3 Hz, 1H), 6.89 (dd, $^{3}J_{HH}$ = 7.3 Hz and $^{4}J_{HH}$ = 1.2 Hz, 1H), 2.47-2.30 (m, 2H), 2.09 (s, 3H), 1.52-1.30 (m, 2H), 1.19 (s, 6H), 1.18 (s, 6H), 0.86 (t, $^{3}J_{HH}$ = 7.3 Hz, 3H), −0.01 (s, 3H), −0.02 (s, 3H). $^{13}C\{^{1}H\}$ NMR ($CDCl_3$): δ 154.7, 143.2, 139.9, 136.0, 133.9, 129.6, 129.4, 128.5, 127.4, 126.5, 125.2, 83.3, 39.1, 25.4, 24.8, 24.8, 24.7, 20.2, 14.4, −1.1, −1.3. HRMS (FD) calcd for $C_{26}H_{37}BO_2Si$ (M^+) 420.2650, found 420.2666.

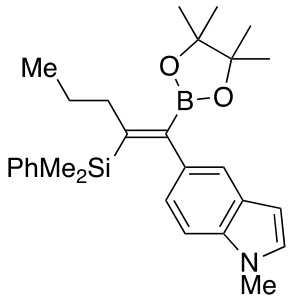

Compound 3ua. The reaction was conducted at 60 °C. Yellow solid. 83% yield (75.4 mg; **3ua**/other isomers = 98/2).

^{1}H NMR ($CDCl_3$): δ 7.41-7.37 (m, 2H), 7.28-7.20 (m, 4H), 7.08 (d, $^{3}J_{HH}$ = 8.3 Hz, 1H), 6.97 (d, $^{3}J_{HH}$ = 3.2 Hz, 1H), 6.93 (dd, $^{3}J_{HH}$ = 8.2 Hz and $^{4}J_{HH}$ = 1.4 Hz, 1H), 6.30 (d, $^{3}J_{HH}$ = 3.2 Hz, 1H), 3.75 (s, 3H), 2.39-2.30 (m, 2H), 1.53-1.41 (m, 2H), 1.23 (s, 12H), 0.88 (t, $^{3}J_{HH}$ = 7.3 Hz, 3H), −0.05 (s, 6H). ^{13}C{^{1}H} NMR ($CDCl_3$): δ 152.3, 141.1, 135.8, 134.8, 134.1, 128.6, 128.24, 128.20 127.4, 122.7, 120.9, 108.3, 101.1, 83.5, 40.3, 32.9, 25.1, 24.8, 14.5, −0.6. HRMS (FAB) calcd for $C_{28}H_{38}BNO_2Si$ (M^+) 459.2759, found 459.2781.

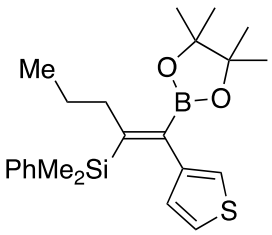

Compound 3va. Yellow viscous oil. 43% yield (35.6 mg; **3va**/other isomers = 97/3).

^{1}H NMR ($CDCl_3$): δ 7.44-7.40 (m, 2H), 7.30-7.25 (m, 3H), 7.06 (dd, $^{3}J_{HH}$ = 4.9 Hz and $^{4}J_{HH}$ = 2.9 Hz, 1H), 6.76 (dd, $^{3}J_{HH}$ = 4.9 Hz and $^{4}J_{HH}$ = 1.2 Hz, 1H), 6.74 (dd, $^{4}J_{HH}$ = 2.9 and 1.2 Hz, 1H), 2.38-2.32 (m, 2H), 1.50-1.40 (m, 2H), 1.25 (s, 12H), 0.88 (t, $^{3}J_{HH}$ = 7.3 Hz, 3H), 0.07 (s, 6H). ^{13}C{^{1}H} NMR ($CDCl_3$): δ 154.8, 143.6, 140.8, 133.9, 128.9, 128.5, 127.6, 124.4, 121.7, 83.7, 40.2, 25.1, 24.8, 14.4, −0.9. HRMS (FAB) calcd for $C_{23}H_{33}BO_2SSi$ (M^+) 412.2058, found 412.2063.

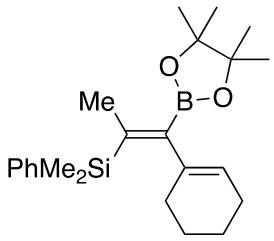

Compound 3wa. White solid. 85% yield (65.0 mg; **3wa**/other isomers = 98/2). The structure was determined by X-ray crystallographic analysis.

^{1}H NMR ($CDCl_3$): δ 7.50-7.44 (m, 2H), 7.32-7.26 (m, 3H), 5.29-5.25 (m, 1H), 1.92 (s, 3H), 1.90-1.80 (m, 4H), 1.43-1.30 (m, 4H), 1.29 (s, 12H), 0.34 (s, 6H). ^{13}C{^{1}H} NMR ($CDCl_3$): δ 145.3, 141.4, 140.7, 133.8, 128.4, 127.6, 123.6, 83.5, 29.0, 25.2, 24.9, 23.3, 22.6, 21.8, −0.5. HRMS (FD) calcd for $C_{23}H_{35}BO_2Si$ (M^+) 382.2494, found 382.2513.

General procedure for Scheme 3.

Compound **2** (0.200 mmol) was added with the aid of THF (0.20 mL) to a mixture of compound **4** (0.240 mmol), CuI (3.8 mg, 20 μmol), and NaO*t*Bu (7.7 mg, 80 μmol) in THF (0.80 mL), and the resulting mixture was stirred for 20 h at 40 °C. This was passed through a pad of silica gel with EtOAc, and the solvent was removed under vacuum. The residue was purified by GPC with $CHCl_3$ to afford compound **5**.

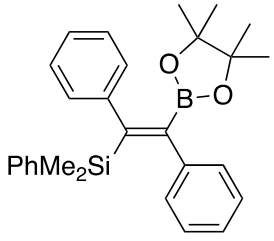

Compound 5aa.[44] (CAS 1443743-82-5) The product was further purified by preparative TLC with EtOAc/hexane = 1/80. White solid. 71% yield (62.6 mg; **5aa**/*syn*-addition product = 99/1).

^{1}H NMR ($CDCl_3$): δ 7.35-7.30 (m, 2H), 7.26-7.19 (m, 5H), 7.19-7.15 (m, 5H), 7.15-7.11 (m, 3H), 0.89 (s, 12H), −0.06 (s, 6H). ^{13}C{^{1}H} NMR ($CDCl_3$): δ 154.0, 145.8, 142.3, 139.6, 134.1, 128.7, 128.6, 128.3, 127.9, 127.6, 127.5, 126.7, 125.8, 83.6, 24.4, −1.1. HRMS (FAB) calcd for $C_{28}H_{33}BO_2Si$ (M^+) 440.2337, found 440.2358.

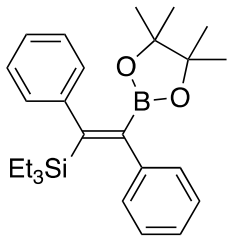

Compound 5ab. The reaction was conducted using **4a** (1.0 equiv) and **2b** (1.2 equiv) at 60 °C. White solid. 66% yield (55.8 mg; **5ab**/*syn*-addition product = 98/2).

^{1}H NMR ($CDCl_3$): δ 7.33-7.28 (m, 4H), 7.28-7.22 (m, 3H), 7.18-7.13 (m, 3H), 0.88 (s, 12H), 0.76 (t, $^3J_{HH}$ = 7.8 Hz, 9H), 0.22 (q, $^3J_{HH}$ = 7.8 Hz, 6H). ^{13}C{^{1}H} NMR ($CDCl_3$): δ 153.6, 146.5, 142.5, 128.4, 128.0, 127.8, 127.6, 126.7, 125.6, 83.4, 24.4, 7.6, 4.5. HRMS (FD) calcd for $C_{26}H_{37}BO_2Si$ (M^+) 420.2650, found 420.2655.

The stereochemistry was confirmed by converting it to a known compound: A mixture of compound **5ab** (8.7 mg, 21 μmol), $[Rh(OH)(cod)]_2$ (1.0 mg, 4.4 μmol Rh), and KOH (4.5 mg, 80 μmol) in 1,4-dioxane (0.30 mL) and H_2O (50 μL) was stirred for 16 h at 60 °C. The reaction mixture was directly passed through a pad of silica gel with EtOAc and the solvent was removed under vacuum. The residue was purified by silica gel preparative TLC with hexane to afford (*Z*)-(1,2-diphenylvinyl)triethylsilane[45] (CAS 91123-51-2) as a colorless oil (3.5 mg; 12 μmol. 57% yield, *Z*/*E* = 86/14).

Z isomer: ^{1}H NMR ($CDCl_3$): δ 7.38-7.27 (m, 8H), 7.24-7.16 (m, 3H), 0.80 (t, $^3J_{HH}$ = 8.0 Hz, 9H), 0.41 (q, $^3J_{HH}$ = 7.9 Hz, 6H).

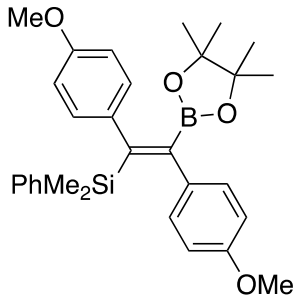

Compound 5ba. Pale yellow solid. 82% yield (81.9 mg; **5ba**/*syn*-addition product > 99/1).

^{1}H NMR ($CDCl_3$): δ 7.37-7.32 (m, 2H), 7.26-7.19 (m, 3H), 7.06 (d, $^3J_{HH}$ = 8.7 Hz, 2H), 7.05 (d, $^3J_{HH}$ = 8.2 Hz, 2H), 6.78 (d, $^3J_{HH}$ = 8.7 Hz, 2H), 6.71 (d, $^3J_{HH}$ = 8.2 Hz, 2H), 3.784 (s, 3H), 3.780 (s, 3H), 0.92 (s, 12H), −0.04 (s, 6H). ^{13}C{^{1}H} NMR ($CDCl_3$): δ 158.6, 158.1, 153.0, 140.0, 138.4, 134.8, 134.0, 129.8, 129.4, 128.5, 127.5, 113.3, 113.1, 83.5, 55.4, 55.2, 24.5, −0.9. HRMS (FAB) calcd for $C_{30}H_{37}BO_4Si$ (M^+) 500.2549, found 500.2577.

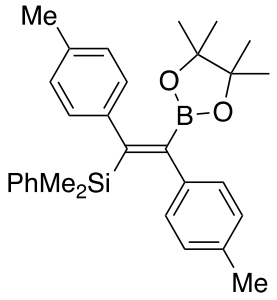

Compound 5ca. White solid. 73% yield (68.6 mg; **5ca**/*syn*-addition product > 99/1).

^{1}H NMR ($CDCl_3$): δ 7.37-7.31 (m, 2H), 7.28-7.18 (m, 3H), 7.06-6.99 (m, 6H), 6.97 (d, $^3J_{HH}$ = 7.8 Hz, 2H), 2.304 (s, 3H), 2.297 (s, 3H), 0.90 (s, 12H), −0.06 (s, 6H). ^{13}C{^{1}H} NMR ($CDCl_3$): δ 153.5, 142.9, 139.9, 139.4, 136.1, 135.2, 134.1, 128.64, 128.55, 128.4, 128.23, 128.20, 127.4, 83.5, 24.4, 21.3, 21.2, −0.9. HRMS (FAB) calcd for $C_{30}H_{37}BO_2Si$ (M^+) 468.2650, found 468.2664.

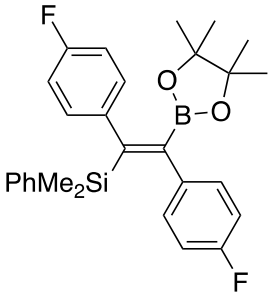

Compound 5da. The reaction was conducted at 60 °C. White solid. 65% yield (62.2 mg; **5da**/*syn*-addition product = 96/4).

^{1}H NMR ($CDCl_3$): δ 7.30-7.19 (m, 5H), 7.11-7.04 (m, 4H), 6.93 (dd, $^{3}J_{HF}$ = 9.2 Hz and $^{3}J_{HH}$ = 8.7 Hz, 2H), 6.86 (t, ^{3}J = 8.7 Hz, 2H), 0.91 (s, 12H), −0.03 (s, 6H). ^{13}C{^{1}H} NMR ($CDCl_3$): δ 162.1 (d, $^{1}J_{CF}$ = 245 Hz), 161.7 (d, $^{1}J_{CF}$ = 244 Hz), 153.9, 141.5 (d, $^{4}J_{CF}$ = 2.9 Hz), 139.1, 138.0 (d, $^{4}J_{CF}$ = 2.9 Hz), 133.9, 130.1 (d, $^{3}J_{CF}$ = 7.7 Hz), 129.8 (d, $^{3}J_{CF}$ = 8.6 Hz), 128.8, 127.6, 114.8 (d, $^{2}J_{CF}$ = 21.1 Hz), 114.5 (d, $^{2}J_{CF}$ = 21.1 Hz), 83.7, 24.4, −1.1. HRMS (FD) calcd for $C_{28}H_{31}BF_2O_2Si$ (M^+) 476.2149, found 476.2148.

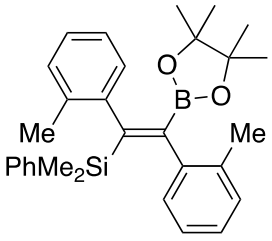

Compound 5ea. The reaction was conducted at 60 °C. White solid. 63% yield (59.2 mg; **5ea**/*syn*-addition product = 97/3).

^{1}H NMR ($CDCl_3$): δ 7.26-7.20 (m, 1H), 7.18-6.96 (m, 12H), 2.24 (s, 3H), 2.20 (bs, 3H), 0.81 (s, 6H), 0.78 (s, 6H), −0.04 (bs, 6H). ^{13}C{^{1}H} NMR ($CDCl_3$): δ 154.0, 144.6, 141.7, 138.6, 136.1, 134.1, 129.6, 129.3, 128.5, 127.2, 126.8, 126.0, 125.3, 124.9, 83.1, 24.4, 24.3, 20.9, 20.3, −1.9. HRMS (FD) calcd for $C_{30}H_{37}BO_2Si$ (M^+) 468.2650, found 468.2650.

General procedure for equation 1

Compound **2a** (0.240 mmol) was added with the aid of THF (0.20 mL) to a mixture of compound **4** (0.200 mmol), CuI (3.8 mg, 20 μmol), and NaO*t*Bu (7.7 mg, 80 μmol) in THF (0.80 mL), and the resulting mixture was stirred for 20 h at 40 °C. This was passed through a pad of silica gel with EtOAc, and the solvent was removed under vacuum. The residue was purified by GPC with $CHCl_3$ to afford compound **5'**.

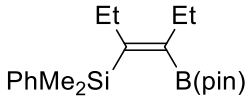

Compound 5fa'. Colorless oil. 54% yield (37.0 mg, 0.107 mmol).

^{1}H NMR ($CDCl_3$): δ 7.54-7.48 (m, 2H), 7.30-7.24 (m, 3H), 2.33 (q, $^3J_{HH}$ = 7.3 Hz, 2H), 2.29 (q, $^3J_{HH}$ = 7.3 Hz, 2H), 1.01 (t, $^3J_{HH}$ = 7.6 Hz, 3H), 1.00 (s, 12H), 0.93 (t, $^3J_{HH}$ = 7.6 Hz, 3H), 0.40 (s, 6H). ^{13}C{^{1}H} NMR ($CDCl_3$): δ 152.8, 141.9, 134.1, 128.2, 127.5, 83.2, 25.3, 25.2, 24.9, 15.1, 15.0, 0.4. HRMS (FD) calcd for $C_{20}H_{33}BO_2Si$ (M^+) 344.2337, found 344.2345.

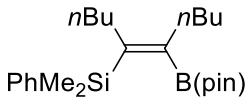

Compound 5ga'. Colorless oil. 52% yield (41.4 mg, 0.103 mmol) (CAS: 185989-99-5).[46]

^{1}H NMR ($CDCl_3$): δ 7.53-7.47 (m, 2H), 7.29-7.24 (m, 3H), 2.29 (t, $^3J_{HH}$ = 7.6 Hz, 2H), 2.23 (t, $^3J_{HH}$ = 7.8 Hz, 2H), 1.38-1.31 (m, 4H), 1.29-1.20 (m, 4H), 0.99 (s, 12H), 0.92 (t, $^3J_{HH}$ = 7.1 Hz, 3H), 0.84 (t, $^3J_{HH}$ = 6.9 Hz, 3H), 0.39 (s, 6H). ^{13}C{^{1}H} NMR ($CDCl_3$): δ 151.5, 141.9, 134.2, 128.2, 127.5, 83.1, 32.8, 32.7, 32.5, 32.1, 25.0, 23.3, 23.2, 14.2, 14.0, 0.4. HRMS (FD) calcd for $C_{24}H_{41}BO_2Si$ (M^+) 400.2963, found 400.2974.

Procedure for Scheme 4a.

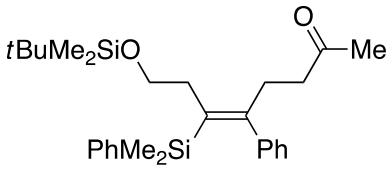

3-Buten-2-one (32.6 μL, 0.40 mmol) and H_2O (0.26 mL) were added to a mixture of compound **3ha** (104 mg, 0.199 mmol), $[Rh(OH)(cod)]_2$ (4.7 mg, 21 μmol Rh), and KOH (22.4 mg, 0.399 mmol) in 1,4-dioxane (1.2 mL), and the resulting mixture was stirred for 13 h at 80 °C. After cooled to room temperature, the reaction mixture was diluted with H_2O and this was extracted with CH_2Cl_2. The organic layer was washed with saturated NaClaq, dried over $MgSO_4$, filtered, and concentrated under vacuum. The residue was purified by silica gel preparative TLC with EtOAc/hexane = 1/20 to afford compound **6** as a colorless viscous oil (67.1 mg, 0.143 mmol; 72% yield).

^{1}H NMR ($CDCl_3$): δ 7.37-7.32 (m, 2H), 7.32-7.24 (m, 3H), 7.22-7.13 (m, 3H), 6.96-6.90 (m, 2H), 3.53 (t, $^3J_{HH}$ = 7.8 Hz, 2H), 2.74 (t, $^3J_{HH}$ = 8.0 Hz, 2H), 2.56 (m, $^3J_{HH}$ = 7.8 Hz, 2H), 2.35 (t, $^3J_{HH}$ = 8.0 Hz, 2H), 2.01 (s, 3H), 0.90 (s, 9H), 0.04 (s, 6H), −0.06 (s, 6H). $^{13}C\{^1H\}$ NMR ($CDCl_3$): δ 208.1, 155.0, 143.9, 140.6, 133.8, 132.1, 129.2, 128.6, 127.9, 127.7, 127.0, 63.0, 42.1, 35.9, 29.9, 29.7, 26.2, 18.5, −0.8, −5.1. HRMS (FD) calcd for $C_{28}H_{42}O_2Si_2$ (M^+) 466.2718, found 466.2716.

Procedure for Scheme 4b.

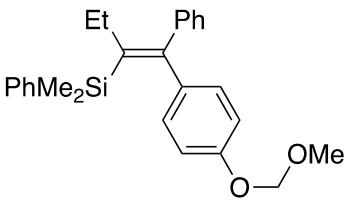

Iodobenzene (114 mg, 0.559 mmol) and compound **3pa** (209 mg, 0.467 mmol) were added with the aid of THF (1.0 mL) to a mixture of $PdCl_2$(dppf) (34.7 mg, 46.7 μmol)

and KOH (134 mg, 2.39 mmol) in THF (3.7 mL) and H_2O (0.47 mL), and the resulting mixture was stirred for 19 h at 60 °C. After cooled to room temperature, the reaction mixture was diluted with H_2O and this was extracted with Et_2O. The organic layer was washed with saturated NaClaq, dried over $MgSO_4$, filtered, and concentrated under vacuum. The residue was purified by silica gel preparative TLC with EtOAc/hexane = 1/80 to afford compound **7** as a pale yellow oil (163 mg, 0.404 mmol; 88% yield).

^{1}H NMR ($CDCl_3$): δ 7.45-7.38 (m, 2H), 7.31-7.25 (m, 5H), 7.20-7.10 (m, 3H), 6.97-6.90 (m, 2H), 6.78-6.72 (m, 2H), 5.10 (s, 2H), 3.45 (s, 3H), 2.19 (q, $^3J_{HH}$ = 7.5 Hz, 2H), 0.84 (t, $^3J_{HH}$ = 7.3 Hz, 3H), 0.13 (s, 6H). ^{13}C{^{1}H} NMR ($CDCl_3$): δ 156.4, 154.6, 144.3, 140.9, 140.6, 138.8, 133.8, 130.5, 128.6, 128.4, 128.2, 127.6, 126.4, 115.6, 94.6, 56.0, 27.1, 15.4, −0.2. HRMS (FD) calcd for $C_{26}H_{30}O_2Si$ (M^+) 402.2010, found 402.2005.

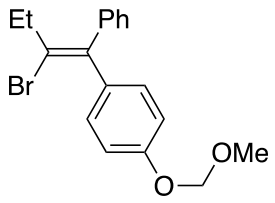

Compound **7** (84.6 mg, 0.210 mmol) was added with the aid of MeCN (1.0 mL) to a mixture of *N*-bromosuccinimide (44.7 mg, 0.251 mmol) in MeCN (1.1 mL), and resulting mixture was stirred for 18 h at room temperature. The solvent was removed under vacuum and the residue was purified by silica gel preparative TLC with EtOAc/hexane = 1/90 to afford compound **8** as a pale yellow oil (72.6 mg, 0.207 mmol; 99% yield).

^{1}H NMR ($CDCl_3$): δ 7.34-7.22 (m, 3H), 7.22-7.13 (m, 4H), 6.99-6.04 (m, 2H), 5.16 (s, 2H), 3.47 (s, 3H), 2.54 (q, $^3J_{HH}$ = 7.3 Hz, 2H), 1.19 (t, $^3J_{HH}$ = 7.3 Hz, 3H). ^{13}C{^{1}H} NMR ($CDCl_3$): δ 156.4, 141.4, 140.8, 136.9, 130.6, 129.4, 128.9, 128.5, 127.3, 115.7, 94.5, 56.2, 32.6, 14.2. HRMS (FAB) calcd for $C_{18}H_{19}BrO_2$ (M^+) 346.0563, found

346.0570.

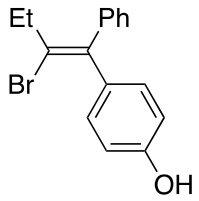

Compound **8** (57.3 mg, 0.165 mmol) was added to a solution of conc. HClaq (43 μL) in MeOH (2.2 mL), and the mixture was stirred for 23 h at room temperature. The reaction mixture was diluted with H_2O and this was extracted with EtOAc. The organic layer was washed with saturated NaClaq, dried over $MgSO_4$, filtered, and concentrated under vacuum. The residue was passed through a pad of silica gel with EtOAc, and the solvent was removed under vacuum. The solid thus obtained was washed with cold hexane to afford compound **9** (CAS 1372129-40-2) as a white solid. (37.0 mg, 0.122 mmol; 74% yield).

^{1}H NMR ($CDCl_3$): δ 7.34-7.22 (m, 3H), 7.18-7.11 (m, 4H), 6.76 (d, $^3J_{HH}$ = 8.3 Hz, 2H), 4.85 (s, 1H), 2.54 (q, $^3J_{HH}$ = 7.2 Hz, 2H), 1.18 (t, $^3J_{HH}$ = 7.3 Hz, 3H). ^{13}C{^{1}H} NMR ($CDCl_3$): δ 154.5, 141.4, 140.7, 135.9, 130.9, 129.4, 128.9, 128.5, 127.3, 115.0, 32.6, 14.2.

Procedure for Scheme 4c.

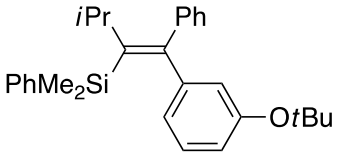

Iodobenzene (166 mg, 0.814 mmol) and compound **3sa** (202 mg, 0.422 mmol) were added with the aid of THF (1.5 mL) to a mixture of $PdCl_2$(dppf) (46.5 mg, 63.5 μmol) and KOH (118 mg, 2.10 mmol) in THF (2.7 mL) and H_2O (0.42 mL), and the resulting mixture was stirred for 32 h at 70 °C. After cooled to room temperature, the reaction

mixture was diluted with H_2O and this was extracted with Et_2O. The organic layer was washed with saturated NaClaq, dried over $MgSO_4$, filtered, and concentrated under vacuum. The residue was purified by silica gel preparative TLC with EtOAc/hexane = 1/90 to afford compound **10** as a colorless viscous oil (148 mg, 0.340 mmol; 81% yield).

^{1}H NMR ($CDCl_3$): δ 7.53-7.47 (m, 2H), 7.33-7.22 (m, 5H), 7.18-7.10 (m, 3H), 6.94 (t, $^3J_{HH}$ = 7.8 Hz, 1H), 6.77-6.72 (m, 2H), 6.70 (dd, $^4J_{HH}$ = 2.3 and 1.8 Hz, 1H), 2.76 (sept, $^3J_{HH}$ = 7.1 Hz, 1H), 1.22 (s, 9H), 1.00 (d, $^3J_{HH}$ = 6.9 Hz, 6H), 0.13 (s, 6H). ^{13}C{^{1}H} NMR ($CDCl_3$): δ 154.9, 154.5, 145.9, 145.2, 144.4, 141.7, 134.2, 128.4, 128.2, 128.1, 127.6, 126.3, 125.1, 124.7, 122.4, 78.4, 34.6, 29.0, 23.3, 1.9. HRMS (EI) calcd for $C_{29}H_{36}OSi$ (M^+) 428.2530, found 428.2516.

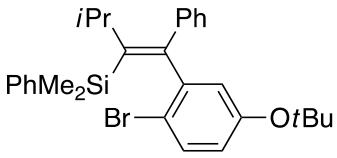

Compound **10** (105 mg, 0.244 mmol) was added with the aid of MeOH (7.0 mL) to a mixture of *N*-bromosuccinimide (131 mg, 0.734 mmol) and NaBr (76.3 mg, 0.741 mmol) in MeOH (3.0 mL), and resulting mixture was stirred for 20 h at room temperature. The solvent was removed under vacuum and the residue was purified by silica gel preparative TLC with EtOAc/hexane = 1/50 to afford compound **11** as a colorless oil (77.8 mg, 0.153 mmol; 63% yield).

^{1}H NMR ($CDCl_3$): δ 7.55-7.50 (m, 2H), 7.34 (d, $^3J_{HH}$ = 7.1 Hz, 2H), 7.32-7.27 (m, 3H), 7.25 (t, $^3J_{HH}$ = 7.7 Hz, 2H), 7.22 (d, $^3J_{HH}$ = 8.5 Hz, 1H), 7.20-7.15 (m, 1H), 6.95 (d, $^4J_{HH}$ = 2.7 Hz, 1H), 6.66 (dd, $^3J_{HH}$ = 8.5 Hz and $^4J_{HH}$ = 2.9 Hz, 1H), 2.82 (sept, $^3J_{HH}$ = 7.0 Hz, 1H), 1.26 (s, 9H), 0.97 (d, $^3J_{HH}$ = 7.0 Hz, 3H), 0.95 (d, $^3J_{HH}$ = 7.0 Hz, 3H), 0.21 (s, 3H), 0.08 (s, 3H). ^{13}C{^{1}H} NMR ($CDCl_3$): δ 154.7, 151.4, 146.2, 145.6, 142.8, 140.7,

134.3, 133.1, 129.2, 128.6, 127.7, 127.6, 127.1, 126.6, 124.2, 118.5, 79.1, 34.0, 28.9, 23.4, 22.8, 1.2, 1.0. HRMS (FD) calcd for $C_{29}H_{35}BrOSi$ (M^+) 506.1635, found 506.1648.

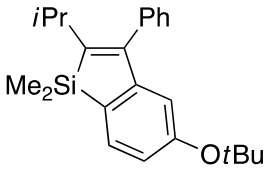

*t*BuLi (201 μL, 0.323 mmol; 1.60 M solution in pentane) was added slowly over 10 min to a solution of compound **11** (74.6 mg, 0.147 mmol) in Et_2O (12 mL) at −75 °C, and the mixture was stirred for 2 h at −75 °C. The reaction was quenched with saturated NH_4Claq and this was extracted with Et_2O. The organic layer was washed with saturated NaClaq, dried over $MgSO_4$, filtered, and concentrated under vacuum. The residue was purified by silica gel preparative TLC with EtOAc/hexane = 1/80 to afford compound **12** as a white solid (39.5 mg, 0.112 mmol; 76% yield).

^{1}H NMR ($CDCl_3$): δ 7.42 (t, $^3J_{HH}$ = 7.3 Hz, 2H), 7.36 (d, $^3J_{HH}$ = 7.8 Hz, 1H), 7.36-7.30 (m, 1H), 7.20-7.15 (m, 2H), 6.77 (dd, $^3J_{HH}$ = 7.8 Hz and $^4J_{HH}$ = 1.8 Hz, 1H), 6.34 (d, $^4J_{HH}$ = 1.8 Hz, 1H), 2.66 (sept, $^3J_{HH}$ = 6.8 Hz, 1H), 1.25 (s, 9H), 1.04 (d, $^3J_{HH}$ = 6.9 Hz, 6H), 0.44 (s, 6H). $^{13}C\{^1H\}$ NMR ($CDCl_3$): δ 157.5, 152.6, 151.6, 151.3, 138.7, 131.5, 131.2, 129.1, 128.4, 126.9, 120.8, 119.3, 78.3, 30.8, 29.0, 24.1, −1.5. HRMS (EI) calcd for $C_{23}H_{30}OSi$ (M^+) 350.2060, found 350.2065.

X-ray crystal structures

Compound 3ja

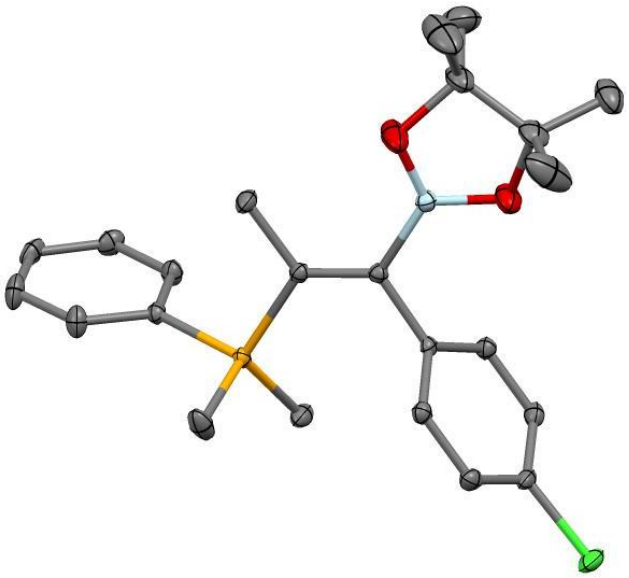

A colorless CH_2Cl_2 solution of compound **3ja** was prepared. Crystals suitable for X-ray analysis were obtained by layering MeOH and slow diffusion of the solvents at room temperature. The crystal structure has been deposited at the Cambridge Crystallographic Data Centre (deposition number: CCDC 2065394). The data can be obtained free of charge via the Internet at www.ccdc.cam.ac.uk/conts/retrieving.html.

Crystal data and structure refinement.

Empirical Formula	$C_{23}H_{30}BClO_2Si$	
Formula Weight	412.82	
Temperature	113 ± 2 K	
Wavelength	0.71075 Å	
Crystal System	Monoclinic	
Space Group	$P2_1/n$	
Unit Cell Dimensions	a = 6.3248(5) Å	α = 90°
	b = 24.8980(19) Å	β = 92.294(2)°

	c = 14.6529(11) Å γ = 90°
Volume	2305.6(3) Å^3
Z Value	4
Calculated Density	1.189 g/cm^3
Absorption coefficient	0.233 mm^{-1}
F(000)	880
Crystal size	0.250 × 0.150 × 0.150 mm
Theta Range for Data Collection	3.228–27.513°
Index Ranges	−8 ≤ h ≤ 7, −31 ≤ k ≤ 32, −19 ≤ l ≤ 17
Reflections Collected	42877
Independent Reflections	5283 [R(int) = 0.0289]
Completeness to Theta = 25.242°	99.7%
Absorption Correction	Semi-empirical from equivalents
Max. and Min. Transmission	0.966 and 0.944
Refinement Method	Full-matrix least-squares on F^2
Data / Restraints / Parameters	5283 / 0 / 260
Goodness-of-Fit on F^2	1.034
Final R Indices [I>2sigma(I)]	R_1 = 0.0615, wR_2 = 0.1739
R Indices (All Data)	R_1 = 0.0681, wR_2 = 0.1807
Largest Diff. Peak and Hole	1.943 and −0.721 e$^-$/Å^3

Compound 3wa

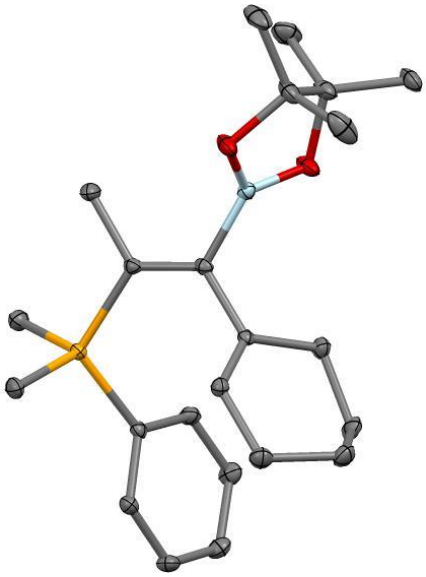

A yellow Et_2O solution of compound **3wa** was prepared. Crystals suitable for X-ray analysis were obtained by layering MeOH and slow diffusion of the solvents at room temperature. The crystal structure has been deposited at the Cambridge Crystallographic Data Centre (deposition number: CCDC 2065393). The data can be obtained free of charge via the Internet at www.ccdc.cam.ac.uk/conts/retrieving.html.

Crystal data and structure refinement.

Empirical Formula	$C_{23}H_{35}BO_2Si$	
Formula Weight	382.41	
Temperature	113 ± 2 K	
Wavelength	0.71075 Å	
Crystal System	Triclinic	
Space Group	$P\bar{1}$	
Unit Cell Dimensions	a = 6.5529(9) Å	α = 101.591(3)°
	b = 10.7620(16) Å	β = 91.243(3)°
	c = 16.245(2) Å	γ = 95.975(4)°

Volume	1115.1(3) Å^3
Z Value	2
Calculated Density	1.139 g/cm^3
Absorption coefficient	0.120 mm^{-1}
F(000)	416
Crystal size	0.150 × 0.050 × 0.050 mm
Theta Range for Data Collection	3.129–27.513°
Index Ranges	$-8 \leq h \leq 8$, $-13 \leq k \leq 13$, $-21 \leq l \leq 19$
Reflections Collected	21005
Independent Reflections	5094 [*R*(int) = 0.0489]
Completeness to Theta = 25.242°	99.7%
Absorption Correction	Semi-empirical from equivalents
Max. and Min. Transmission	0.994 and 0.982
Refinement Method	Full-matrix least-squares on F^2
Data / Restraints / Parameters	5094 / 0 / 251
Goodness-of-Fit on F^2	1.030
Final *R* Indices [*I*>2sigma(*I*)]	R_1 = 0.0454, wR_2 = 0.1181
R Indices (All Data)	R_1 = 0.0669, wR_2 = 0.1257
Largest Diff. Peak and Hole	0.813 and −0.305 e$^-$/Å^3

2.5 References

[1] For reviews: (a) Polák, P.; Vánová, H.; Dvorák, D.; Tobrman, T. *Tetrahedron Lett*. **2016**, *57*, 3684–3693. (b) Negishi, E.-I.; Huang, Z.; Wang, G.; Mohan, S.; Wang, C.; Hattori, H. *Acc. Chem. Res*. **2008**, *41*, 1474–1485. (c) Flynn, A. B.; Ogilvie, W. W. *Chem. Rev*. **2007**, *107*, 4698–4745. (d) Reiser, O. *Angew. Chem.*, *Int. Ed*. **2006**, *45*, 2838–2840.

[2] For reviews: (a) Feng, J.-J.; Mao, W.; Zhang, L.; Oestreich, M. *Chem. Soc. Rev*. **2021**, *50*, 2010–2073. (b) Oestreich, M.; Hartmann, E.; Mewald, M. *Chem. Rev*. **2013**, *113*, 402–441. (c) Suginome, M.; Ohmura, T. In *Boronic Acids, 2nd ed.*, Hall, D. G. Ed., Wiley-VCH, Weinheim, **2011**; pp. 171–212. (d) Ohmura, T.; Suginome, M. *Bull. Chem. Soc. Jpn.* **2009**, *82*, 29–49.

[3] (a) Suginome, M.; Nakamura, H.; Ito, Y. *Chem. Commun*. **1996**, 2777–2778. (b) Suginome, M.; Matsuda, T.; Nakamura, H.; Ito, Y. *Tetrahedron* **1999**, *55*, 2192–8800. (c) Ansell, M. B.; Spencer, J.; Navarro, O. *ACS Catal*. **2016**, *6*, 2192–2196. (d) Morimasa, Y.; Kabasawa, K.; Ohmura, T.; Suginome, M. *Asian J. Org. Chem.* **2019**, *8*, 1092–1096. (e) Zhao, M.; Shan, C.-C.; Wang, Z.-L.; Yang, C.; Fu, Y.; Xu, Y.-H. *Org. Lett.* **2019**, *21*, 6016–6020.

[4] Nagao, K.; Ohmiya, H.; Sawamura, M. *Org. Lett*. **2015**, *17*, 1304–1307.

[5] Fritzemeier, R.; Santos, W. L. *Chem. Eur. J*. **2017**, *23*, 15534–15537.

[6] For addition to terminal alkynes: Ohmura, T.; Oshima, K.; Suginome, M. *Chem. Commun.* **2008**, 1416–1418.

[7] A similar transformation reaction which has recently been reported: Ohmura, T.; Takaoka, Y.; Suginome, M. *Chem. Commun*. **2021**, *57*, 4670–4673.

[8] The structures of **3ja** and **3wa** were determined by X-ray crystallographic analysis. CCDC 2065393 and 2065394 contain the supplementary crystallographic data.

These data can be obtained free of charge via www.ccdc.cam.ac.uk/data_request/cif, or by emailing data_request@ccdc.cam.ac.uk, or by contacting The Cambridge Crystallographic Data Centre, 12 Union Road, Cambridge CB2 1EZ, UK; fax: +44 1223 336033.

[9] For the synthesis of this type of compounds via a palladium-catalyzed *syn*-selective silylboration of alkynylboronates: Jiao, J.; Nakajima, K.; Nishihara, Y. *Org. Lett.* **2013**, *15*, 3294–3297.

[10] For reviews on rhodium-catalyzed 1,4-addition: (a) Berthon-Gelloz, G.; Hayashi, T. in *Boronic Acids, 2nd ed.*, Hall, D. G. Ed., Wiley-VCH, Weinheim, **2011**; pp. 263–313. (b) Edwards, H. J.; Hargrave, J. D.; Penrose, S. D.; Frost, C. G. *Chem. Soc. Rev*. **2010**, *39*, 2093–2105. (c) Hayashi, T.; Yamasaki, K. *Chem. Rev*. **2003**, *103*, 2829–2844. (d) Fagnou, K.; Lautens, M. *Chem. Rev*. **2003**, *103*, 169–196.

[11] Matsumoto, K.; Shindo, M. *Adv. Synth. Catal*. **2012**, *354*, 642–650.

[12] Miller, R. B.; Tsang, T. *Tetrahedron Lett*. **1988**, *29*, 6715–6718.

[13] (a) Konovalov, A. I.; Benet-Buchholz, J.; Martin, E.; Grushin, V. V. *Angew. Chem., Int. Ed.* **2013**, *52*, 11637–11641. (b) Serizawa, H.; Aikawa, K.; Mikami, K. *Chem. Eur. J.* **2013**, *19*, 17692–17697.

[14] (a) Ito, H.; Horita, Y.; Yamamoto, E. *Chem. Commun*. **2012**, *48*, 8006–8008. See also: (b) Wu, H.; Garcia, J. M.; Haeffner, F.; Radomkit, S.; Zhugralin, A. R.; Hoveyda, A. H. *J. Am. Chem. Soc*. **2015**, *137*, 10585–10602.

[15] (a) Xuan, Q.-Q.; Ren, C.-L.; Liu, L.; Wang, D.; Li, C.-J. *Org. Biomol. Chem.* **2015**, *13*, 5871–5874. (b) Liang, H.; Ji, Y.-X.; Wang, R.-H.; Zhang, Z.-H.; Zhang, B. *Org. Lett*. **2019**, *21*, 2750–2754. (c) Ibáñez-Ibáñez, L.; Lázaro, A.; Mejuto, C.; Crespo, M.; Vicent, C.; Rodríguez, L.; Mata, J. *J. Catal*. **2023**, *428*, 115155.

[16] Gaussian 16, Revision C.01, Frisch, M. J.; Trucks, G. W.; Schlegel, H. B.; Scuseria,

G. E.; Robb, M. A.; Cheeseman, J. R.; Scalmani, G.; Barone, V.; Petersson, G. A.; Nakatsuji, H.; Li, X.; Caricato, M.; Marenich, A. V.; Bloino, J.; Janesko, B. G.; Gomperts, R.; Mennucci, B.; Hratchian, H. P.; Ortiz, J. V.; Izmaylov, A. F.; Sonnenberg, J. L.; Williams-Young, D.; Ding, F.; Lipparini, F.; Egidi, F.; Goings, J.; Peng, B.; Petrone, A.; Henderson, T.; Ranasinghe, D.; Zakrzewski, V. G.; Gao, J.; Rega, N.; Zheng, G.; Liang, W.; Hada, M.; Ehara, M.; Toyota, K.; Fukuda, R.; Hasegawa, J.; Ishida, M.; Nakajima, T.; Honda, Y.; Kitao, O.; Nakai, H.; Vreven, T.; Throssell, K.; Montgomery, J. A. Jr.; Peralta, J. E.; Ogliaro, F.; Bearpark, M. J.; Heyd, J. J.; Brothers, E. N.; Kudin, K. N.; Staroverov, V. N.; Keith, T. A.; Kobayashi, R.; Normand, J.; Raghavachari, K.; Rendell, A. P.; Burant, J. C.; Iyengar, S. S.; Tomasi, J.; Cossi, M.; Millam, J. M.; Klene, M.; Adamo, C.; Cammi, R.; Ochterski, J. W.; Martin, R. L.; Morokuma, K.; Farkas, O.; Foresman, J. B.; Fox, D. J. Gaussian, Inc., Wallingford CT, 2019.

[17] (a) Becke, A. D. *J. Chem. Phys.* **1993**, *98*, 5648–5652. (b) Lee, C.; Yang, W.; Parr, R. G. *Phys. Rev. B* **1998**, *37*, 785–789. (c) Stephens, P. J.; Devlin, F. J.; Chabalowski, C. F.; Frisch, M. J. *J. Phys. Chem.* **1994**, *98*, 11623–11627.

[18] Marenich, A. V.; Cramer, C. J.; Truhlar, D. G. *J. Phys. Chem. B* **2009**, *113*, 6378–6396.

[19] CYLview20; Legault, C. Y. Université de Sherbrooke, 2020 (http://www.cylview.org).

[20] (a) Ojima, I.; Clos, N.; Donovan, R. J.; Ingallina, P. *Organometallics* **1990**, *9*, 3127–3133. (b) Tanke, R. S.; Crabtree, R. H. *J. Am. Chem. Soc.* **1990**, *112*, 7984–7989. (c) Zell, D.; Kingston, C.; Jermaks, J.; Smith, S. R.; Seeger, N.; Wassmer, J.; Sirois, L. E.; Han, C.; Zhang, H.; Sigman, M. S.; Gosselin, F. *J. Am. Chem. Soc.* **2021**, *143*, 19078–19090. (d) Shan, C.; He, M.; Luo, X.; Li, R.; Zhang, T. *Org. Chem. Front.*

2023, *10*, 4243–4249. (e) Chandrasekaran, R.; Selvam, K.; Rajeshkumar, T.; Chinnusamy, T.; Maron, L.; Rasappan, R. *Angew. Chem., Int. Ed.* **2024**, *63*, e202318689. (f) Lv, W.; Liu, S.; Chen, Y.; Wen, S.; Lan, Y.; Cheng, G. *ACS Catal.* **2020**, *10*, 10516–10522. (g) Zhou, F.; Shi, W.; Liao, X.; Yang, Y.; Yu, Z.-X.; You, J. *ACS Catal.* **2022**, *12*, 676–686. (h) Yan, X.; Yang, M.; She, Y.-B.; Yang, Y.-F. *Dalton Trans.* **2023**, *52*, 737–746. (i) Sánchez-Page, B.; Munarriz, J.; Jiménez, M. V.; Pérez-Torrente, J. J.; Blasco, J.; Subias, G.; Passarelli, V.; Álvarez, P. *ACS Catal.* **2020**, *10*, 13334–13351. (j) Pérez-Torrente, J. J.; Nguyen, D. H.; Jiménez, M. V.; Modrego, F. J.; Puerta-Oteo, R.; Gómez-Bautista, D.; Iglesias, M.; Oro. L. A. *Organometallics* **2016**, *35*, 2410–2422. (k) Chung, L. W.; Wu, Y.-D.; Trost, B. M.; Ball, Z. T. *J. Am. Chem. Soc.* **2003**, *125*, 11579–11582. (l) Ding, S.; Song, L.-J.; Chung, L. W.; Zhang, X.; Sun, J.; Wu, Y.-D. *J. Am. Chem. Soc.* **2013**, *135*, 13835–13842.

[21] (a) Schleyer, P. V. R.; Clark, T.; Kos, A. J.; Spitznagel, G. W.; Rohde, C.; Arad, D.; Houk, K. N.; Rondan, N. G. *J. Am. Chem. Soc.* **1984**, *106*, 6467–6475. (b) Wetzel, D. M.; Brauman, J. I. *J. Am. Chem. Soc.* **1988**, *110*, 8333–8336. (c) Brinkman, E. A.; Berger, S.; Brauman, J. I. *J. Am. Chem. Soc.* **1994**, *116*, 8304–8310.

[22] (a) Allen, S. R.; Beevor, R. G.; Green, M.; Norman, N. C.; Orpen, A. G.; Williams, I. D. *J. Chem. Soc., Dalton Trans*. **1985**, 435–450. (b) Frohnapfel, D. S.; Templeton, J. L. *Coord. Chem. Rev.* **2000**, *206–207*, 199–235. (c) Brower, D. C.; Birdwhistell, K. R.; Templeton, J. L. *Organometallics* **1986**, *5*, 94–98.

[23] (a) Curtin, D. Y.; Crump, J. W. *J. Am. Chem. Soc.* **1958**, *80*, 1922–1926. (b) Knorr, R.; Menke, T.; Behringer, C.; Ferchland, K.; Mehlstäubl, J.; Lattke, E. *Organometallics* **2013**, *32*, 4070–4081. (c) Yamaguchi, H.; Takahashi, F.; Kurogi, T.; Yorimitsu, H. *Synthesis* **2024**, *56*, DOI: 10.1055/a-2326-6416.

[24] (a) Haszeldine, R. N.; Parish, R. V.; Setchfield, J. H.; *J. Organomet. Chem.* **1973**, *57*, 279–285. (b) Kapoor, P. N.; Kakkar, R.; *J. Mol. Struct. (Theochem)* **2004**, *679*, 149–156. See also: (c) Gao, J.; Ge, Y.; He, C. *Chem. Soc. Rev.* **2024**, *53*, 4648–4673.

[25] (a) Bickelhaupt, F. M. *J. Comput. Chem.* **1999**, *20*, 114–128. (b) Bickelhaupt, F. M.; Houk, K. N. *Angew. Chem., Int. Ed.* **2017**, *56*, 10070–10086. (c) Levandowski, B. J.; Houk, K. N. *J. Org. Chem.* **2015**, *80*, 3530–3537.

[26] Rami, F.; Bächtle, R.; Plietker, B. *Catal. Sci. Technol.* **2020**, *10*, 1492–1497.

[27] Chen, J.; Chen, C.; Chen, J.; Wang, G.; Qu, H. *Chem. Commun.* **2015**, *51*, 1356–1359.

[28] Walkinshaw, A. J.; Xu, W.; Suero, M. G.; Gaunt, M. J. *J. Am. Chem. Soc*. **2013**, *135*, 12532–12535.

[29] Wang, X.; Studer, A. *J. Am. Chem. Soc.* **2016**, *138*, 2977–2980.

[30] Siebeneicher, H.; Doye, S. *Eur. J. Org. Chem.* **2002**, 1213–1220.

[31] Tang, X.; Woodward, S.; Krause, N. *Eur. J. Org. Chem.* **2009**, *2009*, 2836–2844.

[32] Yang, W.; Chen, Y.; Yao, Y.; Yang, X.; Lin, Q.; Yang, D. *J. Org. Chem.* **2019**, *84*, 11080–11090.

[33] Shishido, R.; Uesugi, M.; Takahashi, R.; Mita, T.; Ishiyama, T.; Kubota, K.; Ito, H. *J. Am. Chem. Soc.* **2020**, *142*, 14125–14133.

[34] Jadhav, S. A.; Maccagno, M. *Chem. Pap*. **2014**, *68*, 239–245.

[35] Schmidt, B.; Riemer, M.; Schilde, U. *Eur. J. Org. Chem.* **2015**, *2015*, 7602–7611.

[36] Jakobsson, J. E.; Grønnevik, G.; Rafique, W.; Hartvig, K.; Riss, P. J. *Eur. J. Org. Chem.* **2018**, *2018*, 3701–3704.

[37] Song, J.; Cui, J.; Liang, H.; Liu, Q.; Dong, Y.; Liu, H. P. *Asian J. Org. Chem.* **2018**, *7*, 341–345.

[38] Jurkauskas, V.; Sadighi, J. P.; Buchwald, S. L. *Org. Lett.* **2003**, *5*, 2417–24240.

[39] Uson, R.; Oro, L. A.; Cabeza, J. A. *Inorg*. *Synth*. **1985**, *23*, 126–130.

[40] Mathews, C. J.; Smith, P. J.; Welton, T. *J. Mol. Catal. A: Chem.* **2004**, *214*, 27–32.

[41] Mason, M. R.; Verkade, J. G. *Organometallics* **1992**, *11*, 2212–2220.

[42] Coulson, D. R.; Satek, L. C.; Grim, S. O. *Inorg. Synth*. **1972**, *13*, 121–124.

[43] Hayashi, T.; Konishi, M.; Kumada, M. *Tetrahedron Lett.* **1979**, 1871–1874.

[44] Jiao, J.; Hyodo, K.; Hu, H.; Nakajima, K.; Nishihara, Y. *J. Org. Chem.* **2014**, *79*, 285–295.

[45] (a) Yang, X.; Wang, C. *Angew. Chem.*, *Int. Ed.* **2018**, *57*, 923–928. For *E* isomer: (b) Belger, C.; Plietker, B. *Chem. Commun.* **2012**, *48*, 5419–5421.

[46] Suginome, M.; Matsuda, T.; Nakamura, H.; Ito, Y. *Tetrahedron* **1999**, *55*, 8787–8800.

Chapter 3

Nucleophilic Substitution at Unactivated Arene C–H: Copper-Catalyzed *anti*-Selective Silylative Cyclization of Substituted Benzylacetylenes

3.1 Introduction

For the synthesis of substituted aromatic organic compounds, transition-metal-catalyzed carbon–carbon bond formation at an arene C–H bond has become a common synthetic strategy in modern organic chemistry.[1] Among the various reported methods, one of the most typical approaches is to utilize an arene as a nucleophilic component to form a new bond with a carbon electrophile along with a formal release of H^+ (Scheme 1a).[2] Although this process is attractive in view of its redox neutral nature, the reaction partner is inherently limited. To partially solve this problem, carbon–carbon bond formation of an arene with a nucleophile has also been achieved by conducting the reaction in the presence of a stoichiometric oxidant (Scheme 1b).[2,3] On the other hand, if the arene C–H bond can be directly activated as an electrophile by the release of H^- without using oxidants or extra hydride scavengers, C–H bond functionalization with a nucleophile could be achieved in a more facile and economical way (Scheme 1c). Although this mode of C–H bond functionalization of arenes has been reported for borylation[4] and silylation,[5] it is significantly much less explored for the carbon–carbon bond-forming reaction. Yoshikai *et al*. reported an iron-catalyzed synthesis of naphthalene derivatives by the reaction of arylindium reagents with alkynes, and they proposed electrophilic activation of an arene C–H bond through the formation of an indium hydride via an iron hydride intermediate, but no experimental evidence was

provided regarding the fate of the cleaved hydrogen.[6]

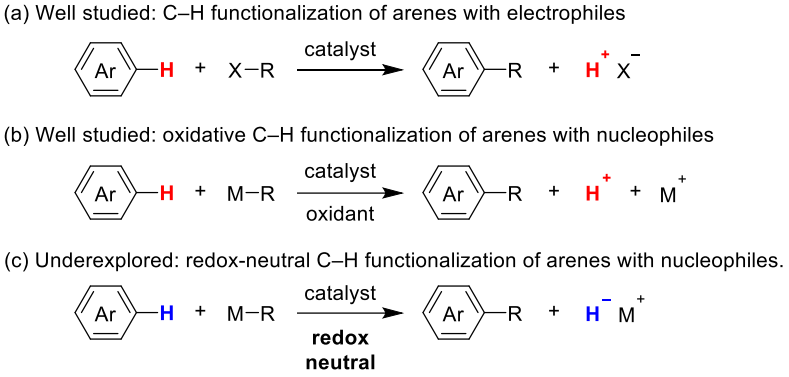

Scheme 1. Classifications of C–H bond functionalization of arenes: (a) and (b) C–H functionalization of arene nucleophiles, and (c) C–H functionalization of arene electrophiles.

Recently, our group has been focusing on the development of copper-catalyzed 1,2-silylfunctionalization of alkynes using silylboronates as the nucleophilic silicon donor toward synthetically useful silicon-substituted alkenes.[7,8] In these reactions, alkenylcopper intermediates generated during catalysis can be effectively coupled with electrophiles either inter- or intramolecularly to form tetrasubstituted alkenes in a stereo-defined manner. Thus, when internal arylalkynes were reacted with silylboronates in the presence of a catalytic amount of CuI in combination with NaO*t*Bu, regio- and *anti*-selective silylboration took place as described in Chapter 2 (Scheme 2a(i)).[7a] On the other hand, internal arylalkynes having a (phenylsilyl)ethyl group selectively gave *anti*-silylative cyclization products through intramolecular displacement of the phenyl group on silicon by an alkenylcopper intermediate with releasing a phenyl anion equivalent as phenylboronate (Scheme 2a(ii)).[7b] Based on these backgrounds, the author imagined that indene derivatives,[9] a useful class of compounds in various fields of research including pharmaceuticals and materials science,[10] could be obtained from benzylacetylenes and

silylboronates under redox-neutral copper catalysis via *anti*-selective silylative cyclization to the benzene ring at the propargylic position,[11,12] if it acts as an electrophile through the activation of a C–H bond with the release of hydrogen as hydride (Scheme 2b).[13] In this context, herein the author describe the development of such a new type of reaction including elucidation of the reaction mechanism.

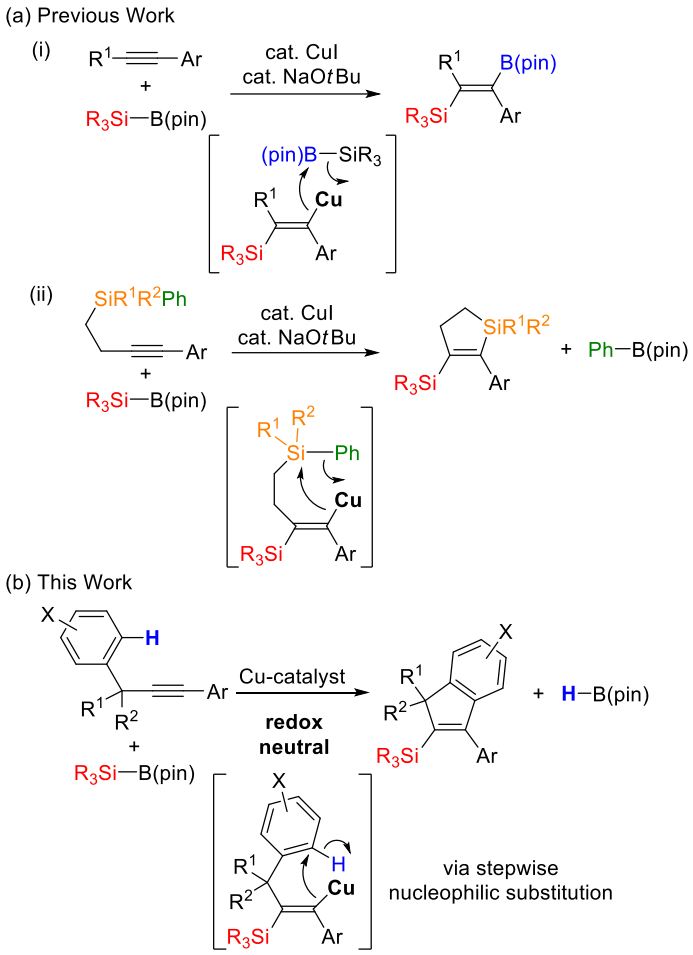

Scheme 2. Copper-catalyzed *anti*-1,2-silylfunctionalization: (a) previous work and (b) this work (pin = $OCMe_2CMe_2O$).

3.2 Results and discussion

3.2.1 Reaction development and product derivatization

Initially, 1,3-diphenyl-3-methyl-1-butyne (**1a**) was employed as a model substrate for the reaction with dimethyl(phenyl)silylboronate **2a** (1.2 equiv) in the presence of CuI (5 mol%) and NaO*t*Bu (1.5 equiv) in THF at 70 °C, and it was found that desired 2-silyl-1*H*-indene **3aa** was obtained as the major product in 66% yield through intramolecular alkenylation of an unactivated arene C–H bond (Table 1, entry 1).[14] The use of phosphine or *N*-heterocyclic carbene ligands such as Binap, PPh_3, JohnPhos, and IPr led to some improvement of the yield of **3aa** (72–82% yield; entries 2–5), and the reaction using 1.5 equiv of **2a** in the presence of JohnPhos gave **3aa** in a high yield of 92% (entry 6).

Table 1. Copper-catalyzed reaction of **1a** with **2a** to give **3aa**: optimization.

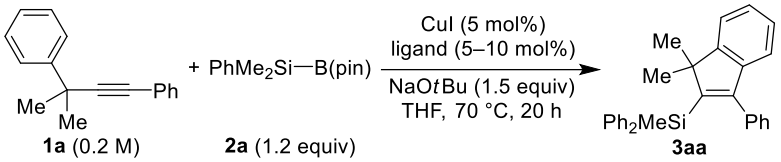

Entry	Ligand	Yield (%) [a]
1	None	66
2	Binap (5 mol%)	72
3	PPh_3 (10 mol%)	78
4	JohnPhos (10 mol%)	82
5[b]	IPr (5mol%)	79
6[c]	JohnPhos (10 mol%)	92[d]

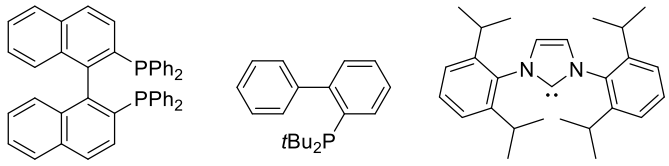

Binap JohnPhos IPr

[a] Determined by ^{1}H NMR against internal standard (dimethyl terephthalate). [b] The reaction was conducted using CuCl(IPr) as the catalyst. [c] 1.5 equiv of **2a** was used. [d] Isolated yield.

Under the conditions in Table 1, entry 6, various aryl(benzyl)acetylenes **1** could be employed for the synthesis of corresponding 2-silyl-1*H*-indenes **3** (Scheme 3). Although simple 1,3-diphenylpropyne was not a suitable substrate presumably due to the existence of highly acidic protons at the propargylic position, introduction of substituents at this position (**1b–e**) led to clean formation of products **3ba–ea** in high yields. Regarding the aryl group on the alkyne, various substituents could be incorporated at *ortho*-, *meta*-, and/or *para*-positions (**1f–l**) such as trimethylsilyl, methoxy, fluoro, and *N*-carbazolyl groups to give **3fa–la** in moderate to high yields. 2-Naphthyl group (**1m**) and several heterocycles (**1n–p**) were compatible in the present catalysis as well and 2-silyl-1*H*-indenes **3ma–pa** were successfully obtained. Various substituents could also be installed on the benzene ring at the propargylic position of substrates **1**. For example, substrates having methoxy (**1q**) or boryl group (**1r**) at the *para*-position gave corresponding 5-substituted indenes **3qa–ra**. It is worth noting that the reaction of chlorinated compound **1s** led to the formation of indene **3sa** with concomitant dechlorinative silylation, despite the fact that neither copper catalyst nor alkali metal alkoxide base has been reported to promote efficient substitution of aryl chlorides with silylboronates to give the corresponding arylsilanes.[15] The use of *meta*-tolyl substrate **1t** gave a mixture of 6-methylindene **3ta** and 4-methylindene **3ta'** in the ratio of 80/20, favoring the cyclization at the less hindered site. On the other hand, substrates having *tert*-butyl (**1u**) or (triisopropylsilyl)ethynyl group (**1v**) at the *meta*-position selectively gave 6-substituted indenes **3ua–va**. In addition to dimethyl(phenyl)silylboronate **2a**, trialkylsilylboronates **2b–c** could also be used for the reaction of **1a** to give 2-silyl-1*H*-indenes **3ab–ac** in high yields by conducting the reactions at a higher temperature (100 °C). Furthermore, a two-fold silylative cyclization reaction of diyne **4** with **2a** proceeded smoothly to give bis(indenyl)benzene **5** in 71% yield (eq 1).

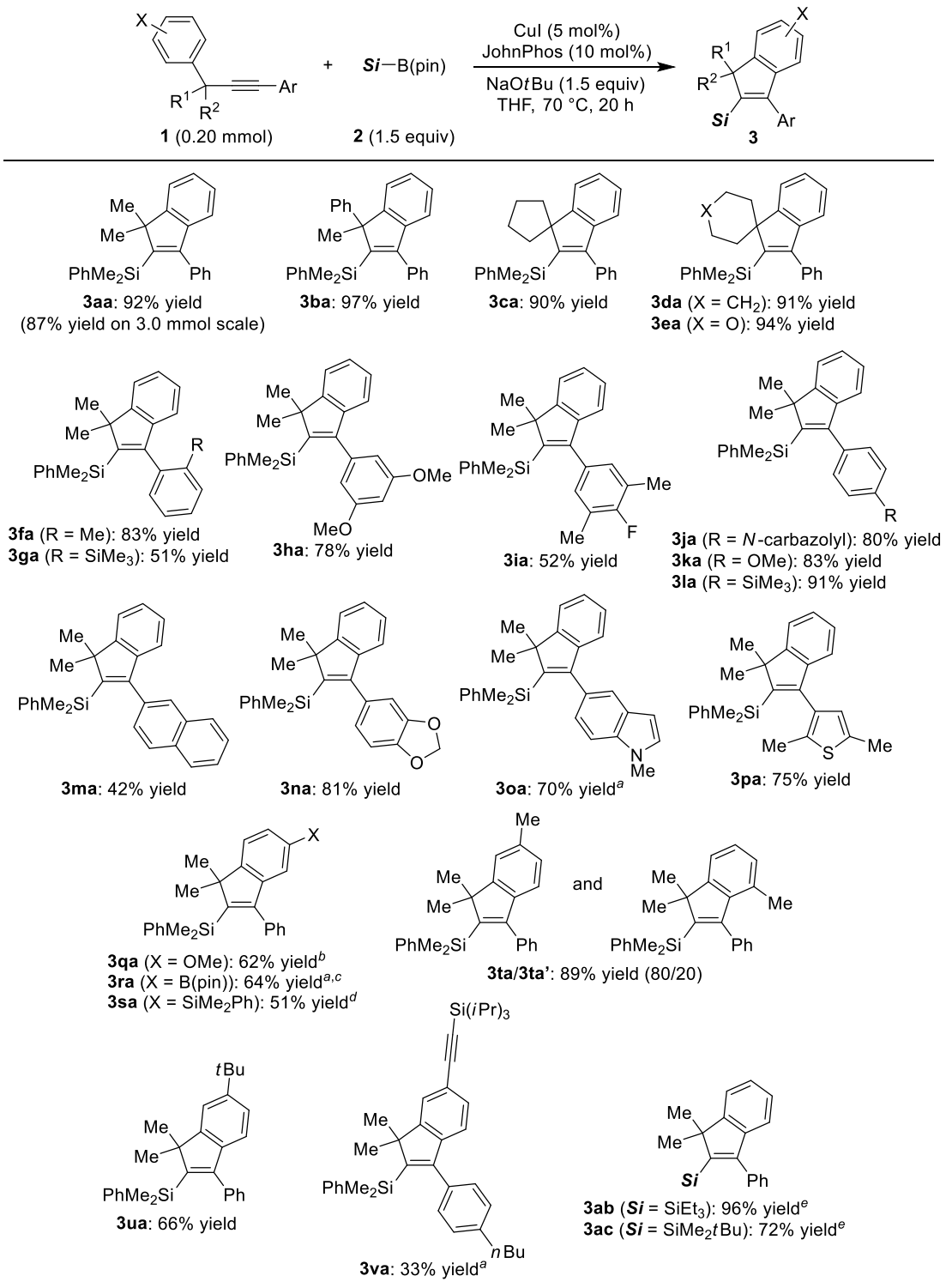

[a] 2.0 equiv of **2a**, 10 mol% of CuI, 20 mol% of JohnPhos, 2.0 equiv of NaO*t*Bu were used. [b] 1.8 equiv of NaO*t*Bu was used. [c] ^{1}H NMR yield. [d] The reaction was conducted using **1s** (X = Cl) with 3.0 equiv of **2a**, 10 mol% of CuI, 20 mol% of JohnPhos, 3.0 equiv of NaO*t*Bu. [e] The reaction was conducted at 100 °C.

Scheme 3. Scope of copper-catalyzed synthesis of 2-silyl-1*H*-indenes **3**.

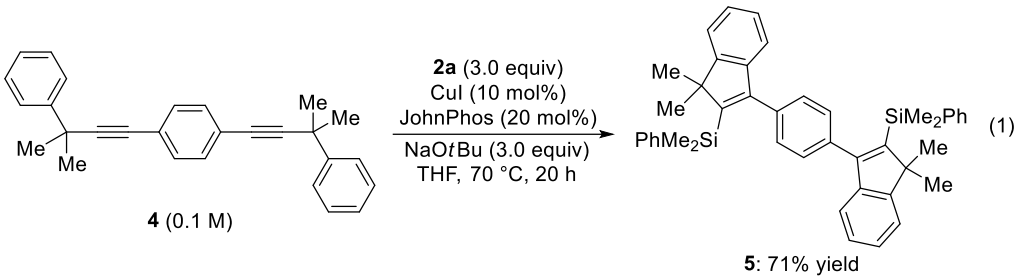

Products **3** obtained in the present catalysis can be further functionalized as exemplified in Scheme 4. Thus, 5-borylindene **3ra** was readily oxidized by hydrogen peroxide to give 5-hydroxyindene **3wa** (Scheme 4a, left). **3ra** could also be cross-coupled with 4-bromopyridine to give 5-(4-pyridyl)indene **3xa** (Scheme 4a, right). These examples demonstrate that peripheral functionalization of **3** is possible to install substituents that are not necessarily easy to incorporate in the catalytic process from **1** to **3**. In addition, transformations of **3** by utilizing the silyl group at the 2-position can be achieved as well. For example, desilylative iodination of **3aa** followed by cross-coupling with 2-bromophenylboronic acid gave 2-(2-bromophenyl)indene **6**, which was further converted to indenophenanthrene **7** by palladium-catalyzed intramolecular C–H bond arylation in a good overall yield (Scheme 4b, top). On the other hand, epoxidation of **3aa** with *m*CPBA proceeded efficiently to give compound **8**, which could be readily transformed to indanone **9** by treating it with trifluoroacetic acid (Scheme 4b, bottom).[16] Furthermore, desilylative bromination of **3ga** having two silyl groups selectively took place at the alkenyl carbon to give 2-bromoindene **10**, and the lithium–halogen exchange followed by the intramolecular nucleophilic attack to the remaining silyl group gave benzoindenosilole **11** in a high yield (Scheme 4c).

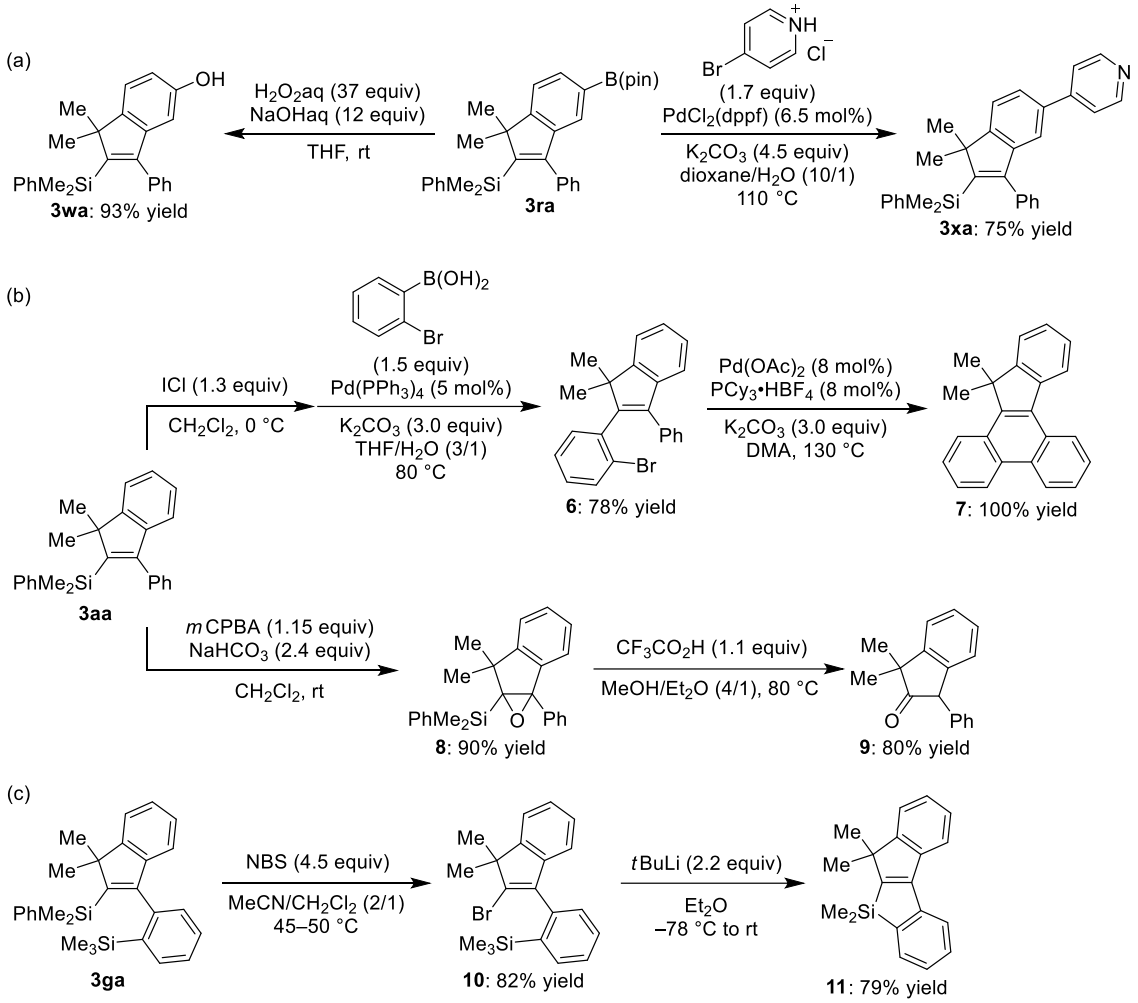

Scheme 4. Functionalization of 2-silyl-1*H*-indenes **3**: (a) functionalization of boron moiety on **3ra**, (b) and (c) transformation reactions of silylindenes **3aa** and **3ga**.

3.2.2 Elucidation of the reaction mechanism

To gain some insights into the fate of the hydrogen atom that is removed from the benzene ring in the present indene formation, the following deuterium-labeling experiment was carried out (Scheme 5a). Thus, the copper-catalyzed reaction was conducted using **1a-*d*$_5$** under the standard conditions, and 4-methoxybenzaldehyde (**12**) was subsequently added to the reaction mixture. As a result, mono-deuterated 4-methoxybenzyl alcohol **13-*d***, a reduced form of **12**, was obtained in 75% yield with 93% deuterium content at the benzylic position along with silylindene **3aa-*d*$_4$** in 83% yield. This result strongly suggests that the cleaved hydrogen atom from the aromatic ring was converted to HB(pin) or its borate form with NaO*t*Bu as NaBH(O*t*Bu)(pin) after the reaction.[17] Therefore, the arene C–H bond was actually activated as an electrophile by releasing H as a hydride. The kinetic isotope effect (KIE) was also examined by comparing the initial rate of the reactions of **1a** and **1a-*d*$_5$** (Scheme 5b). From these experiments, k_H/k_D was determined to be 1.13, indicating that the C–H bond cleavage is not the turnover-limiting step.

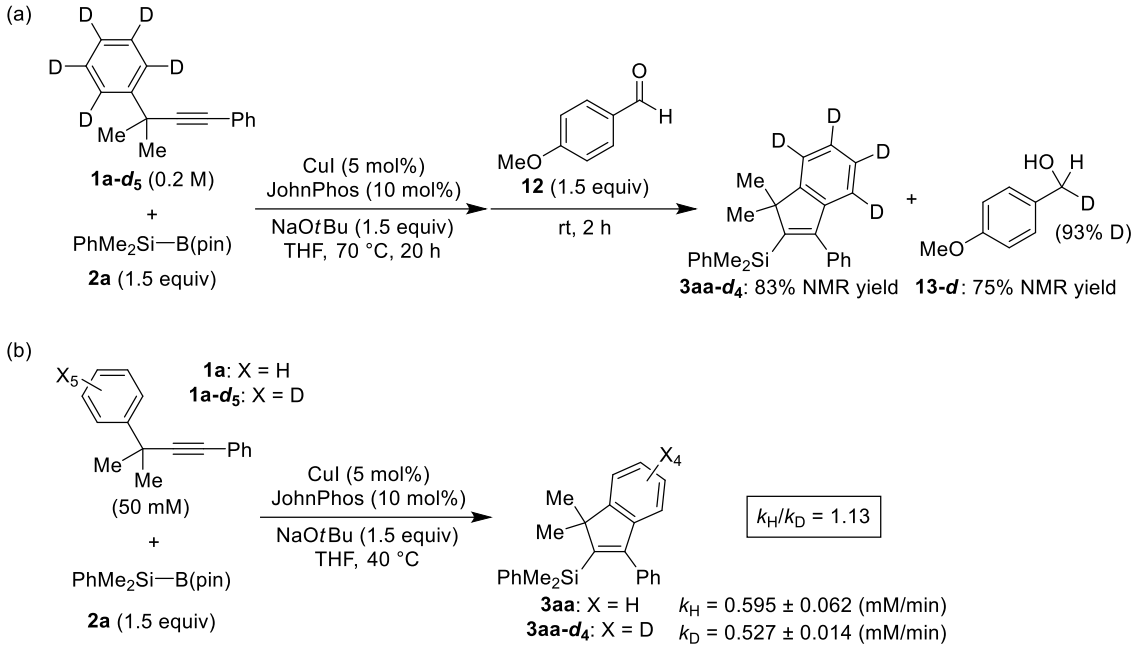

Scheme 5. Deuterium-labeling experiments: (a) tracking deuterium after C–D bond cleavage and (b) kinetic isotope effect.

On the basis of these experimental results and the results in Chapter 2 and Chapter 4 described next, a proposed catalytic cycle for the synthesis of **3aa** from alkyne **1a** and silylboronate **2a** is illustrated in Scheme 6. Thus, silylcopper species **A** in the form of disilylcuprate is initially generated by the reaction of CuI with silylboronate **2a** in the presence of NaO*t*Bu,[18] and this undergoes *syn*-selective insertion of alkyne **1a** to give alkenylcopper intermediate **B**. Subsequent *syn*-to-*anti* alkene isomerization as described in Chapter 2 leads to *anti*-alkenylmetal species **C**, which undergoes an intramolecular C–H bond alkenylation to give **3aa** along with copper hydride **D**. The ligand exchange with silylboronate **2a** then regenerates silylcopper **A** along with the formation of borohydride, HB(pin), which can further react with NaO*t*Bu to give hydroborate, NaBH(O*t*Bu)(pin).[17]

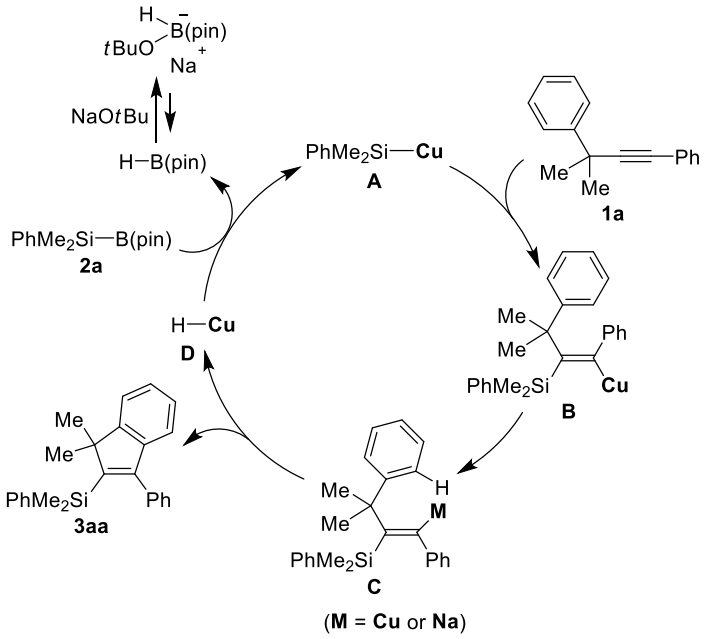

Scheme 6. Proposed catalytic cycle for the synthesis of **3aa** from **1a** and **2a** (**Cu** = $Cu^{-}(SiMe_2Ph)$).

To examine the feasibility of the transformation from copper hydride **D** to silylcopper **A**, a relevant model reaction was conducted. At first, CuH(IPr) was generated *in-situ* by the reaction of Cu(O*t*Bu)(IPr) (Figure 1a) with pinacolborane (1.0 equiv) in THF-d_8 (0.50 mL) as shown in Figure 1b (Cu–H: 2.07 ppm).[19] Subsequent addition of silylboronate **2a** (1.0 equiv) to this mixture resulted in the disappearance of the Cu–H peak, and gave a new set of peaks assignable to Cu($SiMe_2Ph$)(IPr) (Figure 1c). This result suggests that a similar transformation could occur in the present catalytic reactions.

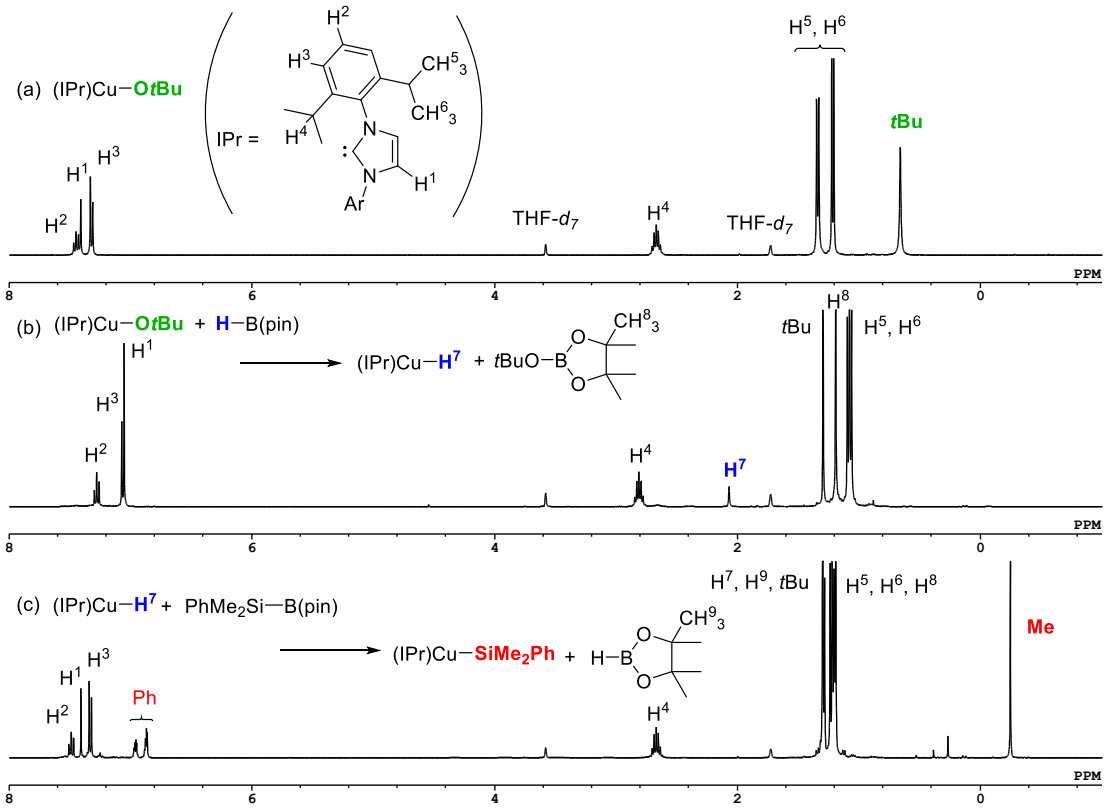

Figure 1. ^{1}H NMR spectra (400 MHz in THF-d_8) of (a) Cu(O*t*Bu)(IPr), (b) CuH(IPr) obtained from Cu(O*t*Bu)(IPr) + HB(pin), and (c) Cu(SiMe$_2$Ph)(IPr) obtained from CuH(IPr) + PhMe$_2$SiB(pin).

To understand how the C–H bond activation step proceeds, the step from **C** to **D** in Scheme 6 was theoretically examined by the density functional theory (DFT) calculations. All calculations were performed with the Gaussian 16 package.[20] Geometry optimizations were performed using the DFT-M06 functional.[21] The LANL2DZ basis set with the associated effective core potential was used for Cu, and the standard 6-31G(d) basis set was used for C, H, P atoms, and the 6-31+G(d) basis set was used for Si atom. Frequency analyses were carried out to confirm that each structure is a local minimum (no imaginary frequency) or a transition state (only one imaginary frequency). The energies were evaluated by single-point calculations using the same level of theory as the geometry optimization, including solvation effect by SCRF-SMD model[22] using THF as

solvent. All the transition states were confirmed with intrinsic reaction coordinate (IRC) analyses. When inevitable errors occur in the IRC calculation, optimization was performed from the structure that was slightly moved in the imaginary vibration direction.at the M06/Cu = LANL2DZ, C, H, P = 6-31G(d) and Si = 6-31+G(d) level theory with the solvation effect of THF (SCRF-SMD model).

The author mainly focused on the three possible pathways as illustrated in Scheme 7. At first, the oxidative addition/reductive elimination pathway was investigated (**path a** in Scheme 7). When alkenyl(silyl)cuprate was employed as **C**, the energy barrier for oxidative addition of aryl C–H bond to the copper was > 45 kcal/mol, and the resulting oxidative adduct **E** was found unstable, spontaneously leading to the Si–H bond-forming reductive elimination to give **F** (Scheme 8). On the other hand, when a neutral alkenylcopper complex coordinated with triphenylphosphine was used (**C'**), both oxidative adduct **E'** and its transition state **TS C'–E'** could be calculated, but the energy barrier of this oxidative addition process was found to be too high ($\Delta G^{\ddagger}$ = 56.4 kcal/mol) (Scheme 9). In addition, the σ-bond metathesis pathway was also attempted to calculate (**path b** in Scheme 7), but the transition state could not be successfully located.

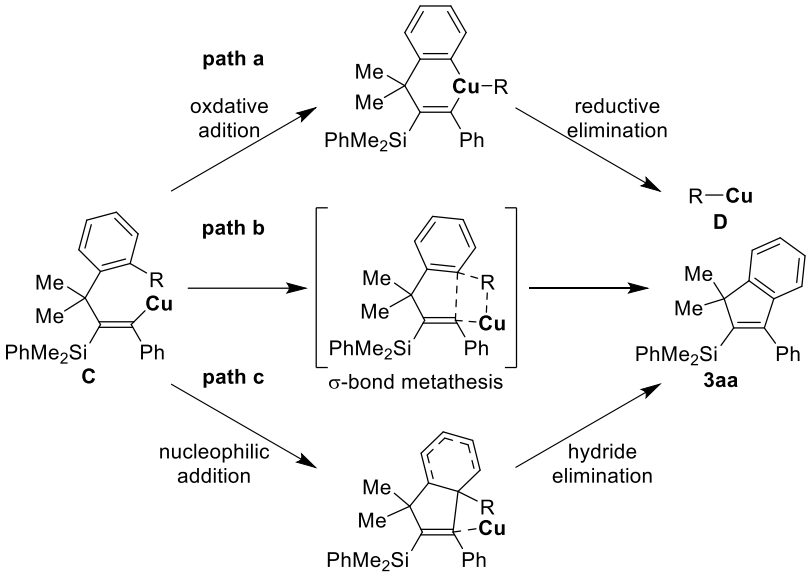

Scheme 7. Possible reaction pathways from alkenylcopper **C** to copper hydride **D** (R = H).

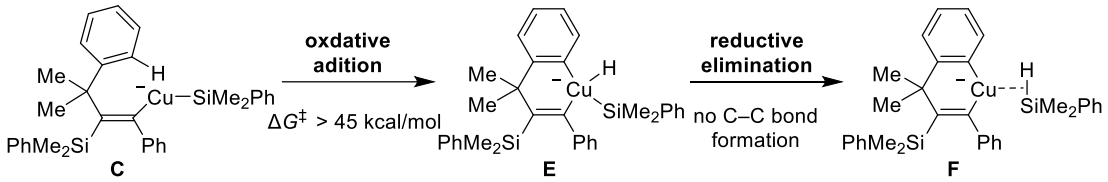

Scheme 8. Calculated reaction pathway from alkenyl(silyl)cuprate **C** via oxidative addition.

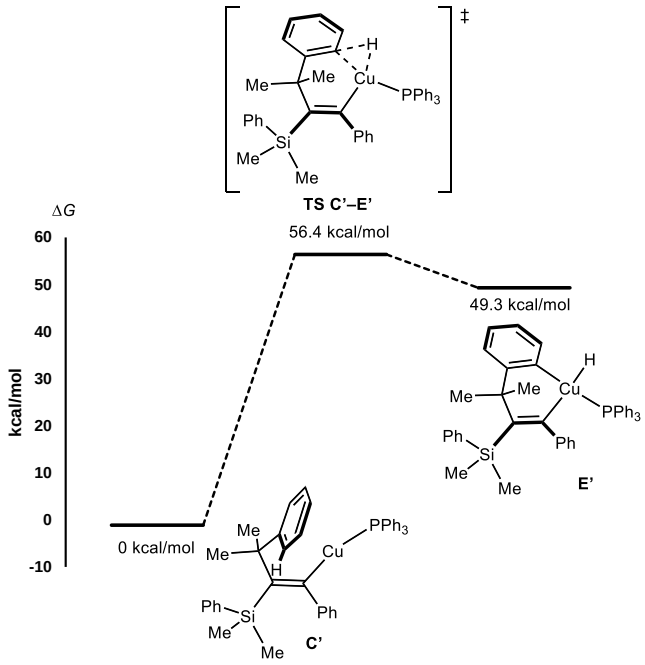

Scheme 9. Calculated energy diagram from PPh_3-coordinated alkenylcopper **C'** to oxidative adduct **E'**.

The author therefore explored an alternative pathway involving an intramolecular nucleophilic attack of alkenylcopper to the arene followed by hydride elimination to form copper hydride (**path c** in Scheme 7). Thus, as shown in Scheme 10, alkenylcopper species **C** (0 kcal/mol) was found to undergo a nucleophilic attack at the *ortho*-position of the pendant phenyl group to give dearomatized Meisenheimer-type intermediate **G** (15.7 kcal/mol) through **TS C–G** ($\Delta G^{\ddagger}$ = 28.0 kcal/mol). This was then led to intermediate **G'** (20.5 kcal/mol) by desorption of the sodium cation, and subsequent elimination of hydride via **TS G'–D** (23.1 kcal/mol, $\Delta G^{\ddagger}$ = 7.4 kcal/mol from **G**) could give rearomatized product **3aa** along with copper hydride intermediate **D** (−15.4 kcal/mol). This addition–elimination pathway is quite unusual, but it is currently thought as most probable. In addition, the result of KIE experiment in Scheme 5b is consistent with this calculated energy diagram.

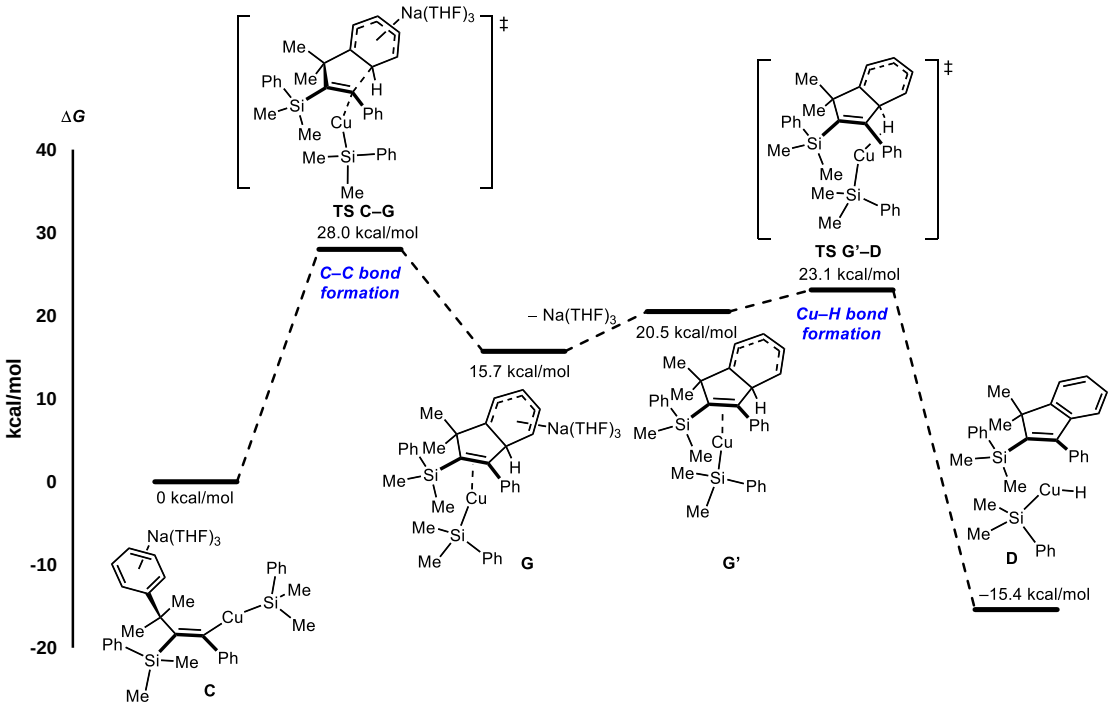

Scheme 10. Calculated energy diagram for the proposed reaction pathway involving a C–H bond cleavage from **C** to **D** (M06/6-31G* for C, H, O, Na, 6-31+G* for Si, and LANL2DZ for Cu).

An additional mechanistic insight was unexpectedly obtained by conducting the present reaction using compound **1y** having *ortho*-tolyl group at the propargylic position. Thus, as shown in eq 2, expected C–H alkenylation product **3ya** was obtained in 49% yield along with the formation of product **3aa** in 12% yield via demethylative cyclization. Although it is a minor product, this represents a rare example of the reaction involving the cleavage of an unstrained and non-polarized C–C bond under mild conditions.[23] The formation of **3aa** from **1y** through oxidative addition of the aryl–methyl bond to copper (**path a** with R = Me in Scheme 7) or σ-bond metathesis between an aryl–methyl bond and an alkenyl–copper bond (**path b** with R = Me in Scheme 7) would be unlikely. On the other hand, nucleophilic attack of an alkenylcopper to the methylated aromatic carbon followed by rearomatization via demethylation (**path c** with R = Me in Scheme 7) would

be more feasible. This reaction pathway was also supported by DFT calculation (Scheme 11), although the formation of methylcopper or methylboron species could not be experimentally detected.

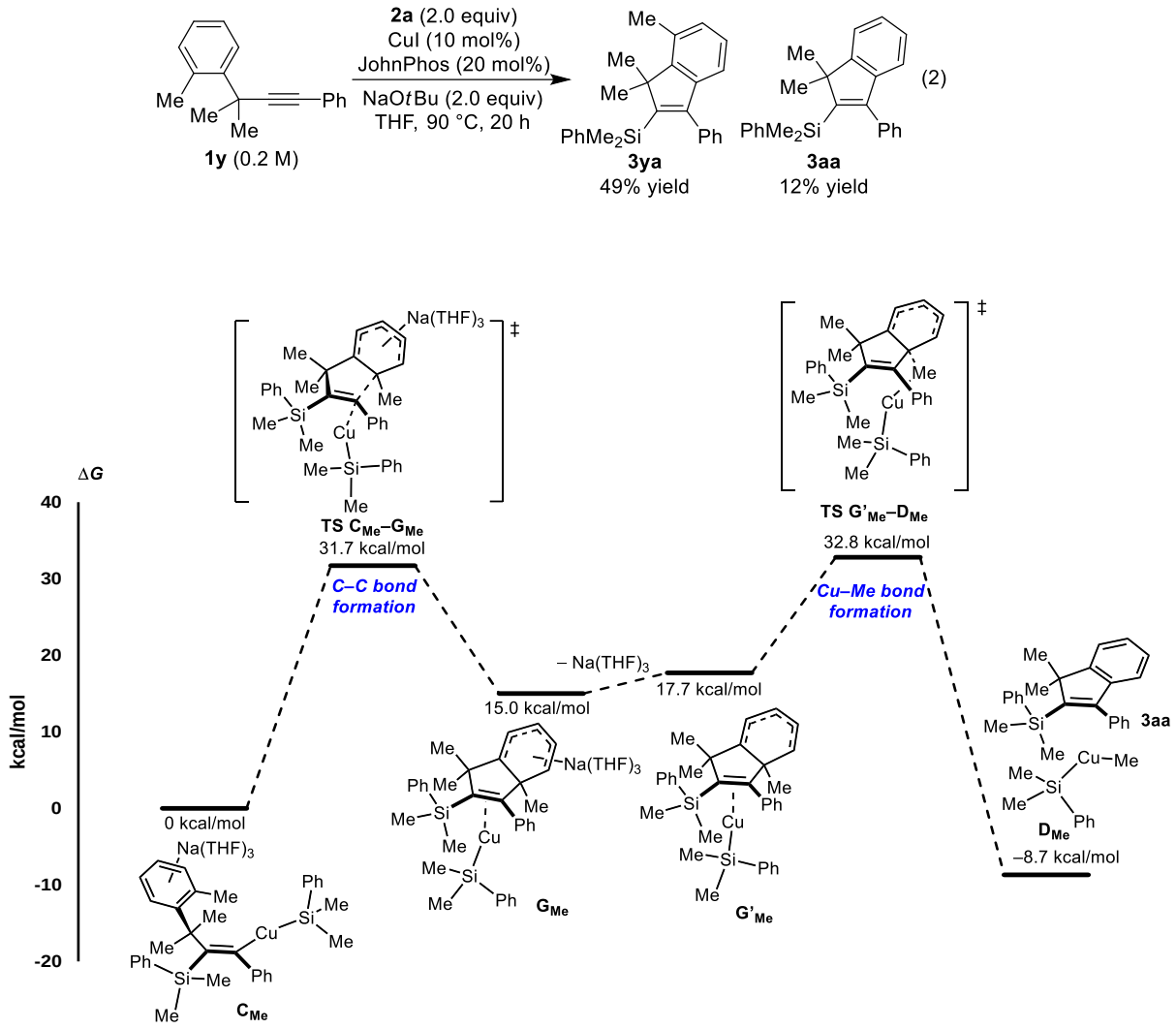

Scheme 11. Calculated energy diagram of C–Me bond cleavage from alkenyl(silyl)cuprate $\mathbf{C_{Me}}$ to give compound **3aa**.

3.3 Conclusion

The author developed a copper-catalyzed *anti*-selective silylarylation of benzylacetylenes with silylboronates to give 2-silyl-1*H*-indenes. The reaction proceeds with high regio- and stereoselectivity for a variety of substituted benzylacetylenes and the resulting products could be further functionalized. The arenes that undergo cyclization acted as an electrophile (aryl cation equivalent) with the release of H^- under redox neutral conditions, and the reaction mechanism was probed by the deuterium-labeling experiments and the DFT calculations. Unusual C–C bond activation was also demonstrated in this reaction system. The results obtained here could promote further investigations for the catalytic transformations involving the activation of unreactive bonds.

3.4 Experimental section

General

All reactions were carried out with standard Schlenk techniques under nitrogen or in a glove box under argon unless otherwise noted. NMR spectra were recorded on JEOL JNM-ECS400, JEOL JNM-ECZL400S, or Agilent Unity-Inova500 spectrometer. High resolution mass spectra were recorded on JEOL JMS700 spectrometer. X-ray crystallographic analysis was performed by RIGAKU XTaLAB P200 with graphite-monochromated Mo-Ka (0.71075 Å) radiation. Preparative GPC was performed with JAI LaboACE LC-5060 equipped with JAIGEL-2HR columns using $CHCl_3$ as an eluent. Computations were performed using workstation at Research Center for Computational Science, National Institutes of Natural Sciences, Okazaki, Japan. IR spectra were recorded on SHIMADZU IRSpirit-T spectrometer with QATR-S. Melting points were measured by Stanford Research System OptiMelt.

Et_3N (FUJIFILM Wako Chemicals) and $(i\mathrm{Pr})_2NH$ (FUJIFILM Wako Chemicals) were distilled over KOH under vacuum. THF-d_8 (Kanto Chemical) was dried over MS4A and degassed by purging argon prior to use. THF (Kanto Chemical; dehydrated), 1,4-dioxane (FUJIFILM Wako Chemicals; dehydrated), Et_2O (FUJIFILM Wako Chemicals; dehydrated), CH_2Cl_2 (Kanto Chemical; dehydrated), MeCN (FUJIFILM Wako Chemicals; dehydrated), DMA (FUJIFILM Wako Chemicals; dehydrated), MeOH (FUJIFILM Wako Chemicals; dehydrated), H_2O (Kishida Chemical), iodobenzene (FUJIFILM Wako Chemicals), 5-bromobenzo[*d*][1,3]dioxole (TCI), 4-bromopyridine hydrochloride (TCI), 4-methoxybenzaldehyde (Kishida Chemical), methyl 2-(4-bromophenyl)-2-methylpropanoate (BLD Pharmatech), *N*-bromosuccinimde (FUJIFILM Wako Chemicals), carbon tetrabromide (FUJIFILM Wako Chemicals), 2-methyl-2-phenylpropanoic acid (TCI), *m*-chloroperbenzoic acid (FUJIFILM Wako Chemicals; 72%

with H_2O), trifluoracetic acid (FUJIFILM Wako Chemicals), 2-bromophenylboronic acid (TCI), (dimethylphenylsilyl)boronic acid pinacol ester (FUJIFILM Wako Chemicals), pinacolborane (TCI), 2-isopropoxy-4,4,5,5-tetramethyl-1,3,2-dioxaborolane (TCI), *n*BuLi (Kanto Chemical; 1.56–1.59 M solution in hexane), *t*BuLi (Kanto Chemical; 1.70 M solution in pentane), $LiAlH_4$ (TCI or Aldrich), diisobutylaluminum hydride (TCI; 1.0 M solution in hexane), NaO*t*Bu (TCI), NaOH (FUJIFILM Wako Chemicals), $NaHCO_3$ (Nacalai Tesque), K_2CO_3 (FUJIFILM Wako Chemicals), H_2O_2 (Kishida Chemical; 30 wt% in H_2O), ICl (FUJIFILM Wako Chemicals), PPh_3 (FUJIFILM Wako Chemicals), JohnPhos (FUJIFILM Wako Chemicals), binap (TCI), P(*t*Bu)$_3$•HBF_4 (TCI), PCy$_3$•HBF_4 (TCI), pyridinium chlorochromate (TCI or Aldrich), $Pd(OAc)_2$ (FUJIFILM Wako Chemicals), CuI (FUJIFILM Wako Chemicals), and Celite (Nacalai Tesque) were used as received. **2b**,[24] **2c**,[24] dimethyl (1-diazo-2-oxopropyl)phosphonate,[25] $PdCl_2(MeCN)_2$,[26] $PdCl_2$(dppf),[27] $Pd(PPh_3)_4$,[28] CuCl(IPr),[29] and Cu(O*t*Bu)(IPr)[30] were synthesized following the literature procedures. Methyl 2-methyl-2-(pentadeuteriophenyl)propanoate was synthesized following the literature procedure for methyl 2-methyl-2-phenylpropanoate.[31]

Synthesis of substrates

Representative procedures for substrates:

1,3-Diphenyl-3-methyl-1-butyne (1a) (CAS 169696-39-3)

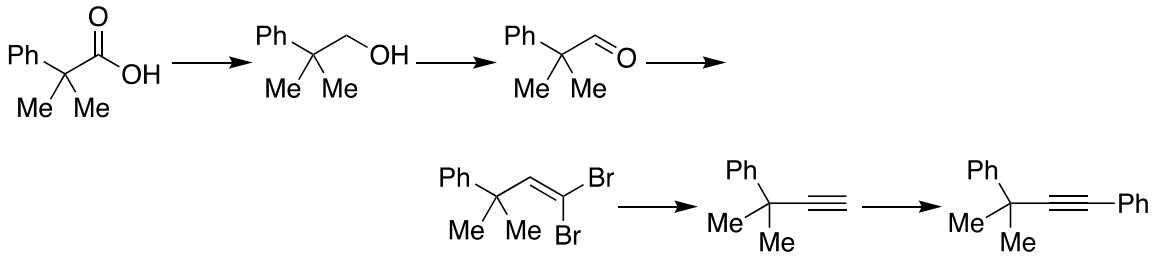

$LiAlH_4$ (1.71 g, 45.0 mmol) was added portionwise over 15 min to a solution of 2-methyl-2-phenylpropanoic acid (4.93 g, 30.0 mmol) in Et_2O (110 mL) at 0 °C, and the mixture was stirred for 22 h at room temperature. The reaction was slowly quenched with 1 M HClaq at 0 °C and this was diluted with H_2O. The precipitates were removed by filtration through Celite, and the filtrate was extracted with Et_2O. The organic layer was washed with saturated NaClaq, dried over $MgSO_4$, filtered, and concentrated under vacuum to afford 2-methyl-2-phenyl-1-propanol (CAS 2173-69-5) as a colorless oil (4.41 g, 29.3 mmol; 98% yield).

^{1}H NMR ($CDCl_3$): δ 7.42-7.37 (m, 2H), 7.35 (t, $^3J_{HH}$ = 7.8 Hz, 2H), 7.23 (tt, $^3J_{HH}$ = 7.1 Hz and $^4J_{HH}$ = 1.9 Hz, 1H), 3.63 (d, $^3J_{HH}$ = 6.4 Hz, 2H), 1.35 (s, 6H), 1.19 (t, $^3J_{HH}$ = 6.6 Hz, 1H).

2-Methyl-2-phenyl-1-propanol (4.41 g, 29.3 mmol) was added with the aid of CH_2Cl_2 (5 mL) to a mixture of pyridinium chlorochromate (8.21 g, 38.1 mmol) and Celite (10 g) in CH_2Cl_2 (55 mL), and the resulting mixture was stirred for 20 h at room temperature. This was passed through a pad of silica gel with CH_2Cl_2 and the solvent was removed under vacuum to afford 2-methyl-2-phenylpropanal (CAS 3805-10-5) as a colorless oil (3.93 g, 26.5 mmol; 91% yield).

^{1}H NMR ($CDCl_3$): δ 9.51 (s, 1H), 7.42-7.35 (m, 2H), 7.32-7.26 (m, 3H), 1.47 (s,

6H).

Carbon tetrabromide (17.3 g, 52.2 mmol) was added to a solution of PPh_3 (27.6 g, 105 mmol) in CH_2Cl_2 (100 mL) at 0 °C, and the mixture was stirred for 30 min at 0 °C. 2-Methyl-2-phenylpropanal (3.93 g, 26.5 mmol) was then added to it, and the resulting mixture was stirred for 23 h while gradually raising the temperature to room temperature. This was diluted with hexane and the precipitates were removed by filtration with hexane. The filtrate was concentrated under vacuum, and the residue was chromatographed on silica gel with hexane to afford 1,1-dibromo-3-methyl-3-phenyl-1-butene (CAS 1620741-89-0) as a colorless oil (7.08 g, 22.3 mmol; 88% yield).

^{1}H NMR ($CDCl_3$): δ 7.35-7.28 (m, 4H), 7.25-7.17 (m, 1H), 6.92 (s, 1H), 1.53 (s, 6H).

*n*BuLi (22.6 mL, 35.3 mmol; 1.56 M solution in hexane) was added slowly over 20 min to a solution of 1,1-dibromo-3-methyl-3-phenyl-1-butene (4.78 g, 15.7 mmol) in THF (72 mL) at −78 °C, and the mixture was stirred for 14 h while gradually raising the temperature to room temperature. The reaction was quenched with saturated NH_4Claq and this was extracted with Et_2O. The organic layer was washed with saturated NaClaq, dried over $MgSO_4$, filtered, and concentrated under vacuum. The residue was chromatographed on silica gel with hexane to afford 3-methyl-3-phenyl-1-butyne (CAS 28129-05-7) as a colorless oil (1.76 g, 12.2 mmol; 78% yield).

^{1}H NMR ($CDCl_3$): δ 7.59-7.54 (m, 2H), 7.34 (t, $^3J_{HH}$ = 7.6 Hz, 2H), 7.26-7.20 (m, 1H), 2.34 (s, 1H), 1.61 (s, 6H).

Et_3N (836 μL, 6.00 mmol), iodobenzene (408 mg, 2.00 mmol), and 3-methyl-3-phenyl-1-butyne (288 mg, 2.00 mmol) were successively added to a mixture of $Pd(PPh_3)_4$ (68.6 mg, 59.4 μmol) and CuI (23.6 mg, 124 μmol) in THF (3.0 mL), and this was stirred for 15 h at room temperature. The reaction mixture was directly passed through a pad of

silica gel with EtOAc and the solvent was removed under vacuum. The residue was chromatographed on silica gel with hexane to afford compound **1a** as a colorless oil (387 mg, 1.76 mmol; 88% yield).

^{1}H NMR ($CDCl_3$): δ 7.66-7.60 (m, 2H), 7.49-7.42 (m, 2H), 7.35 (t, $^{3}J_{HH}$ = 7.6 Hz, 2H), 7.32-7.27 (m, 3H), 7.26-7.21 (m, 1H), 1.68 (s, 6H). ^{13}C{^{1}H} NMR ($CDCl_3$): δ 147.1, 131.8, 128.4, 128.3, 127.8, 126.5, 125.7, 124.0, 96.7, 82.2, 36.6, 31.9.

3-Methyl-3-pentadeuteriophenyl-1-phenyl-1-butyne (1a-*d*$_5$)

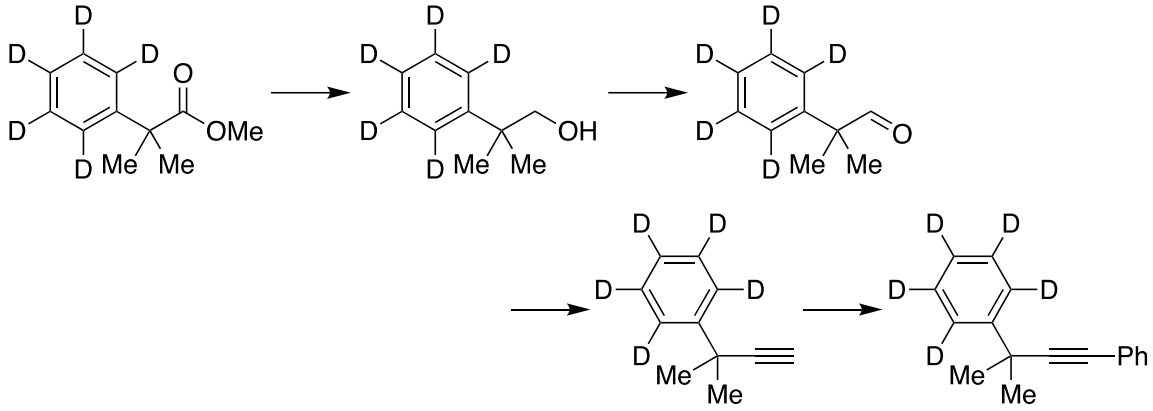

$LiAlH_4$ (238 mg, 6.28 mmol) was added portionwise over 10 min to a solution of methyl 2-methyl-2-(pentadeuteriophenyl)propanoate (577 mg, 3.15 mmol) in Et_2O (15 mL) at 0 °C, and the mixture was stirred for 16 h at room temperature. The reaction was slowly quenched with 1 M HClaq at 0 °C and this was diluted with H_2O. After extraction with Et_2O, the organic layer was washed with saturated NaClaq, dried over $MgSO_4$, filtered, and concentrated under vacuum to afford 2-methyl-2-(pentadeuteriophenyl)-1-propanol as a colorless oil (490 mg, 3.15 mmol; 100% yield).

^{1}H NMR ($CDCl_3$): δ 3.62 (d, $^{3}J_{HH}$ = 6.9 Hz, 2H), 1.35 (s, 6H), 1.19 (t, $^{3}J_{HH}$ = 6.6 Hz, 1H). ^{13}C{^{1}H} NMR ($CDCl_3$): δ 146.3, 128.0 (t, $^{1}J_{CD}$ = 24.4 Hz), 125.9 (t, $^{1}J_{CD}$ = 24.0 Hz), 125.7 (t, $^{1}J_{CD}$ = 24.0 Hz), 73.1, 40.1, 25.4.

2-Methyl-2-(pentadeuteriophenyl)-1-propanol (490 mg, 3.15 mmol) was added

with the aid of CH_2Cl_2 (2.0 mL) to a mixture of pyridinium chlorochromate (880 mg, 4.08 mmol) and Celite in CH_2Cl_2 (8.0 mL), and the resulting mixture was stirred for 18 h at room temperature. This was passed through a pad of silica gel with CH_2Cl_2 and the solvent was removed under vacuum to afford 2-methyl-2-(pentadeuteriophenyl)propanal as a colorless oil (444 mg, 2.90 mmol; 92% yield).

^{1}H NMR ($CDCl_3$): δ 9.51, (s, 1H), 1.47 (s, 6H). $^{13}C\{^1H\}$ NMR ($CDCl_3$): δ 202.3, 141.1, 128.4 (t, $^1J_{CD}$ = 24.4 Hz), 126.8 (t, $^1J_{CD}$ = 24.4 Hz), 126.4 (t, $^1J_{CD}$ = 24.0 Hz), 50.5, 22.6.

Dimethyl (1-diazo-2-oxopropyl)phosphonate (668 mg, 3.48 mmol) was added slowly over 5 min to a mixture of 2-methyl-2-(pentadeuteriophenyl)propanal (444 mg, 2.90 mmol) and K_2CO_3 (1.20 g, 8.68 mmol) in MeOH (9.0 mL), and the resulting mixture was stirred for 15 h at room temperature. This was diluted with H_2O and extracted with Et_2O. The organic layer was washed with saturated NaClaq, dried over $MgSO_4$, filtered, and concentrated under vacuum. The residue was chromatographed on silica gel with hexane to afford 3-methyl-3-(pentadeuteriophenyl)-1-butyne as a colorless oil (279 mg, 1.87 mmol; 64% yield).

^{1}H NMR ($CDCl_3$): δ 2.34 (s, 1H), 1.61 (s, 6H). $^{13}C\{^1H\}$ NMR ($CDCl_3$): δ 146.3, 127.9 (t, $^1J_{CD}$ = 24.0 Hz), 126.1 (t, $^1J_{CD}$ = 24.4 Hz), 125.2 (t, $^1J_{CD}$ = 24.0 Hz), 91.2, 69.8, 35.8, 31.7.

Et_3N (782 μL, 5.61 mmol), iodobenzene (343 mg, 1.68 mmol), and 3-methyl-3-(pentadeuteriophenyl)-1-butyne (251 mg, 1.68 mmol) were successively added to a mixture of $Pd(PPh_3)_4$ (64.2 mg, 55.5 μmol) and CuI (21.3 mg, 0.112 mmol) in THF (2.5 mL), and this was stirred for 15 h at 40 °C. The reaction mixture was directly passed through a pad of silica gel with EtOAc and the solvent was removed under vacuum. The residue was chromatographed on silica gel with hexane to afford compound **1a-*d*$_5$** as a

colorless oil (357 mg, 1.58 mmol; 94% yield).

^{1}H NMR ($CDCl_3$): δ 7.49-7.43 (m, 2H), 7.34-7.27 (m, 3H), 1.68 (s, 6H). $^{13}C\{^{1}H\}$ NMR ($CDCl_3$): δ 147.0, 131.8, 128.3, 127.9 (t, $^{1}J_{CD}$ = 24.4 Hz), 127.8, 126.0 (t, $^{1}J_{CD}$ = 24.4 Hz), 125.3 (t, $^{1}J_{CD}$ = 24.0 Hz), 124.0, 96.7, 82.2, 36.5, 31.9. IR (neat) 2974, 2931, 2276, 1598, 1488, 1442, 1330, 1205, 1066, 829, 753, 690, 544, 491, 455 cm^{-1}. HRMS (EI) calcd for $C_{17}H_{11}D_5$ (M^+) 225.1560, found 225.1560.

5-(3-Methyl-3-phenyl-1-butynyl)benzo[*d*][1,3]dioxole (1n)

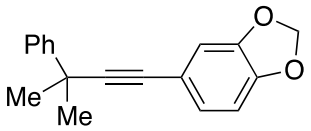

(*i*Pr)$_2$NH (313 μL, 2.25 mmol), 5-bromobenzo[*d*][1,3]dioxole (301 mg, 1.50 mmol), and 3-methyl-3-phenyl-1-butyne (238 mg, 1.65 mmol) were added to a mixture of $PdCl_2(MeCN)_2$ (7.3 mg, 28 μmol), P(*t*Bu)$_3$•HBF_4 (26.9 mg, 92.7 μmol), and CuI (8.6 mg, 45 μmol) in 1,4-dioxane (2.0 mL), and this was stirred for 16 h at 60 °C. The reaction mixture was directly passed through a pad of silica gel with EtOAc and the solvent was removed under vacuum. The residue was chromatographed on silica gel with hexane and further purified by GPC with $CHCl_3$ to afford compound **1n** as a white solid (250 mg, 945 μmol; 63% yield).

^{1}H NMR ($CDCl_3$): δ 7.64-7.58 (m, 2H), 7.34 (t, $^{3}J_{HH}$ = 7.6 Hz, 2H), 7.23 (tt, $^{3}J_{HH}$ = 7.3 Hz and $^{4}J_{HH}$ = 1.8 Hz, 1H), 6.97 (dd, $^{3}J_{HH}$ = 8.2 Hz and $^{4}J_{HH}$ = 1.8 Hz, 1H), 6.91 (d, $^{4}J_{HH}$ = 1.8 Hz, 1H), 6.74 (d, $^{3}J_{HH}$ = 8.2 Hz, 1H), 5.96 (s, 2H), 1.66 (s, 6H). $^{13}C\{^{1}H\}$ NMR ($CDCl_3$): δ 147.51, 147.45, 147.2, 128.4, 126.5, 126.1, 125.7, 117.3, 111.9, 108.4, 101.3, 94.9, 81.9, 36.5, 31.9. IR (neat) 2974, 2890, 1600, 1478, 1429, 1232, 1034, 934, 765, 699, 523 cm^{-1}. Mp: 36.5–37.5 °C. HRMS (FAB) calcd for $C_{18}H_{16}O_2$ (M^+) 264.1145 found 264.1152.

4-(2-Methyl-4-phenyl-3-butyn-2-yl)phenylboronic acid pinacol ester (1r)

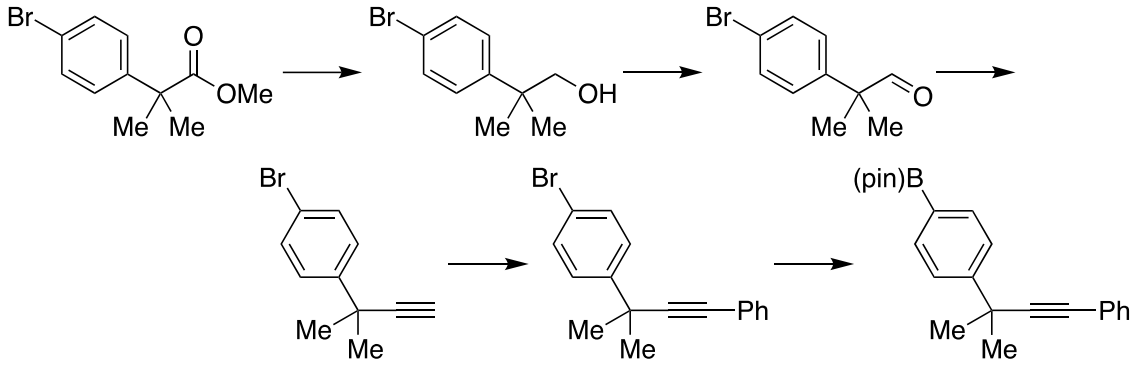

Diisobutylaluminum hydride (22.0 mL, 22.0 mmol; 1.0 M in hexane) was added slowly over 20 min to a solution of methyl 2-(4-bromophenyl)-2-methylpropanoate (2.57 g, 10.0 mmol) in THF (15 mL) at −78 °C, and the mixture was stirred for 37 h while gradually raising the temperature to room temperature. The reaction was quenched with 1 M HClaq and this was extracted with Et_2O. The organic layer was washed with saturated NaClaq, dried over $MgSO_4$, filtered, and concentrated under vacuum to afford 2-(4-bromophenyl)-2-methyl-1-propanol (CAS 32454-37-8) as a dark brown oil (2.56 g), which was used for the next step without further purification.

^{1}H NMR ($CDCl_3$): δ 7.46 (d, $^3J_{HH}$ = 8.7 Hz, 2H), 7.26 (d, $^3J_{HH}$ = 8.7 Hz, 2H), 3.60 (d, $^3J_{HH}$ = 6.4 Hz, 2H), 1.31 (s, 6H), 1.25 (t, $^3J_{HH}$ = 6.0 Hz, 1H).

2-(4-Bromophenyl)-2-methyl-1-propanol (2.56 g) was added with the aid of CH_2Cl_2 (5 mL) to a mixture of pyridinium chlorochromate (2.84 g, 13.2 mmol) and Celite (4.50 g) in CH_2Cl_2 (25 mL), and the resulting mixture was stirred for 24 h at room temperature. This was passed through a pad of silica gel with CH_2Cl_2 and the solvent was removed under vacuum. The residue was chromatographed on silica gel with hexane/EtOAc = 30/1 to afford 2-(4-bromophenyl)-2-methylpropanal (CAS 32454-16-3) as a colorless oil (1.79 g, 7.88 mmol; 79% yield over 2 steps).

^{1}H NMR ($CDCl_3$): δ 9.47 (s, 1H), 7.50 (d, $^3J_{HH}$ = 8.7 Hz, 2H), 7.14 (d, $^3J_{HH}$ = 8.7

Hz, 2H), 1.45 (s, 6H).

Dimethyl (1-diazo-2-oxopropyl)phosphonate (1.82 g, 9.46 mmol) was added slowly over 5 min to a mixture of 2-(4-bromophenyl)-2-methylpropanal (1.79 g, 7.88 mmol) and K_2CO_3 (3.27 g, 23.6 mmol) in MeOH (20 mL), and the resulting mixture was stirred for 15 h at room temperature. This was diluted with H_2O and extracted with Et_2O. The organic layer was washed with saturated NaClaq, dried over $MgSO_4$, filtered, and concentrated under vacuum. The residue was chromatographed on silica gel with hexane to afford 3-methyl-3-(4-bromophenyl)-1-butyne (CAS 2228504-72-9) as a colorless oil (1.52 g, 6.82 mmol; 86% yield).

^{1}H NMR ($CDCl_3$): δ 7.47-7.41 (m, 4H), 2.35 (s, 1H), 1.58 (s, 6H).

Et_3N (2.90 mL, 20.5 mmol), iodobenzene (1.39 g, 6.82 mmol), and 3-methyl-3-(4-bromophenyl)-1-butyne (1.52 g, 6.82 mmol) were successively added to a mixture of $Pd(PPh_3)_4$ (237 mg, 0.205 mmol) and CuI (77.9 mg, 0.409 mmol) in THF (10 mL), and this was stirred for 18 h at room temperature. The reaction mixture was directly passed through a pad of silica gel with EtOAc and the solvent was removed under vacuum. The residue was chromatographed on silica gel with hexane to afford 3-(4-bromophenyl)-3-methyl-1-phenyl-1-butyne (CAS 2247753-41-7) as a colorless oil (2.00 g, 6.67 mmol; 98% yield).

^{1}H NMR ($CDCl_3$): δ 7.53-7.41 (m, 2H), 7.50 (d, $^3J_{HH}$ = 8.7 Hz, 2H), 7.46 (d, $^3J_{HH}$ = 8.7 Hz, 2H), 7.34-7.27 (m, 3H), 1.65 (s, 6H). $^{13}C\{^1H\}$ NMR ($CDCl_3$): δ 146.2, 131.7, 131.4, 128.4, 128.0, 127.7, 123.7, 120.4, 95.9, 82.5, 36.3, 31.7.

*n*BuLi (1.40 mL, 2.22 mmol; 1.59 M solution in hexane) was added slowly over 10 min to a solution of 3-(4-bromophenyl)-3-methyl-1-phenyl-1-butyne (598 mg, 2.01 mmol) in THF (5.5 mL) at −78 °C, and the mixture was stirred for 1 h at −78 °C. 2-Isopropoxy-4,4,5,5-tetramethyl-1,3,2-dioxaborolane (610 μL, 3.00 mmol) was then

added to it at −78 °C, and the resulting mixture was stirred for 21 h while gradually raising the temperature to room temperature. The reaction was quenched with saturated NH_4Claq and this was extracted with Et_2O. The organic layer was washed with saturated NaClaq, dried over $MgSO_4$, filtered, and concentrated under vacuum. The residue was chromatographed on silica gel with hexane/EtOAc = 60/1 → 30/1 to afford compound **1r** as a white solid (452 mg, 1.31 mmol; 65% yield).

^{1}H NMR ($CDCl_3$): δ 7.85 (d, $^3J_{HH}$ = 8.3 Hz, 2H), 7.66 (d, $^3J_{HH}$ = 8.3 Hz, 2H), 7.51-7.45 (m, 2H), 7.35-7.28 (m, 3H), 1.71 (s, 6H), 1.37 (s, 12H). $^{13}C\{^1H\}$ NMR ($CDCl_3$): δ 150.3, 135.0, 131.7, 128.3, 127.8, 125.1, 124.0, 96.5, 83.8, 82.3, 36.7, 31.7, 25.0. IR (neat) 2974, 1607, 1397, 1358, 1142, 1104, 1018, 858, 824, 758, 660 cm^{-1}. Mp: 84.6–85.5 °C. HRMS (FAB) calcd for $C_{23}H_{27}BO_2$ (M^+) 346.2099, found 346.2105.

Analytical data for other substrate:

1,3,3-Triphenyl-1-butyne (1b) (CAS 87734-85-8)

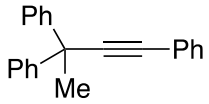

^{1}H NMR ($CDCl_3$): δ 7.53-7.45 (m, 6H), 7.35-7.27 (m, 7H), 7.22 (t, $^3J_{HH}$ = 7.3 Hz, 2H), 2.05 (s, 3H). $^{13}C\{^1H\}$ NMR ($CDCl_3$): δ 146.7, 131.8, 128.38, 128.35, 128.0, 127.2, 126.7, 123.8, 95.4, 84.4, 45.3, 30.7.

1-Phenyl-1-(phenylethynyl)cyclopentane (1c)

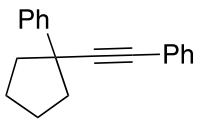

^{1}H NMR ($CDCl_3$): δ 7.62-7.57 (m, 2H), 7.45-7.39 (m, 2H), 7.34 (t, $^3J_{HH}$ = 7.8 Hz, 2H), 7.32-7.26 (m, 3H), 7.26-7.20 (m, 1H), 2.39-2.26 (m, 2H), 2.14-1.99 (m, 4H), 1.94-

1.81 (m, 2H). $^{13}C\{^{1}H\}$ NMR ($CDCl_3$): δ 145.5, 131.7, 128.4, 128.3, 127.7, 126.50, 126.48, 124.2, 96.2, 82.8, 47.9, 42.5, 24.5. IR (neat) 2959, 2867, 1597, 1489, 1443, 1327, 1069, 1028, 753, 696, 520 cm^{-1}. Mp: 52.0–53.4 °C. HRMS (FAB) calcd for $C_{19}H_{18}$ (M^+) 246.1403, found 246.1406.

1-Phenyl-1-(phenylethynyl)cyclohexane (1d)

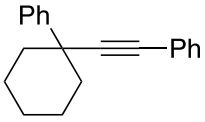

^{1}H NMR ($CDCl_3$): δ 7.67-7.62 (m, 2H), 7.50-7.46 (m, 2H), 7.38-7.33 (m, 2H), 7.33-7.26 (m, 3H), 7.26-7.22 (m, 1H), 2.06-1.92 (m, 4H), 1.84-1.73 (m, 5H), 1.34-1.22 (m, 1H). $^{13}C\{^{1}H\}$ NMR ($CDCl_3$): δ 147.3, 131.7, 128.4, 128.3, 127.8, 126.6, 126.2, 124.2, 94.4, 85.8, 42.5, 39.4, 26.0, 23.9. IR (neat) 3055, 2936, 2920, 2850, 1595, 1488, 1442, 1069, 1010, 756, 693, 526 cm^{-1}. Mp: 66.5–67.7 °C. HRMS (EI) calcd for $C_{20}H_{20}$ (M^+) 260.1560, found 260.1561.

4-Phenyl-4-(phenylethynyl)tetrahydro-2*H*-pyran (1e)

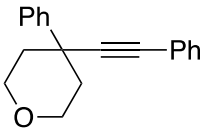

^{1}H NMR ($CDCl_3$): δ 7.66-7.61 (m, 2H), 7.52-7.46 (m, 2H), 7.39 (t, $^{3}J_{HH}$ = 7.6 Hz, 2H), 7.35-7.26 (m, 4H). 4.11-3.98 (m, 4H), 2.18 (td, J_{HH} = 12.4 Hz and $^{3}J_{HH}$ = 5.0 Hz, 2H), 1.92 (d, $^{2}J_{HH}$ = 12.4 Hz, 2H). $^{13}C\{^{1}H\}$ NMR ($CDCl_3$): δ 145.6, 131.7, 128.6, 128.4, 128.2, 127.0, 126.0, 123.5, 92.4, 86.7, 65.5, 40.1, 39.0. IR (neat) 2952, 2919, 2853, 1597, 1489, 1242, 1117, 1026, 835, 755, 700, 560 cm^{-1}. Mp: 85.0–86.0 °C. HRMS (EI) calcd for $C_{19}H_{18}O$ (M^+) 262.1352, found 262.1348.

1-(2-Methylphenyl)-3-methyl-3-phenyl-1-butyne (1f)

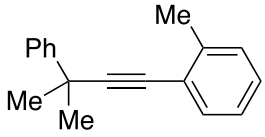

^{1}H NMR ($CDCl_3$): δ 7.66-7.62 (m, 2H), 7.42 (d, $^{3}J_{HH}$ = 7.3 Hz, 1H), 7.35 (t, $^{3}J_{HH}$ = 7.3 Hz, 2H), 7.26-7.22 (m, 1H), 7.21-7.16 (m, 2H), 7.15-7.09 (m, 1H), 2.45 (s, 3H), 1.70 (s, 6H). ^{13}C{^{1}H} NMR ($CDCl_3$): δ 147.2, 140.2, 131.9, 129.5, 128.4, 127.8, 126.5, 125.8, 125.6, 123.7, 100.8, 81.2, 36.8, 32.0, 21.0. IR (neat) 3061, 2974, 2926, 1600, 1494, 1447, 1361, 1269, 1030, 753, 696, 563, 450 cm^{-1}. HRMS (EI) calcd for $C_{18}H_{18}$ (M^+) 234.1403, found 234.1409.

3-Methyl-3-phenyl-1-(2-trimethylsilylphenyl)-1-butyne (1g)

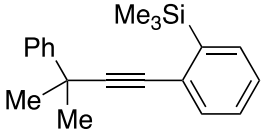

^{1}H NMR ($CDCl_3$): δ 7.65-7.60 (m, 2H), 7.51-7.45 (m, 2H), 7.35 (t, $^{3}J_{HH}$ = 7.8 Hz, 2H), 7.32-7.21 (m, 3H), 1.70 (s, 6H), 0.36 (s, 9H). ^{13}C{^{1}H} NMR ($CDCl_3$): δ 147.0, 141.9, 134.0, 133.1, 129.2, 128.9, 128.5, 127.1, 126.6, 125.9, 99.0, 83.9, 36.7, 31.5, −0.8. IR (neat) 3052, 2973, 1583, 1494, 1447, 1245, 1124, 1074, 1030, 835, 758, 696, 622, 455 cm^{-1}. HRMS (FAB) calcd for $C_{20}H_{24}Si$ (M^+) 292.1642, found 292.1645.

1-(3,5-Dimethoxyphenyl)-3-methyl-3-phenyl-1-butyne (1h)

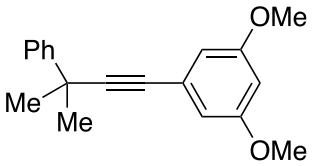

^{1}H NMR ($CDCl_3$): δ 7.62 (d, $^{3}J_{HH}$ = 7.8 Hz, 2H), 7.36 (t, $^{3}J_{HH}$ = 7.8 Hz, 2H), 7.25 (t, $^{3}J_{HH}$ = 7.8 Hz, 1H), 6.62 (d, $^{4}J_{HH}$ = 2.4 Hz, 2H), 6.43 (t, $^{4}J_{HH}$ = 2.4 Hz, 1H), 3.79 (s,

6H), 1.69 (s, 6H). $^{13}C\{^{1}H\}$ NMR ($CDCl_3$): δ 160.6, 147.0, 128.4, 126.6, 125.7, 125.3, 109.6, 101.4, 96.3, 82.2, 55.6, 36.5, 31.8. IR (neat) 2973, 2839, 1587, 1454, 1418, 1205, 1153, 1059, 831, 762, 698, 563 cm^{-1}. HRMS (FAB) calcd for $C_{19}H_{21}O_2$ ($M+H^+$) 281.1536, found 281.1535.

1-(3,5-Dimethyl-4-fluorophenyl)-3-methyl-3-phenyl-1-butyne (1i)

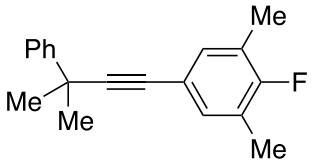

^{1}H NMR ($CDCl_3$): δ 7.64-7.58 (m, 2H), 7.35 (t, $^{3}J_{HH}$ = 7.6 Hz, 2H), 7.24 (t, $^{3}J_{HH}$ = 7.3 Hz, 1H), 7.12 (d, $^{4}J_{HF}$ = 6.8 Hz, 2H), 2.23 (d, $^{4}J_{HF}$ = 2.0 Hz, 6H), 1.66 (s, 6H). $^{13}C\{^{1}H\}$ NMR ($CDCl_3$): δ 159.7 (d, $^{1}J_{CF}$ = 245 Hz), 147.2, 132.3 (d, $^{3}J_{CF}$ = 6.0 Hz), 128.4, 126.5, 125.7, 124.6 (d, $^{2}J_{CF}$ = 18.1 Hz), 118.9 (d, $^{4}J_{CF}$ = 4.0 Hz), 95.4, 81.6, 36.5, 31.9, 14.5 (d, $^{3}J_{CF}$ = 4.0 Hz). IR (neat) 2972, 1601, 1488, 1445, 1216, 1195, 1140, 1030, 877, 766, 702, 566, 471 cm^{-1}. Mp: 69.3–70.3 °C. HRMS (FAB) calcd for $C_{19}H_{19}F$ (M^+) 266.1465, found 266.1471.

1-(4-(9-Carbazolyl)phenyl)-3-methyl-3-phenyl-1-butyne (1j)

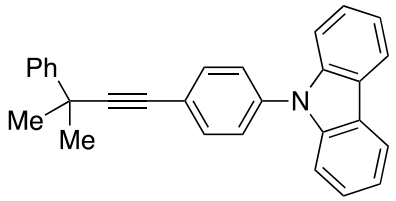

^{1}H NMR ($CDCl_3$): δ 8.14 (d, $^{3}J_{HH}$ = 7.8 Hz, 2H), 7.69 (d, $^{3}J_{HH}$ = 8.2 Hz, 2H), 7.68-7.64 (m, 2H), 7.52 (d, $^{3}J_{HH}$ = 8.7 Hz, 2H), 7.44-7.36 (m, 6H), 7.33-7.27 (m, 3H), 1.73 (s, 6H). $^{13}C\{^{1}H\}$ NMR ($CDCl_3$): δ 146.9, 140.8, 137.2, 133.3, 128.5, 127.0, 126.7, 126.2, 125.7, 123.7, 123.1, 120.5, 120.3, 109.9, 97.8, 81.6, 36.7, 31.8. IR (neat) 2964, 1598,

1511, 1451, 1316, 1233, 1316, 1233, 838, 752, 723, 702, 624 cm^{-1}. Mp: 134.7–137.2 °C. HRMS (FAB) calcd for $C_{29}H_{23}N$ (M^+) 385.1825, found 385.1826.

1-(4-Methoxyphenyl)-3-methyl-3-phenyl-1-butyne (1k)

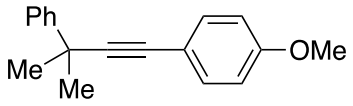

^{1}H NMR ($CDCl_3$): δ 7.62 (d, $^3J_{HH}$ = 7.8 Hz, 2H), 7.39 (d, $^3J_{HH}$ = 8.3 Hz, 2H), 7.34 (t, $^3J_{HH}$ = 7.8 Hz, 2H), 7.23 (t, $^3J_{HH}$ = 7.3 Hz, 1H), 6.83 (d, $^3J_{HH}$ = 8.7 Hz, 2H), 3.81 (s, 3H), 1.67 (s, 6H). $^{13}C\{^1H\}$ NMR ($CDCl_3$): δ 159.3, 147.3, 133.1, 128.4, 126.5, 125.7, 116.2, 113.9, 95.1, 81.9, 55.4, 36.5, 31.9. IR (neat) 2974, 2836, 1606, 1508, 1445, 1243, 1167, 1030, 829, 762, 698, 534 cm^{-1}. HRMS (FAB) calcd for $C_{18}H_{18}O$ (M^+) 250.1352, found 250.1353.

3-Methyl-3-phenyl-1-(4-trimethylsilylphenyl)-1-butyne (1l)

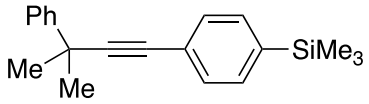

^{1}H NMR ($CDCl_3$): δ 7.65-7.60 (m, 2H), 7.46 (d, $^3J_{HH}$ = 8.2 Hz, 2H), 7.42 (d, $^3J_{HH}$ = 8.2 Hz, 2H), 7.35 (t, $^3J_{HH}$ = 7.6 Hz, 2H), 7.26-7.21 (m, 1H), 1.68 (s, 6H), 0.26 (s, 9H). $^{13}C\{^1H\}$ NMR ($CDCl_3$): δ 147.2, 140.4, 133.2, 130.9, 128.4, 126.5, 125.8, 124.3, 97.1, 82.3, 36.6, 31.9, −1.1. IR (neat) 3064, 2974, 1596, 1494, 1447, 1248, 1106, 836, 817, 756, 696, 628, 566 cm^{-1}. HRMS (FAB) calcd for $C_{20}H_{24}Si$ (M^+) 292.1642, found 292.1642.

3-Methyl-1-(2-naphthyl)-3-phenyl-1-butyne (1m)

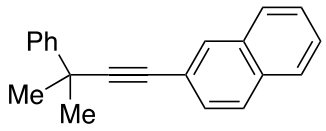

^{1}H NMR ($CDCl_3$): δ 8.03 (s, 1H), 7.87-7.79 (m, 3H), 7.75-7.70 (m, 2H), 7.57 (dd, $^{3}J_{HH}$ = 8.3 Hz and $^{4}J_{HH}$ = 1.7 Hz, 1H), 7.54-7.48 (m, 2H), 7.45-7.40 (m, 2H), 7.31 (tt, $^{3}J_{HH}$ = 7.4 Hz and $^{4}J_{HH}$ = 1.6 Hz, 1H), 1.79 (s, 6H). ^{13}C{^{1}H} NMR ($CDCl_3$): δ 147.1, 133.2, 132.7, 131.3, 128.9, 128.5, 127.94, 127.86, 127.8, 126.6, 126.5, 126.4, 125.8, 121.3, 97.1, 82.6, 36.7, 31.9. IR (neat) 3059, 2974, 1593, 1494, 1447, 1124, 1028, 905, 824, 746, 699, 584, 478 cm^{-1}. Mp: 44.0–46.1 °C. HRMS (FAB) calcd for $C_{21}H_{18}$ (M^+) 270.1403, found 270.1414.

3-Methyl-1-(1-methyl-1*H*-5-indolyl)-3-phenyl-1-butyne (1o)

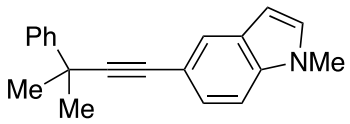

^{1}H NMR ($CDCl_3$): δ 7.77 (s, 1H), 7.68 (d, $^{3}J_{HH}$ = 7.4 Hz, 2H), 7.40-7.30 (m, 3H), 7.27-7.22 (m, 2H), 7.05 (d, $^{3}J_{HH}$ = 3.2 Hz, 1H), 6.45 (d, $^{3}J_{HH}$ = 3.2 Hz, 1H), 3.79 (s, 3H), 1.70 (s, 6H). ^{13}C{^{1}H} NMR ($CDCl_3$): δ 147.7, 136.2, 129.7, 128.44, 128.35, 126.4, 125.8, 125.3, 124.7, 114.6, 109.2, 101.2, 93.8, 83.5, 36.6, 33.0, 32.1. IR (neat) 3100, 2972, 1513, 1487, 1243, 1087, 893, 808, 761, 725, 698, 564, 526, 480 cm^{-1}. Mp: 62.4–64.7 °C. HRMS (FAB) calcd for $C_{20}H_{19}N$ (M^+) 273.1512 found 273.1520.

1-(2,5-Dimethyl-3-thienyl)-3-methyl-3-phenyl-1-butyne (1p)

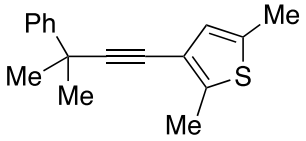

^{1}H NMR ($CDCl_3$): δ 7.65-7.58 (m, 2H), 7.34 (t, $^{3}J_{HH}$ = 7.8 Hz, 2H), 7.23 (tt, $^{3}J_{HH}$

= 7.3 Hz and $^4J_{HH}$ = 1.7 Hz, 1H), 6.64-6.60 (m, 1H), 2.45 (s, 3H), 2.38 (s, 3H), 1.67 (s, 6H). $^{13}C\{^1H\}$ NMR ($CDCl_3$): δ 147.3, 140.4, 135.6, 128.4, 127.5, 126.5, 125.7, 119.8, 98.3, 77.2, 36.7, 32.1, 15.2, 14.4. IR (neat) 2972, 2918, 2859, 1601, 1494, 1445, 1359, 1252, 1142, 1030, 825, 761, 696, 561, 496 cm^{-1}. HRMS (FAB) calcd for $C_{17}H_{18}S$ (M^+) 254.1124 found 254.1126.

3-(4-Methoxyphenyl)-3-methyl-1-phenyl-1-butyne (1q) (CAS 60042-22-0)

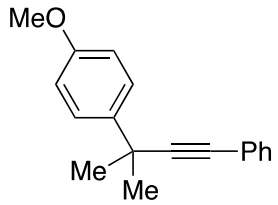

^1H NMR ($CDCl_3$): δ 7.53 (d, $^3J_{HH}$ = 8.7 Hz, 2H), 7.47-7.41 (m, 2H), 7.34-7.26 (m, 3H), 6.88 (d, $^3J_{HH}$ = 9.2 Hz, 2H), 3.81 (s, 3H), 1.65 (s, 6H). $^{13}C\{^1H\}$ NMR ($CDCl_3$): δ 158.2, 139.4, 131.7, 128.3, 127.8, 126.8, 124.0, 113.7, 96.9, 82.0, 55.4, 35.9, 32.0.

3-(4-Chlorophenyl)-3-methyl-1-phenyl-1-butyne (1s) (CAS 2097548-24-6)

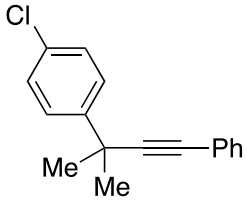

^1H NMR ($CDCl_3$): δ 7.58-7.52 (m, 2H), 7.48-7.42 (m, 2H), 7.35-7.27 (m, 5H), 1.66 (s, 6H). $^{13}C\{^1H\}$ NMR ($CDCl_3$): δ 145.9, 132.4, 131.8, 128.5, 128.4, 128.0, 127.3, 123.9, 96.1, 82.6, 36.3, 31.8.

3-Methyl-3-(3-Methylphenyl)-1-phenyl-1-butyne (1t)

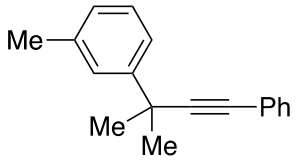

^{1}H NMR ($CDCl_3$): δ 7.48-7.40 (m, 4H), 7.34-7.21 (m, 4H), 7.06 (d, $^{3}J_{HH}$ = 7.3 Hz, 1H), 2.38 (s, 3H), 1.67 (s, 6H). $^{13}C\{^{1}H\}$ NMR ($CDCl_3$): δ 147.1, 137.9, 131.8, 128.3, 127.8, 127.3, 126.5, 124.1, 122.8, 96.8, 82.1, 36.4, 31.9, 21.8. IR (neat) 2973, 2926, 2357, 1598, 1488, 1442, 1292, 1190, 1086, 912, 783, 753, 689, 440 cm^{-1}. HRMS (EI) calcd for $C_{18}H_{18}$ (M^{+}) 234.1403, found 234.1407.

3-(3-(*tert*-Butyl)phenyl)-3-methyl-1-phenyl-1-butyne (1u)

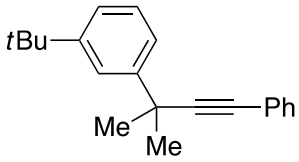

^{1}H NMR ($CDCl_3$): δ 7.74-7.71 (m, 1H), 7.48-7.43 (m, 2H), 7.43-7.38 (m, 1H), 7.33-7.27 (m, 5H), 1.68 (s, 6H), 1.35 (s, 9H). $^{13}C\{^{1}H\}$ NMR ($CDCl_3$): δ 151.2, 146.7, 131.7, 128.4, 128.0, 127.8, 124.1, 123.5, 122.9, 122.7, 97.0, 82.2, 36.8, 35.0, 31.9, 31.6. IR (neat) 2964, 2868, 1598, 1488, 1361, 1222, 1087, 894, 794, 753, 689, 551, 494 cm^{-1}. HRMS (EI) calcd for $C_{21}H_{24}$ (M^{+}) 276.1873, found 273.1874.

1-(4-Butylphenyl)-3-methyl-3-(3-(triisopropylsilylethynyl)phenyl)-1-butyne (1v)

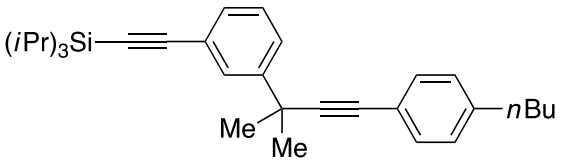

^{1}H NMR ($CDCl_3$): δ 7.72 (t, $^{4}J_{HH}$ = 1.7 Hz, 1H), 7.58 (dt, $^{3}J_{HH}$ = 7.8 Hz and $^{4}J_{HH}$ = 1.5 Hz, 1H), 7.36 (d, $^{3}J_{HH}$ = 8.3 Hz, 2H), 7.38-7.33 (m, 1H), 7.27 (t, $^{3}J_{HH}$ = 7.8 Hz, 1H),

7.11 (d, $^3J_{HH}$ = 8.3 Hz, 2H), 2.60 (t, $^3J_{HH}$ = 7.6 Hz, 2H), 1.66 (s, 6H), 1.63-1.55 (m, 2H), 1.34 (sext, $^3J_{HH}$ = 7.4 Hz, 2H), 1.18-1.10 (m, 21H), 0.92 (t, $^3J_{HH}$ = 7.3 Hz, 3H). $^{13}C\{^1H\}$ NMR ($CDCl_3$): δ 147.4, 142.9, 131.6, 130.3, 129.4, 128.5, 128.3, 126.1, 123.5, 121.0, 107.7, 95.4, 90.2, 82.7, 36.5, 35.7, 33.6, 31.8, 22.4, 18.9, 14.1, 11.5. IR (neat) 2941, 2863, 2151, 1596, 1511, 1462, 1290, 995, 911, 882, 794, 733, 663, 556, 500 cm^{-1}. HRMS (FAB) calcd for $C_{32}H_{44}Si$ (M^+) 456.3207, found 456.3208.

3-Methyl-3-(2-Methylphenyl)-1-phenyl-1-butyne (1y)

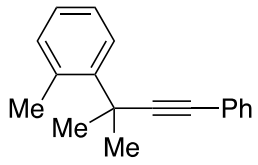

^1H NMR ($CDCl_3$): δ 7.45-7.36 (m, 3H), 7.31-7.24 (m, 3H), 7.22-7.14 (m, 3H), 2.74 (s, 3H), 1.74 (s, 6H). $^{13}C\{^1H\}$ NMR ($CDCl_3$): δ 143.6, 137.2, 132.6, 131.6, 128.3, 127.7, 126.8, 126.0, 125.0, 124.2, 97.0, 81.3, 35.3, 30.7, 21.9. IR (neat) 2975, 2931, 1597, 1488, 1442, 1295, 1056, 753, 725, 689, 602, 570, 474 cm^{-1}. HRMS (FAB) calcd for $C_{18}H_{18}$ (M^+) 234.1403, found 234.1398.

1,4-Bis(3-methyl-3-phenyl-1-butynyl)benzene (4)

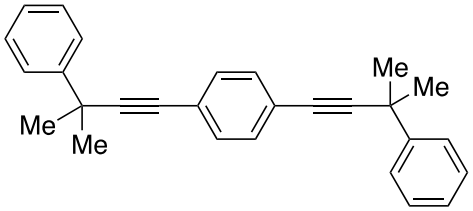

^1H NMR ($CDCl_3$): δ 7.64-7.59 (m, 4H), 7.38 (s, 4H), 7.36 (t, $^3J_{HH}$ = 7.8 Hz, 4H), 7.27-7.21 (m, 2H), 1.68 (s, 12H). $^{13}C\{^1H\}$ NMR ($CDCl_3$): δ 147.0, 131.6, 128.5, 126.6, 125.7, 123.3, 98.2, 82.0, 36.6, 31.8. IR (neat) 2965, 1727, 1493, 1445, 1290, 1028, 766, 700, 567 cm^{-1}. Mp: 166.9–175.9 °C. HRMS (EI) calcd for $C_{28}H_{26}$ (M^+) 362.2029, found

362.2032.

Catalytic reactions and derivatization

General procedure for Scheme 3.

Compound **1** (0.200 mmol) and silylboronate **2** (0.300 mmol) were added with the aid of THF (0.20 mL) to a mixture of CuI (1.9 mg, 10 μmol), JohnPhos (6.0 mg, 20 μmol) and NaO*t*Bu (28.8 mg, 0.300 mmol) in THF (0.80 mL), and this was stirred for 20 h at 70 °C. The reaction mixture was directly passed through a pad of silica gel with EtOAc and the solvent was removed under vacuum. The residue was purified by silica gel preparative TLC with hexane to afford compound **3**.

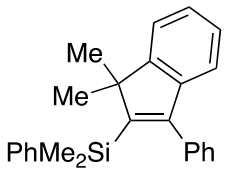

Compound 3aa. White solid. 92% yield (64.9 mg). The reaction could be scaled up using 3.02 mmol of **1a** to give **3aa** in 87% yield (935 mg, 2.64 mmol) after purification by silica gel chromatography with hexane.

^{1}H NMR ($CDCl_3$): δ 7.45-7.40 (m, 2H), 7.34 (d, $^{3}J_{HH}$ = 7.3 Hz, 1H), 7.31-7.19 (m, 7H), 7.18-7.11 (m, 3H), 6.87 (d, $^{3}J_{HH}$ = 7.8 Hz, 1H), 1.40 (s, 6H), 0.25 (s, 6H). ^{13}C{^{1}H} NMR ($CDCl_3$): δ 156.7, 153.8, 151.3, 144.7, 140.2, 137.6, 134.2, 129.5, 128.7, 128.0, 127.6, 127.3, 126.5, 126.0, 120.9, 120.8, 54.9, 25.7, 0.2. IR (neat) 3044, 2959, 1587, 1484, 1425, 1249, 1101, 1013, 918, 815, 759, 698, 620, 471, 411 cm^{-1}. Mp: 73.9–75.2 °C. HRMS (FAB) calcd for $C_{25}H_{26}Si$ (M^+) 354.1798, found 354.1804.

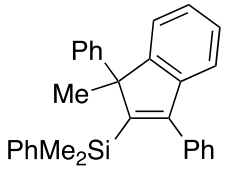

Compound 3ba. Colorless oil. 97% yield (81.0 mg).

^{1}H NMR ($CDCl_3$): δ 7.33-7.27 (m, 3H), 7.26-7.07 (m, 14H), 7.02 (d, $^{3}J_{HH}$ = 6.9 Hz, 1H), 6.91 (d, $^{3}J_{HH}$ = 6.9 Hz, 1H), 1.82 (s, 3H), −0.06 (s, 3H), −0.08 (s, 3H). ^{13}C{^{1}H} NMR ($CDCl_3$): δ 157.9, 155.1, 152.5, 144.8, 142.8, 139.7, 137.1, 134.0, 129.5, 128.5, 128.4, 128.1, 127.5, 127.4, 126.6, 126.54, 126.50, 126.4, 122.2, 120.9, 61.3, 22.4, −0.6, −0.7. IR (neat) 3065, 3022, 2968, 1546, 1488, 1428, 1247, 1104, 1018, 908, 819, 729, 696, 472, 413 cm^{-1}. HRMS (EI) calcd for $C_{30}H_{28}Si$ (M^+) 416.1955, found 416.1958.

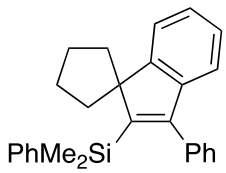

Compound 3ca. White solid. 90% yield (68.3 mg).

^{1}H NMR ($CDCl_3$): δ 7.44-7.36 (m, 3H), 7.33-7.22 (m, 6H), 7.21-7.09 (m, 4H), 6.85-6.80 (m, 1H), 2.36-2.25 (m, 2H), 2.13-2.00 (m, 2H), 1.92-1.80 (m, 2H), 1.80-1.70 (m, 2H), 0.22 (s, 6H). ^{13}C{^{1}H} NMR ($CDCl_3$): δ 158.6, 154.4, 149.7, 144.7, 140.4, 137.6, 134.3, 129.6, 128.7, 128.0, 127.6, 127.2, 126.2, 126.0, 121.3, 120.4, 65.7, 35.4, 26.5, 0.3. IR (neat) 3055, 2949, 1544, 1488, 1247, 1104, 826, 728, 698, 627 474, 411 cm^{-1}. Mp: 116.2–118.4 °C. HRMS (FAB) calcd for $C_{27}H_{28}Si$ (M^+) 380.1955, found 380.1960.

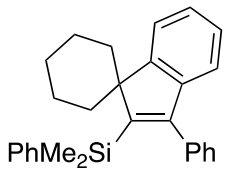

Compound 3da. Colorless viscous oil. 91% yield (72.0 mg).

^{1}H NMR ($CDCl_3$): δ 7.87-7.82 (m, 1H), 7.42-7.38 (m, 2H), 7.32-7.21 (m, 6H), 7.21-7.14 (m, 2H), 7.08-7,03 (m, 2H), 6.84-6.79 (m, 1H), 2.18 (td, $^{3}J_{HH}$ = 13.3 Hz and $^{2}J_{HH}$ = 4.6 Hz, 2H), 2.06-1.87 (m, 3H), 1.80-1.69 (m, 2H), 1.38 (d, $^{3}J_{HH}$ = 12.8 Hz, 2H), 1.33-1.17 (m, 1H), 0.26 (s, 6H). ^{13}C{^{1}H} NMR ($CDCl_3$): δ 155.0, 154.0, 152.2, 146.1, 140.6, 137.5, 134.3, 129.6, 128.6, 127.9, 127.6, 127.2, 126.6, 124.9, 124.4, 121.0, 58.7, 32.1, 25.3, 22.9, 1.0. IR (neat) 3064, 2919, 1548, 1485, 1248, 903, 812, 729, 696, 410 cm^{-1}. Mp: 114.2–120.6 °C. HRMS (FAB) calcd for $C_{28}H_{30}Si$ (M^+) 394.2111, found 394.2121.

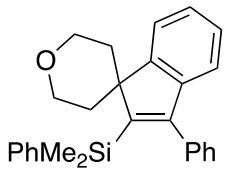

Compound 3ea. White solid. 94% yield (75.1 mg).

^{1}H NMR ($CDCl_3$): δ 8.02-7.96 (m, 1H), 7.40-7.35 (m, 2H), 7.32-7.18 (m, 8H), 7.08-7.03 (m, 2H), 6.88-6.82 (m, 1H), 4.19 (td, J_{HH} = 12.4 Hz and $^{3}J_{HH}$ = 1.8 Hz, 2H), 4.01 (dd, $^{2}J_{HH}$ = 11.9 Hz and $^{3}J_{HH}$ = 5.5 Hz, 2H), 2.61 (td, J_{HH} = 13.3 Hz and $^{3}J_{HH}$ = 5.5 Hz, 2H), 1.32 (d, $^{2}J_{HH}$ = 13.8 Hz, 2H). 0.30 (s, 6H). ^{13}C{^{1}H} NMR ($CDCl_3$): δ 154.8, 154.1, 150.5, 146.1, 140.3, 137.1, 134.0, 129.5, 128.7, 128.0, 127.7, 127.3, 127.1, 125.4, 124.0, 121.4, 64.6, 55.6, 32.0, 0.9. IR (neat) 2948, 1555, 1488, 1427, 1259, 1100, 818, 733, 546 cm^{-1}. Mp: 116.1–121.6 °C. HRMS (FAB) calcd for $C_{27}H_{28}OSi$ (M^+) 396.1904, found 396.1904.

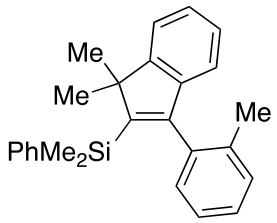

Compound 3fa. The product was further purified by GPC with $CHCl_3$. Colorless oil. 83% yield (60.6 mg).

^{1}H NMR ($CDCl_3$): δ 7.40-7.36 (m, 2H), 7.35-7.32 (m, 1H), 7.32-7.18 (m, 5H), 7.16-7.08 (m, 3H), 7.01 (dd, $^3J_{HH}$ = 7.3 Hz and $^4J_{HH}$ = 1.4 Hz, 1H), 6.71 (d, $^3J_{HH}$ = 7.3 Hz, 1H), 1.97 (s, 3H), 1.42 (s, 3H), 1.35 (s, 3H), 0.27 (s, 3H), 0.20 (s, 3H). ^{13}C{^{1}H} NMR ($CDCl_3$): δ 156.8, 153.4, 151.1, 144.0, 139.6, 137.0, 136.7, 134.2, 130.0, 129.7, 128.7, 127.7, 127.6, 126.5, 125.9, 125.4, 120.9, 120.6, 54.9, 26.3, 25.2, 19.6, −0.3, −0.5. IR (neat) 3067, 2955, 1546, 1428, 1246, 1113, 1020, 826, 751, 699, 468 cm^{-1}. HRMS (EI) calcd for $C_{26}H_{28}Si$ (M^+) 368.1955, found 368.1957.

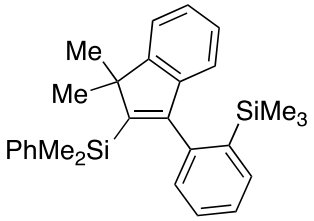

Compound 3ga. The product was purified by GPC with $CHCl_3$ instead of silica gel preparative TLC. White solid. 51% yield (43.2 mg).

^{1}H NMR ($CDCl_3$): δ 7.61 (dd, $^3J_{HH}$ = 7.3 Hz and $^4J_{HH}$ = 1.4 Hz, 1H), 7.50-7.45 (m, 2H), 7.37-7.26 (m, 6H), 7.19 (td, $^3J_{HH}$ = 7.3 Hz and $^4J_{HH}$ = 1.5 Hz, 1H), 7.13 (dd, $^3J_{HH}$ = 7.3 Hz and $^4J_{HH}$ = 1.5 Hz, 1H), 7.09 (dd, $^3J_{HH}$ = 7.3 Hz and $^4J_{HH}$ = 1.5 Hz, 1H), 6.72 (d, $^3J_{HH}$ = 7.3 Hz, 1H), 1.33 (s, 3H), 1.27 (s, 3H), 0.24 (s, 3H), 0.12 (s, 3H), 0.05 (s, 9H). ^{13}C{^{1}H} NMR ($CDCl_3$): δ 156.2, 155.6, 150.3, 145.8, 143.4, 139.8, 139.2, 135.0, 134.4, 130.4, 128.8, 128.6, 127.7, 126.7, 126.3, 126.0, 121.5, 120.8, 54.9, 26.4, 24.6, 1.1, 0.1,

−0.3. IR (neat) 3067, 2956, 1541, 1427, 1248, 1120, 1018, 819, 751, 727, 620, 468, 408 cm^{-1}. Mp: 82.4–87.5 °C. HRMS (FAB) calcd for $C_{28}H_{34}Si_2$ (M^+) 426.2194, found 426.2190.

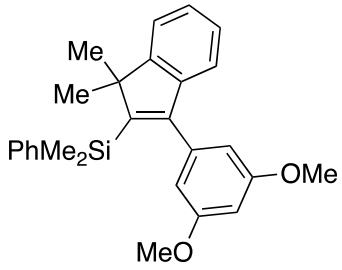

Compound 3ha. The product was purified by GPC with $CHCl_3$ instead of silica gel preparative TLC. White solid. 78% yield (68.8 mg).

^{1}H NMR ($CDCl_3$): δ 7.47-7.42 (m, 2H), 7.35 (d, $^3J_{HH}$ = 7.3 Hz, 1H), 7.30-7.21 (m, 4H), 7.17 (td, $^3J_{HH}$ = 7.3 Hz and $^4J_{HH}$ = 1.0 Hz, 1H), 6.97 (d, $^3J_{HH}$ = 7.3 Hz, 1H), 6.37 (t, $^4J_{HH}$ = 2.4 Hz, 1H), 6.28 (d, $^4J_{HH}$ = 2.4 Hz, 2H), 3.59 (s, 6H), 1.44 (s, 6H), 0.30 (s, 6H). ^{13}C{^{1}H} NMR ($CDCl_3$): δ 160.5, 156.8, 153.8, 150.8, 144.2, 140.6, 139.4, 134.1, 128.6, 127.6, 126.6, 126.1, 120.92, 120.86, 107.2, 100.3, 55.3, 54.8, 25.6, 0.3. IR (neat) 2960, 1588, 1348, 1252, 1203, 1141, 1057, 812, 758, 698, 471 cm^{-1}. Mp: 112.2–113.6 °C. HRMS (FAB) calcd for $C_{27}H_{30}O_2Si$ (M^+) 414.2010, found 414.2017.

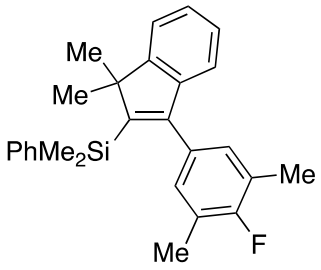

Compound 3ia. The product was further purified by GPC with $CHCl_3$. White solid. 52% yield (41.4 mg).

^{1}H NMR ($CDCl_3$): δ 7.38-7.32 (m, 3H), 7.31-7.19 (m, 4H), 7.15 (td, $^3J_{HH}$ = 7.6

Hz and $^{4}J_{HH}$ = 1.0 Hz, 1H), 6.87 (d, $^{3}J_{HH}$ = 6.8 Hz, 1H), 6.65 (d, $^{4}J_{HF}$ = 6.8 Hz, 2H), 2.13 (d, $^{4}J_{HF}$ = 2.4 Hz, 6H), 1.45 (s, 6H), 0.29 (s, 6H). $^{13}C\{^{1}H\}$ NMR ($CDCl_3$): δ 159.3 (d, $^{1}J_{CF}$ = 242 Hz), 156.7, 153.2, 151.6, 144.5, 140.5, 133.9, 132.3 (d, $^{4}J_{CF}$ = 4.0 Hz), 129.9 (d, $^{3}J_{CF}$ = 5.0 Hz), 128.5, 127.5, 126.5, 126.0, 123.7 (d, $^{2}J_{CF}$ = 18.1 Hz), 120.9, 120.7, 54.7, 25.6, 14.7 (d, $^{3}J_{CF}$ = 4.0 Hz), 0.3. IR (neat) 2956, 1541, 1481, 1246, 1202, 900, 814, 700, 461 cm^{-1}. Mp: 90.6–96.4 °C. HRMS (FAB) calcd for $C_{27}H_{29}FSi$ (M^{+}) 400.2017, found 400.2022.

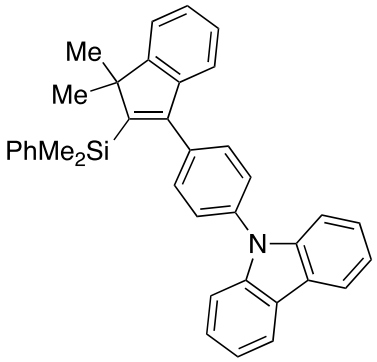

Compound 3ja. The product was purified by GPC with $CHCl_3$ instead of silica gel preparative TLC. White solid. 80% yield (83.2 mg).

^{1}H NMR ($CDCl_3$): δ 8.16 (d, $^{3}J_{HH}$ = 7.8 Hz, 2H), 7.48-7.38 (m, 9H), 7.34-7.21 (m, 9H), 7.01 (d, $^{3}J_{HH}$ = 7.8 Hz, 1H), 1.50 (s, 6H), 0.40 (s, 6H). $^{13}C\{^{1}H\}$ NMR ($CDCl_3$): δ 156.8, 152.9, 152.3, 144.4, 141.0, 140.0, 136.8, 136.7, 134.0, 131.0, 128.8, 127.8, 126.7, 126.5, 126.2, 126.0, 123.5, 121.1, 120.7, 120.4, 120.1, 110.0, 55.1, 25.7, 0.5. IR (neat) 2962, 1596, 1502, 1451, 1229, 1022, 819, 749, 723, 471 cm^{-1}. Mp: 167.0–168.0 °C. HRMS (FAB) calcd for $C_{37}H_{33}NSi$ (M^{+}) 519.2377, found 519.2382.

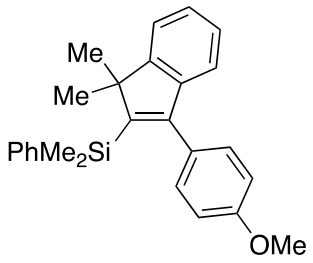

Compound 3ka. The product was purified by GPC with $CHCl_3$ instead of silica gel preparative TLC. White solid. 83% yield (63.4 mg).

^{1}H NMR ($CDCl_3$): δ 7.45-7.40 (m, 2H), 7.33 (d, $^3J_{HH}$ = 7.3 Hz, 1H), 7.30-7.24 (m, 3H), 7.22 (t, $^3J_{HH}$ = 7.3 Hz, 1H), 7.15 (t, $^3J_{HH}$ = 7.3 Hz, 1H), 7.04 (d, $^3J_{HH}$ = 8.2 Hz, 2H), 6.88 (d, $^3J_{HH}$ = 7.3 Hz, 1H), 6.80 (d, $^3J_{HH}$ = 8.7 Hz, 2H), 3.82 (s, 3H), 1.39 (s, 6H), 0.26 (s, 6H). ^{13}C{^{1}H} NMR ($CDCl_3$): δ 158.9, 156.8, 153.5, 151.3, 144.8, 140.4, 134.2, 130.6, 129.8, 128.7, 127.6, 126.5, 125.9, 120.84, 120.77, 113.4, 55.3, 54.7, 25.7, 0.3. IR (neat) 2951, 1610, 1498, 1242, 1175, 842, 759, 630, 413 cm^{-1}. Mp: 155.8–156.8 °C. HRMS (FAB) calcd for $C_{26}H_{28}OSi$ (M^+) 384.1904, found 384.1910.

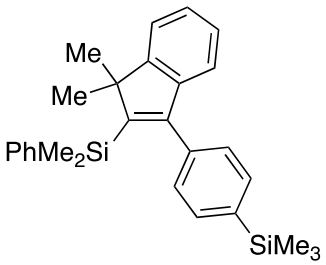

Compound 3la. The product was purified by GPC with $CHCl_3$ instead of silica gel preparative TLC. White solid. 91% yield (77.3 mg).

^{1}H NMR ($CDCl_3$): δ 7.40-7.35 (m, 4H), 7.34 (d, $^3J_{HH}$ = 7.3 Hz, 1H), 7.29-7.19 (m, 4H), 7.14 (td, $^3J_{HH}$ = 7.6 Hz and $^4J_{HH}$ = 0.9 Hz, 1H), 7.08 (d, $^3J_{HH}$ = 8.2 Hz, 2H), 6.88 (d, $^3J_{HH}$ = 7.4 Hz, 1H), 1.41 (s, 6H), 0.28 (s, 9H), 0.27 (s, 6H). ^{13}C{^{1}H} NMR ($CDCl_3$): δ 156.7, 153.8, 151.3, 144.7, 140.1, 139.0, 137.9, 134.1, 132.9, 128.7, 128.6, 127.6, 126.5, 125.9, 120.91, 120.86, 54.9, 25.7, 0.3, −0.9. IR (neat) 2958, 1551, 1427, 1248, 1107, 831,

816, 701, 467 cm^{-1}. Mp: 116.9–120.6 °C. HRMS (EI) calcd for $C_{28}H_{34}Si_2$ (M^+) 426.2194, found 426.2194.

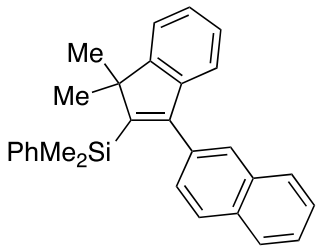

Compound 3ma. The product was further purified by GPC with $CHCl_3$. White solid. 42% yield (34.2 mg).

^1H NMR ($CDCl_3$): δ 7.87-7.81 (m, 1H), 7.76 (d, $^3J_{HH}$ = 8.2 Hz, 1H), 7.63-7.58 (m, 1H), 7.53-7.42 (m, 3H), 7.41-7.35 (m, 3H), 7.30-7.18 (m, 5H), 7.14 (td, $^3J_{HH}$ = 7.3 Hz and $^4J_{HH}$ = 0.9 Hz, 1H), 6.87 (d, $^3J_{HH}$ = 7.3 Hz, 1H), 1.47 (s, 6H), 0.24 (s, 6H). $^{13}C\{^1H\}$ NMR ($CDCl_3$): δ 156.8, 153.6, 152.0, 144.6, 140.4, 135.1, 134.1, 133.2, 132.7, 128.7, 128.6, 128.2, 127.8, 127.64, 127.61, 127.5, 126.6, 126.04, 126.02, 125.9, 120.9, 120.8, 55.0, 25.7, 0.2. IR (neat) 3045, 2961, 1541, 1428, 1248, 1026, 812, 743, 698, 474 cm^{-1}. Mp: 118.4–122.6 °C. HRMS (FAB) calcd for $C_{29}H_{28}Si$ (M^+) 404.1955, found 404.1961.

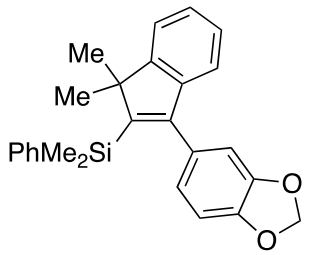

Compound 3na. The product was purified by GPC with $CHCl_3$ instead of silica gel preparative TLC. White solid. 81% yield (64.8 mg).

^1H NMR ($CDCl_3$): δ 7.44-7.38 (m, 2H), 7.33 (d, $^3J_{HH}$ = 7.3 Hz, 1H), 7.31-7.20 (m, 4H), 7.16 (t, $^3J_{HH}$ = 7.3 Hz, 1H), 6.91 (d, $^3J_{HH}$ = 7.3 Hz, 1H), 6.70 (d, $^3J_{HH}$ = 7.8 Hz, 1H),

6.60-6.56 (m, 1H), 6.54 (s, 1H), 5.95 (s, 2H), 1.40 (s, 6H), 0.32 (s, 6H). $^{13}C\{^{1}H\}$ NMR ($CDCl_3$): δ 156.7, 153.2, 151.7, 147.2, 146.8, 144.6, 140.1, 134.1, 131.2, 128.7, 127.6, 126.5, 126.0, 122.9, 120.9, 120.7, 110.0, 108.0, 101.0, 54.7, 25.6, 0.3. IR (neat) 2958, 2878, 1477, 1228, 1034, 813, 728, 698, 468 cm^{-1}. Mp: 112.5–116.6 °C. HRMS (FAB) calcd for $C_{26}H_{26}O_2Si$ (M^+) 398.1697, found 398.1705.

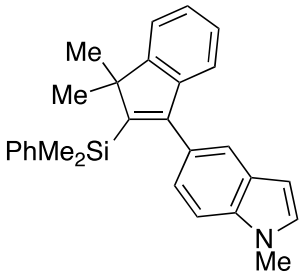

Compound 3oa. The reaction was conducted using 2.0 equiv of **2a** in the presence of 10 mol% of CuI, 20 mol% of JohnPhos, and 2.0 equiv of NaO*t*Bu. The product was purified by silica gel preparative TLC with hexane/EtOAc = 30/1 and further purified by GPC with $CHCl_3$. Pale yellow solid. 70% yield (56.8 mg).

^{1}H NMR ($CDCl_3$): δ 7.48-7.43 (m, 2H), 7.37-7.31 (m, 2H), 7.31-7.23 (m, 4H), 7.20 (td, $^{3}J_{HH}$ = 7.3 Hz and $^{4}J_{HH}$ = 1.4 Hz, 1H), 7.13 (td, $^{3}J_{HH}$ = 7.3 Hz and $^{4}J_{HH}$ = 0.9 Hz, 1H), 7.07-7.02 (m, 2H), 6.91 (d, $^{3}J_{HH}$ = 7.3 Hz, 1H), 6.38 (d, $^{3}J_{HH}$ = 3.2 Hz, 1H), 3.82 (s, 3H), 1.40 (s, 6H), 0.19 (s, 6H). $^{13}C\{^{1}H\}$ NMR ($CDCl_3$): δ 156.8, 154.9, 150.8, 145.3, 140.8, 136.2, 134.3, 129.0, 128.6, 128.4, 128.2, 127.5, 126.4, 125.7, 123.4, 121.9, 121.1, 120.7, 108.7, 101.2, 54.6, 33.0, 25.8, 0.2. IR (neat) 2963, 1513, 1427, 1245, 1101, 1022, 822, 723, 468 cm^{-1}. Mp: 161.9–162.8 °C. HRMS (FAB) calcd for $C_{28}H_{29}NSi$ (M^+) 407.2064, found 407.2062.

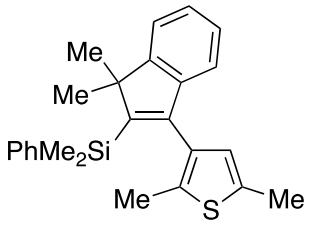

Compound 3pa. The product was further purified by GPC with $CHCl_3$. Colorless oil. 75% yield (58.0 mg).

^{1}H NMR ($CDCl_3$): δ. 7.43-7.38 (m, 2H), 7.34-7.23 (m, 4H), 7.20 (td, $^3J_{HH}$ = 7.3 Hz and $^4J_{HH}$ = 1.0 Hz, 1H), 7.15 (td, $^3J_{HH}$ = 7.3 Hz and $^4J_{HH}$ = 1.5 Hz, 1H), 6.85 (d, $^3J_{HH}$ = 6.8 Hz, 1H), 6.17 (s, 1H), 2.34 (s, 3H), 1.98 (s, 3H), 1.40 (s, 3H), 1.37 (s, 3H), 0.38 (s, 3H), 0.28 (s, 3H). ^{13}C{^{1}H} NMR ($CDCl_3$): δ 156.6, 153.2, 149.0, 144.1, 139.8, 135.2, 134.1, 133.6, 133.3, 128.7, 128.0, 127.5, 126.5, 125.9, 120.8, 120.6, 54.8, 26.3, 25.2, 15.3, 13.6, −0.3, −0.7. IR (neat) 3067, 2955, 2919, 1590, 1534, 1428, 1246, 1112, 908, 809, 699, 468 cm^{-1}. HRMS (FAB) calcd for $C_{25}H_{28}SSi$ (M^+) 388.1675, found 388.1675.

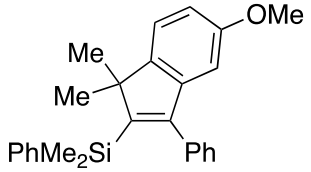

Compound 3qa. The reaction was conducted by using 1.8 equiv of NaO*t*Bu. The product was purified by GPC with $CHCl_3$ instead of silica gel preparative TLC. White solid. 62% yield (47.4 mg).

^{1}H NMR ($CDCl_3$): δ 7.44-7.38 (m, 2H), 7.32-7.22 (m, 6H), 7.22 (d, $^3J_{HH}$ = 8.2 Hz, 1H), 7.15-7.09 (m, 2H), 6.78 (dd, $^3J_{HH}$ = 8.2 Hz and $^4J_{HH}$ = 2.3 Hz, 1H), 6.39 (d, $^4J_{HH}$ = 2.3 Hz, 1H), 3.70 (s, 3H), 1.37 (s, 6H), 0.23 (s, 6H). ^{13}C{^{1}H} NMR ($CDCl_3$): δ 159.1, 153.5, 152.8, 149.1, 146.0, 140.2, 137.4, 134.2, 129.5, 128.7, 128.0, 127.6, 127.3, 121.3, 112.0, 106.1, 55.6, 54.3, 25.9, 0.2. IR (neat) 3064, 2956, 1601, 1488, 1233, 1146, 812, 699, 604 cm^{-1}. Mp: 67.2–68.9 °C. HRMS (FAB) calcd for $C_{26}H_{28}OSi$ (M^+) 384.1904,

found 384.1907.

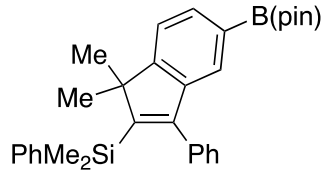

Compound 3ra. The reaction was conducted using 2.0 equiv of **2a** in the presence of 10 mol% of CuI, 20 mol% of JohnPhos, and 2.0 equiv of NaO*t*Bu. The product was not purified and directly used in Scheme 4a. 64% NMR yield.

^{1}H NMR ($CDCl_3$): δ 7.75-7.70 (m, 1H), 7.43-7.38 (m, 2H) 7.36 (d, $^{3}J_{HH}$ = 7.3 Hz, 1H), 7.32 (s, 1H), 7.32-7.22 (m, 5H), 7.31-7.10 (m, 3H), 1.37 (s, 6H), 1.28 (s, 12H), 0.21 (s, 6H).

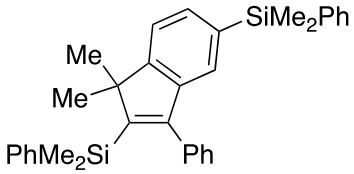

Compound 3sa. The reaction was conducted using 3.0 equiv of **2a** in the presence of 10 mol% of CuI, 20 mol% of JohnPhos, and 3.0 equiv of NaO*t*Bu. The product was further purified by GPC with $CHCl_3$. White solid. 51% yield (50.1 mg).

^{1}H NMR ($CDCl_3$): δ 7.49-7.45 (m, 2H), 7.44-7.40 (m, 2H), 7.37 (dd, $^{3}J_{HH}$ = 7.3 Hz and $^{4}J_{HH}$ = 0.9 Hz, 1H), 7.34-7.29 (m, 4H), 7.29-7.23 (m, 6H), 7.15-7.10 (m, 2H), 7.06 (s, 1H), 1.39 (s, 6H), 0.46 (s, 6H), 0.23 (s, 6H). ^{13}C{^{1}H} NMR ($CDCl_3$): δ 157.9, 153.9, 151.3, 144.1, 140.3, 138.8, 137.4, 135.9, 134.3, 134.2, 132.3, 129.5, 129.1, 128.7, 128.0, 127.8, 127.6, 127.3, 126.3, 120.5, 54.8, 25.7, 0.3, −2.1. IR (neat) 2959, 1588, 1427, 1243, 1112, 1068, 829, 699, 594, 474, 433 cm^{-1}. Mp: 74.2–77.9 °C. HRMS (FAB) calcd for $C_{33}H_{36}Si_2$ (M^+) 488.2350, found 488.2356.

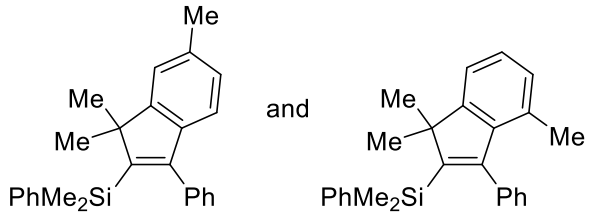

Compounds 3ta and 3ta'. Colorless oil. 89% yield (65.9 mg; **3ta/3ta'** = 80/20).

^{1}H NMR ($CDCl_3$): δ 7.44-7.40 (m, 0.4H), 7.39-7.34 (m, 1.6H), 7.31-7.06 (m, 9.8H), 6.97 (d, $^3J_{HH}$ = 7.8 Hz, 0.2H), 6.89 (d, $^3J_{HH}$ = 7.3 Hz, 0.8H), 6.75 (d, $^3J_{HH}$ = 7.8 Hz, 0.2H), 2.39 (s, 0.6H), 1.68 (s, 2.4H), 1.38 (s, 6H), 0.23 (s, 1.2H), 0.19 (s, 4.8H). ^{13}C{^{1}H} NMR ($CDCl_3$): δ 157.7, 157.0, 154.3, 153.7, 151.7, 150.1, 142.3, 141.0, 140.3, 140.1, 137.8, 135.9, 134.2, 134.1, 132.3, 129.9, 129.6, 129.4, 128.7, 128.6, 128.0, 127.8, 127.62, 127.56, 127.3, 127.2, 127.1, 126.0, 121.8, 120.5, 119.0, 54.6, 53.9, 25.8, 21.7, 19.7, 0.3. IR (neat) 3067, 2956, 1541, 1428, 1248, 1110, 1023, 813, 698, 617, 468 cm^{-1}. HRMS (FAB) calcd for $C_{26}H_{28}Si$ (M^+) 368.1955, found 368.1953.

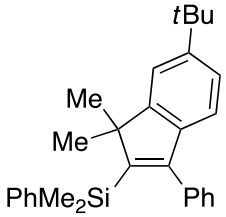

Compound 3ua. White solid. 66% yield (53.9 mg).

^{1}H NMR ($CDCl_3$): δ 7.44-7.39 (m, 2H), 7.37 (d, $^4J_{HH}$ = 1.8 Hz, 1H), 7.31-7.22 (m, 6H), 7.20 (dd, $^3J_{HH}$ = 8.2 Hz and $^4J_{HH}$ = 1.8 Hz, 1H), 7.14-7.09 (m, 2H), 6.80 (d, $^3J_{HH}$ = 8.3 Hz, 1H), 1.40 (s, 6H), 1.34 (s, 9H), 0.23 (s, 6H). ^{13}C{^{1}H} NMR ($CDCl_3$): δ 156.6, 153.6, 150.7, 149.4, 142.3, 140.4, 137.8, 134.2, 129.5, 128.7, 128.0, 127.6, 127.2, 123.6, 120.2, 117.9, 54.9, 35.0, 31.9, 25.9, 0.3. IR (neat) 2950, 1542, 1425, 1245, 1106, 1015, 825, 702, 477, 424 cm^{-1}. Mp: 106.4–110.6 °C. HRMS (FAB) calcd for $C_{29}H_{34}Si$ (M^+)

410.2424, found 410.2437.

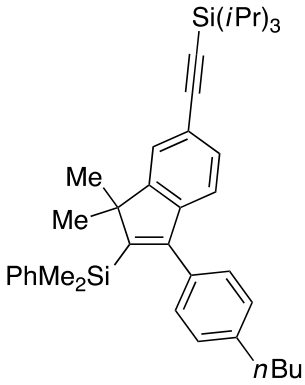

Compound 3va. The reaction was conducted using 2.0 equiv of **2a** in the presence of 10 mol% of CuI, 20 mol% of JohnPhos, and 2.0 equiv of NaO*t*Bu. The product was further purified by GPC with $CHCl_3$. Colorless oil. 33% yield (38.9 mg).

^{1}H NMR ($CDCl_3$): δ 7.42-7.37 (m, 3H), 7.32-7.22 (m, 4H), 7.07 (d, $^3J_{HH}$ = 7.8 Hz, 2H), 6.99 (d, $^3J_{HH}$ = 7.8 Hz, 2H), 6.79 (d, $^3J_{HH}$ = 7.8 Hz, 1H), 2.61 (t, $^3J_{HH}$ = 7.6 Hz, 2H), 1.66-1.56 (m, 2H), 1.43-1.32 (m, 2H), 1.38 (s, 6H), 1.18-1.07 (m, 21H), 0.95 (t, $^3J_{HH}$ = 7.3 Hz, 3H), 0.24 (s, 6H). ^{13}C{^{1}H} NMR ($CDCl_3$): δ 156.6, 153.4, 153.0, 145.0, 142.0, 140.1, 134.3, 134.2, 130.9, 129.3, 128.7, 128.1, 127.6, 124.4, 120.7, 120.6, 108.4, 90.2, 54.8, 35.6, 33.8, 25.6, 22.5, 18.9, 14.2, 11.5, 0.2. IR (neat) 2942, 2863, 2151, 1462, 1248, 1110, 867, 732, 639, 468 cm^{-1}. HRMS (FAB) calcd for $C_{40}H_{54}Si_2$ (M^+) 590.3759, found 590.3756.

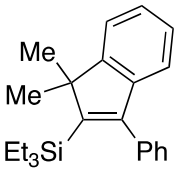

Compound 3ab. The reaction was conducted at 100 °C. White solid. 96% yield (64.5 mg).

^{1}H NMR ($CDCl_3$): δ 7.43-7.33 (m, 4H), 7.30-7.26 (m, 2H), 7.21 (td, $^3J_{HH}$ = 7.8

Hz and $^4J_{HH}$ = 0.9 Hz, 1H), 7.14 (td, $^3J_{HH}$ = 7.3 Hz and $^4J_{HH}$ = 0.9 Hz, 1H), 6.79 (d, $^3J_{HH}$ = 7.3 Hz, 1H), 1.46 (s, 6H), 0.86 (t, $^3J_{HH}$ = 7.8 Hz, 9H), 0.51 (q, $^3J_{HH}$ = 7.8 Hz, 6H). $^{13}C\{^1H\}$ NMR ($CDCl_3$): δ 156.8, 152.9, 151.4, 145.0, 138.0, 129.3, 128.0, 127.4, 126.5, 125.7, 120.8, 120.6, 54.7, 25.6, 7.7, 4.6. IR (neat) 2953, 2872, 1544, 1485, 1238, 1000, 799, 722, 699, 597 cm^{-1}. Mp: 34.9–37.8 °C. HRMS (FAB) calcd for $C_{23}H_{30}Si$ (M^+) 334.2111, found 334.2117.

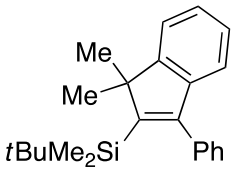

Compound 3ac. The reaction was conducted at 100 °C. The product was further purified by GPC with $CHCl_3$. White solid. 72% yield (48.3 mg).

^1H NMR ($CDCl_3$): δ 7.40-7.30 (m, 4H), 7.29-7.24 (m, 2H), 7.24-7.18 (m, 1H) 7.13 (td, $^3J_{HH}$ = 7.6 Hz and $^4J_{HH}$ = 0.9 Hz, 1H), 6.74 (d, $^3J_{HH}$ = 7.3 Hz, 1H), 1.50 (s, 6H), 0.74 (s, 9H), 0.10 (s, 6H). $^{13}C\{^1H\}$ NMR ($CDCl_3$): δ 156.7, 153.8, 151.3, 145.3, 138.1, 130.4, 127.7, 127.3, 126.5, 125.9, 120.9, 120.7, 55.2, 28.4, 26.2, 18.5, −0.7. IR (neat) 2956, 2924, 2852, 1468, 1246, 1006, 809, 751, 683 cm^{-1}. Mp: 62.1–69.2 °C. HRMS (FAB) calcd for $C_{23}H_{31}Si$ ($M+H^+$) 335.2190, found 335.2194.

Procedure for equation 1.

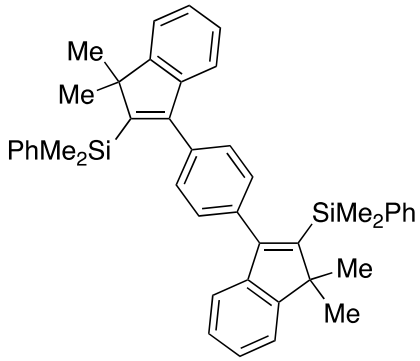

Compound **4** (36.4 mg, 0.100 mmol) and silylboronate **2a** (81.8 μL, 0.300 mmol) were added with the aid of THF (0.20 mL) to a mixture of CuI (1.9 mg, 10 μmol), JohnPhos (6.0 mg, 20 μmol), and NaO*t*Bu (28.9 mg, 0.301 mmol) in THF (0.80 mL), and this was stirred for 20 h at 70 °C. The reaction mixture was directly passed through a pad of silica gel with EtOAc and the solvent was removed under vacuum. The residue was purified by silica gel preparative TLC with hexane and further purified by GPC with $CHCl_3$ to afford compound **5** as a white solid (44.8 mg, 71.0 μmol; 71% yield).

^{1}H NMR ($CDCl_3$): δ 7.49-7.45 (m, 4H), 7.35 (d, $^3J_{HH}$ = 7.1 Hz, 2H), 7.32-7.18 (m, 10H), 7.07 (s, 4H), 6.85 (d, $^3J_{HH}$ = 7.5 Hz, 2H), 1.41 (s, 12H), 0.31 (s, 12 H). ^{13}C{^{1}H} NMR ($CDCl_3$): δ 156.8, 153.6, 151.2, 144.7, 140.3, 136.4, 134.2, 129.1, 128.8, 127.7, 126.5, 126.0, 120.9, 120.8, 54.9, 25.7, 0.5. IR (neat) 3068, 2955, 1491, 1426, 1243, 905, 811, 756, 576 cm^{-1}. Mp: 218.8–234.7 °C. HRMS (EI) calcd for $C_{44}H_{46}Si_2$ (M^+) 630.3133, found 630.3133

Procedure for Scheme 4a, compound 3wa.

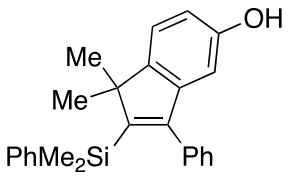

Compound **3ra** obtained by the reaction of **1r** and **2a** (0.104 mmol by ^{1}H NMR) was dissolved in THF (1.0 mL). 3 M NaOHaq (0.40 mL, 1.2 mmol) and H_2O_2 (0.40 mL, 3.9 mmol; 30 wt% in H_2O) were added to it, and the resulting mixture was stirred for 4 h at room temperature. This was diluted with H_2O and extracted with Et_2O. The organic layer was washed with saturated NaClaq, dried over $MgSO_4$, filtered, and concentrated under vacuum. The residue was purified by silica gel preparative TLC with hexane/EtOAc = 30/1 → 20/1 and further purified by preparative HPLC on Daicel

Chiralpak IF column with hexane/*i*PrOH = 95/5 to afford compound **3wa** as a yellow solid (36.0 mg, 97.1 μmol; 93% yield).

^{1}H NMR ($CDCl_3$): δ 7.41 (dd, $^{3}J_{HH}$ = 7.8 and $^{4}J_{HH}$ = 1.8 Hz, 2H), 7.32-7.22 (m, 6H), 7.17 (d, $^{3}J_{HH}$ = 7.8 Hz, 1H), 7.13-7.08 (m, 2H), 6.69 (dd, $^{3}J_{HH}$ = 8.3 Hz and $^{4}J_{HH}$ = 2.3 Hz, 1H), 6.30 (d, $^{4}J_{HH}$ = 2.3 Hz, 1H), 4.52 (s, 1H), 1.37 (s, 6H), 0.23 (s, 6H). $^{13}C\{^{1}H\}$ NMR ($CDCl_3$): δ 154.8, 153.2, 153.0, 149.2, 146.3, 140.1, 137.4, 134.2, 129.4, 128.7, 128.0, 127.6, 127.3, 121.5, 112.8, 107.6, 54.3, 25.9, 0.2. IR (neat) 3551, 2959, 1600, 1546, 1229, 1144, 961, 820, 698, 600 cm^{-1}. Mp: 119.2–121.5 °C. HRMS (FAB) calcd for $C_{25}H_{26}OSi$ (M^{+}) 370.1747, found 370.1753.

Procedure for Scheme 4a, compound 3xa.

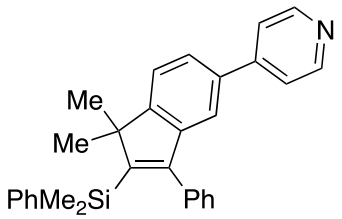

Compound **3ra** obtained by the reaction of **1r** and **2a** (0.128 mmol by ^{1}H NMR) was purified by GPC with $CHCl_3$, and this was added to a mixture of $PdCl_2$(dppf) (6.0 mg, 8.3 μmol), K_2CO_3 (79.8 mg, 0.578 mmol), and 4-bromopyridine hydrochloride (41.7 mg, 0.215 mmol) in 1,4-dioxane (0.80 mL) and H_2O (80 μL). The resulting mixture was stirred for 17 h at 110 °C and this was diluted with H_2O. After extraction with Et_2O, the organic layer was washed with saturated NaClaq, dried over Na_2SO_4, filtered, and concentrated under vacuum. The residue was purified by silica gel preparative TLC with hexane/EtOAc/Et_3N = 24/6/1 and further purified by preparative HPLC on Daicel Chiralpak IB-N column with hexane/*i*PrOH = 95/5 to afford compound **3xa** as a white solid (41.4 mg, 95.9 μmol; 75% yield).

^{1}H NMR ($CDCl_3$): δ 8.57 (bs, 2H), 7.50 (dd, $^{3}J_{HH}$ = 7.8 Hz and $^{4}J_{HH}$ = 2.0 Hz, 1H), 7.46-7.37 (m, 5H), 7.34-7.24 (m, 6H), 7.19-7.13 (m, 2H), 7.08 (d, $^{4}J_{HH}$ = 1.9 Hz, 1H), 1.43 (s, 6H), 0.26 (s, 6H). $^{13}C\{^{1}H\}$ NMR ($CDCl_3$): δ 157.8, 153.2, 153.0, 150.2, 148.9, 145.7, 139.9, 137.1, 137.0, 134.2, 129.5, 128.8, 128.2, 127.7, 127.6, 125.0, 121.9, 121.5, 119.2, 54.8, 25.6, 0.2. IR (neat) 2953, 1597, 1546, 1249, 1102, 816, 735, 622, 536 cm^{-1}. Mp: 120.2–121.3 °C. HRMS (FAB) calcd for $C_{30}H_{30}NSi$ ($M+H^{+}$) 432.2142, found 432.2158.

Procedure for Scheme 4b, compound 7 via compound 6.

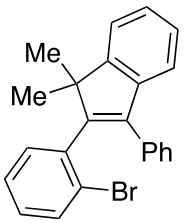

A solution of ICl (34.0 μL, 0.649 mmol) in CH_2Cl_2 (5 mL) was added slowly over 5 min to a solution of compound **3aa** (177 mg, 0.499 mmol) in CH_2Cl_2 (10 mL) at 0 °C, and the mixture was stirred for 2 h at 0 °C. The reaction was quenched with 5% Na_2SO_3aq and this was extracted with Et_2O. The organic layer was washed with saturated NaClaq, dried over $MgSO_4$, filtered, and concentrated under vacuum. The residue was passed through a pad of silica gel with EtOAc and purified by GPC with $CHCl_3$ to afford 2-iodo-1,1-dimethyl-3-phenyl-1*H*-indene (CAS 1860883-35-7) as a white solid (161 mg). This was dissolved in THF (1.0 mL) and added to a mixture of $Pd(PPh_3)_4$ (28.9 mg, 25.0 μmol), K_2CO_3 (207 mg, 1.50 mmol), and 2-bromophenylboronic acid (151 mg, 0.753 mmol) in THF (2.0 mL) and H_2O (0.9 mL). This was stirred for 17 h at 80 °C, and the resulting mixture was diluted with H_2O. After extraction with Et_2O, the organic layer was washed with saturated NaClaq, dried over $MgSO_4$, filtered, and concentrated under

vacuum. The residue was chromatographed on silica gel with hexane/EtOAc = 40/1 → 20/1 to afford compound **6** as a white solid (147 mg, 0.392 mmol; 78% yield over 2 steps).

^{1}H NMR ($CDCl_3$): δ 7.51 (d, $^{3}J_{HH}$ = 8.2 Hz, 1H), 7.46-7.41 (m, 1H), 7.41-7.36 (m, 1H), 7.34-7.19 (m, 9H), 7.12 (ddd, $^{3}J_{HH}$ = 8.3 and 6.0 Hz and $^{4}J_{HH}$ = 3.2 Hz, 1H), 1.46 (s, 3H), 1.40 (s, 3H). $^{13}C\{^{1}H\}$ NMR ($CDCl_3$): δ 153.4, 150.5, 142.4, 139.7, 137.3, 135.1, 133.3, 132.1, 129.1, 128.8, 128.1, 127.2, 126.72, 126.68, 125.8, 124.9, 121.7, 121.0, 52.7, 25.3, 24.2. IR (neat) 2966, 1460, 1260, 1019, 782, 748, 698, 655, 534 cm^{-1}. Mp: 124.5–127.3 °C. HRMS (FAB) calcd for $C_{23}H_{19}Br$ (M^{+}) 374.0665, found 374.0678.

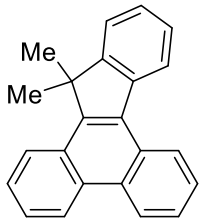

A mixture of compound **6** (34.5 mg, 91.9 μmol), $Pd(OAc)_2$ (1.8 mg, 8.0 μmol), PCy_3•HBF_4 (3.1 mg, 8.4 μmol), and K_2CO_3 (41.5 mg, 0.300 mmol) in DMA (0.5 mL) was stirred for 12 h at 130 °C. The resulting mixture was diluted with H_2O and this was extracted with Et_2O. The organic layer was washed with saturated NaClaq and concentrated under vacuum. The residue was passed through a pad of silica gel with CH_2Cl_2 and the solvent was removed under vacuum. The residue was purified by GPC with $CHCl_3$ to afford compound **7** (CAS 1313594-39-6) as a white solid (27.0 mg, 91.7 μmol; 100% yield).

^{1}H NMR ($CDCl_3$): δ 8.96 (dd, $^{3}J_{HH}$ = 8.0 Hz and $^{4}J_{HH}$ = 1.2 Hz, 1H), 8.85 (dd, $^{3}J_{HH}$ = 7.6 Hz and $^{4}J_{HH}$ = 1.5 Hz, 2H), 8.45 (d, $^{3}J_{HH}$ = 7.8 Hz, 1H), 8.39-8.34 (m, 1H), 7.76 (ddd, $^{3}J_{HH}$ = 8.3 and 6.8 Hz and $^{4}J_{HH}$ =1.5 Hz, 1H), 7.73-7.66 (m, 3H), 7.63 (dd, $^{3}J_{HH}$ = 7.5 Hz and $^{4}J_{HH}$ = 0.7 Hz, 1H), 7.49 (td, $^{3}J_{HH}$ = 7.5 Hz and $^{4}J_{HH}$ = 1.5 Hz, 1H), 7.43 (td,

$^{3}J_{HH}$ = 7.3 Hz and $^{4}J_{HH}$ = 0.9 Hz, 1H), 1.80 (s, 6H). $^{13}C\{^{1}H\}$ NMR ($CDCl_3$): δ 156.8, 148.9, 147.4, 139.9, 131.2, 131.1, 129.3, 128.9, 127.14, 127.10, 126.6, 126.5, 126.1, 126.0, 125.4, 124.8, 123.9, 123.6, 123.3, 122.2, 48.3, 26.6.

Procedure for Scheme 4b, compound 9 via compound 8.

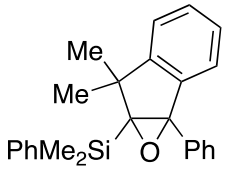

m-Chloroperbenzoic acid (54.8 mg, 0.229 mmol; 72 wt%) was added to a mixture of compound **3aa** (70.9 mg, 0.200 mmol) and $NaHCO_3$ (40.5 mg, 0.482 mmol) in CH_2Cl_2 (3.0 mL), and the resulting mixture was stirred for 4 h at room temperature. The reaction was quenched with 5% Na_2SO_3aq and this was extracted with Et_2O. The organic layer was washed with saturated NaClaq, dried over $MgSO_4$, filtered, and concentrated under vacuum. The residue was purified by silica gel preparative TLC with hexane/EtOAc = 30/1 to afford compound **8** as a colorless viscous oil (66.9 mg, 0.181 mmol; 90% yield).

^{1}H NMR ($CDCl_3$): δ 7.49-7.41 (m, 3H), 7.38-7.20 (m, 8H), 7.09 (d, $^{3}J_{HH}$ = 7.8 Hz, 1H), 7.06 (td, $^{3}J_{HH}$ = 7.3 Hz and $^{4}J_{HH}$ = 1.0 Hz, 1H), 6.88 (d, $^{3}J_{HH}$ = 7.3 Hz, 1H), 1.32 (s, 3H), 1.17 (s, 3H), 0.29 (s, 3H), 0.07 (s, 3H). $^{13}C\{^{1}H\}$ NMR ($CDCl_3$): δ 153.7, 143.8, 137.5, 134.9, 134.6, 129.3, 128.8, 128.53, 128.48, 128.2, 127.8, 127.7, 127.5, 126.0, 124.7, 123.2, 73.4, 73.2, 48.9, 28.5, 23.7, −1.8, −2.0. IR (neat) 2962, 1478, 1428, 1249, 1114, 908, 809, 730, 699, 626, 471 cm^{-1}. HRMS (FAB) calcd for $C_{25}H_{26}OSi$ (M^{+}) 370.1747, found 370.1747.

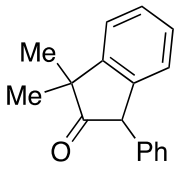

Trifluoroacetic acid (16 μL, 0.21 mmol) was added to a solution of compound **8** (66.9 mg, 0.181 mmol) in Et_2O (1.5 mL) and MeOH (6.0 mL), and the mixture was stirred for 3 h at 80 °C. The reaction was quenched with saturated $NaHCO_3$aq and this was extracted with Et_2O. The organic layer was washed with saturated NaClaq, dried over $MgSO_4$, filtered, and concentrated under vacuum. The residue was purified by silica gel preparative TLC with hexane/EtOAc = 30/1 to afford compound **9** (CAS 2097255-81-5) as a white solid (34.0 mg, 0.144 mmol; 80% yield).

^{1}H NMR ($CDCl_3$): δ 7.41-7.35 (m, 1H), 7.35-7.23 (m, 5H), 7.20 (d, $^3J_{HH}$ = 7.3 Hz, 1H), 7.15-7.10 (m, 2H), 4.74 (s, 1H), 1.41 (s, 3H), 1.35 (s, 3H). $^{13}C\{^1H\}$ NMR ($CDCl_3$): δ 219.3, 148.2, 138.7, 138.6, 128.8, 128.7, 128.5, 127.9, 127.3, 126.0, 123.1, 57.9, 49.9, 26.4, 26.0.

Procedure for Scheme 4c, compound 11 via compound 10.

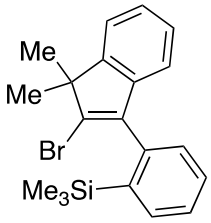

A mixture of *N*-bromosuccinimide (137 mg, 0.742 mmol) and compound **3ga** (70.3 mg, 0.165 mmol) in MeCN (1.0 mL) and CH_2Cl_2 (0.5 mL) was stirred for 24 h at 45 °C and for 26 h at 50 °C. The solvents were removed under vacuum, and the residue was purified by silica gel preparative TLC with hexane to afford compound **10** as a white solid (50.2 mg, 0.135 mmol; 82% yield).

^{1}H NMR ($CDCl_3$): δ 7.71-7.66 (m, 1H), 7.46-7.38 (m, 2H), 7.37 (d, $^3J_{HH}$ = 7.3 Hz,

1H), 7.21 (td, $^{3}J_{HH}$ = 7.6 Hz and $^{4}J_{HH}$ = 1.0 Hz, 1H), 7.15 (td, $^{3}J_{HH}$ = 7.6 Hz and $^{4}J_{HH}$ = 1.0 Hz, 1H), 7.13-7.09 (m, 1H), 6.82 (d, $^{3}J_{HH}$ = 7.3 Hz, 1H), 1.39 (s, 3H), 1.37 (s, 3H), 0.07 (s, 9H). $^{13}C\{^{1}H\}$ NMR ($CDCl_3$): δ 151.1, 144.0, 142.8, 140.4, 139.4, 137.7, 135.2, 129.8, 129.3, 127.3, 126.8, 125.5, 121.6, 121.0, 51.7, 25.3, 23.1, 0.5. IR (neat) 2966, 1461, 1248, 1121, 1004, 835, 748, 673, 621, 440 cm^{-1}. Mp: 41.7–45.8 °C. HRMS (FAB) calcd for $C_{20}H_{23}BrSi$ (M^{+}) 370.0747, found 370.0755.

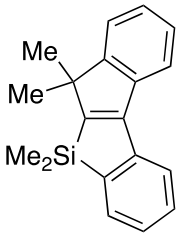

*t*BuLi (171 μL, 0.290 mmol; 1.70 M solution in pentane) was slowly added to a solution of compound **10** (49.0 mg, 0.132 mmol) in Et_2O (11 mL) at −78 °C, and the mixture was stirred for 21 h while gradually raising the temperature to room temperature. The reaction was quenched with saturated NH_4Claq and this was extracted with Et_2O. The organic layer was washed with saturated NaClaq, dried over $MgSO_4$, filtered, and concentrated under vacuum. The residue was purified by silica gel preparative TLC with hexane to afford compound **11** as a white solid (28.9 mg, 0.104 mmol; 79% yield).

^{1}H NMR ($CDCl_3$): δ 7.93 (d, $^{3}J_{HH}$ = 7.8 Hz, 1H), 7.89 (d, $^{3}J_{HH}$ = 7.3 Hz, 1H), 7.56 (d, $^{3}J_{HH}$ = 7.3 Hz, 1H), 7.43 (td, $^{3}J_{HH}$ = 7.5 Hz and $^{4}J_{HH}$ = 1.5 Hz, 1H), 7.41 (d, $^{3}J_{HH}$ = 7.3 Hz, 1H), 7.34 (td, $^{3}J_{HH}$ = 7.3 Hz and $^{4}J_{HH}$ = 1.0 Hz, 1H), 7.31-7.23 (m, 2H), 1.43 (s, 6H), 0.41 (s, 6H). $^{13}C\{^{1}H\}$ NMR ($CDCl_3$): δ 161.3, 160.2, 155.3, 145.2, 143.2, 139.6, 132.3, 129.7, 126.6, 126.5, 125.8, 122.0, 121.9, 121.1, 50.2, 26.0, −3.5. IR (neat) 2952, 1586, 1508, 1351, 1246, 1041, 839, 746, 657, 573 cm^{-1}. Mp: 90.5–91.7 °C. HRMS (FAB) calcd for $C_{19}H_{20}Si$ (M^{+}) 276.1329, found 276.1328.

Procedure for Scheme 5a.

Compound **1a-*d*$_5$** (45.3 mg, 0.201 mmol) and silylboronate **2a** (81.8 μL, 0.300 μmol) were added with the aid of THF (0.10 mL) to a mixture of CuI (1.9 mg, 10 μmol), JohnPhos (6.0 mg, 20 μmol), and NaO*t*Bu (29.2 mg, 0.304 mmol) in THF (0.90 mL), and this was stirred for 20 h at 70 °C. The reaction mixture was cooled to room temperature and 4-methoxybenzaldehyde (**12**; 40.8 mg, 0.300 mmol) was added to it. This was further stirred for 2 h at room temperature, and the reaction was quenched with saturated NH_4Claq. After extraction with Et_2O, the organic layer was washed with saturated NaClaq, dried over $MgSO_4$, filtered, and concentrated under vacuum. The yields of compound **3aa-*d*$_4$** and 4-methoxybenzyl alcohol-*d* (**13-*d***) were determined by ^{1}H NMR against internal standard (dimethyl terephthalate).

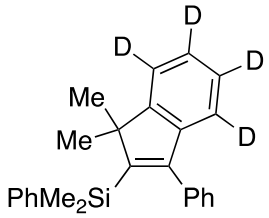

Compound 3aa-*d*$_5$. The product was purified by silica gel preparative TLC with hexane/EtOAc = 15/2 and further purified by GPC with $CHCl_3$. White solid. 64% yield (45.6 mg).

^{1}H NMR ($CDCl_3$): δ 7.45-7.40 (m, 2H), 7.33-7.22 (m, 6H), 7.17-7.10 (m, 2H), 1.39, (s, 6H), 0.24 (s, 6H). ^{13}C{^{1}H} NMR ($CDCl_3$): δ 156.7, 153.7, 151.3, 144.6, 140.2, 137.6, 134.2, 129.5, 128.7, 128.0, 127.6, 127.3, 126.0 (t, $^1J_{CD}$ = 23.5 Hz), 125.5 (t, $^1J_{CD}$ = 23.5 Hz), 120.5 (t, $^1J_{CD}$ = 23.5 Hz), 120.4 (t, $^1J_{CD}$ = 24.0 Hz), 54.9, 25.7, 0.2. IR (neat) 3044, 2960, 1484, 1256, 1017, 811, 698, 583, 470 cm^{-1}. Mp: 73.3–75.5 °C. HRMS (FAB) calcd for $C_{25}H_{22}D_4Si$ (M^+) 358.2049, found 358.2052.

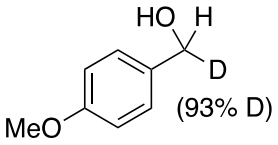

Compound 13-*d*.

^{1}H NMR ($CDCl_3$): δ 7.30 (d, $^3J_{HH}$ = 8.2 Hz, 2H), 6.90 (d, $^3J_{HH}$ = 8.7 Hz, 2H), 4.64-4.58 (m, 1.07H), 3.81 (s, 3H), 1.52 (d, $^3J_{HH}$ = 5.5 Hz, 1H).

Procedure for equation 2.

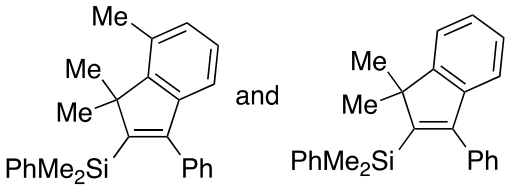

Compound **1y** (47.2 mg, 0.202 mmol) and silylboronate **2a** (109 μL, 0.400 μmol) were added with the aid of THF (0.20 mL) to a mixture of CuI (3.8 mg, 20 μmol), JohnPhos (12.0 mg, 40.1 μmol), and NaO*t*Bu (38.5 mg, 0.401 mmol) in THF (0.80 mL), and this was stirred for 20 h at 90 °C. The reaction mixture was directly passed through a pad of silica gel with EtOAc and the solvent was removed under vacuum. The residue was purified by silica gel preparative TLC with hexane to afford a mixture of compound **3ya** and compound **3aa** as a white solid (44.3 mg, 0.121 mmol combined; 61% yield, **3ya**/**3aa** = 81/19).

3ya: ^{1}H NMR ($CDCl_3$): δ 7.43-7.39 (m, 2H), 7.29-7.22 (m, 6H), 7.11-7.06 (m, 2H), 7.05 (d, $^3J_{HH}$ = 7.3 Hz, 1H), 6.96 (d, $^3J_{HH}$ = 7.3 Hz, 1H), 6.65 (d, $^3J_{HH}$ = 7.3 Hz, 1H), 2.52 (s, 3H), 1.51 (s, 6H), 0.24 (s, 6H). $^{13}C\{^1H\}$ NMR ($CDCl_3$): δ 153.5, 152.9, 152.0, 145.6, 140.4, 137.7, 134.2, 132.2, 129.6, 128.7, 128.6, 128.0, 127.6, 127.2, 126.7, 118.7, 56.2, 22.6, 19.1, 0.5. IR (neat) 3044, 2966, 1551, 1425, 1246, 1106, 814, 699, 650, 471 cm^{-1}. Mp: 93.2–95.3 °C. HRMS (EI) calcd for $C_{26}H_{28}Si$ (M^+) 368.1955, found 368.1954.

Kinetic experiments

Data collection for Scheme 5b.

Compound **1a** or **1a-*d*$_5$** (0.200 mmol) and silylboronate **2a** (81.8 µL, 0.300 mmol) were added to a mixture of CuI (1.9 mg, 10 µmol), JohnPhos (6.0 mg, 20 µmol), NaO*t*Bu (28.8 mg, 0.300 mmol), and 1,3,5-trimethoxybenzene (8.4 mg, 50 µmol; internal standard) in THF (4.0 mL) at 40 °C. The resulting mixture was stirred at 40 °C and aliquots (ca. 0.2 mL each) were taken every 3–4 minutes. They were immediately quenched by H_2O and extracted with Et_2O, and the organic layer was concentrated under vacuum. The residues were analyzed by ^{1}H NMR to determine the reaction progress (production of **3aa** or **3aa-*d*$_4$**). Each experiment was carried out twice.

Reaction of 1a. Initial rate = 0.595 (mM/min)

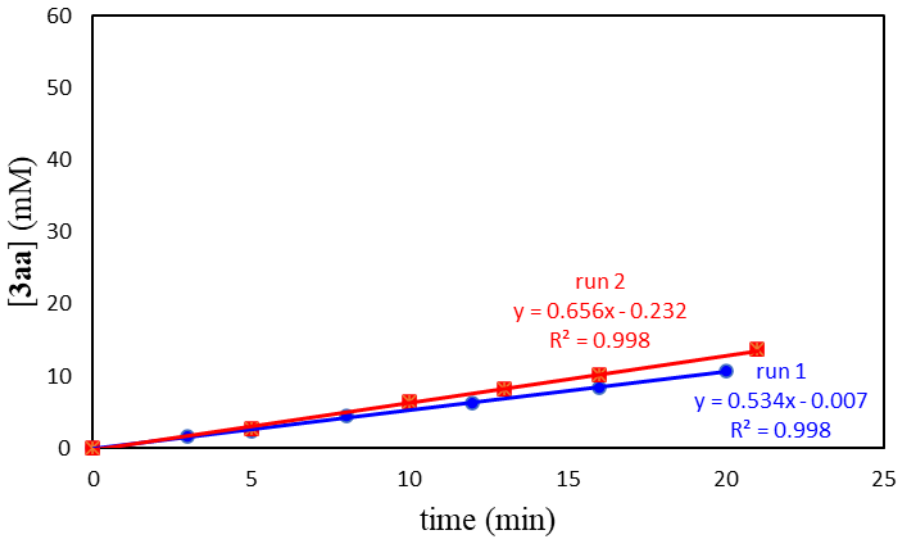

Reaction of 1a-d_5. Initial rate = 0.527 (mM/min)

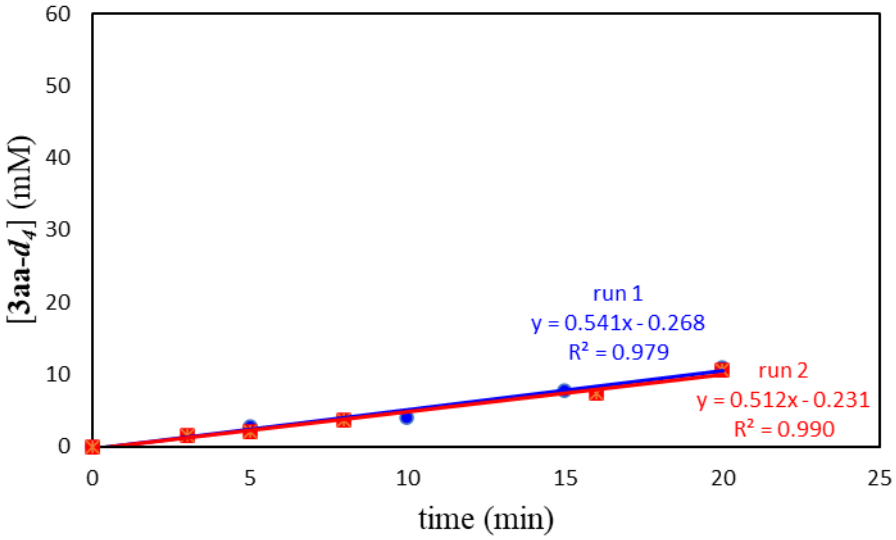

X-ray crystal structure

Compound 3aa

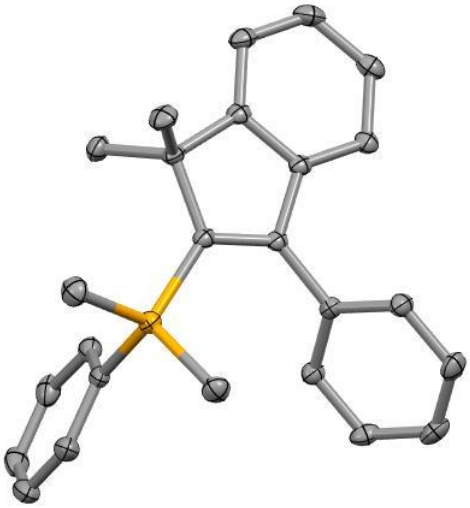

A colorless CH_2Cl_2 solution of compound **3aa** was prepared. Crystals suitable for X-ray analysis were obtained by layering MeOH and slow diffusion of the solvents at room temperature. The crystal structure has been deposited at the Cambridge Crystallographic Data Centre (deposition number: CCDC 2363760). The data can be obtained free of charge via the Internet at https://www.ccdc.cam.ac.uk/structures/.

Crystal data and structure refinement.

Empirical Formula	$C_{25}H_{26}Si$	
Formula Weight	354.55	
Temperature	113 ± 2 K	
Wavelength	0.71075 Å	
Crystal System	Triclinic	
Space Group	$P\bar{1}$	
Unit Cell Dimensions	a = 9.5633(13) Å	α = 65.097(7)°
	b = 10.1666(11) Å	β = 81.059(9)°

	c = 11.7074(12) Å γ = 85.282(9)°
Volume	1019.7(2) Å^3
Z Value	2
Calculated Density	1.155 g/cm^3
Absorption coefficient	0.120 mm^{-1}
F(000)	380
Crystal size	0.290 × 0.130 × 0.080 mm
Theta Range for Data Collection	3.059–27.471°
Index Ranges	−12 ≤ h ≤ 12, −13 ≤ k ≤ 13, −15 ≤ l ≤ 15
Reflections Collected	19242
Independent Reflections	4636 [R(int) = 0.0312]
Completeness to Theta = 25.242°	99.7%
Absorption Correction	Semi-empirical from equivalents
Max. and Min. Transmission	0.990 and 0.966
Refinement Method	Full-matrix least-squares on F^2
Data / Restraints / Parameters	4636 / 0 / 239
Goodness-of-Fit on F^2	1.110
Final R Indices [I>2sigma(I)]	R_1 = 0.0327, wR_2 = 0.0914
R Indices (All Data)	R_1 = 0.0371, wR_2 = 0.0979
Largest Diff. Peak and Hole	0.296 and −0.287 e$^-$/Å^3

3.5 References

[1] (a) Chand, T.; Kapur, M. *Synthesis* **2024**, *56*, 1505–1540. (b) Wu, K.; Lam, N.; Strassfeld, D. A.; Fan, Z.; Qiao, J. X.; Liu, T.; Stamos, D.; Yu, J.-Q. *Angew. Chem., Int. Ed.* **2024**, *63*, e202400509. (c) Pradhan, C.; Punji, B. *Org. Chem. Front.* **2024**, *11*, 2397–2417. (d) Docherty, J. H.; Lister, T. M.; Mcarthur, G.; Findlay, M. T.; Domingo-Legarda, P.; Kenyon, J.; Choudhary, S.; Larrosa, I. *Chem. Rev.* **2023**, *123*, 7692–7760. (e) Sinha, S. K.; Ghosh, P.; Jain, S.; Maiti, S.; Al-Thabati, S. A.; Alshehri, A. A.; Mokhtar, M.; Maiti, D. *Chem. Soc. Rev.* **2023**, *52*, 7461–7503. (f) Pati, B. V.; Puthalath, N. N.; Banjare, S. K.; Nanda, T.; Ravikumar, P. C. *Org. Biomol. Chem.* **2023**, *21*, 2842–2869. (g) Dalton, T.; Faber, T.; Glorius, F. *ACS Cent. Sci.* **2021**, *7*, 245–261. (h) Gandeepan, P.; Müller, T.; Zell, D.; Cera, G.; Warratz, S.; Ackermann, L. *Chem. Rev*. **2019**, *119*, 2192–2452. (i) Shi, X.-Y.; Han, W.-J.; Li, C.-J. *Chem. Rec.* **2016**, *16*, 1178–1190.

[2] (a) Požgan, F.; Grošelj, U.; Svete, J.; Štefane, B.; Al Mamari, H. H. *Molecules* **2024**, *29*, 1917. (b) Sunny, S.; Maingle, M.; Sheeba, L.; Pathan, F. R.; J., G. S.; Juloori, H.; Gadewar, S. G.; Seth, K. *Synthesis* **2024**, *56*, 611–638. (c) Sinha, S. K.; Guin, S.; Maiti, S.; Biswas, J. P.; Porey, S.; Maiti, D. *Chem. Rev*. **2022**, *122*, 5682–5841. (d) Joshi, A.; De, S. R. *Eur. J. Org. Chem.* **2021**, *2021*, 1837–1858. (e) Yang, Z.; Yu, J.-T.; Pan, C. *Org. Biomol. Chem.* **2021**, *19*, 8442–8465. (f) Ankade, S. B.; Shabade, A. B.; Soni, V.; Punji, B. *ACS Catal.* **2021**, *11*, 3268–3292.

[3] (a) Basak, S.; Biswas, J. P.; Maiti, D. *Synthesis* **2021**, *53*, 3151–3179. (b) Fricke, C.; Reid, W. B.; Schoenebeck, F. *Eur. J. Org. Chem.* **2020**, *2020*, 7119–7130. (c) Nareddy, P.; Jordan, F.; Szostak, M. *ACS Catal*. **2017**, *7*, 5721–5745. See also: (d) Changmai, S.; Sultana, S.; Saikia, A. K. *ChemistrySelect* **2023**, *8*, e202203530. (e) Tian, T.; Li,

Z.; Li, C.-J. *Green Chem*, **2021**, *23*, 6789–6862. (f) Yeung, C. S.; Dong, V. M. *Chem. Rev*. **2011**, *111*, 1215–1292.

[4] (a) Hassan, M. M. M.; Guria, S.; Dey, S.; Das, J.; Chattopadhyay, B. *Sci. Adv*. **2023**, *9*, eadg3311. (b) Bisht, R.; Haldar, C.; Hassan, M. M. M.; Hoque, M. E.; Chaturvedi, J.; Chattopadhyay, B. *Chem. Soc. Rev*. **2022**, *51*, 5042–5100. (c) Hartwig, J. F. *Acc. Chem. Res.* **2012**, *45*, 864–873. (d) Ishiyama, T.; Miyaura, N. *Pure Appl. Chem.* **2006**, *78*, 1369–1375.

[5] (a) Kong, Y.; Mu, D. *Chem. Asian J.* **2022**, *17*, e202200104. (b) Cheng, C.; Hartwig, J. F. *Chem. Rev.* **2015**, *115*, 8946–8975. (c) Xu, Z.; Huang, W.-S.; Zhang, J.; Xu, L.-W. *Synthesis* **2015**, *47*, 3645–3668.

[6] Adak, L.; Yoshikai, N. *Tetrahedron* **2012**, *68*, 5167–5171.

[7] (a) Moniwa, H.; Shintani, R. *Chem. Eur. J.* **2021**, *27*, 7512–7515. (b) Kondo, R.; Moniwa, H.; Shintani, R. *Org. Lett.* **2023**, *25*, 4193–4197.

[8] For reviews on silylboron reagents in organic synthesis: (a) Feng, J.-J.; Mao, W.; Zhang, L.; Oestreich, M. *Chem. Soc. Rev.* **2021**, *50*, 2010–2073. (b) Moberg, C. *Synthesis* **2020**, *52*, 3129–3139. (c) Wilkinson, J. R.; Nuyen, C. E.; Carpenter, T. S.; Harruff, S. R.; Van Hoveln, R. *ACS Catal.* **2019**, *9*, 8961–8979. (d) Oestreich, M.; Hartmann, E.; Mewald, M. *Chem. Rev.* **2013**, *113*, 402–441. (e) Ohmura, T.; Suginome, M. *Bull. Chem. Soc. Jpn.* **2009**, *82*, 29–49.

[9] For reviews on indene synthesis: (a) Wu, W.-Q.; Shi, H. *J. Org. Chem.* **2023**, *88*, 14264–14273. (b) Rinaldi, A.; Scarpi, D.; Occhiato, E. G. *Eur. J. Org. Chem.* **2019**, *2019*, 7401–7419.

[10] (a) Prasher, P.; Sharma, M. *ChemistrySelect* **2021**, *6*, 2658–2677. (b) Han, J.; Meng, J.-B. *J. Photochem. Photobiol. C: Photochem. Rev.* **2009**, *10*, 141–147.

[11] For examples of *anti*-selective silylarylation of alkynes: (a) Yan, Z.; Xie, J.; Zhu, C. *Adv. Synth. Catal.* **2017**, *359*, 4153–4157. (b) Lv, W.; Liu, S.; Chen, Y.; Wen, S.; Lan, Y.; Cheng, G. *ACS Catal.* **2020**, *10*, 10516–10522. (c) Cheng, C.; Zhang, Y. *Org. Lett*. **2021**, *23*, 5772–5776. (d) Zuo, H.; Klare, H. F. T.; Oestreich, M. *J. Org. Chem*. **2023**, *88*, 4024–4027.

[12] For examples of *anti*-selective carbosilylation of alkynes using silylboronates: (a) Vercruysse, S.; Cornelissen, L.; Nahra, F.; Collard, L.; Riant, O. *Chem. Eur. J.* **2014**, *20*, 1834–1838. (b) Iwamoto, T.; Nishikori, T.; Nakagawa, N.; Takaya, H.; Nakamura, M. *Angew. Chem*., *Int. Ed*. **2017**, *56*, 13298–13301. (c) Yang, L.-F.; Wang, Q.-A.; Li, J.-H. *Org. Lett.* **2021**, *23*, 6553–6557.

[13] For reviews on copper-catalyzed C(sp^2)–H bond functionalization: (a) Parmar, H. V.; Adodariya, Y. J.; Patel, U. P.; Shrivastav, P. S.; Maru, J. J. *ChemistrySelect* **2024**, *9*, e202303474. (b) Bhaskaran, R. P.; Nayak, K. H.; Sreelekha, M. K.; Babu, B. P. *Org. Biomol. Chem.* **2023**, *21*, 237–251. (c) Guo, X.-X.; Gu, D.-W.; Wu, Z.; Zhang, W. *Chem. Rev.* **2015**, *115*, 1622–1651. See also: (d) Almasalma, A. A.; Mejía, E. *Synthesis* **2020**, *52*, 2613–2622.

[14] The structure of **3aa** was confirmed by X-ray crystallographic analysis. Deposition number 2363760 contains the supplementary crystallographic data for this paper. These data are provided free of charge by the joint Cambridge Crystallographic Data Centre and Fachinformationszentrum Karlsruhe Access Structures service.

[15] (a) Jia, J.; Zeng, X.; Liu, Z.; Zhao, L.; He, C.-Y.; Li, X.-F.; Feng, Z. *Org. Lett.* **2020**, *22*, 2816–2821. (b) Yamamoto, E.; Izumi, K.; Horita, Y.; Ito, H. *J. Am. Chem. Soc.* **2012**, *134*, 19997–20000.

[16] Cooke, F.; Magnus, P. *J. Chem. Soc., Chem. Commun.* **1977**, 513–513.

[17] Query, I. P.; Squier, P. A.; Larson, E. M.; Isley, N. A.; Clark, T. B. *J. Org. Chem*. **2011**, *76*, 6452–6456.

[18] Moniwa, H.; Yamanaka, M.; Shintani, R. *J. Am. Chem. Soc.* **2023**, *145*, 23470–23477.

[19] (a) Shintani, R.; Nozaki, K. *Organometallics* **2013**, *32*, 2459–2462. (b) DiBenedetto, T. A.; Parsons, A. M.; Jones, W. D. *Organometallics* **2019**, *38*, 3322–3326.

[20] Gaussian 16, Revision C.01, Frisch, M. J.; Trucks, G. W.; Schlegel, H. B.; Scuseria, G. E.; Robb, M. A.; Cheeseman, J. R.; Scalmani, G.; Barone, V.; Petersson, G. A.; Nakatsuji, H.; Li, X.; Caricato, M.; Marenich, A. V.; Bloino, J.; Janesko, B. G.; Gomperts, R.; Mennucci, B.; Hratchian, H. P.; Ortiz, J. V.; Izmaylov, A. F.; Sonnenberg, J. L.; Williams-Young, D.; Ding, F.; Lipparini, F.; Egidi, F.; Goings, J.; Peng, B.; Petrone, A.; Henderson, T.; Ranasinghe, D.; Zakrzewski, V. G.; Gao, J.; Rega, N.; Zheng, G.; Liang, W.; Hada, M.; Ehara, M.; Toyota, K.; Fukuda, R.; Hasegawa, J.; Ishida, M.; Nakajima, T.; Honda, Y.; Kitao, O.; Nakai, H.; Vreven, T.; Throssell, K.; Montgomery, J. A. Jr.; Peralta, J. E.; Ogliaro, F.; Bearpark, M. J.; Heyd, J. J.; Brothers, E. N.; Kudin, K. N.; Staroverov, V. N.; Keith, T. A.; Kobayashi, R.; Normand, J.; Raghavachari, K.; Rendell, A. P.; Burant, J. C.; Iyengar, S. S.; Tomasi, J.; Cossi, M.; Millam, J. M.; Klene, M.; Adamo, C.; Cammi, R.; Ochterski, J. W.; Martin, R. L.; Morokuma, K.; Farkas, O.; Foresman, J. B.; Fox, D. J. Gaussian, Inc., Wallingford CT, 2019.

[21] Zhao, Y.; Truhlar, D. G. *Theor. Chem. Acc.* **2008**, *120*, 215–241.

[22] Marenich, A. V.; Cramer, C. J.; Truhlar, D. G. *J. Phys. Chem. B* **2009**, *113*, 6378–6396.

[23] For reviews: (a) Liang, Y.-F.; Bilal, M.; Tang, L.-Y.; Wang, T.-Z.; Guan, Y.-Q.; Cheng, Z.; Zhu, M.; Wei, J.; Jiao, N. *Chem. Rev*. **2023**, *123*, 12313–12370. (b) Karimzadeh-Younjali, M.; Wendt, O. F. *Helv. Chim. Acta* **2021**, *104*, e2100114. (c)

Dai, P.-F.; Wang, H.; Cui, X.-C.; Qu, J.-P.; Kang, Y.-B. *Org. Chem. Front*. **2020**, *7*, 896–904.

[24] Shishido, R.; Uesugi, M.; Takahashi, R.; Mita, T.; Ishiyama, T.; Kubota, K.; Ito, H. *J. Am. Chem. Soc.* **2020**, *142*, 14125–14133.

[25] Meffre, P.; Hermann, S.; Durand, P.; Reginato, G.; Riu, A. *Tetrahedron* **2002**, *58*, 5159–5162.

[26] Mathews, C. J.; Smith, P. J.; Welton, T. *J. Mol. Catal. A: Chem.* **2004**, *214*, 27–32.

[27] Hayashi, T.; Konishi, M.; Kumada, M. *Tetrahedron Lett*. **1979**, 1871–1874.

[28] Coulson, D. R.; Satek, L. C.; Grim, S. O. *Inorg. Synth*. **1972**, *13*, 121–124.

[29] Jurkauskas, V.; Sadighi, J. P.; Buchwald, S. L. *Org. Lett.* **2003**, *5*, 2417–24240.

[30] Mankad, N. P.; Laitar, D. S.; Sadighi, J. P. *Organometallics* **2004**, *23*, 3369–3371.

[31] Jørgensen, M.; Lee, S.; Liu, X.; Wolkowski, J. P.; Hartwig, J. F. *J. Am. Chem. Soc*. **2002**, *124*, 12557–12565.

Chapter 4

Copper-Catalyzed Regio- and Stereoselective Formal Hydro(borylmethylsilyl)ation of Internal Alkynes via Alkenyl-to-Alkyl 1,4-Copper Migration

4.1 Introduction

C–H bond functionalization through 1,*n*-metal migration from carbon to carbon under transition-metal catalysis can provide a non-classical way of constructing organic molecular skeletons, allowing the facile synthesis of complex molecules from relatively simple precursors.[1] In particular, 1,4-metal migration has been most widely explored using palladium[2] or rhodium[3] as the metals of choice, and some reactions involving 1,5-migration of these metals have also been reported.[4,5] In contrast, the use of less precious and more abundant 3d transition metals has been much less explored, and only scattered examples have been known to date using chromium,[6] iron,[7] cobalt,[8] or nickel[9] as the migrating metal.[10] It is therefore highly desirable to expand the scope of 1,*n*-metal migration processes under 3d transition-metal catalysis, as it could lead to new and more sustainable synthetic methods for various organic compounds that are difficult to prepare using existing protocols.

Recently, our group has been focusing on the development of new synthetic methods of various organosilanes with high synthetic utility using silylboronates as the nucleophilic silicon donor,[11,12] and, as described in Chapter 2, the author developed a copper-catalyzed regio- and *anti*-selective silylboration of unsymmetric internal alkynes to give silicon- and boron-containing tetrasubstituted alkenes (Scheme 1a).[11d,13] During the course of this study, it was found that the reaction of *tert*-butyl(phenyl)acetylene (**1a**)

with silylboronate **2** gave alkenylsilylmethylboronate **3a** as a minor product in addition to silylboration product **4a** (eq 1).[14] The formation of **3a** presumably occurs through a sequence of silylcupration of **1a**, 1,4-copper migration, and borylation of the resulting silylmethylcopper species.[15] To date, a related functionalization of a methyl group on silicon via 1,*n*-metal migration is limited to a palladium-catalyzed process for a pre-installed MeR_2Si-group on bromonaphthalenes via 1,5-palladium migration.[4c] In this context, as a new entry of 1,*n*-metal migration using a 3d transition metal, herein the author describe the development of a copper-catalyzed regio- and stereoselective synthesis of alkenylsilylmethylboronates[16,17] from unsymmetric internal alkynes and silylboronates by formal hydro(borylmethylsilyl)ation[12a–c,18] involving a 1,4-copper migration process from an alkenyl carbon to an alkyl carbon,[19,20] which has never been reported for any 3d transition metals (Scheme 1b).

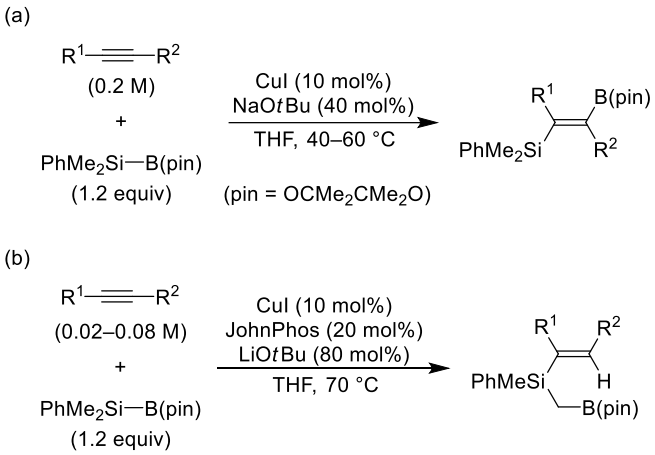

Scheme 1. (a) Copper-catalyzed *anti*-selective silylboration of internal alkynes (previous work described in Chapter 2) and (b) Formal hydro(borylmethylsilyl)ation of internal alkynes via 1,4-copper migration (this work).

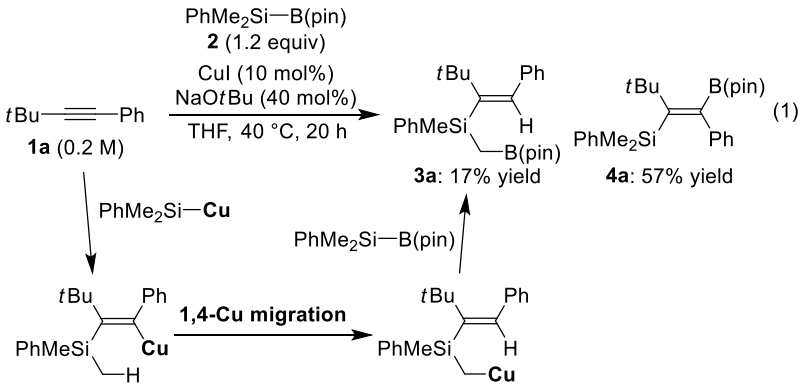
PhMe2Si—B(pin)
2 (1.2 equiv)
CuI (10 mol%)
NaOtBu (40 mol%)
THF, 40 °C, 20 h
tBu
Ph
1a (0.2 M)
PhMeSi
H
B(pin)
3a: 17% yield
B(pin)
PhMe2Si
Ph
4a: 57% yield
(1)
PhMe2Si—Cu
PhMe2Si—B(pin)
1,4-Cu migration
Cu

4.2 Results and discussion

4.2.1 Reaction development and product derivatization.

As a starting point, based on the result in eq 1, the reaction of alkyne **1a** with silylboronate **2** was examined to improve the yield of **3a** (Table 1). In the presence of CuI (10 mol%) and NaO*t*Bu (40 mol%) in THF, the yield of **3a** became slightly higher by raising the reaction temperature from 40 °C to 70 °C (entry 1). While the use of KO*t*Bu instead of NaO*t*Bu did not show any improvement (entry 2), the use of LiO*t*Bu led to preferential formation of **3a** in 48% yield along with 33% yield of **4a** (entry 3). Although only small differences were observed by the addition of phosphine ligands to copper (entries 4–7), a slightly higher yield of 54% was achieved by using JohnPhos as the ligand (entry 7). It was subsequently found that the yield and selectivity of **3a** became significantly higher by lowering the initial concentration of **1a** from 0.2 M to 0.04–0.02 M for both 'ligandless' (entries 8 and 11) and phosphine-added (entries 9–10 and 12–13) conditions (58–71% yield, **3a**/**4a** = up to 94/6).

Table 1. Copper-catalyzed reaction of **1a** with **2** to give **3a** and **4a**: Optimization.

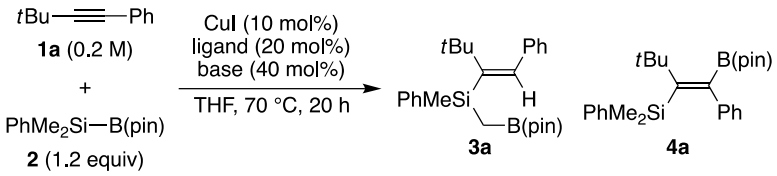

entry	ligand	base	yield of **3a** (%)[a]	yield of **4a** (%)[a]	**3a**/**4a**[a]
1	none	NaO*t*Bu	24	57	30/70
2	none	KO*t*Bu	24	28	46/54
3	none	LiO*t*Bu	48	33	59/41
4	PPh_3	LiO*t*Bu	52	28	65/35
5	PCy_3	LiO*t*Bu	48	37	56/44
6	$P(t\text{Bu})_3$	LiO*t*Bu	53	27	66/34
7	JohnPhos	LiO*t*Bu	54	33	62/38
8[b]	none	LiO*t*Bu	69	14	83/17
9[b]	$P(t\text{Bu})_3$	LiO*t*Bu	69	9	88/12
10[b]	JohnPhos	LiO*t*Bu	70	11	86/14
11[c]	none	LiO*t*Bu	58	4	94/6
12[c]	$P(t\text{Bu})_3$	LiO*t*Bu	71	5	93/7
13[c]	JohnPhos	LiO*t*Bu	66	4	94/6

[a] Determined by ^{1}H NMR (internal standard: dimethyl terephthalate). [b] The reaction was conducted at 0.04 M of **1a**. [c] The reaction was conducted at 0.02 M of **1a** in the presence of 80 mol% of LiO*t*Bu.

Considering the slightly higher yields with phosphine-added conditions (entries 12–13 vs. entry 11) and the ease of handling of JohnPhos over P(*t*Bu)$_3$, the author decided to employ the conditions in Table 1, entry 13 for further study. Under these conditions, **3a** was isolated in 65% yield as a 94/6 mixture of **3a**/**4a**, and similar results were obtained for the reactions of *para*- or *meta*- substituted *tert*-butyl(aryl)acetylenes **1b–d** to give corresponding hydro(borylmethylsilyl)ation products **3b–d** (Scheme 2). In addition, it is remarkable that even more sterically demanding *tert*-butyl(aryl)acetylenes **1e–g** having an *ortho*-substituted aryl group and *tert*-butyl(1-naphthyl)acetylene (**1i**) could also undergo the present regioselective hydrofunctionalization, and alkenylsilylmethylboronates **3e–g** and **3i** were obtained exclusively in somewhat higher yields (74–82% yield). On the other hand, chlorine-containing substrate **1h** could also be employed, but the yield and selectivity of product **3h** became lower. Furthermore, while *tert*-butyl(2-naphthyl)acetylene (**1j**) showed a lower selectivity (**3j**/**4j** = 86/14), alkynes having 4- and 5-indolyl groups (**1k** and **1l**) as well as a substituted thienyl group (**1m**) gave products **3k–m** with high selectivity. With regard to the R group on the alkyne, in addition to *tert*-butyl group, several other tertiary alkyl groups such as triethylmethyl (**1n**), thexyl (**1o**), and 2-silyloxy-1,1-dimethylethyl (**1p**) groups could be incorporated to give corresponding products **3n–p** in relatively high yields (65–71% yield with **3**/**4** = 90/10–97/3). Alkynes having carbo- or heterocyclic alkyl groups **1q–s** were also applicable as shown for the synthesis of **3q–s**. In contrast, less bulky alkyl groups were found to be more challenging to promote 1,4-copper migration (vide infra), and alkynes having secondary or primary alkyl groups (**1t–v**) led to diminished yields of hydro(borylmethylsilyl)ation products **3t–v**. Unfortunately, diaryl- and dialkylacetylenes turned out to be inapplicable to the present catalysis. Regarding the functional group compatibility, halogens and electron-withdrawing groups were not well tolerated. To

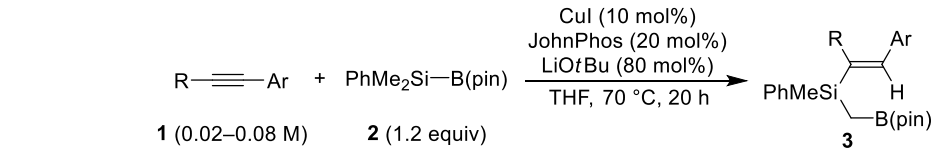

1 (0.02–0.08 M) **2** (1.2 equiv) **3**

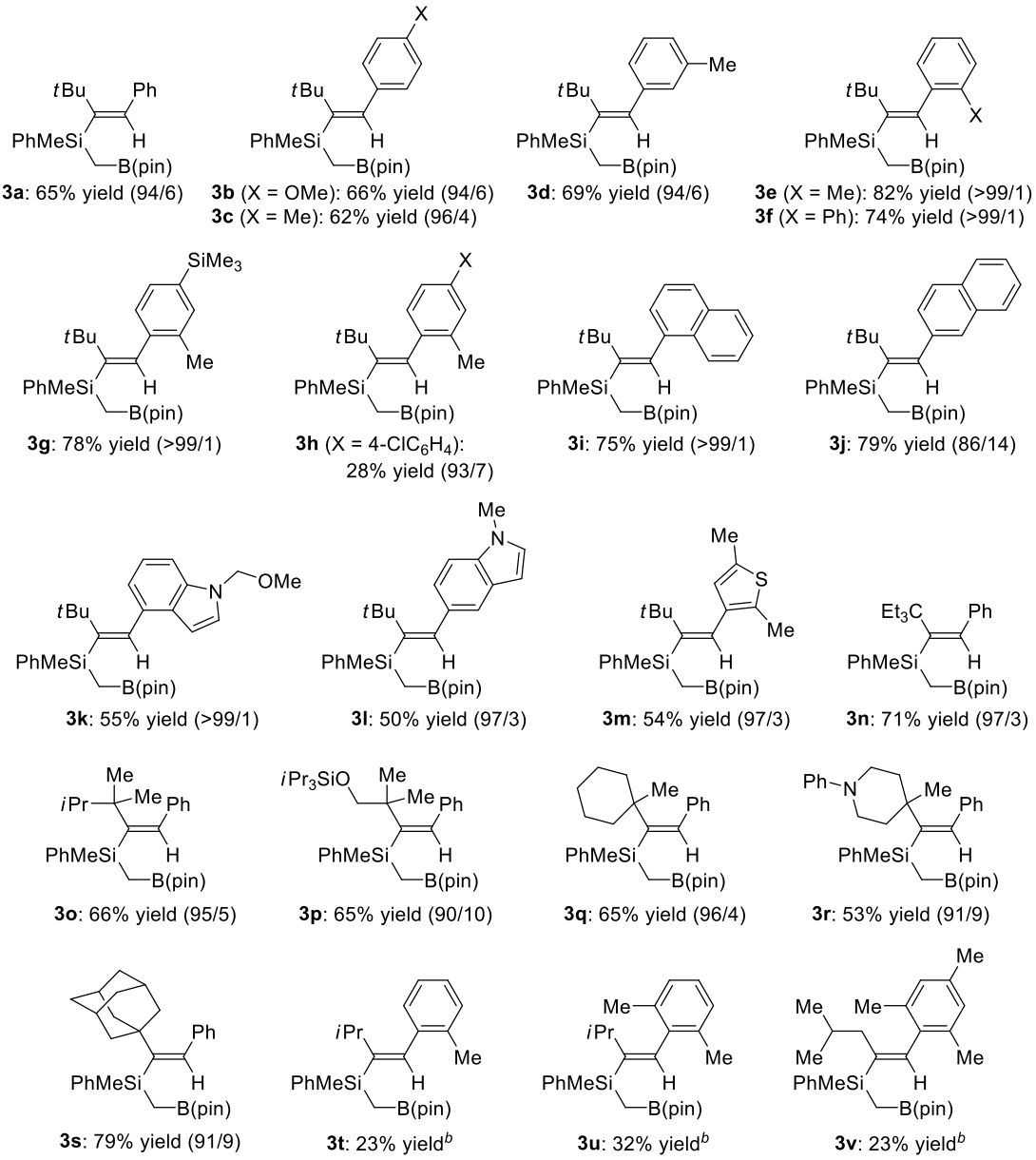

3a: 65% yield (94/6)
3b (X = OMe): 66% yield (94/6)
3c (X = Me): 62% yield (96/4)
3d: 69% yield (94/6)
3e (X = Me): 82% yield (>99/1)
3f (X = Ph): 74% yield (>99/1)
3g: 78% yield (>99/1)
3h (X = 4-ClC$_6$H$_4$): 28% yield (93/7)
3i: 75% yield (>99/1)
3j: 79% yield (86/14)
3k: 55% yield (>99/1)
3l: 50% yield (97/3)
3m: 54% yield (97/3)
3n: 71% yield (97/3)
3o: 66% yield (95/5)
3p: 65% yield (90/10)
3q: 65% yield (96/4)
3r: 53% yield (91/9)
3s: 79% yield (91/9)
3t: 23% yield[b]
3u: 32% yield[b]
3v: 23% yield[b]

[a] The reactions were conducted on a 0.20 mmol scale. The yields are combined isolated yields of **3** and **4**, and the ratios of **3**/**4** are given in parentheses by analogy to **3a**/**4a** in Table 1. [b] Isolated yield of **3**.

Scheme 2. Scope of copper-catalyzed formal hydro(borylmethylsilyl)ation of internal alkynes[a].

partially solve this problem indirectly, trimethylsilylated product **3g** was treated with *N*-bromosuccinimide (NBS) to give corresponding bromodesilylated compound **3w** in 78% yield (eq 2), demonstrating the possibility to install various other functional groups to this molecular skeleton utilizing rich chemistry of bromoarenes. It is also worth noting that the present regioselective hydro(borylmethylsilyl)ation reaction can be conducted on a preparative scale. For example, the reaction of 3.0 mmol of **1e** with **2** gave 1.08 g of **3e** (83% yield; eq 3).

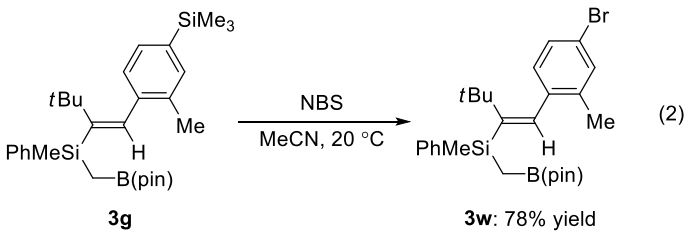

3g **3w**: 78% yield (2)

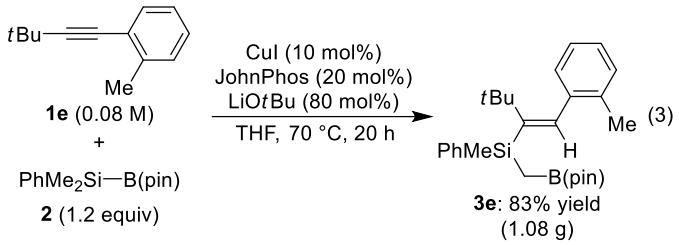

3e: 83% yield (1.08 g) (3)

The silylmethylboronate moiety of compounds **3** obtained in the present catalysis can be converted to various other functional groups as exemplified in Scheme 3. Thus, Matteson homologation of **3e** by treatment with *n*-butyllithium in the presence of bromochloromethane gave silylethylboronate **5** in 60% yield,[21] and allylsilane **6** was obtained in 49% yield by Zweifel olefination of **3e** using vinylmagnesium bromide followed by treating it with iodine in methanol.[16d,22] In addition, oxidation of **3e** by hydrogen peroxide under basic conditions gave silylmethanol **7** in 92% yield.[23]

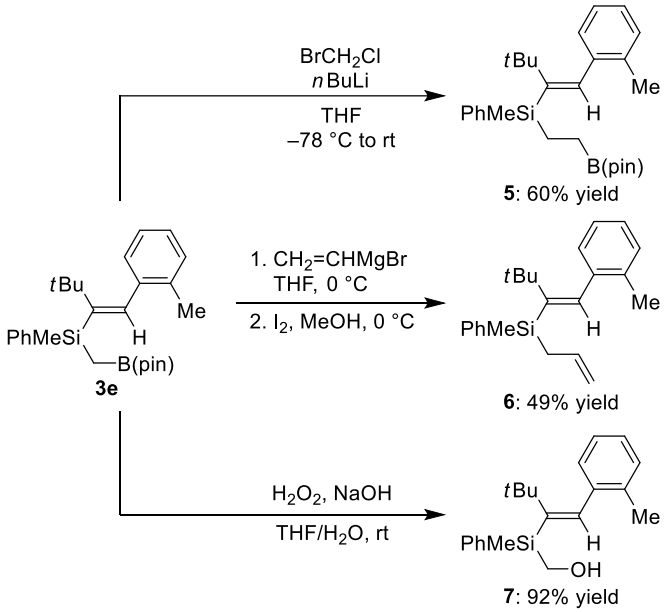

Scheme 3. Functionalization of silylmethylboronate **3e**.

4.2.2 Mechanistic investigation

With regard to the mechanism of the present catalysis toward **3** and **4**, proposed catalytic cycles are shown in Scheme 4.[11d,12a–c] Silylcopper species **A**, which is initially generated *in-situ* by the reaction of copper(I) salt with silylboronate **2** in the presence of LiO*t*Bu, undergoes regioselective *syn*-insertion of alkyne **1** to give silylalkenylcopper **B**. Subsequently, either 1,4-copper migration giving silylmethylcopper **C** (Cycle I) or *syn*-to-*anti* alkene isomerization giving *anti*-silylalkenylmetal **D** (Cycle II) takes place, and borylation of these organocopper species by silylboronate **2** leads to the formation of **3** and **4**, respectively, along with regeneration of silylcopper **A**. As demonstrated in Table 1, the selectivity toward **3a** became higher by lowering the reaction concentration, and this trend could be explained as follows. The alkene stereoisomerization between **B** and **D** is reversible and takes place faster than the alkenyl-to-alkyl 1,4-copper migration from **B** to **C**, which would be a virtually irreversible process. In this scenario, the subsequent

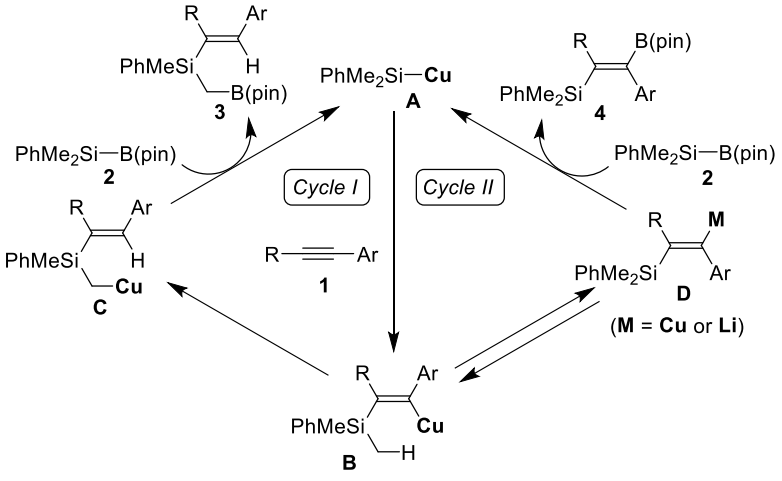

Scheme 4. Proposed catalytic cycles for the reaction of **1** with **2** to give **3** (Cycle I) and **4** (Cycle II).

intermolecular borylation of **D** by silylboronate **2** is decelerated at a low reaction concentration, leading to the preferential formation of **3** via **C**. In addition, the selectivity of **3** over **4** became higher for the alkynes **1** having an *ortho*-substituted aryl group as shown in Scheme 2. This would be partially attributable to the slower borylation of **D** by **2** due to the steric effect of the adjacent Ar group. The bulky Ar group could also be in favor of the 1,4-copper migration from **B** to **C** by making the copper moiety geometrically closer to the methyl group on silicon. Along this line, as shown in Scheme 2, the size of an alkyl group (R) on the alkyne **1** was found to significantly affect the reaction outcome as well. Thus, alkyne **1a** having *tert*-butyl group selectively gave alkeynylsilylmethylboronate **3a** over silylalkenylboronate **4a** under the present reaction conditions, but alkyne **1x** having less bulky isopropyl group led to the preferential formation of **4x** over **3x** (eq 4). These results also suggest the importance of geometrical closeness of the copper moiety and the methyl group on silicon in intermediate **B** in order to promote the alkenyl-to-alkyl 1,4-copper migration efficiently.

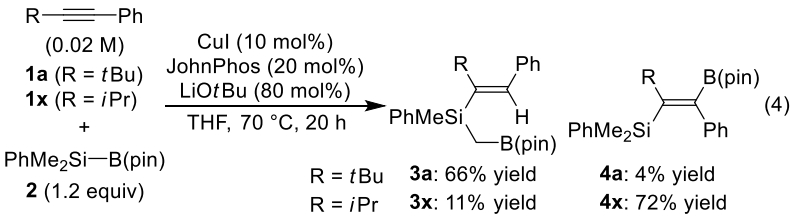

To further understand the origin of selectivity difference between alkynes **1a** and **1x** in eq 4, the author compared the structures of silylalkenylcopper intermediates **B-a** and **B-x** having P(*t*Bu)$_3$ (**B-a_P**; corresponding to the phosphine-added conditions) and $SiMe_2Ph^-$ (**B-x_Si**; corresponding to the 'ligandless' conditions) as the ligand for copper, respectively, by theoretical calculations. All the calculations were performed using

Gaussian 16 program.[24] Geometry optimizations were performed at the B3LYP/6-31G(d) for C, H, P, 6-31+G(d) for Si, LANL2DZ for Cu. As shown in Table 2, due to the steric effect of *tert*-butyl group, $\angle C^1–C^2–C^3$ and $\angle C^4–C^3–C^2$ of **B-a_P** and **B-a_Si** are significantly larger than those of **B-x_P** and **B-x_Si**, which tends to make $\angle Si–C^2–C^3$ and $\angle Cu–C^3–C^2$ of **B-a** smaller than those of **B-x**. As a result, the distances between the silyl group and Cu in **B-a_P** (Si–Cu = 3.35 Å) and **B-a_Si** (Si–Cu = 3.41 Å) become shorter than those in **B-x_P** (Si–Cu = 3.55 Å) and **B-x_Si** (Si–Cu = 3.50 Å). Those structural distortions on **B-a_P** and **B-a_Si** would promote 1,4-copper migration. This could partially explain the higher ratio of 1,4-copper migration for the reaction of **1a** than that of **1x**.

Table 2. Selected bond angles of silylalkenylcopper species **B-a** and **B-x**.

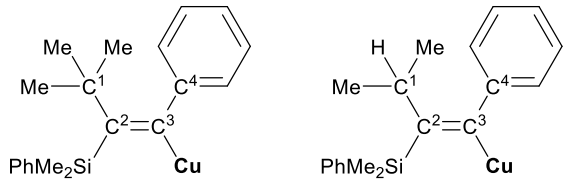

B-a_P (**Cu** = CuP(*t*Bu)$_3$)
B-a_Si (**Cu** = Cu$^-$(SiMe$_2$Ph))
B-x_P (**Cu** = CuP(*t*Bu)$_3$)
B-x_Si (**Cu** = Cu$^-$(SiMe$_2$Ph))

	B-a_P	**B-a_Si**	**B-x_P**	**B-x_Si**
$\angle C^1–C^2–C^3$	128.6°	128.6°	121.9°	122.4°
$\angle C^4–C^3–C^2$	127.7°	128.7°	121.3°	122.0°
$\angle Si–C^2–C^1$	121.0°	121.6°	122.7°	123.9°
$\angle Cu–C^3–C^4$	101.5°	98.6°	105.5°	105.6°
$\angle Si–C^2–C^3$	110.3°	109.8°	115.3°	113.7°
$\angle Cu–C^3–C^2$	130.8°	132.7°	133.2°	132.3°

To gain more insights into the present catalysis, a series of kinetic experiments were conducted for the reaction of alkyne **1e** with silylboronate **2**, which is essentially composed of only Cycle I to give **3e** (Scheme 4). As shown in Figure 1, the reaction rate (v) shows first-order dependency on the concentration of copper catalyst ([**Cu**]) and a positive order (ca. 0.5-order) dependency on the initial concentration of alkyne **1e** ([**1e**]$_0$). On the other hand, the initial concentrations of silylboronate **2** and LiO*t*Bu have no influence on the initial rate of the production of **3e**, indicating that the reaction is zero-order in these components. These results suggest that borylation of silylmethylcopper **C** by silylboronate **2** in Scheme 4 proceeds much faster than the preceding alkyne insertion (**A** to **B**) and 1,4-copper migration (**B** to **C**). Due to the positive order dependency of v on [**1e**]$_0$ and the first-order dependency on [**Cu**], the alkyne insertion step would be partly involved in the turnover-limiting step of Cycle I, but $v \propto [\mathbf{1e}]_0^{0.5}$ (not $v \propto [\mathbf{1e}]_0^{1}$) indicates that subsequent 1,4-copper migration should also be comparably slow or even slower.

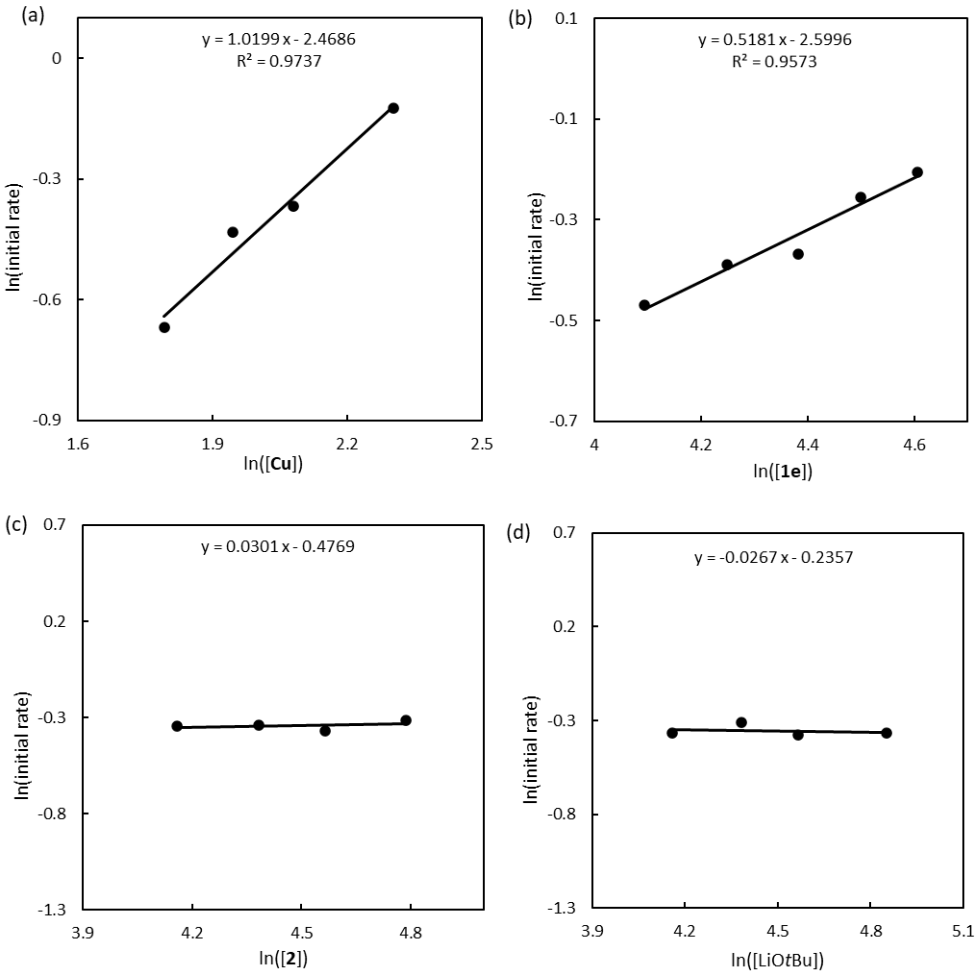

Figure 1. Kinetic experiments for the reaction of **1e** with **2**: ln plots of the initial rate (mM/min) vs. (a) concentration of Cu/Johnphos catalyst (mM) ([**Cu**]$_0$ = 6–10 mM, [LiO*t*Bu]$_0$ = 64 mM, [**1e**]$_0$ = 80 mM, [**2**]$_0$ = 96 mM), (b) concentration of **1e** (mM) ([**Cu**]$_0$ = 8 mM, [LiO*t*Bu]$_0$ = 64 mM, [**1e**]$_0$ = 60–100 mM, [**2**]$_0$ = 96 mM), (c) concentration of **2** (mM) ([**Cu**]$_0$ = 8 mM, [LiO*t*Bu]$_0$ = 64 mM, [**1e**]$_0$ = 80 mM, [**2**] = 64–120 mM), and (d) concentration of LiO*t*Bu (mM) ([**Cu**]$_0$ = 8 mM, [LiO*t*Bu]$_0$ = 64–128 mM, [**1e**]$_0$ = 80 mM, [**2**]$_0$ = 96 mM).

Additional mechanistic information was obtained by monitoring the model reactions in THF-d_8 by ^{1}H NMR. As was described in Chapter 2, a 1:1 mixture of CuI and silylboronate **2** in the presence of LiO*t*Bu (4.0 equiv) in THF-d_8 gave a singlet peak at 0.31 ppm, which can be assigned as methyl protons on the silicon of Cu(SiMe$_2$Ph) (**A1**) (Figure 2a). On the other hand, a 1:2 mixture of CuI and **2** with LiO*t*Bu (4.0 equiv) gave a new singlet at 0.02 ppm as the major peak, presumably corresponding to methyl protons of $Li^+Cu^-(SiMe_2Ph)_2$ (**A2**) (Figure 2b). Furthermore, the same species **A2** was mainly observed even when JohnPhos (1.0 equiv) was added to the 1:2 mixture of CuI and **2** with LiO*t*Bu (4.0 equiv), and the signals for JohnPhos were the same as their original ones (Figure 2c and 2d). These results indicate that the phosphine ligand plays only a subordinate role and the active copper species may be phosphine-free.

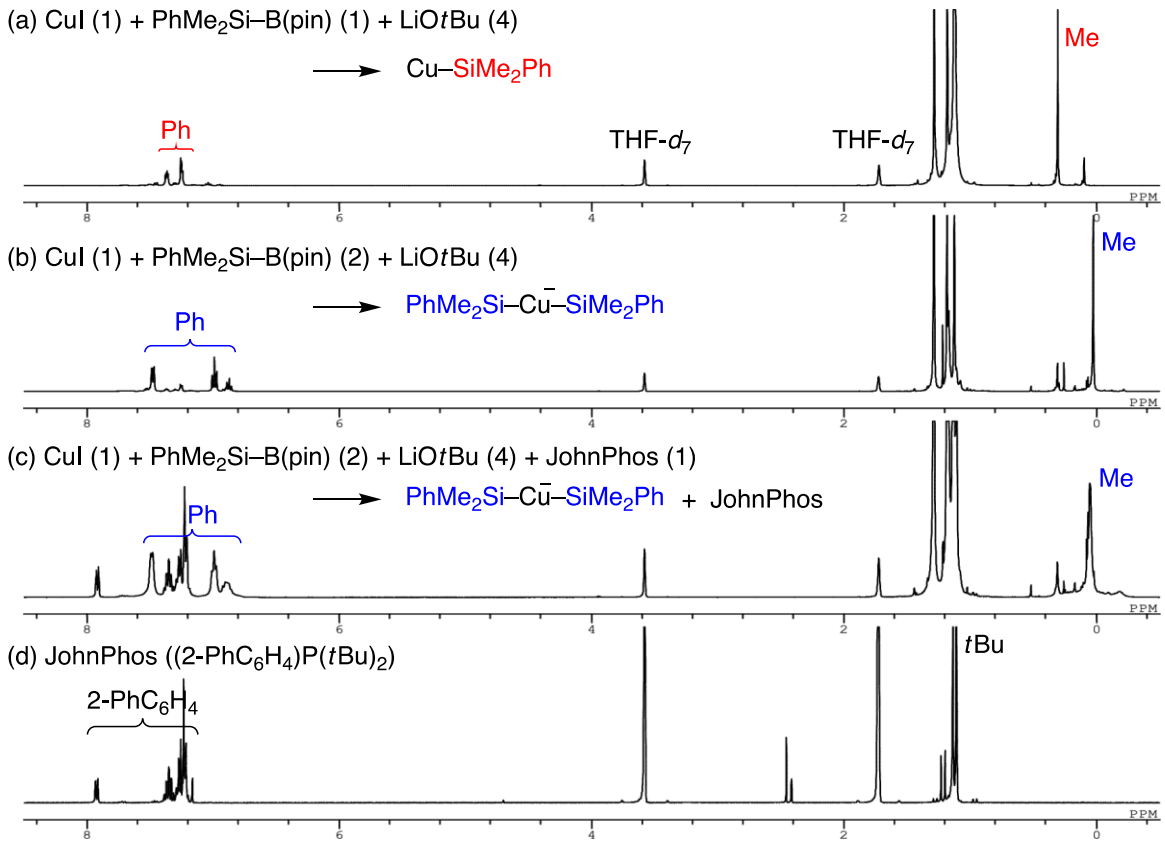

Figure 2. ^{1}H NMR spectra of (a) *in-situ* generated Cu(SiMe$_2$Ph), (b) *in-situ* generated Li$^+$Cu$^-$(SiMe$_2$Ph)$_2$, (c) *in-situ* generated Li$^+$Cu$^-$(SiMe$_2$Ph)$_2$ + JohnPhos, and (d) JohnPhos (400 MHz in THF-d_8).

When *tert*-butyl(phenyl)acetylene (**1a**; 2.0 equiv) was added to *in-situ* generated **A1**, no reaction took place at room temperature or at 60 °C (Figure 3a and 3b). On the other hand, a smooth reaction was found to proceed at room temperature when **1a** was added to *in-situ* generated **A2** to give new signals at 0.99, 0.26, and −0.03 ppm, which could be assigned as *tert*-butyl and methyl protons of silylalkenyl(silyl)cuprate **B2'** (Figure 3c and 3d), indicating that disilylcuprate **A2** rather than silylcopper **A1** is the one that promotes insertion of an alkyne. Protonolysis of this species led to the formation of alkene **8** derived from silylprotonation of **1a**. It is remarkable that the structure of **8** was assigned as (*E*)-(2-*tert*-butyl-1-phenylvinyl)dimethyl(phenyl)silane, not the expected (1-*tert*-butyl-2-phenylvinyl)dimethyl(phenyl)silane, by the NOE experiment (Figure 4).

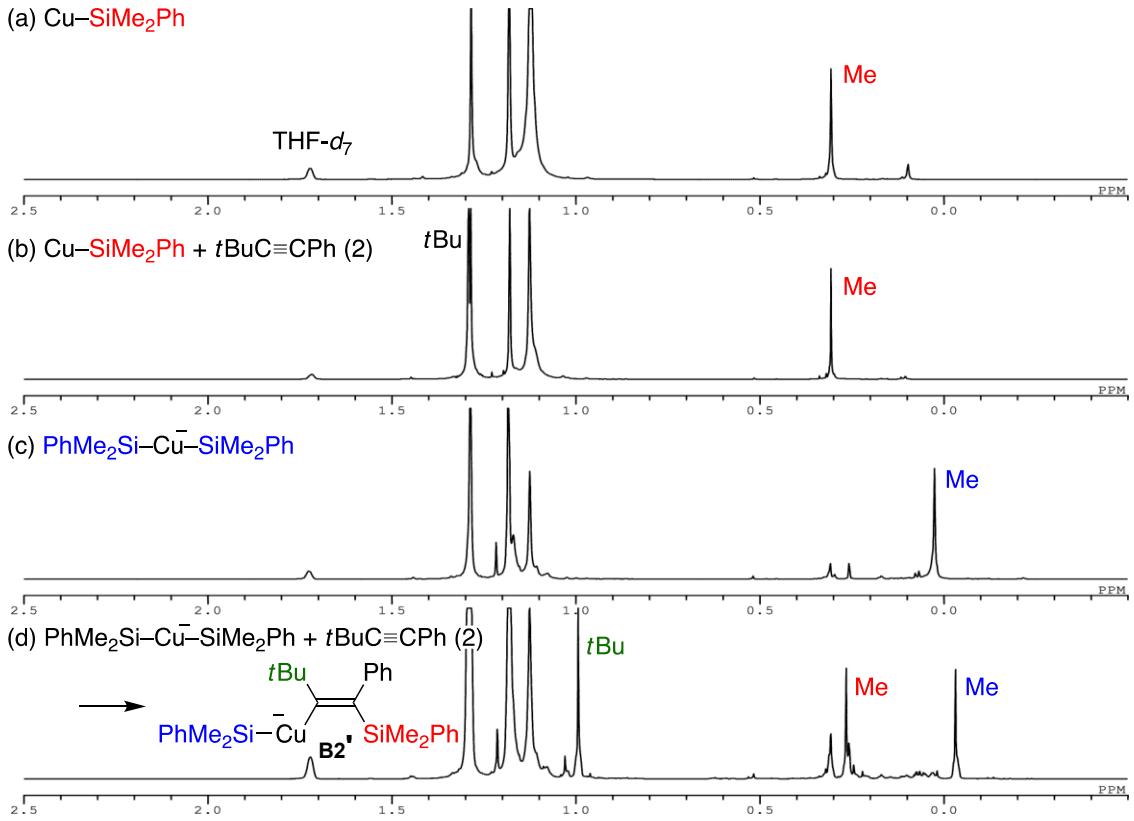

Figure 3. ^{1}H NMR spectra of (a) *in-situ* generated CuSiMe$_2$Ph, (b) *in-situ* generated Cu(SiMe$_2$Ph) + alkyne **1a** at room temperature, (c) *in-situ* generated Li^{+}Cu^{-}(SiMe$_2$Ph)$_2$, and (d) *in-situ* generated Li^{+}Cu^{-}(SiMe$_2$Ph)$_2$ + alkyne **1a** (400 MHz in THF-d_8).

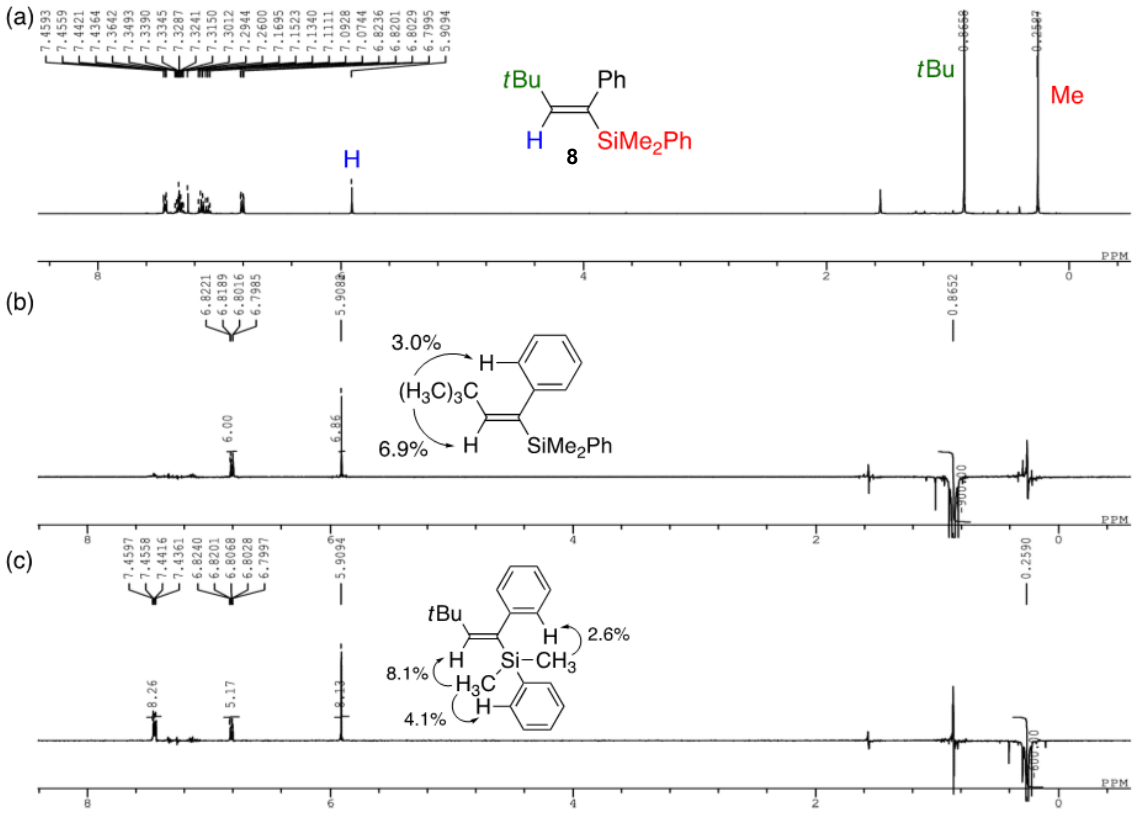

Figure 4. (a) ^{1}H NMR spectrum and (b, c) the NOE spectra of compound **8** (400 MHz in $CDCl_3$).

Furthermore, addition of silylboronate **2** (2.0 equiv) to *in-situ* generated **B2'** and warming the mixture at 60 °C led to the formation of alkenylsilylmethylboronate **3a** and *anti*-silylboration product **4a** (Figure 5a and 5b), both of which are the products obtained in the present catalytic reaction. Treatment of this mixture with MeOH gave 54% yield of **3a**, 78% yield of **4a**, and 40% yield of **8** with respect to the amount of copper employed. (Note that the ratio of **3a**/**4a** is significantly affected by the reaction temperature and concentration of each component.) In addition, when **1a** (2.0 equiv) was added to a 1:4 mixture of CuI and **2** in the presence of LiO*t*Bu (4.0 equiv) and the mixture was warmed to 60 °C, **B2'** was observed along with the formation of **3a** and **4a** (Figure 5c). Treatment of this mixture with MeOH gave 48% yield of **3a**, 38% yield of **4a**, and 36% yield of **8** with respect to the amount of copper employed in this case.

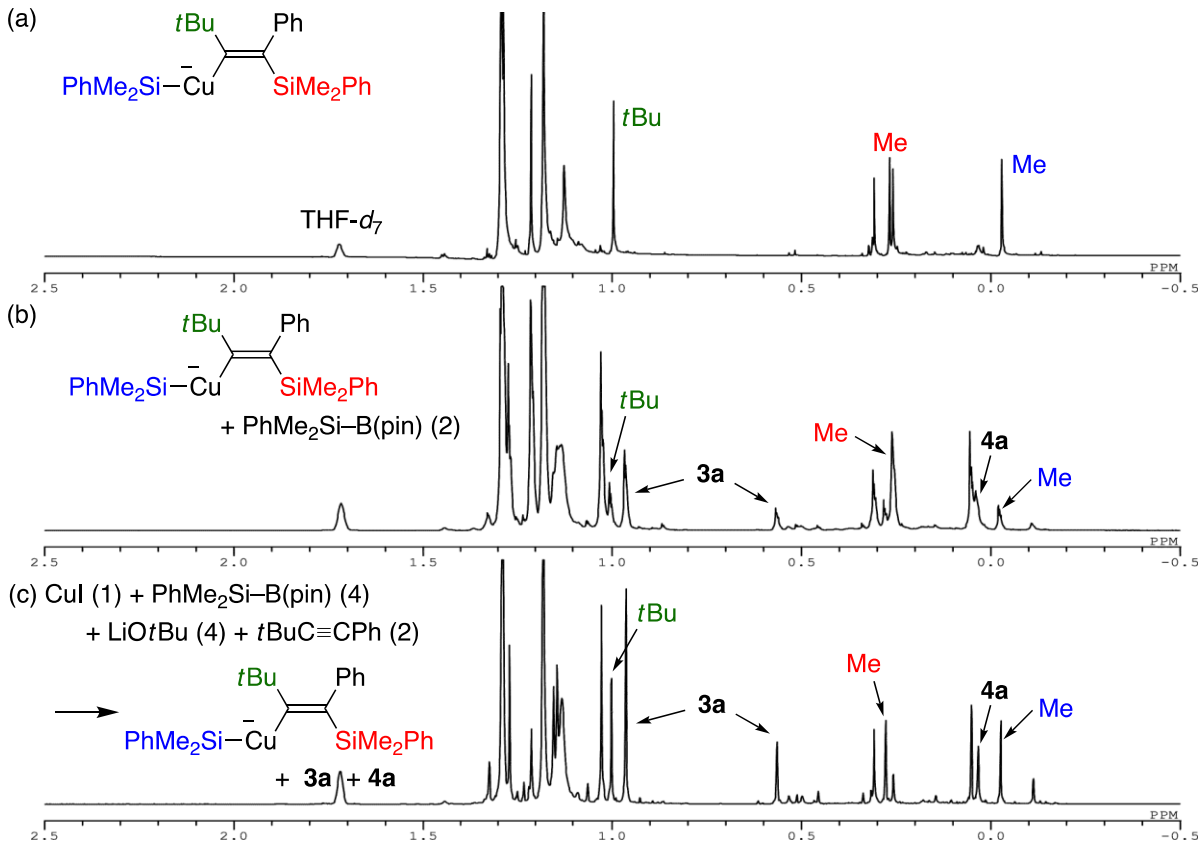

Figure 5. ^{1}H NMR spectra of (a) *in-situ* generated **B2'**, (b) *in-situ* generated **B2'** + silylboronate **2** (2.0 equiv) at 60 °C, and (c) CuI + silylboronate **2** (4.0 equiv) + LiO*t*Bu (4.0 equiv) + **1a** (2.0 equiv) at 60 °C (400 MHz in THF-d_8).

Based on these results, catalytically active species corresponding to **A** in Scheme 4 is most likely bis(phenyldimethylsilyl)cuprate **A2** regardless of the presence/absence of a phosphine ligand (Scheme 5). Disilylcuprate **A2** preferentially undergoes 2,1-insertion of alkyne **1a** to give **B2'**. This process is reversible and when 1,2-insertion giving reigoisomeric alkenyl(silyl)cuprate **B2** takes place,[25] this undergoes either 1,4-copper migration to give **C2** or *syn*-to-*anti*-isomerization to give **D2**. Borylations of **C2** and **D2** give **3a** and **4a**, respectively.

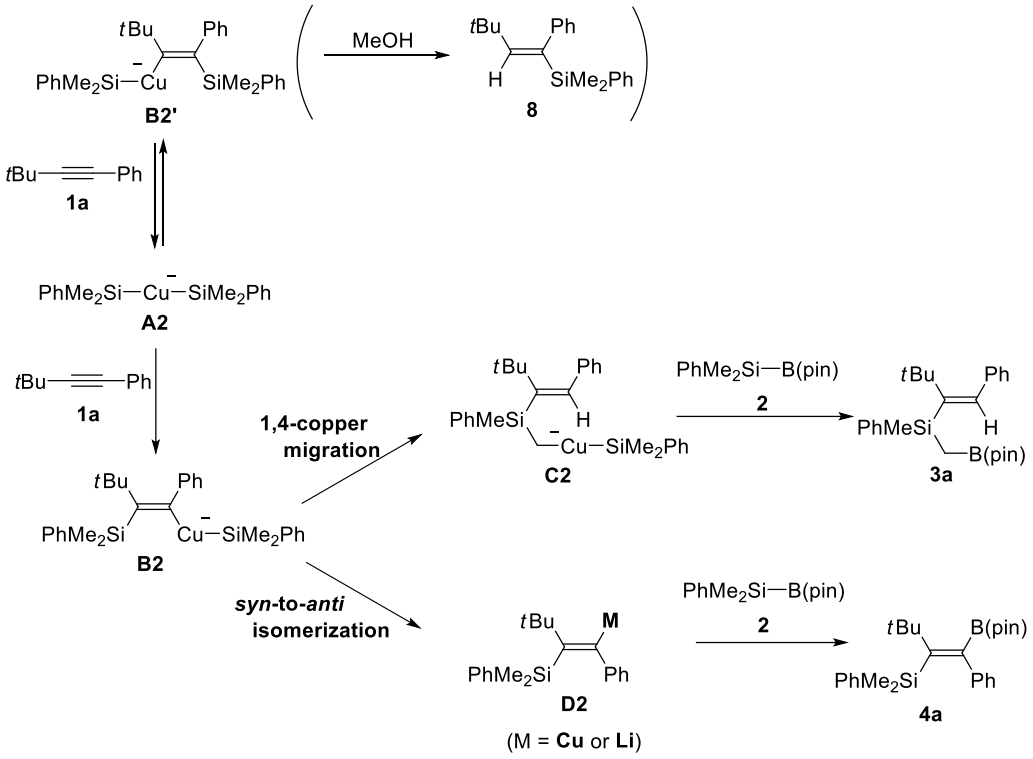

Scheme 5. Reaction pathways proposed by the ^{1}H NMR experiments.

Some control experiments using deuterium-labeled silylboronates were also carried out. As shown in Scheme 6, while the reaction of alkyne **1a** with 1.2 equiv of non-deuterated silylboronate **2** gave **3a** in a good yield with high selectivity (Scheme 6a), the use of 1.2 equiv of deuterated **2-*d*$_6$** having two CD_3 groups on the silicon significantly decreased the overall reactivity, and the yield and selectivity of **3a-*d*$_6$** became much lower (Scheme 6b). These results show that the reaction rate toward **3a** is strongly affected by replacement of methyl C–H on silicon with C–D, indicating that 1,4-copper migration is involved in the turnover-limiting step. It is also worth noting that a deuterium of the CD_3 group was quantitatively incorporated at the alkenyl carbon in the resulting **3a-*d*$_6$**, which confirms that alkenyl-to-alkyl 1,4-copper migration actually took place. On the other hand, the use of 1.2 equiv of silylboronate **2-*d*$_3$** having one CD_3 group gave a moderate yield of **3a-*d*$_3$** and 1,4-migration toward non-deuterated CH_3 group occurred with 93/7 selectivity (Scheme 6c). In addition, when these three reactions were conducted using 2.4 equiv of silylboronates, the selectivity toward **4a** became higher in all cases, and the degree was larger by having more CD_3 groups. This trend suggests that borylation of **D** in Scheme 4 is accelerated by increasing the concentration of **2**, and the relative rates between Cycles I and II are in a fine balance depending on the ease or difficulty of 1,4-copper migration from **B** to **C** and borylation of **D**.

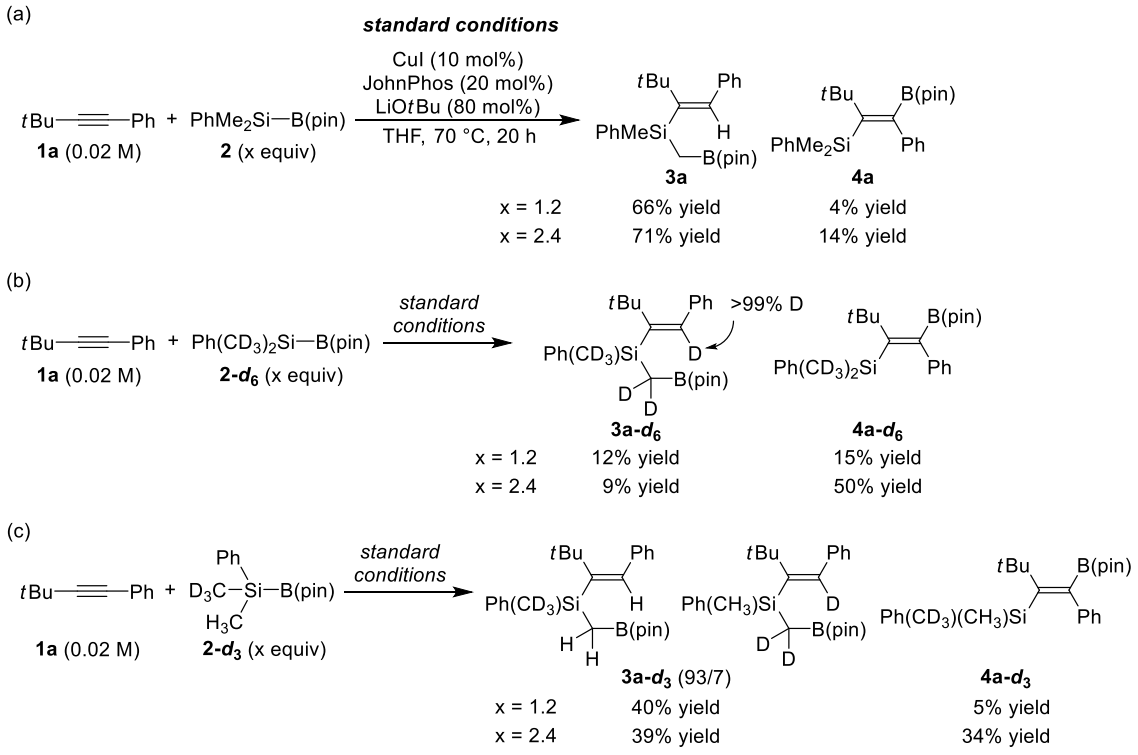

Scheme 6. Control experiments using (a) silylboronate **2a**, (b) **2a-*d*$_6$**, and (c) **2a-*d*$_3$**.

4.3 Conclusion

The author achieved a copper-catalyzed formal hydro(borylmethylsilyl)ation of internal alkynes with silylboronates through 1,4-copper migration to give alkenylsilylmethylboronates. The reaction proceeds with high chemo-, regio-, and stereoselectivity for a variety of sterically demanding alkyl(aryl)acetylenes and the resulting boryl groups could be further functionalized. The reaction mechanism and the origin of selectivity were investigated through kinetic, NMR, and deuterium-labeling experiments. The results of this study will lead to expansion of the catalytic transformations involving 1,*n*-copper migration.

4.4 Experimental section

General

All air- and moisture-sensitive manipulations were carried out with standard Schlenk techniques under nitrogen or in a glove box under argon. Preparative GPC was performed with JAI LaboACE LC-5060 equipped with JAIGEL-2HR columns using $CHCl_3$ as an eluent. NMR spectra were recorded on JEOL JNM-ECS400, JEOL JNM-ECZL400S, or Agilent Unity-Inova500 spectrometer. High resolution mass spectra were recorded on JEOL JMS700 spectrometer. X-ray crystallographic analysis was performed by RIGAKU XTaLAB P200 with graphite-monochromated Mo-Kα (0.71075 Å) radiation.

Et_3N (FUJIFILM Wako Chemicals) and $(i\text{Pr})_2NH$ (FUJIFILM Wako Chemicals) were distilled over KOH under vacuum. CCl_4 (FUJIFILM Wako Chemicals) was dried over $MgSO_4$ and degassed by purging nitrogen prior to use. THF (Kanto Chemical; dehydrated), 1,4-dioxane (FUJIFILM Wako Chemicals; dehydrated), Et_2O (FUJIFILM Wako Chemicals; dehydrated), hexane (FUJIFILM Wako Chemicals; dehydrated), CH_2Cl_2 (Kanto Chemical; dehydrated), MeCN (FUJIFILM Wako Chemicals; dehydrated), MeOH (FUJIFILM Wako Chemicals; dehydrated), 3,3-dimethyl-1-butyne (TCI), 4-methyl-1-pentyne (TCI), iodobenzene (FUJIFILM Wako Chemicals), iodomethane-d_3 (CIL), iodoethane (FUJIFILM Wako Chemicals), mesityl iodide (TCI), 2-bromonaphthalene (TCI), bromochloromethane (FUJIFILM Wako Chemicals), ethyl 2-ethylbutyrate (TCI), *N*-bromosuccinimde (FUJIFILM Wako Chemicals), dichlorophenylsilane (BLD Pharmatech), (dimethylphenylsilyl)boronic acid pinacol ester (FUJIFILM Wako Chemicals), isopropoxy 4,4,5,5-tetramethyl-1,3,2-dioxaborolane (TCI), pyridinium chlorochromate (TCI), *n*BuLi (Kanto Chemical; 1.56–1.57 M solution in hexane), vinylmagnesium bromide (Aldrich; 1.0 M solution in THF), $LiAlH_4$ (TCI), iodine (FUJIFILM Wako Chemicals), H_2O_2 (Kishida Chemical; 35 wt% in H_2O), PPh_3

(FUJIFILM Wako Chemicals), PCy_3 (Aldrich), P(*t*Bu)$_3$ (Strem Chemicals; 10 wt% solution in hexane), JohnPhos (FUJIFILM Wako Chemicals), P(*t*Bu)$_3$•HBF_4 (TCI), LiO*t*Bu (Aldrich), NaO*t*Bu (TCI), KO*t*Bu (Nacalai Tesque), K_2CO_3 (FUJIFILM Wako Chemicals), Li (Kishida Chemical: stick in paraffin), Mg turnings (FUJIFILM Wako Chemicals), $PdCl_2$ (Tanaka Kinzoku), CuI (FUJIFILM Wako Chemicals), and $ZnCl_2$ (TCI) were used as received. **1b**,[26] **1e**,[27] **1f**,[28] **1x**,[29] dimethyl (1-diazo-2-oxopropyl)phosphonate,[30] $PdCl_2(MeCN)_2$,[31] and $Pd(PPh_3)_4$[32] were synthesized following the literature procedures.

Synthesis of substrates

Representative procedures for substrates:

(3,3-Dimethyl-1-butynyl)benzene (1a) (CAS 4250-82-2)

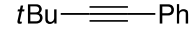

Et_3N (2.10 mL, 15.0 mmol), iodobenzene (1.03 g, 5.05 mmol), and 3,3-dimethyl-1-butyne (644 μL, 5.25 mmol) were successively added to a mixture of $Pd(PPh_3)_4$ (57.8 mg, 50.0 μmol) and CuI (19.8 mg, 104 μmol) in THF (7.5 mL), and this was stirred for 26 h at 40 °C. The reaction mixture was directly passed through a pad of silica gel with EtOAc and the solvent was removed under vacuum. The residue was chromatographed on silica gel with hexane to afford compound **1a** as a colorless oil (740 mg, 4.68 mmol; 94% yield).

^1H NMR ($CDCl_3$): δ 7.41-7.39 (m, 2H), 7.30-7.20 (m, 3H), 1.32 (s, 9H). $^{13}C\{^1H\}$ NMR ($CDCl_3$): δ 131.7, 128.3, 127.5, 124.2, 98.7, 79.2, 31.2, 28.1.

2-(3,3-Dimethyl-1-butynyl)naphthalene (1j) (CAS 1391145-01-9)

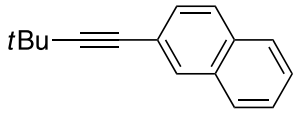

(iPr)$_2$NH (355 μL, 2.53 mmol) and 3,3-dimethyl-1-butyne (294 μL, 2.40 mmol) were added to a mixture of 2-bromonaphthalene (415 mg, 2.00 mmol), $PdCl_2(MeCN)_2$ (15.7 mg, 60.5 μmol), P(tBu)$_3$•HBF_4 (34.8 mg, 0.120 mmol), and CuI (7.6 mg, 40 μmol) in 1,4-dioxane (3.0 mL), and this was stirred for 15 h at 40 °C. The reaction mixture was directly passed through a pad of silica gel with EtOAc and the solvent was removed under vacuum. The residue was chromatographed on silica gel with hexane and further purified by GPC with $CHCl_3$ to afford compound **1j** as a pale purple solid (293 mg, 1.40 mmol; 70% yield).

^1H NMR ($CDCl_3$): δ 7.90 (s, 1H), 7.82-7.71 (m, 3H), 7.49-7.41 (m, 3H), 1.36 (s, 9H). $^{13}C\{^1H\}$ NMR ($CDCl_3$): δ 133.2, 132.6, 131.1, 129.0, 127.84, 127.82, 127.7, 126.4, 126.3,

121.6, 99.1, 79.5, 31.2, 28.2.

(3,3-Diethyl-1-pentynyl)benzene (1n) (CAS 80025-09-8)

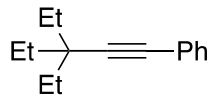

*n*BuLi (10.6 mL, 16.5 mmol; 1.56 M solution in hexane) was added slowly over 20 min to a solution of (*i*Pr)$_2$NH (2.43 mL, 17.3 mmol) in THF (10 mL) at −78 °C, and the mixture was stirred for 30 min at −78 °C. Ethyl 2-ethylbutyrate (2.48 mL, 15.0 mmol) was added to it slowly over 5 min at −78 °C. The resulting mixture was stirred for 30 min at 0 °C and iodoethane (1.44 mL, 18.0 mmol) was added to it. This was stirred for 22 h at room temperature, and the reaction was quenched with saturated NH_4Claq. After extraction with Et_2O, the organic layer was washed with saturated NaClaq, dried over $MgSO_4$, filtered, and concentrated under vacuum to afford ethyl 2,2-diethylbutanoate (CAS 34666-17-6) as a colorless oil (3.89 g containing THF and Et_2O), which was used for the next step without further purification.

^{1}H NMR ($CDCl_3$): δ 4.13 (q, $^3J_{HH}$ = 7.2 Hz, 2H), 1.57 (q, $^3J_{HH}$ = 7.5 Hz, 6H), 1.24 (t, $^3J_{HH}$ = 7.3 Hz, 3H), 0.76 (t, $^3J_{HH}$ = 7.6 Hz, 9H).

$LiAlH_4$ (1.14 g, 30.0 mmol) was added portionwise over 10 min to a solution of ethyl 2,2-diethylbutanoate obtained above in Et_2O (45 mL) at 0 °C, and the mixture was stirred for 23 h at room temperature. The reaction was quenched slowly with 1 M HClaq at 0 °C and diluted with H_2O. This was extracted with Et_2O, and the organic layer was washed with saturated NaClaq, dried over $MgSO_4$, filtered, and concentrated under vacuum to afford 2,2-diethyl-1-butanol (CAS 13023-60-4) as a colorless oil (2.37 g containing Et_2O), which was used for the next step without further purification.

^{1}H NMR ($CDCl_3$): δ 3.36 (s, 2H), 1.60 (bs, 1H), 1.24 (q, $^3J_{HH}$ = 7.5 Hz, 6H), 0.79 (t,

$^3J_{HH}$ = 7.3 Hz, 9H).

A solution of 2,2-diethyl-1-butanol obtained above in CH_2Cl_2 (10 mL) was added to a mixture of pyridinium chlorochromate (4.85 g, 22.5 mmol) and Celite in CH_2Cl_2 (30 mL), and the resulting mixture was stirred for 17 h at room temperature. The reaction mixture was passed through a pad of silica gel with CH_2Cl_2 and the solvent was removed under vacuum to afford 2,2-diethylbutanal (CAS 26254-89-7) as a colorless oil (2.78 g containing CH_2Cl_2 and Et_2O), which was used for the next step without further purification.

^{1}H NMR ($CDCl_3$): δ 9.41 (s, 1H), 1.52 (q, $^3J_{HH}$ = 7.6 Hz, 6H), 0.78 (t, $^3J_{HH}$ = 7.6 Hz, 9H).

Dimethyl (1-diazo-2-oxopropyl)phosphonate (3.46 g, 18.0 mmol) was added slowly over 5 min to a mixture of 2,2-diethylbutanal obtained above and K_2CO_3 (6.20 g, 44.9 mmol) in MeOH (40 mL), and this was stirred for 27 h at room temperature. The reaction mixture was diluted with H_2O and this was extracted with pentane. The organic layer was washed with saturated NaClaq, dried over $MgSO_4$, filtered, and passed through a pad of silica gel with pentane. The solvents were distilled off at 55 °C under atmospheric pressure to afford 3,3-diethyl-1-pentyne (CAS 919-23-3) as a colorless oil (1.94 g, 10.7 mmol; 71% yield over 4 steps, 69 wt% with pentane and 2,2-diethylbutanal).

^{1}H NMR ($CDCl_3$): δ 2.08 (s, 1H), 1.46 (q, $^3J_{HH}$ = 7.5 Hz, 6H), 0.91 (t, $^3J_{HH}$ = 7.6 Hz, 9H).

Et_3N (1.00 mL, 7.17 mmol), iodobenzene (510 mg, 2.50 mmol), and 3,3-diethyl-1-pentyne (471 mg, 2.63 mmol; 69 wt%) were successively added to a mixture of $Pd(PPh_3)_4$ (57.8 mg, 50.0 μmol) and CuI (18.7 mg, 98.2 μmol) in THF (4.5 mL), and this was stirred for 42 h at 50 °C. The reaction mixture was directly passed through a pad of silica gel with EtOAc and the solvent was removed under vacuum. The residue was

chromatographed on silica gel with hexane to afford compound **1n** as a colorless oil (330 mg, 1.65 mmol; 66% yield).

^{1}H NMR ($CDCl_3$): δ 7.42-7.36 (m, 2H), 7.30-7.21 (m, 3H), 1.53 (q, $^{3}J_{HH}$ = 7.3 Hz, 6H), 0.97 (t, $^{3}J_{HH}$ = 7.6 Hz, 9H). $^{13}C\{^{1}H\}$ NMR ($CDCl_3$): δ 131.7, 128.2, 127.4, 124.6, 96.2, 82.5, 40.1, 30.0, 8.9.

1,3,5-Trimethyl-2-(4-methyl-1-pentynyl)benzene (1v) (CAS 2629763-08-0)

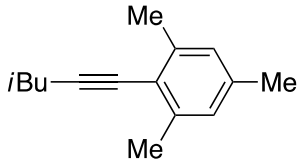

*n*BuLi (2.90 mL, 4.52 mmol; 1.56 M solution in hexane) was added slowly over 10 min to a solution of 4-methyl-1-pentyne (540 µL, 4.60 mmol) in THF (4.5 mL) at −78 °C, and the mixture was stirred for 40 min at −78 °C. This was added to $ZnCl_2$ (638 mg, 4.68 mmol) in THF (1.0 mL) at −78 °C, and the resulting mixture was stirred for 30 min at −78 °C. $Pd(PPh_3)_4$ (174 mg, 0.151 mmol) and mesityl iodide (739 mg, 3.00 mmol) were then added to it, and the mixture was stirred for 41 h at room temperature. The reaction was quenched with saturated NH_4Claq and this was extracted with Et_2O. The organic layer was washed with saturated NaClaq, dried over $MgSO_4$, filtered, and concentrated under vacuum. The residue was chromatographed on silica gel with hexane to afford compound **1v** as a colorless oil (521 mg, 2.60 mmol; 87% yield).

^{1}H NMR ($CDCl_3$): δ 6.84 (s, 2H), 2.39 (d, $^{3}J_{HH}$ = 7.3 Hz, 2H), 2.38 (s, 6H), 2.26 (s, 3H), 1.92 (non, $^{3}J_{HH}$ = 6.6 Hz, 1H), 1.06 (d, $^{3}J_{HH}$ = 6.4 Hz, 6H). $^{13}C\{^{1}H\}$ NMR ($CDCl_3$): δ 140.0, 136.7, 127.5, 121.0, 97.0, 79.2, 29.1, 28.5, 22.2, 21.3, 21.2.

(Di(methyl-d_3)phenylsilyl)boronic acid pinacol ester (2-d_6)

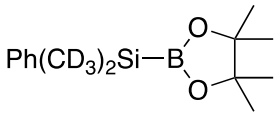

A solution of iodomethane-d_3 (1.40 mL, 22.0 mmol) in Et_2O (10 mL) was added dropwise over 30 min to a suspension of Mg turnings (588 mg, 24.2 mmol) in Et_2O (20 mL), and the mixture was stirred for 1 h at room temperature. A solution of dichlorophenylsilane (1.46 mL, 10.0 mmol) in Et_2O (20 mL) was added to it slowly over 15 min, and the resulting mixture was stirred for 18 h at room temperature. The reaction was quenched with saturated NH_4Claq and this was extracted with Et_2O. The organic layer was washed with saturated NaClaq, dried over $MgSO_4$, filtered, and concentrated under vacuum (300 hPa at 25 °C). The residue was chromatographed on silica gel with pentane to afford di(methyl-d_3)phenylsilane (CAS 106710-82-1) as a colorless oil (1.24 g, 8.45 mmol; 85% yield, 97 wt% with pentane).

^{1}H NMR ($CDCl_3$): δ 7.59-7.51 (m, 2H), 7.41-7.33 (m, 3H), 4.41 (s, 1H).

Di(methyl-d_3)phenylsilane (1.24 g, 8.45 mmol; 97 wt%) was added to a suspension of $PdCl_2$ (30.5 mg, 17.2 μmol) in CCl_4 (10 mL), and the mixture was stirred for 22 h at room temperature. The reaction mixture was filtered through Celite with THF (20 mL) and concentrated under vacuum. The residue was added with the aid of THF (3 mL) to a suspension of Li (235 mg, 33.9 mmol; cut in small pieces) in THF (7 mL) at 0 °C, and the mixture was stirred for 20 h at 0 °C. The resulting mixture was added slowly over 20 min with the aid of hexane (3 mL) to a solution of 2-isopropoxy-4,4,5,5-tetramethyl-1,3,2-dioxaborolane (3.40 mL, 16.8 mmol) in hexane (7 mL) at 0 °C, and the mixture was stirred for 30 min at 0 °C and for 19 h at room temperature. The reaction mixture was passed through a pad of Celite with hexane and concentrated under vacuum. The residue was purified by bulb-to-bulb distillation under 90–100 Pa at 120 °C to afford compound

2-*d*$_6$ as a colorless oil (732 mg, 2.73 mmol; 32% yield, ca. 88% pure).

^{1}H NMR ($CDCl_3$): δ 7.59-7.55 (m, 2H), 7.35-7.31 (m, 3H), 1.25 (s, 12H).

Analytical data for other substrates:

1-(3,3-Dimethyl-1-butynyl)-4-methylbenzene (1c) (CAS 79756-95-9)

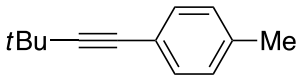

^{1}H NMR ($CDCl_3$): δ 7.27 (d, $^3J_{HH}$ = 8.3 Hz, 2H), 7.07 (d, $^3J_{HH}$ = 8.3 Hz, 2H), 2.32 (s, 3H), 1.31 (s, 9H). ^{13}C{^{1}H} NMR ($CDCl_3$): δ 137.4, 131.6, 129.0, 121.1, 97.9, 79.1, 31.3, 28.1, 21.5.

1-(3,3-Dimethyl-1-butynyl)-3-methylbenzene (1d) (CAS 210171-75-8)

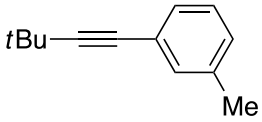

^{1}H NMR ($CDCl_3$): δ 7.23 (s, 1H), 7.22-7.13 (m, 2H), 7.07 (d, $^3J_{HH}$ = 7.3 Hz, 1H), 2.31 (s, 3H), 1.32 (s, 9H). ^{13}C{^{1}H} NMR ($CDCl_3$): δ 137.9, 132.3, 128.7, 128.4, 128.2, 124.0, 98.3, 79.3, 31.2, 28.1, 21.3.

1-(3,3-Dimethyl-1-butynyl)-2-methyl-4-(trimethylsilyl)benzene (1g)

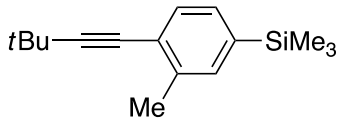

^{1}H NMR ($CDCl_3$): δ 7.31 (d, $^3J_{HH}$ = 7.8 Hz, 1H), 7.30 (s, 1H), 7.24 (d, $^3J_{HH}$ = 7.8 Hz, 1H), 2.40 (s, 3H), 1.33 (s, 9H), 0.24 (s, 9H). ^{13}C{^{1}H} NMR ($CDCl_3$): δ 139.9, 139.0, 134.3, 130.8, 130.4, 124.4, 103.4, 78.2, 31.3, 28.4, 20.8, −1.0. HRMS (EI) calcd for $C_{16}H_{24}Si$ (M^+) 244.1642, found 244.1647.

1-(3,3-Dimethyl-1-butynyl)-2-methyl-4-(4-chlorophenyl)benzene (1h)

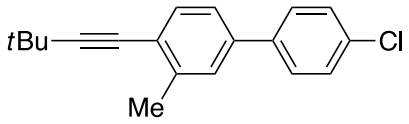

^{1}H NMR ($CDCl_3$): δ 7.50 (d, $^{3}J_{HH}$ = 8.8 Hz, 2H), 7.43-7.35 (m, 4H), 7.29 (dd, $^{3}J_{HH}$ = 7.8 Hz, and $^{4}J_{HH}$ = 2.0 Hz, 1H), 2.45 (s, 3H), 1.35 (s, 9H). ^{13}C{^{1}H} NMR ($CDCl_3$): δ 156.5, 154.9, 154.4, 147.6, 146.0, 142.0, 141.2, 140.6, 135.8, 134.9, 110.6, 78.0, 19.8, 16.2, 6.9. HRMS (FAB) calcd for $C_{19}H_{19}Cl$ (M^+) 282.1170, found 282.1169.

1-(3,3-Dimethyl-1-butynyl)naphthalene (1i) (CAS 124153-66-8)

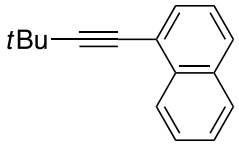

^{1}H NMR ($CDCl_3$): δ 8.31 (d, $^{3}J_{HH}$ = 8.7 Hz, 1H), 7.82 (d, $^{3}J_{HH}$ = 8.7 Hz, 1H), 7.76 (d, $^{3}J_{HH}$ = 8.2 Hz, 1H), 7.60 (dd, $^{3}J_{HH}$ = 7.3 Hz and $^{4}J_{HH}$ = 1.4 Hz, 1H), 7.55 (ddd, $^{3}J_{HH}$ = 8.2 and 6.9 Hz and $^{4}J_{HH}$ = 1.4 Hz, 1H), 7.49 (ddd, $^{3}J_{HH}$ = 8.2 and 6.9 Hz and $^{4}J_{HH}$ = 1.4 Hz, 1H), 7.39 (dd, $^{3}J_{HH}$ = 8.2 and 7.4 Hz, 1H), 1.43 (s, 9H). ^{13}C{^{1}H} NMR ($CDCl_3$): δ 133.6, 133.3, 130.0, 128.3, 128.0, 126.6, 126.4, 126.3, 125.3, 121.8, 103.9, 77.2, 31.3, 28.5.

4-(3,3-Dimethyl-1-butynyl)-1-methoxymethyl-1*H*-indole (1k)

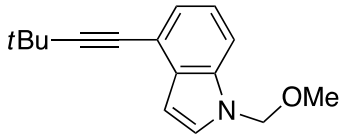

^{1}H NMR ($CDCl_3$): δ 7.41 (dt, $^{3}J_{HH}$ = 8.2 Hz and J_{HH} = 0.9 Hz, 1H), 7.21 (dd, $^{3}J_{HH}$ = 7.4 Hz and $^{4}J_{HH}$ = 1.4 Hz, 1H), 7.20 (d, $^{3}J_{HH}$ = 3.2 Hz, 1H), 7.15 (t, $^{3}J_{HH}$ = 7.8 Hz, 1H), 6.67 (dd, $^{3}J_{HH}$ = 3.2 Hz and $^{5}J_{HH}$ = 0.9 Hz, 1H), 5.44 (s, 2H), 3.21 (s, 3H), 1.39 (s, 9H).

$^{13}C\{^{1}H\}$ NMR ($CDCl_3$): δ 136.1, 130.9, 128.4, 123.7, 122.1, 116.2, 109.7, 102.4, 101.5, 77.6, 77.5, 55.9, 31.4, 28.3. HRMS (EI) calcd for $C_{16}H_{19}NO$ (M^+) 241.1461, found 241.1462.

5-(3,3-Dimethyl-1-butynyl)-1-methyl-1*H*-indole (1l) (CAS 2519944-45-5)

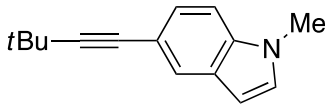

^{1}H NMR ($CDCl_3$): δ 7.70 (t, J_{HH} = 0.9 Hz, 1H), 7.26 (dd, $^{3}J_{HH}$ = 8.2 Hz and $^{4}J_{HH}$ = 1.4 Hz, 1H), 7.21 (dd, $^{3}J_{HH}$ = 8.2 Hz and $^{5}J_{HH}$ = 0.9 Hz, 1H), 7.03 (d, $^{3}J_{HH}$ = 3.2 Hz, 1H), 6.43 (d, $^{3}J_{HH}$ = 2.8 Hz, 1H), 3.77 (s, 3H), 1.35 (s, 9H). $^{13}C\{^{1}H\}$ NMR ($CDCl_3$): δ 136.1, 129.6, 128.4, 125.4, 124.6, 114.8, 109.1, 101.1, 95.8, 80.3, 33.0, 31.4, 28.1.

3-(3,3-Dimethyl-1-butynyl)-2,5-dimethylthiophene (1m) (CAS 2494387-99-2)

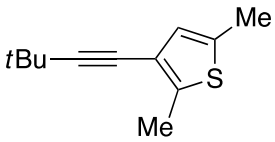

^{1}H NMR ($CDCl_3$): δ 6.56 (s, 1H), 2.41 (s, 3H), 2.36 (s, 3H), 1.31 (s, 9H). $^{13}C\{^{1}H\}$ NMR ($CDCl_3$): δ 139.9, 135.4, 127.4, 120.0, 100.4, 73.9, 31.4, 28.2, 15.2, 14.2.

(3,3,4-Trimethyl-1-pentynyl)benzene (1o) (CAS 174744-88-8)

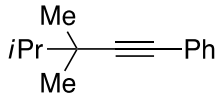

^{1}H NMR ($CDCl_3$): δ 7.42-7.36 (m, 2H), 7.31-7.21 (m, 3H), 1.64 (sept, $^{3}J_{HH}$ = 6.8 Hz, 1H), 1.25 (s, 6H), 1.03 (d, $^{3}J_{HH}$ = 6.9 Hz, 6H). $^{13}C\{^{1}H\}$ NMR ($CDCl_3$): δ 131.7, 128.3, 127.4, 124.4, 97.0, 81.0, 38.0, 35.6, 27.1, 18.6.

(3,3-Dimethyl-4-triisopropylsilyloxy-1-butynyl)benzene (1p)

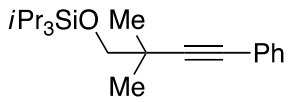

^{1}H NMR ($CDCl_3$): δ 7.40-7.35 (m, 2H), 7.29-7.23 (m, 3H), 3.64 (s, 2H), 1.29 (s, 6H), 1.18-1.04 (m, 21H). $^{13}C\{^{1}H\}$ NMR ($CDCl_3$): δ 131.7, 128.2, 127.6, 124.2, 96.3, 80.7, 71.9, 34.5, 25.7, 18.2, 12.2. HRMS (EI) calcd for $C_{21}H_{34}OSi$ (M^+) 330.2373, found 330.2376.

((1-Methylcyclohexyl)ethynyl)benzene (1q) (CAS 1931126-45-2)

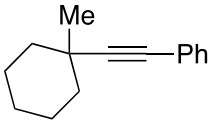

^{1}H NMR ($CDCl_3$): δ 7.43-7.37 (m, 2H), 7.31-7.23 (m, 3H), 1.85-1.77 (m, 2H), 1.75-1.54 (m, 6H), 1.27 (s, 3H), 1.27-1.12 (m, 2H). $^{13}C\{^{1}H\}$ NMR ($CDCl_3$): δ 131.7, 128.3, 127.5, 124.4, 96.9, 81.9, 39.7, 33.3, 30.4, 26.1, 23.6.

4-Methyl-1-phenyl-4-(phenylethynyl)piperidine (1r)

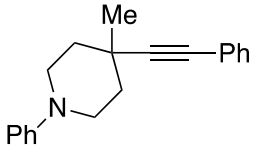

^{1}H NMR ($CDCl_3$): δ 7.43-7.36 (m, 2H), 7.32-7.22 (m, 5H), 6.98 (d, $^{3}J_{HH}$ = 8.7 Hz, 2H), 6.83 (t, $^{3}J_{HH}$ = 7.3 Hz, 1H), 3.59 (dt, $^{2}J_{HH}$ = 12.8 Hz and $^{3}J_{HH}$ = 3.4 Hz, 2H), 3.16 (td, J_{HH} = 12.4 Hz and $^{3}J_{HH}$ = 2.3 Hz, 2H), 1.90 (d, $^{2}J_{HH}$ = 13.3 Hz, 2H), 1.70 (td, J_{HH} = 12.6 Hz and $^{3}J_{HH}$ = 3.7 Hz, 2H), 1.37 (s, 3H). $^{13}C\{^{1}H\}$ NMR ($CDCl_3$): δ 151.7, 131.7, 129.2, 128.3, 127.8, 123.8, 119.3, 116.5, 94.7, 83.4, 47.1, 38.5, 31.7, 29.7. HRMS (EI) calcd for $C_{20}H_{21}N$ (M^+) 275.1669, found 275.1674.

(1-Adamantylethynyl)benzene (1s) (CAS 74203-39-7)

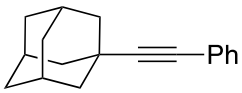

^{1}H NMR ($CDCl_3$): δ 7.42-7.35 (m, 2H), 7.30-7.21 (m, 3H), 2.03-1.94 (m, 9H), 1.75-1.69 (m, 6H). $^{13}C\{^{1}H\}$ NMR ($CDCl_3$): δ 131.8, 128.2, 127.5, 124.3, 98.5, 79.5, 43.0, 36.6, 30.2, 28.2.

1-Methyl-2-(3-methyl-1-butynyl)benzene (1t) (CAS 2443556-88-3)

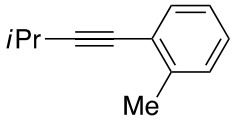

^{1}H NMR ($CDCl_3$): δ 7.35 (d, $^{3}J_{HH}$ = 8.3 Hz, 1H), 7.19-7.13 (m, 2H), 7.12-7.07 (m, 1H), 2.82 (sept, $^{3}J_{HH}$ = 6.8 Hz, 1H), 2.41 (s, 3H), 1.28 (d, $^{3}J_{HH}$ = 6.8 Hz, 6H). $^{13}C\{^{1}H\}$ NMR ($CDCl_3$): δ 140.1, 131.8, 129.4, 127.6, 125.5, 123.9, 100.1, 78.7, 23.4, 21.5, 20.8.

1,3-Dimethyl-2-(3-methyl-1-butynyl)benzene (1u) (CAS 2532523-82-1)

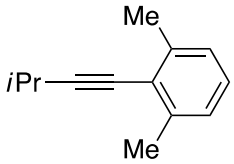

^{1}H NMR ($CDCl_3$): δ 7.08-6.98 (m, 3H), 2.86 (sept, $^{3}J_{HH}$ = 6.9 Hz, 1H), 2.40 (s, 6H), 1.30 (d, $^{3}J_{HH}$ = 6.9 Hz, 6H). $^{13}C\{^{1}H\}$ NMR ($CDCl_3$): δ 140.0, 127.0, 126.6, 123.8, 104.8, 77.4, 23.5, 21.7, 21.2.

(Methyl(methyl-*d*$_3$)phenylsilyl)boronic acid pinacol ester (2-*d*$_3$)

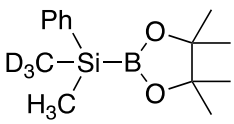

^{1}H NMR ($CDCl_3$): δ 7.61-7.55 (m, 2H), 7.36-7.30 (m, 3H), 1.25 (s, 12H), 0.33 (s, 3H).

Catalytic reactions and derivatization

General procedure for Scheme 2.

Compound **1** (0.200 mmol) and (dimethylphenylsilyl)boronic acid pinacol ester (**2**) (65.4 μL, 0.240 mmol) were added with the aid of THF (1.0 mL) to a mixture of CuI (3.8 mg, 20 μmol), JohnPhos (11.9 mg, 39.9 μmol), and Li*O*tBu (12.8 mg, 0.160 mmol) in THF (9.0 mL), and this was stirred for 20 h at 70 °C. The reaction mixture was directly passed through a pad of silica gel with EtOAc and the solvent was removed under vacuum. The residue was purified by GPC with $CHCl_3$ to afford compound **3**.

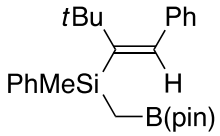

Compound 3a. White solid. 65% yield (55.3 mg; **3a**/**4a** = 94/6).

^{1}H NMR ($CDCl_3$): δ 7.66-7.61 (m, 2H), 7.38-7.31 (m, 3H), 7.30-7.24 (m, 2H), 7.22-7.13 (m, 3H) 7.09 (s, 1H), 1.18 (s, 6H), 1.16 (s, 6H), 0.94 (s, 9H), 0.62 (d, $^2J_{HH}$ = 12.8 Hz, 1H), 0.60-0.53 (m, 4H). ^{13}C{^{1}H} NMR ($CDCl_3$): δ 151.3, 142.9, 142.0, 140.9, 134.2, 128.7, 128.2, 127.73, 127.71, 126.0, 82.9, 38.2, 32.8, 25.1, 25.0, 1.1. HRMS (FAB) calcd for $C_{26}H_{37}BO_2Si$ (M^+) 420.2650, found 420.2664.

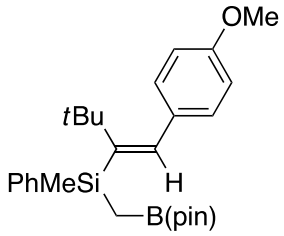

Compound 3b. Colorless oil. 66% yield (58.6 mg; **3b**/**4b** = 94/6).

^{1}H NMR ($CDCl_3$): δ 7.65-7.59 (m, 2H), 7.37-7.29 (m, 3H), 7.06 (d, $^3J_{HH}$ = 8.7 Hz, 2H), 7.04 (s, 1H), 6.82 (d, $^3J_{HH}$ = 8.7 Hz, 2H), 3.80 (s, 3H), 1.18 (s, 6H), 1.16 (s, 6H),

0.95 (s, 9H), 0.61 (d, $^{2}J_{HH}$ = 12.8 Hz, 1H), 0.58-0.52 (m, 4H). $^{13}C\{^{1}H\}$ NMR ($CDCl_3$): δ 157.9, 151.4, 141.8, 141.0, 135.0, 134.2, 129.3, 128.6, 127.7, 113.2, 82.9, 55.3, 38.0, 32.8, 25.1, 25.0, 1.2. HRMS (EI) calcd for $C_{27}H_{39}BO_3Si$ (M^+) 450.2756, found 450.2755.

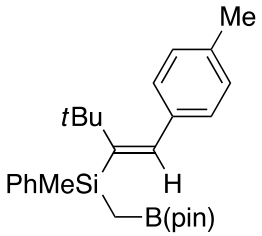

Compound 3c. White solid. 62% yield (54.0 mg; **3c**/**4c** = 96/4).

^{1}H NMR ($CDCl_3$): δ 7.65-7.60 (m, 2H), 7.37-7.29 (m, 3H), 7.08 (d, $^{3}J_{HH}$ = 7.8 Hz, 2H), 7.06 (s, 1H), 7.03 (d, $^{3}J_{HH}$ = 7.8 Hz, 2H), 2.33 (s, 3H), 1.18 (s, 6H), 1.16 (s, 6H), 0.94 (s, 9H), 0.61 (d, $^{2}J_{HH}$ = 12.8 Hz, 1H), 0.58-0.53 (m, 4H). $^{13}C\{^{1}H\}$ NMR ($CDCl_3$): δ 151.2, 142.2, 141.0, 139.8, 135.4, 134.2, 128.6, 128.4, 128.1, 127.7, 82.9, 38.1, 32.8, 25.1, 25.0, 21.3, 1.2. HRMS (EI) calcd for $C_{27}H_{39}BO_2Si$ (M^+) 434.2807, found 434.2809.

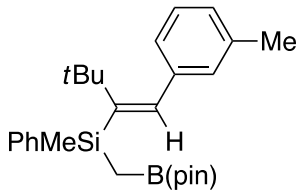

Compound 3d. Colorless oil. 69% yield (59.3 mg; **3d**/**4d** = 94/6).

^{1}H NMR ($CDCl_3$): δ 7.65-7.60 (m, 2H), 7.37-7.29 (m, 3H), 7.16 (dd, $^{3}J_{HH}$ = 7.8 and 7.4 Hz, 1H), 7.06 (s, 1H), 7.02-6.92 (m, 3H), 2.33 (s, 3H), 1.18 (s, 6H), 1.16 (s, 6H), 0.94 (s, 9H), 0.61 (d, $^{2}J_{HH}$ = 12.4 Hz, 1H), 0.58-0.53 (m, 4H). $^{13}C\{^{1}H\}$ NMR ($CDCl_3$): δ 150.9, 142.8, 142.2, 140.9, 137.2, 134.2, 128.8, 128.6, 127.7, 127.6, 126.6, 125.2, 82.9, 38.1, 32.8, 25.1, 25.0, 21.6, 1.1. HRMS (EI) calcd for $C_{27}H_{39}BO_2Si$ (M^+) 434.2807, found 434.2815.

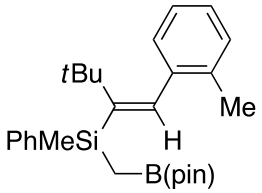

Compound 3e. The reaction was conducted in 2.5 mL of THF. White solid. 82% yield (72.0 mg; **3e**/**4e** > 99/1).

^{1}H NMR ($CDCl_3$): δ 7.66-7.61 (m, 2H), 7.36-7.29 (m, 3H), 7.15-7.09 (m, 4H), 6.93 (s, 1H), 2.26 (s, 3H), 1.15 (s, 6H), 1.13 (s, 6H), 0.92 (s, 9H), 0.61 (s, 3H), 0.60 (s, 2H). ^{13}C{^{1}H} NMR ($CDCl_3$): δ 150.8, 142.2, 141.5, 141.0, 134.9, 134.2, 129.5, 128.6, 128.5, 127.7, 126.4, 125.0, 82.9, 38.2, 32.3, 25.1, 24.9, 20.6, 1.1. HRMS (FAB) calcd for $C_{27}H_{39}BO_2Si$ (M^+) 434.2807, found 434.2808.

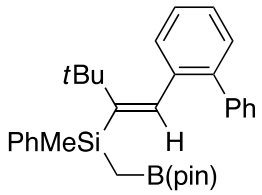

Compound 3f. The reaction was conducted in 2.5 mL of THF. Colorless oil. 74% yield (72.1 mg; **3f**/**4f** > 99/1).

^{1}H NMR ($CDCl_3$): δ 7.44-7.33 (m, 5H), 7.32-7.18 (m, 9H), 7.03 (s, 1H), 1.13 (s, 6H), 1.11 (s, 6H), 0.82 (s, 9H), 0.54-0.48 (m, 4H), 0.46 (d, $^{2}J_{HH}$ = 12.8 Hz, 1H). ^{13}C{^{1}H} NMR ($CDCl_3$): δ 149.9, 142.1, 141.3, 141.0, 140.8, 140.1, 134.2, 129.64, 129.57, 129.4, 128.4, 128.1, 127.5, 126.9, 126.8, 126.4, 82.9, 38.0, 32.2, 25.0, 24.9, 0.8. HRMS (EI) calcd for $C_{32}H_{41}BO_2Si$ (M^+) 496.2963, found 496.2974.

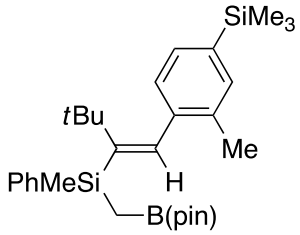

Compound 3g. The reaction was conducted in 2.5 mL of THF. Colorless oil. 78% yield (79.5 mg; **3g**/**4g** > 99/1).

^{1}H NMR ($CDCl_3$): δ 7.67-7.60 (m, 2H), 7.36-7.22 (m, 5H), 7.08 (d, $^{3}J_{HH}$ = 7.3 H, 1H), 6.90 (s, 1H), 2.26 (s, 3H), 1.15 (s, 6H), 1.12 (s, 6H), 0.94 (s, 9H), 0.62 (d, $^{2}J_{HH}$ = 12.4 Hz, 1H), 0.60 (s, 3H), 0.58 (d, $^{2}J_{HH}$ = 12.4 Hz, 1H), 0.25 (s, 9H). ^{13}C{^{1}H} NMR ($CDCl_3$): δ 150.7, 142.9, 141.6, 141.0, 138.1, 134.5, 134.2, 134.0, 130.0, 128.6, 127.9, 127.7, 82.9, 38.2, 32.3, 25.1, 24.9, 20.7, 1.1, −0.9. HRMS (EI) calcd for $C_{30}H_{47}BO_2Si_2$ (M^+) 506.3202, found 506.3202.

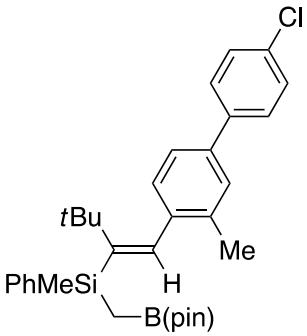

Compound 3h. The reaction was conducted in 2.5 mL of THF. Colorless oil. 28% yield (30.9 mg; **3h**/**4h** = 93/7).

^{1}H NMR ($CDCl_3$): δ 7.68-7.62 (m, 2H), 7.52 (d, $^{3}J_{HH}$ = 8.3 Hz, 2H), 7.38 (d, $^{3}J_{HH}$ = 8.3 Hz, 2H), 7.36-7.28 (m, 5H), 7.16 (d, $^{3}J_{HH}$ = 7.8 Hz, 1H), 6.93 (s, 1H), 2.32 (s, 3H), 1.15 (s, 6H), 1.13 (s, 6H), 0.96 (s, 9H), 0.63 (s, 3H), 0.65-0.57 (m, 2H). ^{13}C{^{1}H} NMR ($CDCl_3$): δ 151.5, 141.8, 140.94, 140.90, 139.7, 138.0, 135.5, 134.2, 133.2, 129.2, 128.9, 128.7, 128.3, 128.0, 127.7, 123.6, 83.0, 38.3, 32.3, 25.1, 24.9, 20.8, 1.1. HRMS (FAB)

calcd for $C_{33}H_{42}BClO_2Si$ (M^+) 544.2730, found 544.2729.

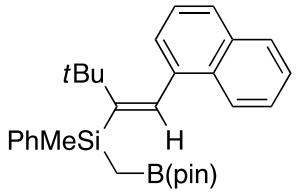

Compound 3i. The reaction was conducted in 2.5 mL of THF. Pale yellow viscous oil. 75% yield (70.7 mg; **3i**/**4i** > 99/1).

^{1}H NMR ($CDCl_3$): δ 8.02-7.96 (m, 1H), 7.85-7.79 (m, 1H), 7.76-7.69 (m, 3H), 7.51-7.45 (m, 2H), 7.43-7.33 (m, 4H), 7.30-7.24 (m, 2H), 1.18 (s, 6H), 1.16 (s, 6H), 0.90 (s, 9H), 0.68 (s, 5H). ^{13}C{^{1}H} NMR ($CDCl_3$): δ 153.1, 140.9, 140.5, 140.2, 134.3, 133.5, 131.4, 128.7, 128.3, 127.8, 126.7, 126.5, 125.8, 125.7, 125.4, 125.1, 83.0, 38.5, 32.4, 25.1, 25.0, 1.2. HRMS (EI) calcd for $C_{30}H_{39}BO_2Si$ (M^+) 470.2807, found 470.2798.

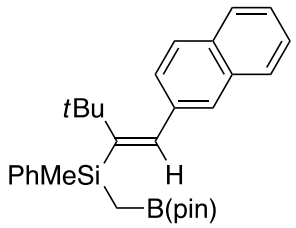

Compound 3j. Pale yellow oil. 79% yield (75.0 mg; **3j**/**4j** = 86/14).

^{1}H NMR ($CDCl_3$): δ 7.84-7.73 (m, 3H), 7.70-7.64 (m, 2H), 7.59 (s, 1H), 7.49-7.41 (m, 2H), 7.38-7.28 (m, 4H), 7.22 (s, 1H), 1.19 (s, 6H), 1.18 (s, 6H), 0.96 (s, 9H), 0.65 (d, $^2J_{HH}$ = 12.8 Hz, 1H), 0.63-0.56 (m, 4H). ^{13}C{^{1}H} NMR ($CDCl_3$): δ 151.9, 141.9, 140.9, 140.5, 134.3, 133.3, 133.2, 131.9, 128.7, 127.82, 127.75, 127.22, 127.17, 126.3, 126.1, 125.5, 83.0, 38.2, 32.9, 25.2, 25.0, 1.2. HRMS (EI) calcd for $C_{30}H_{39}BO_2Si$ (M^+) 470.2807, found 470.2810.

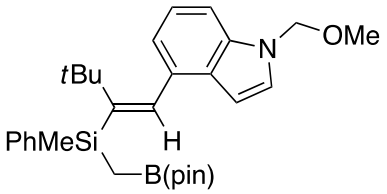

Compound 3k. The reaction was conducted in 2.5 mL of THF. Pale yellow viscous oil. 55% yield (59.8 mg; **3k**/**4k** > 99/1).

^{1}H NMR ($CDCl_3$): δ 7.73-7.68 (m, 2H), 7.39-7.30 (m, 4H), 7.20 (s, 1H), 7.19-7.13 (m, 2H), 6.93 (d, $^{3}J_{HH}$ = 6.9 Hz, 1H), 6.50 (d, $^{3}J_{HH}$ = 3.2 Hz, 1H), 5.45 (s, 2H), 3.24 (s, 3H), 1.18 (s, 6H), 1.16 (s, 6H), 0.93 (s, 9H), 0.65 (s, 2H), 0.64 (s, 3H). ^{13}C{^{1}H} NMR ($CDCl_3$): δ 152.1, 141.1, 140.1, 136.1, 135.9, 134.2, 128.6, 127.70, 127.68, 127.6, 121.9, 119.8, 107.9, 102.7, 82.9, 77.6, 56.0, 38.3, 32.5, 25.1, 25.0, 1.2. HRMS (EI) calcd for $C_{30}H_{42}BNO_3Si$ (M^+) 503.3022, found 503.3026.

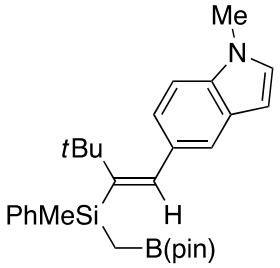

Compound 3l. Yellow viscous oil. 50% yield (47.8 mg; **3l**/**4l** = 97/3).

^{1}H NMR ($CDCl_3$): δ 7.70-7.63 (m, 2H), 7.40-7.30 (m, 4H), 7.28-7.21 (m, 2H), 7.05-7.00 (m, 2H), 6.43 (d, $^{3}J_{HH}$ = 3.2 Hz, 1H), 3.78 (s, 3H), 1.19 (s, 6H), 1.17 (s, 6H), 0.96 (s, 9H), 0.64 (d, $^{2}J_{HH}$ = 12.8 Hz, 1H), 0.592 (s, 3H), 0.586 (d, $^{2}J_{HH}$ = 12.4 Hz, 1H). ^{13}C{^{1}H} NMR ($CDCl_3$): δ 150.3, 143.5, 141.3, 135.4, 134.3, 133.7, 129.0, 128.5, 128.1, 127.7, 122.5, 120.0, 108.4, 100.9, 82.9, 38.1, 33.0, 32.9, 25.2, 25.0, 1.3. HRMS (EI) calcd for $C_{29}H_{40}BNO_2Si$ (M^+) 473.2916, found 473.2923.

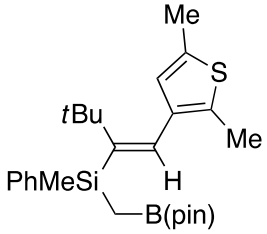

Compound 3m. The reaction was conducted using 5.0 mL of THF. Colorless oil. 54% yield (49.4 mg; **3m**/**4m** = 97/3).

^{1}H NMR ($CDCl_3$): δ 7.64-7.57 (m, 2H), 7.36-7.28 (m, 3H), 6.64 (s, 1H), 6.40 (s, 1H), 2.39 (s, 3H), 2.24 (s, 3H), 1.15 (s, 6H), 1.13 (s, 6H), 0.97 (s, 9H), 0.57 (s, 2H), 0.56 (s, 3H). ^{13}C{^{1}H} NMR ($CDCl_3$): δ 154.0, 140.9, 138.3, 136.8, 134.8, 134.2, 130.0, 128.6, 127.7, 127.4, 82.9, 37.8, 32.0, 25.1, 24.9, 15.3, 14.2, 1.1. HRMS (FAB) calcd for $C_{26}H_{39}BO_2SSi$ (M^+) 454.2528, found 454.2526.

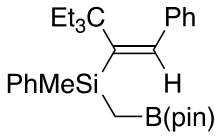

Compound 3n. The reaction was conducted in 2.5 mL of THF. Colorless oil. 71% yield (64.6 mg; **3n**/**4n** = 97/3).

^{1}H NMR ($CDCl_3$): δ 7.65-7.60 (m, 2H), 7.33-7.26 (m, 3H), 7.24-7.19 (m, 3H), 7.14 (t, $^{3}J_{HH}$ = 7.3 Hz, 1H), 7.07 (d, $^{3}J_{HH}$ = 7.0 Hz, 2H), 1.33-1.22 (m, 6H), 1.08 (s, 6H), 1.06 (s, 6H), 0.67-0.57 (m, 13H), 0.57 (d, $^{2}J_{HH}$ = 13.1 Hz, 1H). ^{13}C{^{1}H} NMR ($CDCl_3$): δ 149.4, 143.6, 143.3, 140.9, 134.5, 128.5, 127.49, 127.47, 127.1, 125.7, 82.8, 49.1, 28.5, 24.93, 24.90, 8.7, 1.4. HRMS (EI) calcd for $C_{29}H_{43}BO_2Si$ (M^+) 462.3120, found 462.3129.

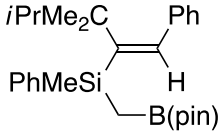

Compound 3o. The reaction was conducted in 5.0 mL of THF. Colorless oil. 66% yield

(59.1 mg; **3o**/**4o** = 95/5).

^{1}H NMR ($CDCl_3$): δ 7.66-7.61 (m, 2H), 7.36-7.29 (m, 3H), 7.27-7.21 (m, 2H), 7.19-7.08 (m, 4H), 1.82 (sept, $^{3}J_{HH}$ = 6.9 Hz, 1H), 1.13 (s, 6H), 1.11 (s, 6H), 0.86 (s, 3H), 0.85 (s, 3H), 0.69 (d, $^{3}J_{HH}$ = 6.8 Hz, 3H), 0.68 (d, $^{3}J_{HH}$ = 6.9 Hz, 3H), 0.62 (s, 3H), 0.58 (s, 2H). ^{13}C{^{1}H} NMR ($CDCl_3$): δ 151.8, 143.2, 141.5, 141.1, 134.3, 128.6, 127.7, 127.62, 127.58, 125.8, 82.9, 44.7, 34.9, 26.7, 26.3, 25.0, 24.9, 18.13, 18.07, 1.3. HRMS (EI) calcd for $C_{28}H_{41}BO_2Si$ (M^+) 448.2963, found 448.2975.

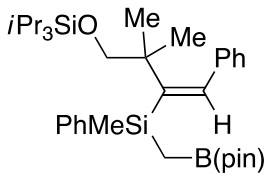

Compound 3p. The reaction was conducted using 2.5 mL of THF. Colorless oil. 65% yield (77.0 mg; **3p**/**4p** = 90/10).

^{1}H NMR ($CDCl_3$): δ 7.65-7.59 (m, 2H), 7.36-7.30 (m, 3H), 7.28-7.22 (m, 2H), 7.21-7.15 (m, 2H), 7.15-7.10 (m, 2H), 3.38 (d, $^{2}J_{HH}$ = 13.3 Hz, 1H), 3.36 (d, $^{2}J_{HH}$ = 13.8 Hz, 1H), 1.17 (s, 6H), 1.15 (s, 6H), 0.962 (s, 3H), 0.957 (s, 3H), 0.93-0.85 (m, 21H), 0.61 (d, $^{2}J_{HH}$ = 12.8 Hz, 1H), 0.58 (s, 3H), 0.55 (d, $^{2}J_{HH}$ = 12.8 Hz, 1H). ^{13}C{^{1}H} NMR ($CDCl_3$): δ 148.9, 143.3, 142.9, 140.7, 134.2, 128.7, 128.0, 127.80, 127.76, 126.1, 82.9, 71.4, 44.2, 26.63, 26.59, 25.1, 25.0, 18.1, 12.0, 1.2. HRMS (EI) calcd for $C_{35}H_{57}BO_3Si_2$ (M^+) 592.3934, found 592.3934.

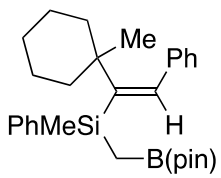

Compound 3q. Pale yellow oil. 65% yield (59.8 mg; **3q**/**4q** = 96/4).

^{1}H NMR ($CDCl_3$): δ 7.67-7.61 (m, 2H), 7.36-7.28 (m, 3H), 7.28-7.22 (m, 2H), 7.19-7.11 (m, 3H), 7.08 (s, 1H), 1.55-1.47 (m, 2H), 1.36-1.09 (m, 7H), 1.16 (s, 6H), 1.14 (s, 6H), 1.03-0.94 (m, 1H), 0.97 (s, 3H), 0.63 (d, $^2J_{HH}$ = 12.4 Hz, 1H), 0.62 (s, 3H), 0.58 (d, $^2J_{HH}$ = 12.8 Hz, 1H). ^{13}C{^{1}H} NMR ($CDCl_3$): δ 152.5, 143.3, 142.0, 141.2, 134.3, 128.6, 128.0, 127.7, 127.6, 125.8, 82.9, 41.8, 38.91, 38.87, 26.1, 25.1, 25.0, 22.7, 1.7. HRMS (EI) calcd for $C_{29}H_{41}BO_2Si$ (M^+) 460.2963, found 460.2973.

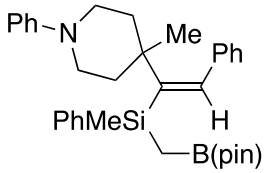

Compound 3r. Colorless oil. 53% yield (57.4 mg; **3r**/**4r** = 91/9).

^{1}H NMR ($CDCl_3$): δ 7.67-7.61 (m, 2H), 7.38-7.31 (m, 3H), 7.31-7.26 (m, 2H), 7.24-7.12 (m, 6H), 6.77-6.71 (m, 3H), 3.08-2.97 (m, 2H), 2.78-2.66 (m, 2H), 1.90-1.78 (m, 2H), 1.51-1.39 (m, 2H), 1.14 (s, 6H), 1.13 (s, 6H), 1.11 (s, 3H), 0.64 (s, 3H), 0.61 (s, 2H). ^{13}C{^{1}H} NMR ($CDCl_3$): δ 151.7, 150.8, 142.8, 142.6, 140.6, 134.3, 129.0, 128.8, 127.92, 127.89, 127.8, 126.2, 118.8, 115.8, 83.0, 46.0, 45.8, 39.7, 37.9, 26.0, 25.1, 24.9, 1.4. HRMS (EI) calcd for $C_{34}H_{44}BNO_2Si$ (M^+) 537.3229, found 537.3235.

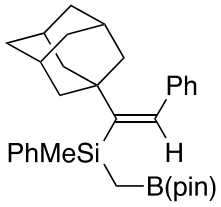

Compound 3s. White solid. 79% yield (79.6 mg; **3s**/**4s** = 91/9)

^{1}H NMR ($CDCl_3$): δ 7.67-7.61 (m, 2H), 7.37-7.29 (m, 3H), 7.28-7.22 (m, 2H), 7.20-7.11 (m, 3H), 7.05 (s, 1H), 1.75-1.64 (m, 9H), 1.51-1.36 (m, 6H) 1.17 (s, 6H), 1.16 (s, 6H), 0.66-060 (m, 4H), 0.57 (d, $^2J_{HH}$ = 12.8 Hz, 1H). ^{13}C{^{1}H} NMR ($CDCl_3$): δ 151.6,

143.3, 141.7, 141.2, 134.3, 128.6, 128.0, 127.6, 127.3, 125.8, 82.9, 43.4, 41.2, 36.7, 29.0, 25.1, 25.0, 1.7. HRMS (EI) calcd for $C_{32}H_{43}BO_2Si$ (M^+) 498.3120, found 498.3125.

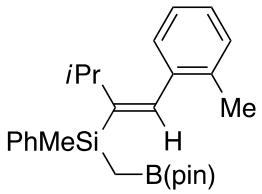

Compound 3t. The selectivity of **3t**/**4t** was 46/54. Compound **3t** was separated from compound **4t** by GPC with $CHCl_3$. Colorless oil. 23% yield (19.4 mg).

^{1}H NMR ($CDCl_3$): δ 7.68-7.61 (m, 2H), 7.36-7.30 (m, 3H), 7.18-7.10 (m, 3H), 7.10-7.04 (m, 1H), 6.79 (s, 1H), 2.83 (sept, $^3J_{HH}$ = 7.1 Hz, 1H), 2.21 (s, 1H), 1.13 (s, 6H), 1.11 (s, 6H), 0.92 (d, $^3J_{HH}$ = 6.9 Hz, 3H), 0.88 (d, $^3J_{HH}$ = 6.9 Hz, 3H), 0.618 (s, 3H), 0.617 (d, $^2J_{HH}$ = 12.8 Hz, 1H), 0.57 (d, $^2J_{HH}$ = 12.8 Hz, 1H). ^{13}C{^{1}H} NMR ($CDCl_3$): δ 149.0, 139.94, 139.87, 139.1, 135.9, 134.5, 129.7, 128.8, 128.6, 127.6, 126.7, 125.3, 82.9, 31.5, 25.0, 24.9, 23.4, 23.2, 20.2, −0.2. HRMS (EI) calcd for $C_{26}H_{37}BO_2Si$ (M^+) 420.2650, found 420.2653.

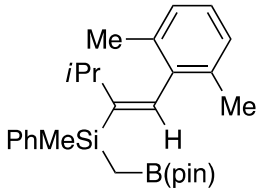

Compound 3u. The selectivity of **3u**/**4u** was 65/35. Compound **3u** was separated from compound **4u** by GPC with $CHCl_3$. Colorless oil. 32% yield (27.4 mg).

^{1}H NMR ($CDCl_3$): δ. 7.70-7.62 (m, 2H), 7.37-7.29 (m, 3H), 7.07-6.95 (m, 3H), 6.61 (s, 1H), 2.47 (sept, $^3J_{HH}$ = 7.2 Hz, 1H), 2.18 (s, 3H), 2.16 (s, 3H), 1.12 (s, 6H), 1.10 (s, 6H), 0.86 (d, $^3J_{HH}$ = 6.9 Hz, 3H), 0.84 (d, $^3J_{HH}$ = 7.3 Hz, 3H), 0.68 (d, $^2J_{HH}$ = 12.8 Hz,

1H), 0.63 (s, 3H), 0.59 (d, $^2J_{HH}$ = 12.8 Hz, 1H). $^{13}C\{^1H\}$ NMR ($CDCl_3$): δ 149.4, 139.9, 139.3, 139.0, 135.4, 135.3, 134.5, 128.8, 127.6, 127.1, 126.3, 83.0, 32.3, 25.0, 24.9, 22.72, 22.69, 20.6, −0.2. HRMS (EI) calcd for $C_{27}H_{39}BO_2Si$ (M^+) 434.2807, found 434.2803.

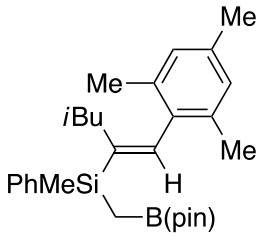

Compound 3v. The selectivity of **3v**/**4v** was 71/29. Compound **3v** was separated from compound **4v** by GPC with $CHCl_3$. Colorless oil. 23% yield (21.5 mg).

^1H NMR ($CDCl_3$): δ. 7.66-7.59 (m, 2H), 7.36-7.30 (m, 3H), 6.81 (s, 2H), 6.76 (s, 1H), 2.26 (s, 3H), 2.14 (s, 3H), 2.12 (s, 3H), 1.90-1.83 (m, 2H), 1.32-1.23 (m, 1H), 1.14 (s, 6H), 1.11 (s, 6H), 0.61 (d, $^2J_{HH}$ = 12.8 Hz, 1H), 0.57-0.49 (m, 10H). $^{13}C\{^1H\}$ NMR ($CDCl_3$): δ 143.1, 140.6, 139.0, 135.7, 135.5, 135.4, 134.3, 128.8, 127.9, 127.6, 83.0, 41.1, 27.5, 25.1, 24.9, 22.78, 22.75, 21.1, 20.4, −1.8. HRMS (FAB) calcd for $C_{29}H_{43}BO_2Si$ (M^+) 462.3120, found 462.3121.

Procedure for equation 2.

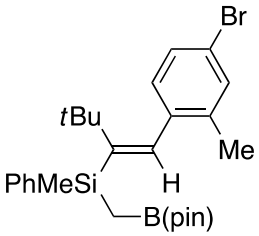

N-Bromosuccinimide (21.0 mg, 0.118 mmol) was added to a solution of compound **3g** (54.5 mg, 0.108 mmol) in MeCN (1.1 mL) at 0 °C, and the mixture was stirred for 10 min at 0 °C and for 49 h at 20 °C. The reaction was quenched with saturated $NaHCO_3$aq and this was extracted with Et_2O. The organic layer was washed with saturated NaClaq

and concentrated under vacuum. The residue was chromatographed on silica gel with hexane → EtOAc/hexane = 1/30 and further purified by GPC with $CHCl_3$ to afford compound **3w** as a colorless viscous oil (43.3 mg, 84.3 μmol; 78% yield).

^{1}H NMR ($CDCl_3$): δ 7.64-7.58 (m, 2H), 7.37-7.30 (m, 3H), 7.28 (d, $^4J_{HH}$ = 1.8 Hz, 1H), 7.23 (dd $^3J_{HH}$ = 8.2 Hz and $^4J_{HH}$ = 1.8 Hz, 1H), 6.96 (d, $^3J_{HH}$ = 8.2 Hz, 1H), 6.80 (s, 1H), 2.23 (s, 3H), 1.14 (s, 6H), 1.12 (s, 6H), 0.92 (s, 9H), 0.61 (s, 3H), 0.58 (s, 2H). ^{13}C{^{1}H} NMR ($CDCl_3$): δ 152.1, 141.2, 140.7, 140.0, 137.3, 134.2, 132.3, 130.1, 128.7, 128.0, 127.7, 120.0, 82.9, 38.3, 32.3, 25.1, 24.9, 20.5, 1.0. HRMS (EI) calcd for $C_{27}H_{38}BBrO_2Si$ (M^+) 512.1912, found 512.1917.

Procedure for equation 3.

Compound **1e** (517 mg, 3.00 mmol) and (dimethylphenylsilyl)boronic acid pinacol ester (**2**) (981 μL, 3.60 mmol) were added with the aid of THF (5.0 mL) to a mixture of CuI (57.2 mg, 0.300 mmol), JohnPhos (179 mg, 0.600 mmol), and Li*O*t*Bu (192 mg, 2.40 mmol) in THF (32.5 mL), and this was stirred for 20 h at 70 °C. The reaction mixture was directly passed through a pad of silica gel with EtOAc and the solvent was removed under vacuum. The residue was chromatographed on silica gel with EtOAc/hexane = 1/40 and further purified by GPC with $CHCl_3$ to afford compound **3e** as a white solid (1.08 g, 2.48 mmol; 83% yield).

Procedure for Scheme 3.

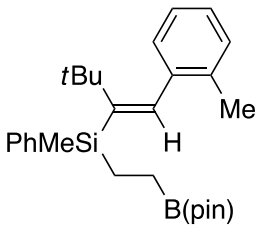

*n*BuLi (380 μL, 0.597 mmol; 1.57 M solution in hexane) was added slowly over 10 min to a solution of compound **3e** (132 mg, 0.304 mmol) and bromochloromethane (40.2 μL, 0.597 mmol) in Et_2O (0.75 mL) at −78 °C, and the mixture was stirred for 1 h at −78 °C and for 21 h at room temperature. The reaction was quenched with saturated NH_4Claq and this was extracted with Et_2O. The organic layer was washed with saturated NaClaq, dried over $MgSO_4$, filtered, and concentrated under vacuum. The residue was chromatographed on silica gel with EtOAc/hexane = 1/40 and further purified by GPC with $CHCl_3$ to afford compound **5** as a colorless oil (81.8 mg, 0.182 mmol; 60% yield).

^{1}H NMR ($CDCl_3$): δ 7.63-7.57 (m, 2H), 7.37-7.29 (m, 3H), 7.16-7.08 (m, 4H), 6.87 (s, 1H), 2.26 (s, 3H), 1.23 (s, 12H), 1.12-0.97 (m, 2H), 0.92 (s, 9H), 0.89-0.69 (m, 2H), 0.51 (s, 3H). ^{13}C{^{1}H} NMR ($CDCl_3$): δ 149.9, 142.2, 141.4, 140.1, 134.8, 134.3, 129.5, 128.6, 127.8, 126.5, 125.1, 83.1, 38.1, 32.2, 24.9, 20.7, 9.3, −1.5. HRMS (FD) calcd for $C_{28}H_{41}BO_2Si$ (M^+) 448.2963, found 448.2978.

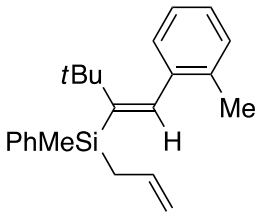

Vinylmagnesium bromide (1.20 mL, 1.20 mmol; 1.0 M solution in THF) was added slowly over 10 min to a solution of compound **3e** (134 mg, 0.309 mmol) in THF (2.4 mL) at 0 °C, and the mixture was stirred for 4 h at 0 °C. A solution of iodine (307 mg, 1.21 mmol) in MeOH (2.4 mL) was added to it and the resulting mixture was stirred for 2 h 30 min at 0 °C. The reaction was quenched with 5 wt% Na_2SO_3aq and the volatiles were removed under vacuum. This was extracted with Et_2O and the organic layer was washed with saturated NaClaq, dried over $MgSO_4$, filtered, and concentrated under vacuum. The

residue was purified by silica gel preparative TLC with hexane and further purified by GPC with $CHCl_3$ to afford compound **6** as a colorless oil (49.4 mg, 0.148 mmol; 49% yield).

^{1}H NMR ($CDCl_3$): δ 7.65-7.57 (m, 2H), 7.41-7.32 (m, 3H), 7.18-7.08 (m, 4H), 6.88 (s, 1H), 5.87-5.73 (m, 1H), 4.96-4.86 (m, 2H), 2.26 (s, 3H), 2.10-1.95 (m, 2H) 0.94 (s, 9H), 0.54 (s, 3H). ^{13}C{^{1}H} NMR ($CDCl_3$): δ 149.5, 142.0, 141.9, 139.6, 135.0, 134.8, 134.3, 129.6, 128.9, 128.6, 127.9, 126.6, 125.1, 114.3, 38.1, 32.2, 24.7, 20.7, −1.2. HRMS (FD) calcd for $C_{23}H_{30}Si$ (M^+) 334.2111, found 334.2109.

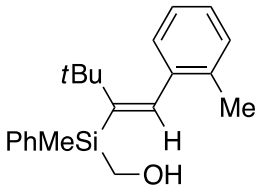

3.0 M NaOHaq (0.40 mL, 12 mmol) and H_2O_2 (0.40 mL, 4.0 mmol; 35 wt% in H_2O) were added to a solution of compound **3e** (87.0 mg, 0.200 mmol) in THF (1.0 mL) and the mixture was stirred for 4 h at room temperature. The reaction was quenched with H_2O and this was extracted with Et_2O. The organic layer was washed with saturated NaClaq, dried over $MgSO_4$, filtered, and concentrated under vacuum. The residue was chromatographed on silica gel with EtOAc/hexane = 1/20 → 1/10 to afford compound **7** as a colorless oil (62.4 mg, 0.184 mmol; 92% yield).

^{1}H NMR ($CDCl_3$): δ 7.70-7.64 (m, 2H), 7.43-7.36 (m, 3H), 7.16-7.09 (m, 4H), 6.91 (s, 1H), 3.80 (dd, $^2J_{HH}$ = 14.2 Hz and $^3J_{HH}$ = 5.0 Hz, 1H), 3.75 (dd, $^2J_{HH}$ = 14.2 Hz and $^3J_{HH}$ = 5.5 Hz, 1H), 2.25 (s, 3H), 0.96 (s, 9H), 0.89 (dd, $^3J_{HH}$ = 5.5 and 5.0 Hz, 1H), 0.64 (s, 3H). ^{13}C{^{1}H} NMR ($CDCl_3$): δ 149.0, 142.3, 141.5, 137.6, 134.7, 134.5, 129.6, 129.4, 128.5, 128.2, 126.7, 125.1, 56.1, 38.1, 32.1, 20.6, −2.7. HRMS (FAB, matrix NPOE) calcd for $C_{21}H_{27}OSi$ ([M–H]$^-$) 323.1837, found 323.1830.

Procedure for equation 4 (R = *i*Pr).

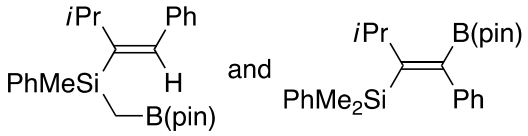

Compound **1x** (28.8 mg, 0.200 mmol) and (dimethylphenylsilyl)boronic acid pinacol ester (**2**) (65.4 μL, 0.240 mmol) were added with the aid of THF (1.0 mL) to a mixture of CuI (3.8 mg, 20 μmol), JohnPhos (11.9 mg, 39.9 μmol), and Li*O*t*Bu (12.8 mg, 0.160 mmol) in THF (9.0 mL), and this was stirred for 20 h at 70 °C. The reaction mixture was directly passed through a pad of silica gel with EtOAc and the solvent was removed under vacuum. The residue was purified by GPC with $CHCl_3$ to afford a mixture of compounds **3x** and **4x** as a colorless oil (67.6 mg, 0.166 mmol; 83% yield, **3x**/**4x** = 13/87).

3x: ^{1}H NMR ($CDCl_3$): δ 7.64-7.60 (m, 2H), 7.38-7.00 (m, 8H), 6.87 (s, 1H), 3.19-3.07 (m, 1H), 1.13 (s, 6H), 1.12 (s, 6H), 0.98 (d, $^3J_{HH}$ = 6.8 Hz, 3H), 0.95 (d, $^3J_{HH}$ = 6.9 Hz, 3H), 0.62 (s, 3H), 0.58 (s, 2H). **4x**: ^{1}H NMR ($CDCl_3$): δ 7.42-7.35 (m, 2H), 7.27-7.18 (m, 3H), 7.14-7.06 (m, 3H), 7.05-6.98 (m, 2H), 2.71 (sept, $^3J_{HH}$ = 7.0 Hz, 1H), 1.19 (s, 12H), 1.16 (d, $^3J_{HH}$ = 6.9 Hz, 6H), 0.00 (s, 6H). ^{13}C{^{1}H} NMR ($CDCl_3$): δ 156.9, 143.2, 141.1, 134.0, 128.7, 128.3, 127.7, 127.5, 126.2, 83.7, 37.3, 24.7, 23.4, 0.6. HRMS (EI) calcd for $C_{25}H_{35}BO_2Si$ (M^+) 406.2494, found 406.2503.

(*E*)-(2-*tert*-Butyl-1-phenylvinyl)dimethyl(phenyl)silane (8)

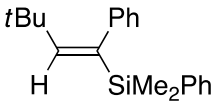

^{1}H NMR ($CDCl_3$): δ 7.48-7.44 (m, 2H), 7.37-7.28 (m, 3H), 7.18-7.07 (m, 3H), 6.85-6.78 (m, 2H), 5.91 (s, 1H), 0.87 (s, 9H), 0.26 (s, 6H). ^{13}C{^{1}H} NMR ($CDCl_3$): δ 151.3, 142.3, 140.0, 138.4, 134.3, 128.9, 128.6, 127.7, 127.3, 125.1, 36.2, 31.2, −3.0. HRMS (EI) calcd for $C_{20}H_{26}Si$ (M^+) 294.1798, found 294.1801.

General procedure for Scheme 6.

Compound **1a** (0.200 mmol) and silylboronate **2**, **2-*d*$_6$**, or **2-*d*$_3$** (0.240 or 0.480 mmol) were added with the aid of THF (1.0 mL) to a mixture of CuI (3.8 mg, 20 μmol), JohnPhos (11.9 mg, 39.9 μmol), and Li*O*t*Bu (12.8 mg, 0.160 mmol) in THF (9.0 mL), and this was stirred for 20 h at 70 °C. The reaction mixture was directly passed through a pad of silica gel with EtOAc and the solvent was removed under vacuum. The yields and selectivity of the products were determined by ^{1}H NMR against an internal standard (dimethyl terephthalate).

X-ray crystal structure

Compound 3a

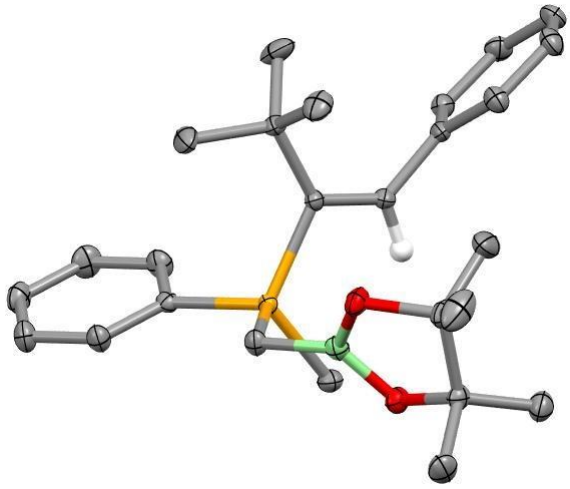

A colorless CH_2Cl_2 solution of compound **3a** was prepared. Crystals suitable for X-ray analysis were obtained by layering MeOH and slow diffusion of the solvents at room temperature. The crystal structure has been deposited at the Cambridge Crystallographic Data Centre (deposition number: CCDC 2268930). The data can be obtained free of charge via the Internet at www.ccdc.cam.ac.uk/conts/retrieving.html.

Crystal data and structure refinement.

Empirical Formula	$C_{26}H_{37}BO_2Si$	
Formula Weight	420.45	
Temperature	113 ± 2 K	
Wavelength	0.71075 Å	
Crystal System	Triclinic	
Space Group	$P\bar{1}$	
Unit Cell Dimensions	a = 7.4596 (6) Å	α = 71.606(6)°
	b = 11.7979 (8) Å	β = 80.803 (8)°
	c = 15.2801 (10) Å	γ = 78.356(7)°

Volume	1243.09(16) Å^3
Z Value	2
Calculated Density	1.123 g/cm^3
Absorption coefficient	0.113 mm^{-1}
F(000)	456
Crystal size	0.300 × 0.200 × 0.130 mm
Theta Range for Data Collection	3.006–27.514°
Index Ranges	$-9 \leq h \leq 9$, $-15 \leq k \leq 15$, $-19 \leq l \leq 18$
Reflections Collected	23449
Independent Reflections	5674 [R(int) = 0.0321]
Completeness to Theta = 25.242°	99.6%
Absorption Correction	Semi-empirical from equivalents
Max. and Min. Transmission	0.985 and 0.967
Refinement Method	Full-matrix least-squares on F^2
Data / Restraints / Parameters	5674 / 0 / 279
Goodness-of-Fit on F^2	1.181
Final R Indices [I>2sigma(I)]	R_1 = 0.0342, wR_2 = 0.1089
R Indices (All Data)	R_1 = 0.0429, wR_2 = 0.1245
Largest Diff. Peak and Hole	0.431 and −0.567 e$^-$/Å^3

Kinetic experiments

Data collection for Figure 1a.

Compound **1e** (34.5 mg, 0.200 mmol) and (dimethylphenylsilyl)boronic acid pinacol ester (**2**) (65.4 µL, 0.240 mmol) were added to a mixture of CuI (15–25 µmol), JohnPhos (30–50 µmol), LiO*t*Bu (0.160 mmol), and 1,3,5-trimethoxybenzene (8.4 mg, 50 µmol; internal standard) in THF (2.5 mL) at 70 °C. The resulting mixture was stirred at 70 °C and aliquots (ca. 0.2 mL each) were taken every 5 minutes. They were immediately quenched by H_2O and extracted with Et_2O, and the organic layer was concentrated under vacuum. The residues were analyzed by ^1H NMR to determine the reaction progress (production of **3e**). Each experiment was carried out twice.

15 µmol/30 µmol of CuI/JohnPhos: initial rate = 0.512 (mM/min)

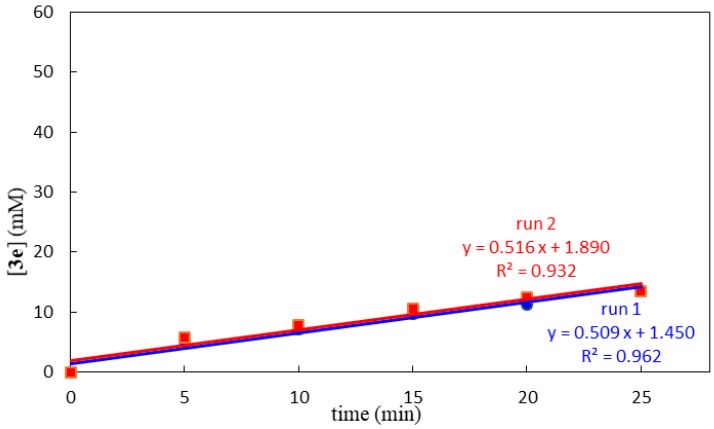

17.5 µmol/35 µmol of CuI/JohnPhos: initial rate = 0.650 (mM/min)

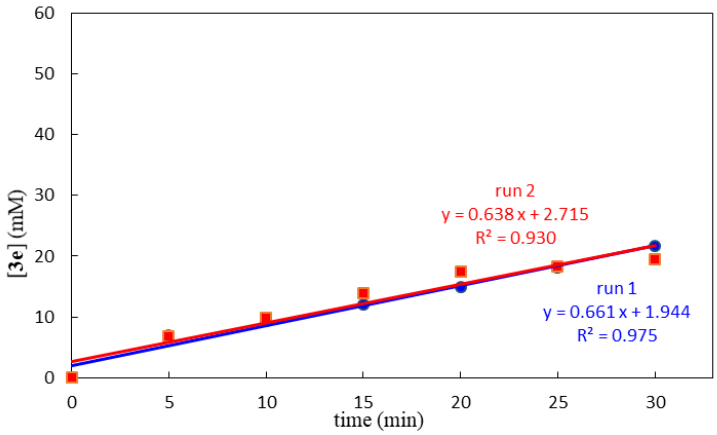

20 µmol/40 µmol of CuI/JohnPhos: initial rate = 0.692 (mM/min)

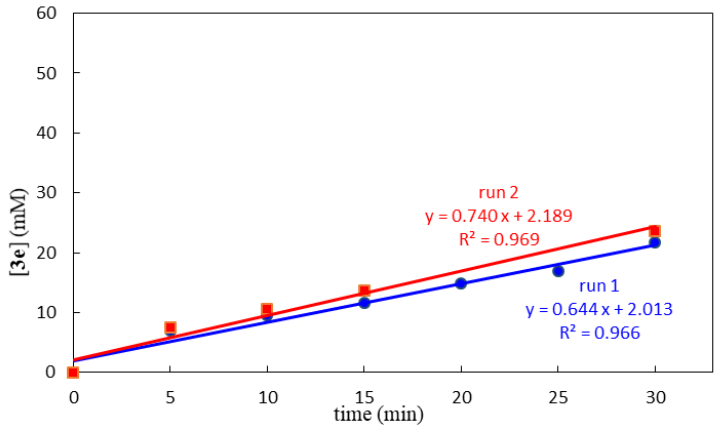

25 µmol/50 µmol of CuI/JohnPhos: initial rate = 0.883 (mM/min)

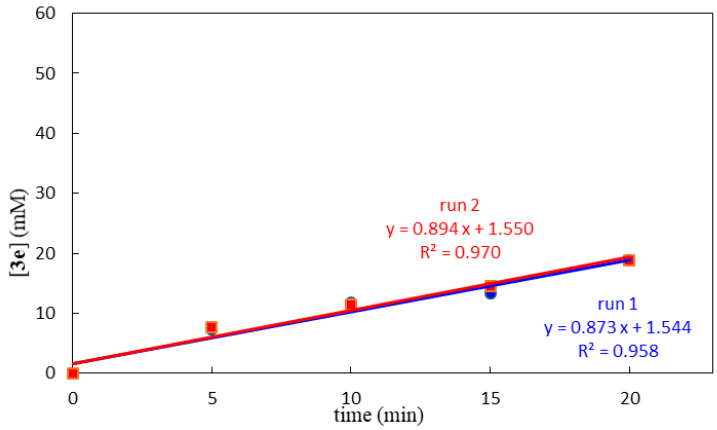

Data collection for Figure 1b.

Compound **1e** (0.150–0.250 mmol) and (dimethylphenylsilyl)boronic acid pinacol ester (**2**) (65.4 µL, 0.240 mmol) were added to a mixture of CuI (3.8 mg, 20 µmol), JohnPhos (11.9 mg, 39.9 µmol), LiO*t*Bu (12.8 mg, 0.160 mmol), and 1,3,5-trimethoxybenzene (8.4 mg, 50 µmol; internal standard) in THF (2.5 mL) at 70 °C. The resulting mixture was stirred at 70 °C and aliquots (ca. 0.2 mL each) were taken every 5 minutes. They were immediately quenched by H_2O and extracted with Et_2O, and the organic layer was concentrated under vacuum. The residues were analyzed by ^1H NMR to determine the reaction progress (production of **3e**). Each experiment was carried out twice.

0.150 mmol of **1e**: initial rate = 0.625 (mM/min)

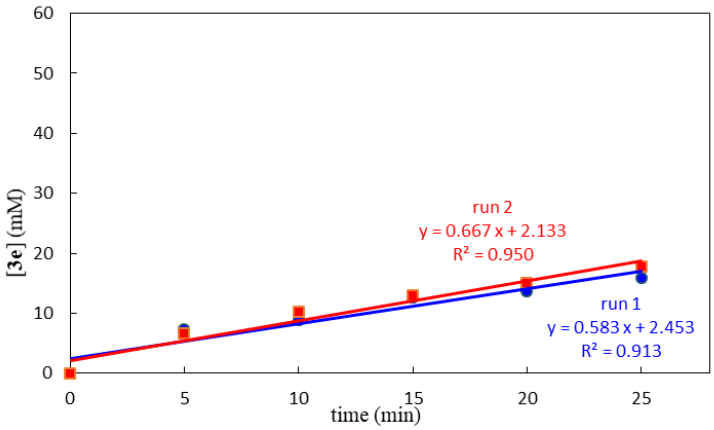

0.175 mmol of **1e**: initial rate = 0.677 (mM/min)

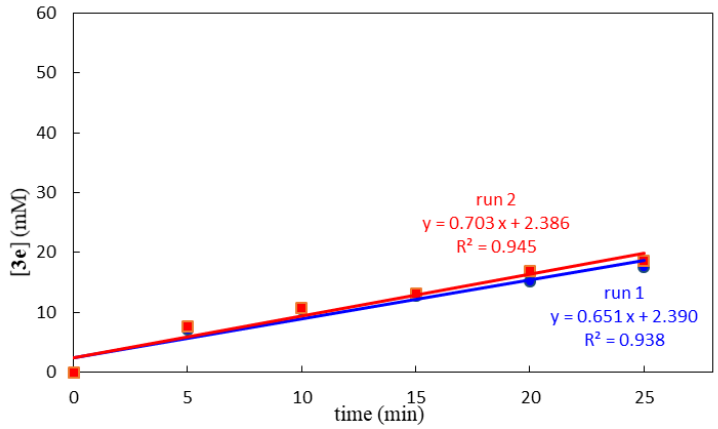

0.200 mmol of **1e**: initial rate = 0.692 (mM/min)

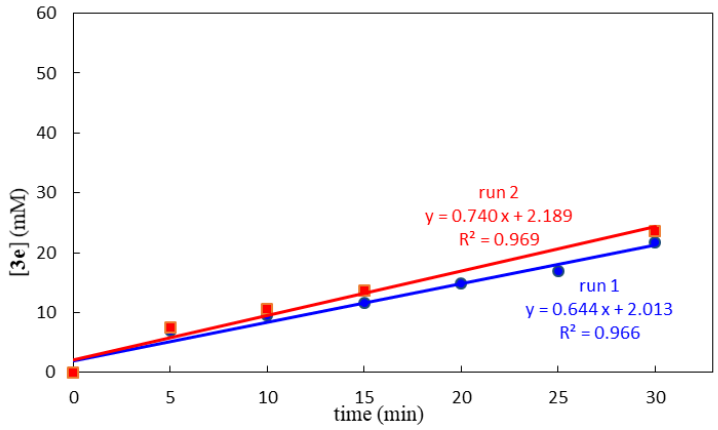

0.225 mmol of **1e**: initial rate = 0.775 (mM/min)

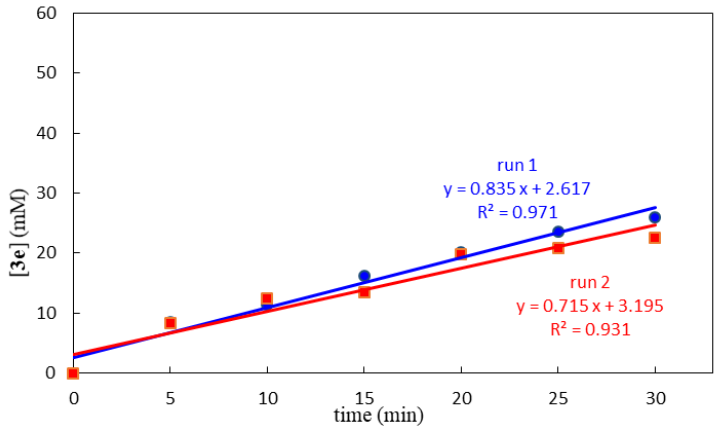

0.250 mmol of **1e**: initial rate = 0.815 (mM/min)

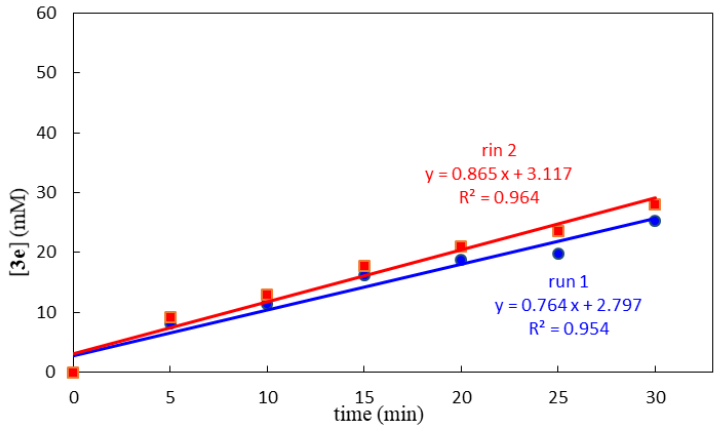

Data collection for Figure 1c.

Compound **1e** (34.5 mg, 0.200 mmol) and (dimethylphenylsilyl)boronic acid pinacol ester (**2**) (0.160–0.300 mmol) were added to a mixture of CuI (3.8 mg, 20 μmol), JohnPhos (11.9 mg, 39.9 μmol), LiO*t*Bu (12.8 mg, 0.160 mmol), and 1,3,5-trimethoxybenzene (8.4 mg, 50 μmol; internal standard) in THF (2.5 mL) at 70 °C. The resulting mixture was stirred at 70 °C and aliquots (ca. 0.2 mL each) were taken every 5 minutes. They were immediately quenched by H_2O and extracted with Et_2O, and the organic layer was concentrated under vacuum. The residues were analyzed by ^1H NMR to determine the reaction progress (production of **3e**). Each experiment was carried out twice.

0.160 mmol of **2**: initial rate = 0.709 (mM/min)

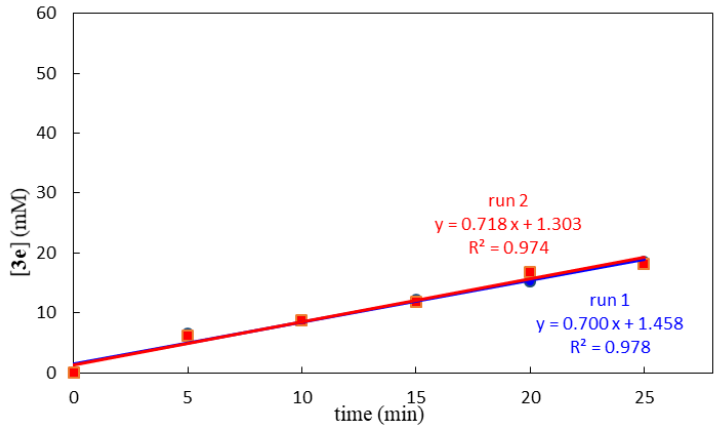

0.200 mmol of **2**: initial rate = 0.711 (mM/min)

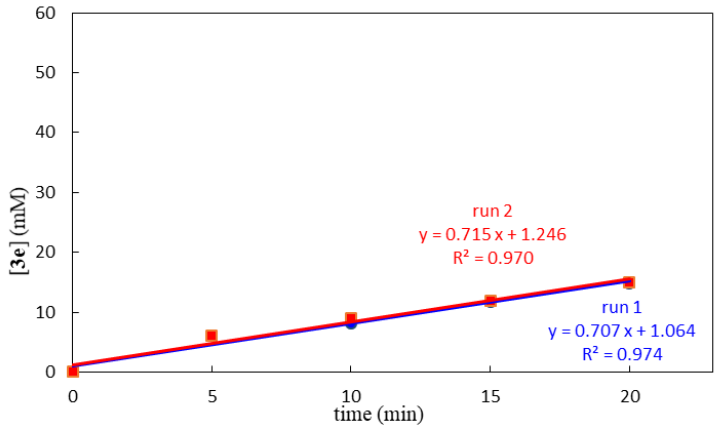

0.200 mmol of **2**: initial rate = 0.692 (mM/min)

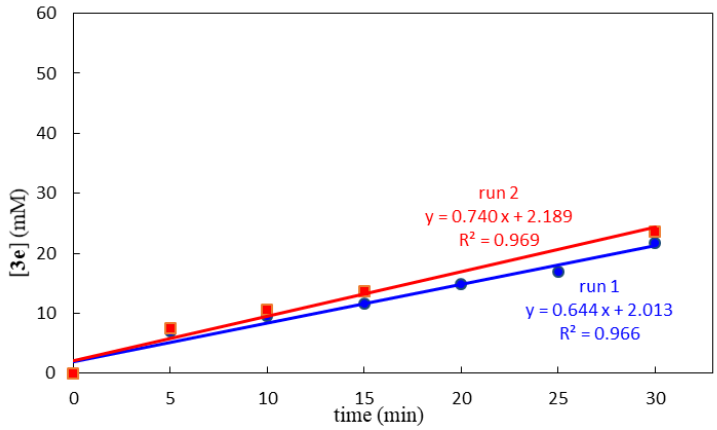

0.300 mmol of **2**: initial rate = 0.730 (mM/min)

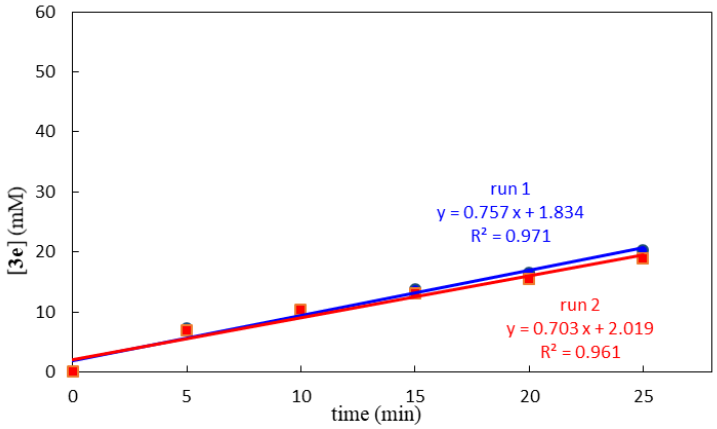

Data collection for Figure 1d.

Compound **1e** (34.5 mg, 0.200 mmol) and (dimethylphenylsilyl)boronic acid pinacol ester (**2**) (65.4 µL, 0.240 mmol) were added to a mixture of CuI (3.8 mg, 20 µmol), JohnPhos (11.9 mg, 39.9 µmol), Li*O*t*Bu (0.160–0.320 mmol), and 1,3,5-trimethoxybenzene (8.4 mg, 50 µmol; internal standard) in THF (2.5 mL) at 70 °C. The resulting mixture was stirred at 70 °C and aliquots (ca. 0.2 mL each) were taken every 5 minutes. They were immediately quenched by H_2O and extracted with Et_2O, and the organic layer was concentrated under vacuum. The residues were analyzed by ^1H NMR to determine the reaction progress (production of **3e**). Each experiment was carried out twice.

0.160 mmol of LiO*t*Bu: initial rate = 0.692 (mM/min)

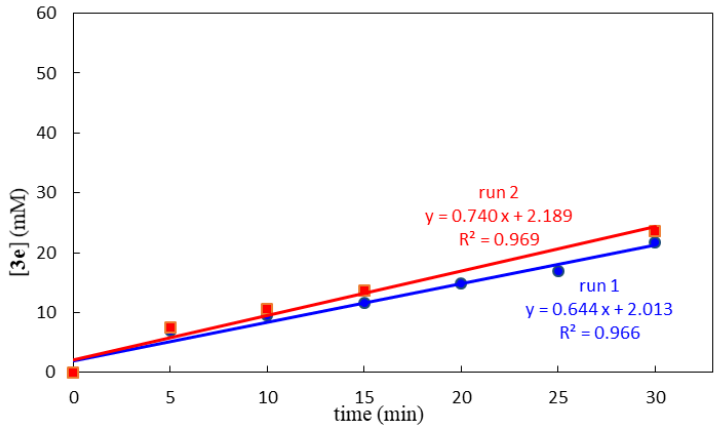

0.200 mmol of LiO*t*Bu: initial rate = 0.735 (mM/min)

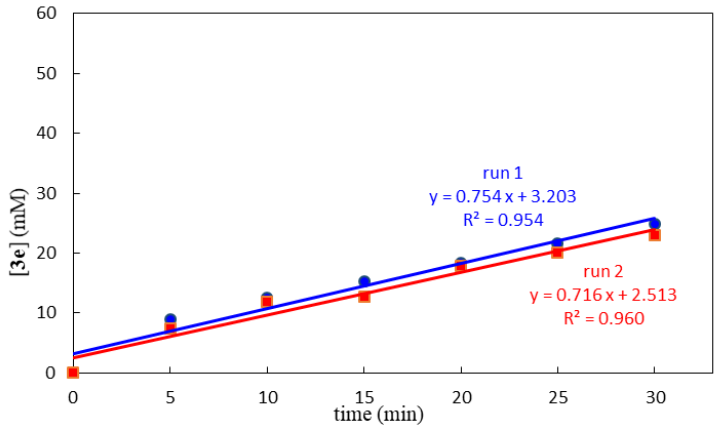

0.240 mmol of LiO*t*Bu: initial rate = 0.684 (mM/min)

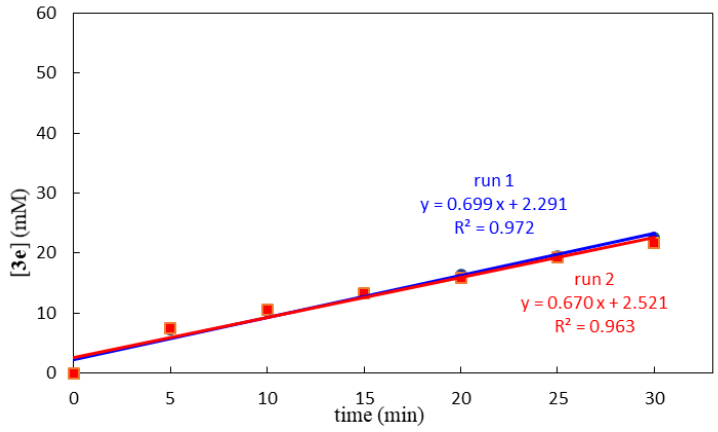

0.320 mmol of LiO*t*Bu: initial rate = 0.692 (mM/min)

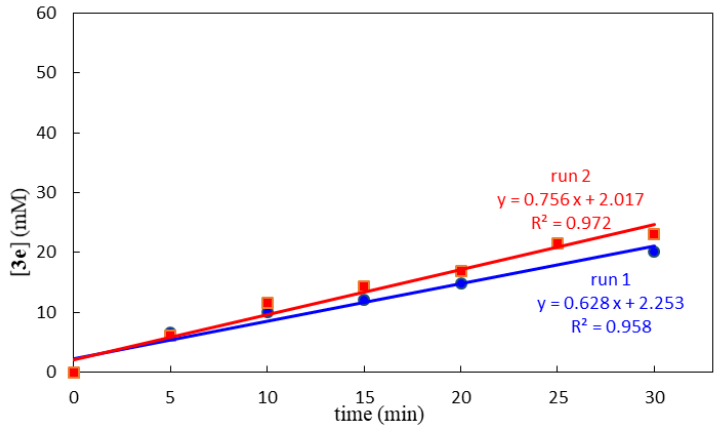

Additional kinetic experiments using alkyne 1a.

In addition to the kinetic experiments using alkyne **1e**, the rate dependency on alkyne **1a** was also investigated to examine the effect of alkyne substituents on the reaction profile. As a result, no significant difference was observed between **1e** and **1a** (Figure 1b vs. Figure 6).

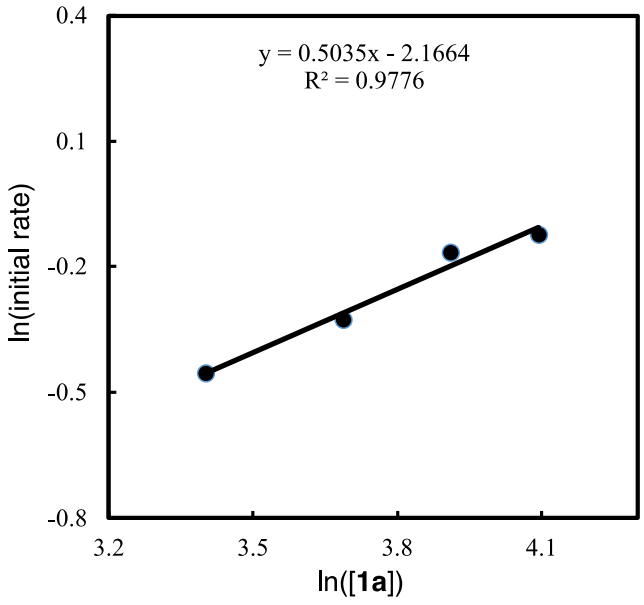

Figure 6. Ln plot of the initial rate (mM/min) vs. concentration of **1a** (mM) ([**Cu**]$_0$ = 4 mM, [LiO*t*Bu]$_0$ = 32 mM, [**1a**]$_0$ = 30–60 mM, [**2**]$_0$ = 48 mM).

Data collection for Figure 6.

Compound **1a** (0.150–0.300 mmol) and (dimethylphenylsilyl)boronic acid pinacol ester (**2**) (65.4 µL, 0.240 mmol) were added to a mixture of CuI (3.8 mg, 20 µmol), JohnPhos (11.9 mg, 39.9 µmol), Li*O*t*Bu (12.8 mg, 0.160 mmol), and 1,3,5-trimethoxybenzene (8.4 mg, 50 µmol; internal standard) in THF (5.0 mL) at 70 °C. The resulting mixture was stirred at 70 °C and aliquots (ca. 0.5 mL each) were taken every 2–3 minutes. They were immediately quenched by H_2O and extracted with Et_2O, and the organic layer was concentrated under vacuum. The residues were analyzed by ^1H NMR to determine the reaction progress (production of **3a**). Each experiment was carried out twice.

0.150 mmol of **1a**: initial rate = 0.636 (mM/min)

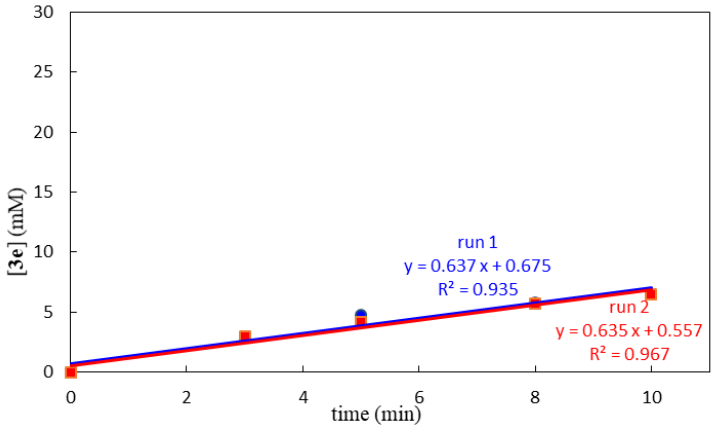

0.200 mmol of **1a**: initial rate = 0.723 (mM/min)

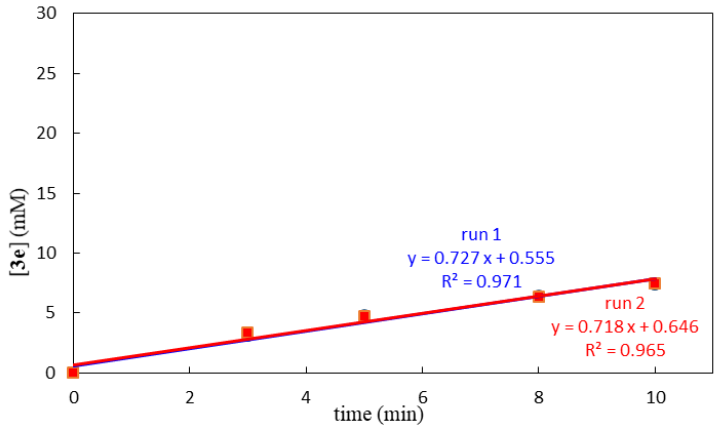

0.250 mmol of **1a**: initial rate = 0.848 (mM/min)

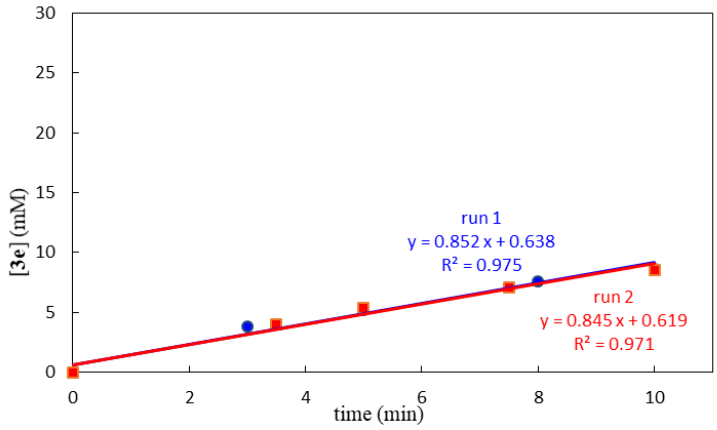

0.300 mmol of **1a**: initial rate = 0.885 (mM/min)

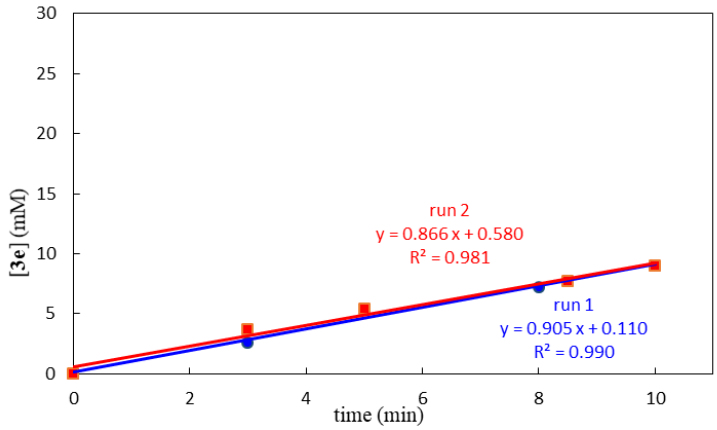

4.5 References

[1] For reviews: (a) Dong, X.; Wang, H.; Liu, H.; Wang, F. *Org. Chem. Front.* **2020**, *7*, 3530–3556. (b) Rahim, A.; Feng, J.; Gu, Z. *Chin. J. Chem.* **2019**, *37*, 929–945. (c) Shi, F.; Larock, R. C. *Top. Curr. Chem.* **2010**, *292*, 123–164. See also: (d) Corpas, J.; Mauleón, P.; Arrayás, R. G.; Carretero, J. C. *ACS Catal.* **2021**, *11*, 7513–7551.

[2] For selected examples: (a) Campo, M. A.; Larock, R. C. *J. Am. Chem. Soc.* **2002**, *124*, 14326–14327. (b) Campo, M. A.; Huang, Q.; Yao, T.; Tian, Q.; Larock, R. C. *J. Am. Chem. Soc.* **2003**, *125*, 11506–11507. (c) Huang, Q.; Fazio, A.; Dai, G.; Campo, M. A.; Larock, R. C. *J. Am. Chem. Soc.* **2004**, *126*, 7460–7461. (d) Zhao, J.; Campo, M.; Larock, R. C. *Angew. Chem.*, *Int. Ed.* **2005**, *44*, 1873–1875. (e) Singh, A.; Sharp, P. R. *J. Am. Chem. Soc.* **2006**, *128*, 5998–5999. (f) Zhao, J.; Yue, D.; Campo, M. A.; Larock, R. C. *J. Am. Chem. Soc.* **2007**, *129*, 5288–5295. (g) Pan, J.; Su, M.; Buchwald, S. L. *Angew. Chem*., *Int. Ed.* **2011**, *50*, 8647–8651. (h) Piou, T.; Bunescu, A.; Wang, Q.; Neuville, L.; Zhu, J. *Angew. Chem.*, *Int. Ed.* **2013**, *52*, 12385–12389. (i) Hu, T.-J.; Zhang, G.; Chen, Y.-H.; Feng, C.-G.; Lin, G.-Q. *J. Am. Chem. Soc.* **2016**, *138*, 2897–2900. (j) Rocaboy, R.; Anastasiou, I.; Baudoin, O. *Angew. Chem.*, *Int. Ed.* **2019**, *58*, 14625–14628. (k) Tsuda, T.; Kawakami, Y.; Choi, S.-M.; Shintani, R. *Angew. Chem*., *Int. Ed.* **2020**, *59*, 8057–8061.

[3] For selected examples: (a) Oguma, K.; Miura, M.; Satoh, T.; Nomura, M. *J. Am. Chem. Soc.* **2000**, *122*, 10464–10465. (b) Hayashi, T.; Inoue, K.; Taniguchi, N.; Ogasawara, M. *J. Am. Chem. Soc.* **2001**, *123*, 9918–9919. (c) Matsuda, T.; Shigeno, M.; Murakami, M. *J. Am. Chem. Soc.* **2007**, *129*, 12086–12087. (d) Shintani, R.; Isobe, S.; Takeda, M.; Hayashi, T. *Angew. Chem.*, *Int. Ed.* **2010**, *49*, 3795–3798. (e) Sasaki, K.; Nishimura, T.; Shintani, R.; Kantchev, E. A. B.; Hayashi, T. *Chem. Sci.* **2012**, *3*, 1278–1283. (f) Hepburn, H. B.; Lam, H. W. *Angew. Chem*., *Int. Ed.* **2014**,

53, 11605–11610. (g) Callingham, M.; Partridge, B. M.; Lewis, W.; Lam, H. W. *Angew. Chem.*, *Int. Ed.* **2017**, *56*, 16352–16356. (h) Ming, J.; Shi, Q.; Hayashi, T. *Chem. Sci.* **2018**, *9*, 7700–7704. (i) Zhang, S.-S.; Hu, T.-J.; Li, M.-Y.; Song, Y.-K.; Yang, X.-D.; Feng, C.-G.; Lin, G.-Q. *Angew. Chem*., *Int. Ed.* **2019**, *58*, 3387–3391. (j) Groves, A.; Sun, J.; Parke, H. R. I.; Callingham, M.; Argent, S. P.; Taylor, L. J.; Lam, H. W. *Chem. Sci.* **2020**, *11*, 2759–2764.

[4] (a) Bour, C.; Suffert, J. *Org. Lett.* **2005**, *7*, 653–656. (b) Sato, Y.; Takagi, C.; Shintani, R.; Nozaki, K. *Angew. Chem.*, *Int. Ed.* **2017**, *56*, 9211–9216. (c) Han, J.-L.; Qin, Y.; Ju, C.-W.; Zhao, D. *Angew. Chem.*, *Int. Ed.* **2020**, *59*, 6555–6560. (d) Tsuda, T.; Choi, S.-M.; Shintani, R. *J. Am. Chem. Soc.* **2021**, *143*, 1641–1650.

[5] (a) Tobisu, M.; Hasegawa, J.; Kita, Y.; Kinuta, H.; Chatani, N. *Chem. Commun.* **2012**, *48*, 11437–11439. (b) Ishida, N.; Shimamoto, Y.; Yano, T.; Murakami, M. *J. Am. Chem. Soc.* **2013**, *135*, 19103–19106. (c) Matsuda, T.; Yuihara, I. *Chem. Commun.* **2015**, *51*, 7393–7396. (d) Font, M.; Cendón, B.; Seoane, A.; Mascareñas, J. L.; Gulías, M. *Angew. Chem.*, *Int. Ed.* **2018**, *57*, 8255–8259. See also: (e) So, C. M.; Kume, S.; Hayashi, T. *J. Am. Chem. Soc.* **2013**, *135*, 10990–10993. (f) Miwa, T.; Shintani, R. *Org. Lett.* **2019**, *21*, 1627–1631.

[6] Yan, J.; Yoshikai, N. *Org. Chem. Front.* **2017**, *4*, 1972–19075.

[7] (a) Mo, J.; Müller, T.; Oliveira, J. C. A.; Ackermann, L. *Angew. Chem.*, *Int. Ed.* **2018**, *57*, 7719–7723. (b) Kimura, N.; Kochi, T.; Kakiuchi, F. *Asian J. Org. Chem.* **2019**, *8*, 1115–1117.

[8] (a) Tan, B.-H.; Dong, J.; Yoshikai, N. *Angew. Chem.*, *Int. Ed.* **2012**, *51*, 9610–9614. (b) Tan, B.-H.; Yoshikai, N. *Org. Lett.* **2014**, *16*, 3392–3395. (c) Yan, J.; Yoshikai, N. *ACS Catal.* **2016**, *6*, 3738–3742.

[9] (a) Börjesson, M.; Janssen-Müller, D.; Sahoo, B.; Duan, Y.; Wang, X.; Martin, R. *J. Am. Chem. Soc.* **2020**, *142*, 16234–16239. (b) He, Y.; Börjesson, M.; Song, H.; Xue, Y.; Zeng, D.; Martin, R.; Zhu, S. *J. Am. Chem. Soc.* **2021**, *143*, 20064–20070. (c) Yang, J.; Gui, Z.; He, Y.; Zhu, S. *Angew. Chem.*, *Int. Ed.* **2023**, *62*, e202304713. (d) Wang, C.-T.; Liang, P.-Y.; Li, M.; Wang, B.; Wang, Y.-Z.; Li, X.-S.; Wei, W.-X.; Gou, X.-Y.; Ding, Y.-N.; Zhang, Z.; Li, Y.-K.; Liu, X.-Y.; Liang, Y.-M. *Angew. Chem.*, *Int. Ed.* **2023**, *62*, e202304447. (e) Zhang, H.; Rodrigalvarez, J.; Martin, R. *J. Am. Chem. Soc.* **2023**, *145*, 17564–17569. See also: (f) Keen, A. L.; Doster, M.; Johnson, S. A. *J. Am. Chem. Soc.* **2007**, *129*, 810–819.

[10] For a relevant review: Gandeepan, P.; Müller, T.; Zell, D.; Cera, G.; Warratz, S.; Ackermann, L. *Chem. Rev.* **2019**, *119*, 2192–2452.

[11] (a) Takeda, M.; Shintani, R.; Hayashi, T. *J. Org. Chem.* **2013**, *78*, 5007–5017. (b) Shintani, R.; Fujie, R.; Takeda, M.; Nozaki, K. *Angew. Chem.*, *Int. Ed.* **2014**, *53*, 6546–6549. (c) Shintani, R.; Kurata, H.; Nozaki, K. *J. Org. Chem.* **2016**, *81*, 3065–3069. (d) Moniwa, H.; Shintani, R. *Chem. Eur. J.* **2021**, *27*, 7512–7515. (e) Kondo, R.; Moniwa, H.; Shintani, R. *Org. Lett.* **2023**, *25*, 4193–4197.

[12] For reviews on silylboronates: (a) Feng, J.-J.; Mao, W.; Zhang, L.; Oestreich, M. *Chem. Soc. Rev.* **2021**, *50*, 2010–2073. (b) Wilkinson, J. R.; Nuyen, C. E.; Carpenter, T. S.; Harruff, S. R.; Van Hoveln, R. *ACS Catal.* **2019**, *9*, 8961–8979. (c) Oestreich, M.; Hartmann, E.; Mewald, M. *Chem. Rev.* **2013**, *113*, 402–411. (d) Suginome, M.; Ohmura, T. In *Boronic Acids, 2nd Ed.*; Hall, D. G., Ed.; Wiley-VCH: Weinheim, 2011; pp. 171–212. (e) Ohmura, T.; Suginome, M. *Bull. Chem. Soc. Jpn.* **2009**, *82*, 29–49.

[13] (a) Ohmura, T.; Takaoka, Y.; Suginome, M. *Chem. Commun.* **2021**, *57*, 4670–4673. See also: (b) Zhao, M.; Shan, C.-C.; Wang, Z.-L.; Yang, C.; Fu, Y.; Xu, Y.-H. *Org. Lett.* **2019**, *21*, 6016–6020.

[14] The structure of **3a** was confirmed by X-ray crystallographic analysis. CCDC Deposition Number 2268930 contains the supplementary crystallographic data for this paper. These data are provided free of charge by the joint Cambridge Crystallographic Data Centre and Fachinformationszentrum Karlsruhe Access Structures service.

[15] For examples of C–H borylation of methyl groups on silicon under transition-metal catalysis: (a) Ohmura, T.; Torigoe, T.; Suginome, M. *J. Am. Chem. Soc.* **2012**, *134*, 17416–17419. (b) Ohmura, T.; Torigoe, T.; Suginome, M. *Organometallics* **2013**, *32*, 6170–6173. (c) Torigoe, T.; Ohmura, T.; Suginome, M. *J. Org. Chem.* **2017**, *82*, 2943–2956. See also: (d) Liang, Y.; Geng, W.; Wei, J.; Ouyang, K.; Xi, Z. *Org. Biomol. Chem.* **2012**, *10*, 1537–1542. (e) Han, J.-L.; Qin, Y.; Zhao, D. *ACS Catal.* **2019**, *9*, 6020–6026.

[16] For a review on silylmethylboronates: (a) Sun, W.; Hu, Y.; Xia, C.; Liu, C. *New J. Chem.* **2021**, *45*, 14847–14854. For selected examples of the synthesis of silylmethylboronates using silylboronate reagents: (b) Shimizu, M.; Kitagawa, H.; Kurahashi, T.; Hiyama, T. *Angew. Chem*., *Int. Ed.* **2001**, *40*, 4283–4286. (c) Shimizu, M.; Kurahashi, T.; Kitagawa, H.; Shimono, K.; Hiyama, T. *J. Organomet. Chem.* **2003**, *686*, 286–293. (d) Aggarwal, V. K.; Binanzer, M.; Carolina de Ceglie, M.; Gallanti, M.; Glasspoole, B. W.; Kendrick, S. J. F.; Sonawane, R. P.; Vázquez-Romero, A.; Webster, M. P. *Org. Lett.* **2011**, *13*, 1490–1493. (e) Li, H.; Shangguan, X.; Zhang, Z.; Huang, S.; Zhang, Y.; Wang, J. *Org. Lett.* **2014**, *16*, 448–451. (f) Millán, A.; Grigol Martinez, P. D.; Aggarwal, V. K. *Chem. Eur. J.* **2018**, *24*, 730–735.

(g) Qi, W.-Y.; Zhen, J.-S.; Xu, X.; Du, X.; Li, Y.; Yuan, H.; Guan, Y.-S.; Wei, X.; Wang, Z.-Y.; Liang, G.; Luo, Y. *Org. Lett.* **2021**, *23*, 5988–5992.

[17] Alkenylsilylmethylboronates are underexplored compounds and only one report has been made on their synthesis to date: Zhang, G.; Li, Y.; Wang, Y.; Zhang, Q.; Xiong, T.; Zhang, Q. *Angew. Chem.*, *Int. Ed.* **2020**, *59*, 11927–11931.

[18] For reviews on copper-catalyzed hydrofunctionalization of alkynes and related topics: (a) Alam, S.; Karim, R.; Khan, A.; Pal, A. K.; Maruani, A. *Eur. J. Org. Chem.* **2021**, *2021*, 6115–6160. (b) Whyte, A.; Torelli, A.; Mirabi, B.; Zhang, A.; Lautens, M. *ACS Catal.* **2020**, *10*, 11578–11622. (c) Chen, J.; Guo, J.; Lu, Z. *Chin. J. Chem.* **2018**, *36*, 1075–1109. (d) Suess, A. M.; Lalic, G. *Synlett* **2016**, *27*, 1165–1174. (e) Yun, J. *Asian J. Org. Chem.* **2013**, *2*, 1016–1025.

[19] Stoichiometric copper-mediated 1,4-Brook rearrangements have been reported: (a) Taguchi, H.; Ghoroku, K.; Tadaki, M.; Tsubouchi, A.; Takeda, T. *Org. Lett.* **2001**, *3*, 3811–3814. (b) Taguchi, H.; Miyashita, H.; Tsubouchi, A.; Takeda, T. *Chem. Commun.* **2002**, 2218–2219. See also: (c) Tsubouchi, A.; Itoh, M.; Onishi, K.; Takeda, T. *Synthesis* **2004**, *2004*, 1504–1508. (d) Tsubouchi, A.; Onishi, K.; Takeda, T. *J. Am. Chem. Soc.* **2006**, *128*, 14268–14269.

[20] For a review on copper-catalyzed C–H bond functionalization: Yang, Y.; Gao, W.; Wang, Y.; Wang, X.; Cao, F.; Shi, T.; Wang, Z. *ACS Catal.* **2021**, *11*, 967–984.

[21] (a) Matteson, D. S.; Mah, R. W. H. *J. Am. Chem. Soc.* **1963**, *85*, 2599–2603. (b) Matteson, D. S. *J. Org. Chem.* **2013**, *78*, 10009–10023.

[22] (a) Zweifel, G.; Arzoumanian, H.; Whitney, C. C. *J. Am. Chem. Soc.* **1967**, *89*, 3652–3653. (b) Armstrong, R. J.; Aggarwal, V. K. *Synthesis* **2017**, *49*, 3323–3336.

[23] Bhat, N. G.; Garza, A. *Tetrahedron Lett.* **2003**, *44*, 6833–6835.

[24] Gaussian 16, Revision E.01: Frisch, M. J.; Trucks, G. W.; Schlegel, H. B.; Scuseria,

G. E.; Robb, M. A.; Cheeseman, J. R.; Scalmani, G.; Barone, V.; Mennucci, B.; Petersson, G. A.; Nakatsuji, H.; Caricato, M.; Li, X.; Hratchian, H. P.; Izmaylov, A. F.; Bloino, J.; Zheng, G.; Sonnenberg, J. L.; Hada, M.; Ehara, M.; Toyota, K.; Fukuda, R.; Hasegawa, J.; Ishida, M.; Nakajima, T.; Honda, Y.; Kitao, O.; Nakai, H.; Vreven, T.; Montgomery, J. A., Jr.; Peralta, J. E.; Ogliaro, F.; Bearpark, M.; Heyd, J. J.; Brothers, E.; Kudin, K. N.; Staroverov, V. N.; Keith, T.; Kobayashi, R.; Normand, J.; Raghavachari, K.; Rendell, A.; Burant, J. C.; Iyengar, S. S.; Tomasi, J.; Cossi, M.; Rega, N.; Millam, J. M.; Klene, M.; Knox, J. E.; Cross, J. B.; Bakken, V.; Adamo, C.; Jaramillo, J.; Gomperts, R.; Stratmann, R. E.; Yazyev, O.; Austin, A. J.; Cammi, R.; Pomelli, C.; Ochterski, J. W.; Martin, R. L.; Morokuma, K.; Zakrzewski, V. G.; Voth, G. A.; Salvador, P.; Dannenberg, J. J.; Dapprich, S.; Daniels, A. D.; Farkas, Ö.; Foresman, J. B.; Ortiz, J. V.; Cioslowski, J.; Fox, D. J. Gaussian, Inc., Wallingford CT, 2019.

[25] Reversible β-elimination of alkenylpalladium species has been reported: (a) Ebran, J.-P.; Hansen, A. L.; Gøgsig, T. M.; Skrydstrup, T. *J. Am. Chem. Soc.* **2007**, *129*, 6931–6942. (b) Ohmura, T.; Oshima, K.; Taniguchi, H.; Suginome, M. *J. Am. Chem. Soc.* **2010**, *132*, 12194–12196.

[26] Batey, R. A.; Shen, M.; Lough, A. J. *Org. Lett.* **2002**, *4*, 1411–1414.

[27] Antenucci, A.; Flamini, P.; Fornaiolo, M. V.; Di Silvio, S.; Mazzetti, S.; Mencarelli, P.; Salvio, R.; Bassetti, M. *Adv. Synth. Catal.* **2019**, *361*, 4517–4526.

[28] Zhao, M.; Barrado, A. G.; Sprenger, K.; Golz, C.; Mata, R. A.; Alcarazo, M. *Org. Lett*. **2020**, *22*, 4932–4937.

[29] Rami, F.; Bächtle, R.; Plietker, B. *Catal. Sci. Technol.* **2020**, *10*, 1492–1497.

[30] Meffre, P.; Hermann, S.; Durand, P.; Reginato, G.; Riu, A. *Tetrahedron* **2002**, *58*, 5159–5162.

[31] Mathews, C. J.; Smith, P. J.; Welton, T. *J. Mol. Catal. A: Chem.* **2004**, *214*, 27–32.

[32] Coulson, D. R.; Satek, L. C.; Grim, S. O. *Inorg. Synth*. **1972**, *13*, 121–124.

List of Publications

Publications

1. Copper-Catalyzed Synthesis of Tetrasubstituted Alkenes via Regio- and *anti*-Selective Addition of Silylboronates to Internal Alkynes
   Moniwa, H.; Shintani, R. *Chem. Eur. J*. **2021**, *27*, 7512–7515.

2. Copper-Catalyzed Regio- and Stereoselective Formal Hydro(borylmethylsilyl)ation of Internal Alkynes via Alkenyl-to-Alkyl 1,4-Copper Migration
   Moniwa, H.; Yamanaka, M.; Shintani, R. *J. Am. Chem. Soc.* **2023**, *145*, 23470–23477.

3. Theoretical Investigation on the Copper-Catalyzed *anti*-Selective 1,2-Silylboration of Internal Alkynes
   Moniwa, H.; Yamanaka, M.; Shintani, R. *Eur. J. Org. Chem*. **2025**, e202401155.

4. Nucleophilic Substitution at Unactivated Arene C–H: Copper Catalyzed *anti*-Selective Silylative Cyclization of Substituted Benzylacetylenes
   Moniwa, H.; Shintani, R. *Org. Lett*. **2025**, *accepted*.

Related publications

5. Copper-Catalyzed Synthesis of 3-Silyl-1-silacyclopent-2-enes via Regio- and *anti*-Selective Addition of Silylboronates to Silicon-Containing Internal Alkynes
   Kondo, R.; Moniwa, H.; Shintani, R. *Org. Lett.* **2023**, *25*, 4193–4197.

6. Synthesis of (1-silyl)allylboronates by KO*t*Bu-catalyzed ring-opening *gem*-silylborylation of cyclopropenes
   Fujii, I.; Hirata, H.; Moniwa, H.; Shintani, R. *Chem. Commun.* **2024**, *60*, 6921–6924.

Acknowledgement

This research presented in this thesis was conducted during 2020–2024 at Graduate School of Engineering Science, Osaka University.

I would first like to express the deepest appreciation to Professor Dr. Ryo Shintani for his invaluable and precise guidance throughout this work. By virtue of his guidance, I could complete this work. The six-years study at Shintani group has taught me how difficult and exciting chemistry is.

I would next like to appreciate Professor Dr. Ichiro Hisaki and Professor Dr. Jun Takaya for their fruitful advice for this dissertation.

I wish to thank Professor Dr. Shuichi Suzuki and Ms. Rika Miyake for HRMS analysis. I would like to appreciate Professor Dr. Masahiro Yamanaka at Graduate School of Science, Rikkyo University for precious guidance on DFT calculation.

I also appreciate all the members in Shintani group. I would like to thank Professor Dr. Akihiro Shimizu and Professor Dr. Ikuya Fujii for insightful discussion in my research. I would like to thank Ms. Shoko Ueno and Ms. Yuko Inaba for their kind assistance throughout my stay in Shintani group. I give special thanks to Dr. Tomohiro Tsuda, Dr. Sho Ikeda, Dr. Shinobu Arikawa, Mr. Yuta Ochi, Ms. Ayase Oozono, Ms. Ayane Kayama, Mr. Mamoru Yokota, Mr. Masaaki Hayashida, Mr. Tetsuya Morikoshi, Ms. Honoka Tsuda, Mr. Tatsuki Takagi, Mr. Soya Togawa, Mr. Atsuo Fujita, Mr. Naoya Hamada, Mr. Daigo Hayashi, Mr. Yuki Haga, Mr. Yuki Misaki, Mr. Ryosuke Kondo, Mr. Masaki Morita, Mr. Hamachan, Ms. Yuka Kuno, Mr. Taihei Mori, Mr. Kanta Ueji, Mr. Yoshiaki Kasai, and all the past and current members in Shintani group for sharing a tough and enjoyable laboratory life. Especially, I am most grateful to Mr. Donghyeon Lee, my best friend who has been with me for sharing the longest time in Shintani group. Thanks to him, I could overcome the hard times.

Finally, my deepest thanks go to my family, Masahiro, Akemi, and Ayaka for their warm and continuous supports and encouragement throughout my life.

March, 2025

Hirokazu Moniwa